A SYSTEMS BIOLOGY APPROACH TO THE HUMAN HAIR CYCLE

A thesis submitted to The University of Manchester for the degree of
Doctor of Philosophy
in the Faculty of Engineering and Physical Sciences

2011

Yusur Mamoon Al-Nuaimi

School of Chemical Engineering and Analytical Science
Doctoral Training Centre in Integrative Systems Biology

TABLE OF CONTENTS

LIST OF FIGURES

LIST OF TABLES

Word count: 57,062

ABSTRACT

"A Systems Biology Approach to the Human Hair Cycle". A thesis submitted to The University of Manchester for the degree of Doctor of Philosophy by Yusur Mamoon Al-Nuaimi, 2011.

The hair cycle represents a dynamic process during which a complex mini-organ, the hair follicle, rhythmically regresses and regenerates. The control mechanism that governs the hair cycle ("hair cycle clock") is thought to be an autonomous oscillator system, however, its exact nature is not known. This thesis aims to understand the human hair cycle as a systems biology problem using theoretical and experimental techniques in three distinct study approaches.

Using mathematical modelling, a simple two-compartment model of the human hair cycle was developed. The model concentrates on the growth control of matrix keratinocytes, a key cell population responsible for hair growth, and bi-directional communication between these cells and the inductive fibroblasts of the dermal papilla. A bistable switch and feedback inhibition produces key characteristics of human hair cycle dynamics. This study represents the first mathematically formulated theory of the "hair cycle clock".

A second chronobiological approach was adopted to explore the molecular control of the human hair follicle by a peripheral clock mechanism. The hypothesis was tested that selected circadian clock genes regulate the human hair cycle, namely the clinically crucial follicle transformation from organ growth (anagen) to organ regression (catagen). This revealed that intra-follicular expression of core clock and clock-controlled genes display a circadian rhythm and is hair cycle-dependent. Knock-down of *Period1* and *Clock* promotes anagen maintenance, hair matrix keratinocyte proliferation and stimulates hair follicle pigmentation. This provides the first evidence that peripheral *Period1* and *Clock* gene activity is a component of the human "hair cycle clock" mechanism.

Lastly, an unbiased gene expression profiling approach was adopted to establish important genes and signalling pathways that regulate the human hair cycle. This revealed that similar genes and pathways previously shown to control the murine hair cycle *in vivo*, such as *Sgk3, Msx2* and the BMP pathway, are also differentially regulated during the anagen-catagen transformation of human hair follicles.

In summary, by using a three-pronged systems biology approach, the thesis has shed new light on the control of human hair follicle cycling and has generated clinically relevant information: a) The hair cycle model may predict how hair cycle modulatory agents alter human hair growth. b) *Period1* and *Clock* are new therapeutic targets for human hair growth manipulation. c) Gene expression profiling points to additional key players in human hair cycle control with potential for future therapeutic targets.

Declaration

The author declares that no portion of the work referred to in the thesis has been submitted in support of an application for another degree or qualification of this or any other university or other institute of learning.

COPYRIGHT STATEMENT

i. The author of this thesis (including any appendices and/or schedules to this thesis) owns certain copyright or related rights in it (the "Copyright") and s/he has given The University of Manchester certain rights to use such Copyright, including for administrative purposes.

ii. Copies of this thesis, either in full or in extracts and whether in hard or electronic copy, may be made **only** in accordance with the Copyright, Designs and Patents Act 1988 (as amended) and regulations issued under it or, where appropriate, in accordance with licensing agreements which the University has from time to time. This page must form part of any such copies made.

iii. The ownership of certain Copyright, patents, designs, trade marks and other intellectual property (the "Intellectual Property") and any reproductions of copyright works in the thesis, for example graphs and tables ("Reproductions"), which may be described in this thesis, may not be owned by the author and may be owned by third parties. Such Intellectual Property and Reproductions cannot and must not be made available for use without the prior written permission of the owner(s) of the relevant Intellectual Property and/or Reproductions.

iv. Further information on the conditions under which disclosure, publication and commercialisation of this thesis, the Copyright and any Intellectual Property and/or Reproductions described in it may take place is available in the University IP Policy (see http://www.campus.manchester.ac.uk/medialibrary/policies/intellectual-property.pdf), in any relevant Thesis restriction declarations deposited in the University Library, The University Library's regulations (see http://www.manchester.ac.uk/library/aboutus/regulations) and in The University's policy on presentation of Theses.

ACKNOWLEDGEMENTS

I would like to acknowledge and thank Professor Ralf Paus, Dr Rachel Watson and Dr Gerold Baier for their supervision, support and guidance through my PhD. You have all taught me a great deal and each provided me with inspiration in my work and for the future. I would like to acknowledge the DTC in Integrative Systems biology, in particular, Professor Westerhoff for providing the environment to develop as a novice Systems Biologist. Professor Griffiths, thank you for acting as my PhD advisor, for all your support and for inspiring me in my career goal as an academic dermatologist. I would like to thank the Paus group in Germany, particularly Dr Jennifer Kloepper for their support, guidance and hospitality during my stay at the University of Luebeck and the lab technician Nadine Doerwald for experimental support. Thanks to the Watson group (especially Dr Abigail Langton) and the Paus UK group (Drs David Pattwell, Iain Haslam and Craig Portsmouth) for lab support and advice. I acknowledge and thank Marc Goodfellow (Baier Research Group), fellow DTC student, for dynamical systems tutorials (MATLAB advice and explanations) used for the dynamic introduction section Chapter 4 and the mathematical model presented in Chapter 5 in the thesis. I am grateful for the collaborations with Professor Mike Philpott, London, and Dr Tamas Biro, Hungary and for their contributions to the clock work and qPCR experiments, respectively. I acknowledge and thank Dr Qing-Jun Meng for his advice and suggestions on the circadian clock work (The University of Manchester). In addition, I acknowledge the University of Manchester Genomic Technologies Core Facility for performing the microarray experiment (Leanne Wardleworth) and initial analyses (Dr. Leo Zeef) that is presented in this thesis. Thank you, my best friend M, for always encouraging and believing in me. Finally, thank you Mama, Baba and Dania for your endless support.

LIST OF ABBREVIATIONS

ACTB	actin, beta
AKR1C1	aldo-keto reductase (AKR) superfamily
APM	arrector pili muscle
BAMBI	BMP and activin membrane-bound inhibitor homolog
BDNF	brain-derived neurotrophic factor
BM	basement membrane
BMAL1	aryl hydrocarbon receptor nuclear translocator-like
BMP	bone morphogenetic protein
BMPR1A	bone morphogenetic protein receptor 1A
CCG	clock controlled gene
CDKN1A	cyclin-dependent kinase inhibitor 1A (p21, Cip1)
cDNA	complementary deoxyribonucleic acid
CLOCK	clock homolog (mouse)
c-MYC	v-myc myelocytomatosis viral oncogene homolog (avian)
CRY	cryptochrome
CTS	connective tissue sheath
ΔCT	delta Ct
DAPI	4', 6-diamidino-2-phenylindole
DLX	distal less homeobox
DNA	deoxyribonucleic acid
DP	dermal papilla
DSG4	desmoglein 4
EGF	epidermal growth factor
EMI	endogenous mitotic inhibitor
EP	epithelium
FAM	follicular automaton model
FITC	fluorescein isothiocyanate
FKBPL	FK506 binding like protein

FGF-5	fibroblast growth factor 5
FGF5S	fibroblast growth factor 5 splice variant
FZD10	frizzled 10
GAPDH	glyceraldehyde 3-phosphate dehydrogenase
GO	gene ontology
HCC	hair cycle clock
HFPU	hair follicle pigmentary unit
HF	hair follicle
HGF	hepatocyte growth factor
HS	hair shaft
IF	immunofluorescence
IGF-1	insulin-like growth factor 1
IGF-R	insulin-like growth factor receptor
IHC	immunohistochemistry
ISH	in situ hybridisation
IRS	inner root sheath
K	keratin
KAP	keratin-associated protein
Ki-67	proliferation-related Ki-67 antigen
ODE	ordinary differential equation
ORS	outer root sheath
M	matrix
MAPK	mitogen-activated protein (MAP) kinases
MF	masson-fontana
mRNA	messenger ribonucleic acid
MSX2	msh homeobox 2
MK	matrix keratinocyte
NOG	noggin
NR1D1	nuclear receptor subfamily 1, group D, member 1
NT	neurotrophin

NT-3	neurotrophin 3
P13K	phosphatidylinositol-3-kinase
P21	cyclin-dependent kinase inhibitor 1A (p21, Cip1)
PBS	phosphate buffered saline
PERIOD1	period homolog (mouse)
PFA	paraformaldehyde
PM	papilla morphogen
PPIA	peptidylprolyl isomerase A
qPCR	quantitative polymerase chain reaction
RNA	ribonucleic acid
RNase	ribonuclease
SC	stem cell
siRNA	small interfering RNA
SG	sebaceous gland
SGK3	serum glucocorticoid regulated kinase 3
SPP1	secreted phosphoprotein 1 (osteopontin)
TAC	transient amplifying cell
TBS	tris buffered saline
TGF-β1	transforming growth factor β1/ β2
TRH	thyrotropin hormone
TUNEL	terminal deoxynucleotidyl transferase dUTP nick end labelling
VEGF	vascular endothelial growth factor
WNT	wingless-type MMTV integration site

1 CHAPTER 1: INTRODUCTION

This chapter provides an overview of the aims of the thesis and an explanation of the thesis structure. A short background describing the motivation of the project is provided with the specific aims of the thesis detailed. Following this, the format of the thesis is outlined.

1.1 MOTIVATION AND AIMS

The hair follicle (HF) undergoes continuous cyclical organ transformations involving co-ordinated regeneration (proliferation) and apoptotic regression of the HF in its own unique biorhythm (the hair cycle). This dynamic process relies on the co-ordinated spatio-temporal interactions of various cell compartments that exhibit both molecular and population changes in expression patterns.

Understanding how the hair cycle mechanism occurs is of clinical importance as disruption of normal hair cycling is responsible for most hair disorders. In addition the current treatment options available are disappointingly ineffective. Although multiple molecules have been identified that alter hair cycling, the research relies heavily on other mammalian species such as mice. There remains neither an existing mechanistic explanation of how the human hair cycle rhythm may come about nor confirmation that synergy exists between established research findings in other mammalian species with the human HF.

Systems biology aims to understand the complex interactions within a biological system that result in its normal function or dysfunction. The discipline involves interdisciplinary approaches and often mathematical modelling to elucidate the systems properties of the biological system of interest.

The goal of this thesis is to apply a systems biology approach to understand the human hair cycle mechanism as a complex dynamic process. Within this work there is a particular focus on elucidating the controls of the transition from the growth stage of the hair cycle (anagen) to the regressive state (catagen).

In order to address the problem from a systems biology perspective, three specific approaches will be taken for the thesis. Firstly, a theoretical

approach is applied via the use of mathematical modelling. Secondly, a directed experimental investigation elucidating the role of circadian clock genes and proteins as novel candidates in the human anagen-to-catagen transition is adopted. Finally, these two hypothesis-driven approaches are complemented by a gene expression profiling strategy to identify key genes and signalling pathways that control the transformation of human HFs from the anagen to catagen hair cycle stages.

This three-pronged systems biology investigation aims to shed new light on the controls of human HF cycling and to generate clinically relevant information for the future management of human hair growth disorders.

1.2 STRUCTURE OF THE THESIS

The thesis is presented in the alternative format, as such; some chapters are in the form of a manuscript. Where this is the case this is clearly identified on the chapter title page and the nature of the authors' contributions are also detailed there. This format was chosen so that these chapters may be understood independently with their own introduction, methods and discussion sections and reflects the various techniques and approaches adopted in the thesis.

An introduction to the thesis aims and structure is provided in this chapter. Chapter 2 comprises a literature review introducing the human HF, the hair cycle and explores existing theories of the hair cycle mechanism. The chapter concludes that a systems biology approach may be adopted to address this problem. Additional literature reviews are also found in the relevant introductory sections of "manuscript" chapters. Chapter 3 is a viewpoint article that was published in *Experimental Dermatology*. This chapter argues that the HF is an ideal systems biology research tool, introduces systems biology and mathematical modelling and its status in terms of hair biology.

The theoretical approaches utilised in the thesis are found in Chapters 4 and 5, where Chapter 4 introduces dynamical systems theory and terminologies. Chapter 5 contains a proposed mathematical model of the human hair cycle using a dynamical systems approach. It concludes that the human hair cycle

rhythm is an autonomous process which requires the presence of bistability and feedback inhibition to produce the dynamic behaviour of the human hair cycle.

Chapters 6-8 comprise the experimental work of the thesis beginning with experimental methodologies found in Chapter 6. The role of circadian genes and proteins in the human HF is presented in Chapter 7, which concludes that *Period1* and *Clock* play a role in regulating the anagen-to-catagen transition in human organ-cultured HFs. Chapter 8 details a transcriptome study which identifies global gene expression profiles of human anagen and catagen organ-cultured HFs. Novel genes that represent each state are identified.

Finally, the conclusions along with future research perspectives are presented in Chapter 9.

2 CHAPTER 2: LITERATURE REVIEW

In this chapter the literature is reviewed in order to introduce HF anatomy, the hair cycle, current theories of the controls of hair cycling and the anagen-to-catagen transition. There are additional literature reviews located in subsequent chapters that introduce specific topics relevant to the chapter.

2.1 BASIC HUMAN HAIR DATA

The human body is covered in 5 million hairs and, of that, approximately 80,000 to 150,000 are found on the scalp (Krause and Foitzik, 2006). Hair is produced by the multi-cellular entity; the HF. There are two types of HFs in adult humans; vellus and terminal. These produce a small, fine vellus hair and thick, pigmented terminal hair respectively (Whiting, 2004, Paus and Cotsarelis, 1999, White and Cox, 2006).

2.2 THE HAIR FOLLICLE

The HF resides as an appendage of the skin and makes up one entity of the pilo-sebaceous unit. The pilo-sebaceous unit consists of the HF, sebaceous gland, apocrine gland and arrector pili muscle. The HF, in adult life, undergoes cycles of growth (anagen), regression (catagen) and relative resting (telogen). Anatomically, the HF is most commonly described when it is in the mature anagen stage; anagen VI (Figure 2.1).

In the mature anagen state the HF can be divided into an upper "permanent" portion the infundibulum and isthmus, which does not cycle, and a lower "non-permanent" segment comprising the suprabulbar region and the bulb (Figure 2.1A). It is the lower region of the HF which undergoes re-modelling during the hair cycle.

The infundibulum, at its proximal end, marks the opening of the hair canal to the surface of the skin. The infundibulum is lined by epidermis which is continuous with the surface of the skin. The lower part of the infundibulum is defined by the attachment of the duct of the sebaceous gland and it is via this duct that sebum is excreted into the HF and onto the skin's surface (Schneider et al., 2009, Whiting, 2004). Distal to the infundibulum is the isthmus. The hair

shaft is not attached to either the isthmus or infundibulum and this allows free movement of the hair shaft.

The isthmus of the HF extends upwards from the point of arrector pili muscle insertion, also known as the bulge area, to the sebaceous duct (Figure 2.1B). The bulge region is of functional importance as it is here where melanocytic and epithelial stem cells reside and are responsible for activation of a new hair cycle (Cotsarelis, 2006). In human scalp HFs, the follicular trochanter, a protrusion of the outer root sheath (ORS), has been shown to represent the bulge region (Tiede et al., 2007). The isthmus marks where the inner root sheath (IRS) gradually disappears and is replaced by trichemmal keratin produced by the ORS until this layer is no longer visible. The lower end of the isthmus also marks the end of the "permanent" section of the HF.

The supra-bulbar region is located between the isthmus and hair bulb (Figure 2.1). Proximal to the bulb, the IRS and ORS thicken and are well-defined. The keratinisation process in the IRS is completed half way up the supra-bulbar region of the HF (Whiting, 2004).

The anagen hair bulb is the centre of the hair shaft factory (Figure 2.1C). The epithelial cells of the bulb; hair matrix keratinocytes (MKs) and melanocytes, surround the dermal papilla (DP). Melanocytes are interspersed between the MKs. The MKs are rapidly proliferating cells and the number of these cells determines the diameter of the hair shaft and hair bulb size (Legué and Nicolas, 2005). When these cells withdraw from the cell cycle (i.e. stop proliferating) they differentiate and migrate upwards to form concentric cylinders of cells (Figure 2.1D). Each cylinder comprises cells of different morphology which have followed separate differentiation patterns to form the various cell lineages of the hair shaft and IRS.

The cells which make up the hair shaft are known as trichocytes. The shaft comprises three layers; the innermost medulla, cortex and cuticle (Figure 2.1D). Hair matrix cells centrally located at the apex of the DP form the medulla of the hair shaft, whilst those lateral to these form cylinders around the shaft in a concentric formation. The hair shaft cells become compacted and keratinised as they move proximally in the HF. The outer area of matrix cells form the

cuticle of the hair shaft, which consists of 6-10 overlapping cuticle cells, and the IRS (Whiting, 2004). The hair keratins and their associated proteins, keratin associated proteins (KAPs), are the main structural components of the hair shaft. Hair keratins are structural proteins and can be subdivided into two families; the type I (acidic) and type II (neutral) hair keratins (Langbein and Schweizer, 2005). The expression patterns of type I and II keratins differ depending on their location in the hair shaft (see Figure 2.1E). Copolymers of type I and II hair keratins make up the intermediate filaments found in trichocytes. In the hair fibre, KAPs act to link keratin intermediate filaments within trichocytes. KAPs are classified according to their chemical composition; high sulphur KAPs, ultrahigh sulphur KAPs and high glycine tyrosine KAPs. mRNA expression of human KAPs has been mainly located to the cortex of the hair shaft with expression also seen in the hair cuticle and hair matrix-cortex cell region (Rogers et al., 2006). As with the hair keratins, the KAPs exhibit location specific expression patterns. In the hair cortex the KAP gene families KAP 1-4, 7, 8 are strongly expressed, whereas in the cuticle one finds KAPs 5, 10 and 12. The KAP gene families found in the matrix-cortex region are KAP8 and KAP1J.

The IRS comprises three layers; the Henley, Huxley and innermost cuticle layer. The latter interlocks with the cuticle of the hair shaft via outward projections. The IRS is itself surrounded by the ORS, though separated by the companion layer. The ORS derives from progenitor cells of polyclonal origin, which are different to those that form the IRS and hair shaft (Legué and Nicolas, 2005). The ORS is continuous with the epidermis of the skin and is covered by the hyaline membrane laterally and this is continuous with the epidermal basement membrane surrounding the DP. The expression patterns of hair follicle keratins within the IRS and ORS is found in Figure 2.1E. The IRS hair keratins are K71-74 and K25-28, whereas those expressed in the ORS are K5, K6a/b, K14-17 and K19 (Porter, 2006, Schweizer et al., 2007). Another important structural component of the anagen hair follicle that is located in the IRS is trichohyalin. This large insoluble protein makes up a third of the total protein content of the IRS of the HF. It is also located in the medulla of the hair

shaft (Steinert et al., 2003). Trichohyalin is an important structural protein that forms multiple cross links between keratin chains in the IRS and serves to harden this layer of the HF (Steinert et al., 2003).

The DP contains blood vessels and fibroblasts (Stenn and Paus, 2001, Tobin et al., 2003, Whiting, 2004) and has been shown to be important for determining the size of hair bulb, hair shaft diameter and the duration of anagen (Cotsarelis, 2006, Rendl et al., 2005, Stenn and Paus, 2001). Around this layer is the connective tissue sheath (CTS) which is continuous with the DP and surrounds the epithelial HF (Whiting, 2004). The CTS comprises loosely connected stromal cells and mesenchymal stem cells which act to replace DP cells (Tobin et al., 2003).

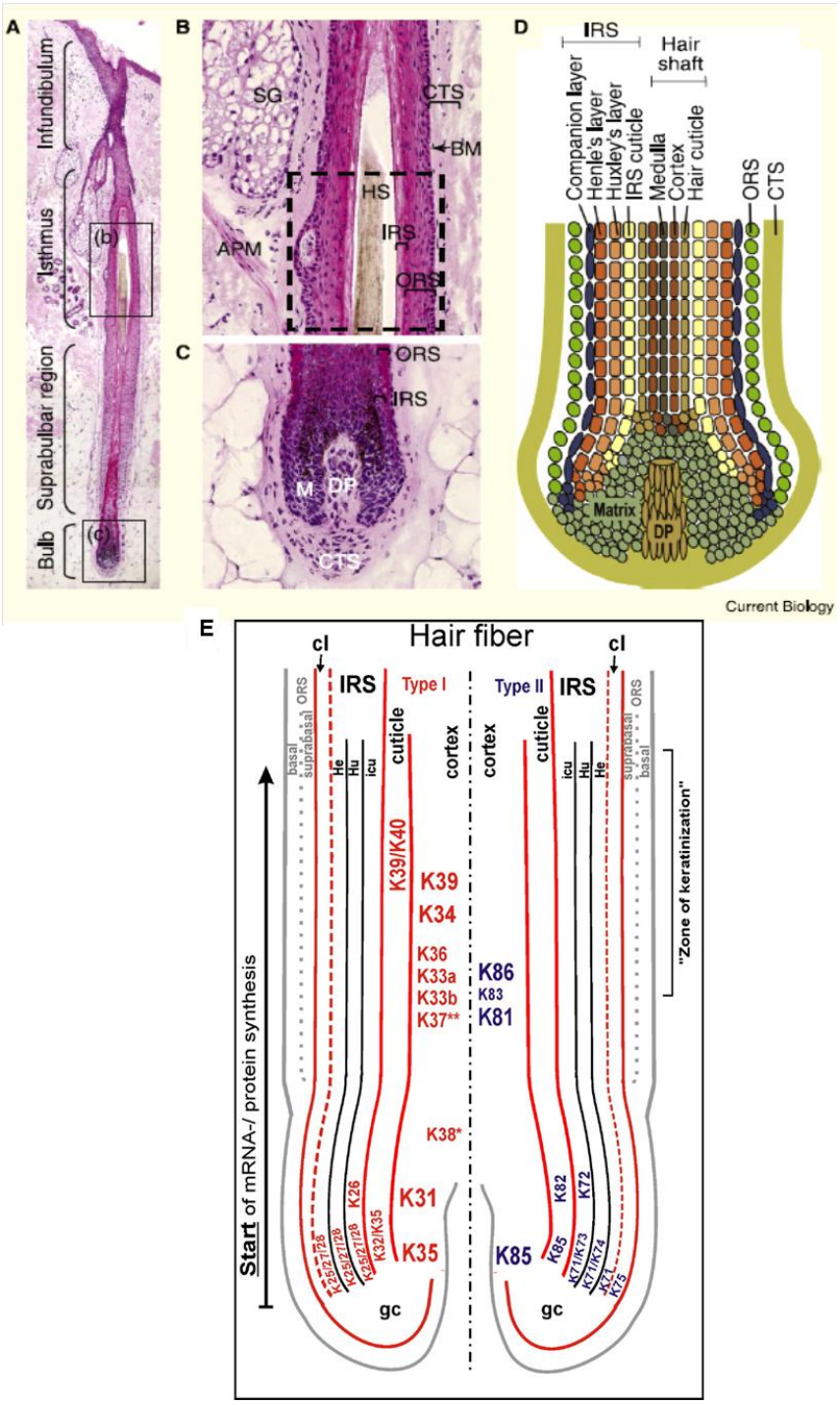

Figure 2.1 Histomorphology of the human hair follicle

(A) Sagittal section human scalp anagen HF. (B) The isthmus region of the HF. (C) The hair bulb. (D) The concentric layers of hair follicle bulb. (E) Pattern of expression of the human HF keratins. APM Arrector pili muscle; BM, basement membrane; CL, companion layer; CTS, connective tissue sheath; DP, dermal papilla; GC, germative cells; He, Henley layer; Hu, Huxley layer; HS, hair shaft; ICU, IRS cuticle; IRS, Inner root sheath; K, keratin; ORS, outer root sheath; M, matrix; SG: sebaceous gland;. Figure comprised from Schneider et al 2009 and Schweizer 2007 with permission.

2.3 THE HUMAN HAIR CYCLE

The hair cycle describes the continuous cyclical regression and regeneration of the HF (Figure 2.2). In 1924 Trotter documented the cyclical growth of hair in humans (Trotter, 1924). However, in 1959, Kligman first characterised and documented the structural changes in the HF during the human hair cycle (Kligman, 1959). The hair cycle commences immediately following morphogenesis of the HF and consists of distinct stages; anagen, catagen, telogen and exogen (Paus et al., 1999a, Milner et al., 2002). Each stage has an approximate length of duration, with anagen in scalp HFs ranging from 2 to 7 years. Catagen normally lasts 10-14 days and telogen 2-4 months in humans (Krause and Foitzik, 2006, Whiting, 2004). Exogen describes the process of hair shedding (Higgins et al., 2009, Milner et al., 2002). There is a wide variation in HF size and hair cycle length between individuals and body regions (Saitoh et al., 1970). The variation in hair cycle length is attributed, in the main, to different lengths of the anagen phase (Krause and Foitzik, 2006). As hair is produced solely in anagen, this phase also determines the length of the hair.

2.4 DYNAMIC CHANGES IN HAIR FOLLICLE ANATOMY DURING THE HAIR CYCLE

As mentioned above, the HF is a mini-organ which perpetually cycles in three stages; anagen (active growth), catagen (apoptosis-driven regression) and telogen (relative "resting") (Schneider et al., 2009). The HF is unique among mammalian organs in that it rhythmically undergoes these massive organ transformation events for the entire lifespan of the organism. During these organ remodelling events, the HF shows complex, patterned phenomena that are temporo-spatially restricted (Chuong et al., 2006, Widelitz et al., 2006). During anagen, matrix cells in the bulb of the HF proliferate and differentiate into the hair shaft trichocytes and IRS (Stenn and Paus, 2001, Legué and Nicolas,

2005). HF melanogenesis is tightly coupled to the anagen phase of the hair cycle (Slominski et al., 2005). This process is halted early in catagen and does not recommence until the next anagen.

Catagen is coupled with the apoptosis of melanocytes (Slominski et al., 2005). During catagen, apoptosis occurs in the lower two thirds of the HF involving the matrix, IRS and ORS cells. The hair shaft retracts upwards leaving behind an epithelial stela. During this process, the hair shaft and IRS slide upwards leaving trichemmal ORS below. The base of the retreating hair shaft becomes club shaped (club hair) and is surrounded by trichilemmal keratin, which produces a small white "cap" at the end of the hair shaft (often noticed at the end of shed hair). Apoptosis of the ORS produces a reduction in the volume of the ORS layer and there is a thickening of the surrounding hyaline layer. The DP is drawn upwards to the base of the permanent epithelial part of the HF until it lies close to the HF bulge.

The HF has retracted to the level of the bulge when telogen commences. A germinal unit is found beneath the club hair and consists of trichilemma surrounded by basaloid cells. The telogen club is found to have a central mass of trichilemmal keratin, surrounded by trichilemma and a fibrous sheath which connects the telogen germinal unit and the hair shaft. It is thought that telogen ends when a signal arises between the DP and bulge region to initiate regeneration of the follicular epithelial cells which then act to regenerate the lower portion of the HF (Schneider et al., 2009, Stenn and Paus, 2001, Fuchs et al., 2001). This re-traces many HF morphological steps that occurred during HF development and the new anagen bud grows down the existing follicular stela forming an anagen HF.

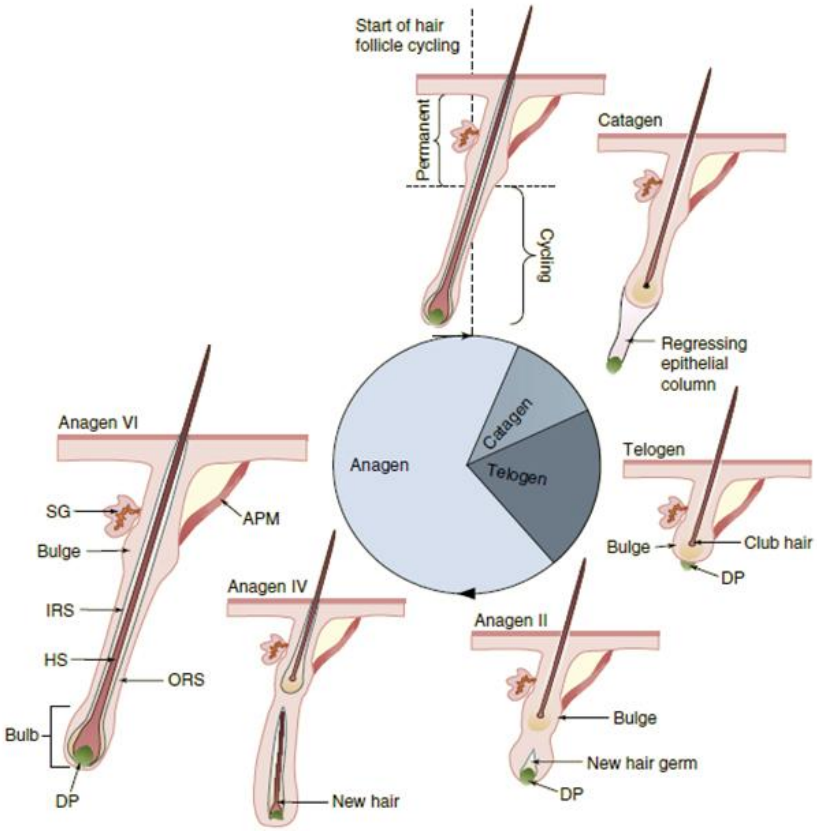

Figure 2.2: The hair cycle

The hair follicle enters a continuous cyclical process of organ regression (catagen; lasting a few weeks), a relative "resting" phase (telogen; lasting approx. few months) and a growth and pigmentation phase (anagen which lasts months in mice and years in man) in the hair cycle. This process is altered in hair disorders such as hirsutism in which HFs exhibit a prolonged anagen phase. This process demonstrates the dynamic nature of the HF with drastic molecular and structural changes associated with the passing of time (stage of hair cycle). The hair cycle occurs as a result of precisely co-ordinated and collective functioning of the component parts of the HF. Key: DP Dermal papilla, ORS Outer root sheath, HS Hair shaft, IRS inner root sheath, SG Sebaceous gland. Figure and figure legend presented as found in (Al-Nuaimi et al., 2010). Adapted after Schneider et al 2009 Current Biology (Schneider et al., 2009).

2.5 THE RELEVANCE OF HAIR CYCLING TO HAIR DISEASES

A wide range of pathologies affect the HF, its cycling and hair shaft structure (White and Cox, 2006). This section briefly introduces the relevance of the hair cycle to hair disorders. Pure structural diseases of the hair shaft are not addressed here.

Hair growth disorders may be divided into those causing hair loss and those leading to excessive hair growth. The common hair growth disorders include androgenetic alopecia, alopecia areata, telogen effluvium, anagen effluvium, hirsutism and hypertrichosis. The hair cycle is intrinsically important to these hair disorders as all of these pathologies exhibit alterations in normal hair cycling (Paus, 2006, Paus et al., 1999a).

Anagen length is shortened in androgenetic alopecia, aging HFs and the effluviums (telogen effluvium and anagen effluvium). This results in shortened effective hair (White and Cox, 2006). In addition, in androgenetic alopecia, miniaturisation of the HF occurs which involves a transformation of the HF from a terminal to vellus follicle. The cyclical nature of the HF is therefore central to the occurrence of HF transformations (Stenn and Paus, 2001, Tobin et al., 2003). Transition from a vellus to terminal follicle results in a prolonged anagen phase as occurs in hirsutism and hypertrichosis (Schneider et al., 2009, Krause and Foitzik, 2006). The transition from anagen to catagen is of high clinical importance as an alteration in anagen length results in changes in the resultant hair shaft.

In humans, synchronised hair cycling is lost in post-natal life and exhibits a mosaic or asynchronous cycling pattern (Whiting, 2004, Paus and Foitzik, 2004)**.** Therefore, the normal dynamics of multiple human HFs in relation to each other entails the asynchronous HF cycle in terms of one HF in comparison to its neighbours. This may also be described as the population cycling dynamics. Therefore, an abnormality of normal human HF dynamics is synchronisation. The synchronisation of populations of HFs leads to a patch or the whole scalp of hair shedding together. This occurs in the pathologies anagen effluvium and telogen effluvium whereby anagen is abrogated by factors such as chemotherapy and stress, respectively (Hadshiew et al., 2004, Paus, 2006) (see Figure 2.3).

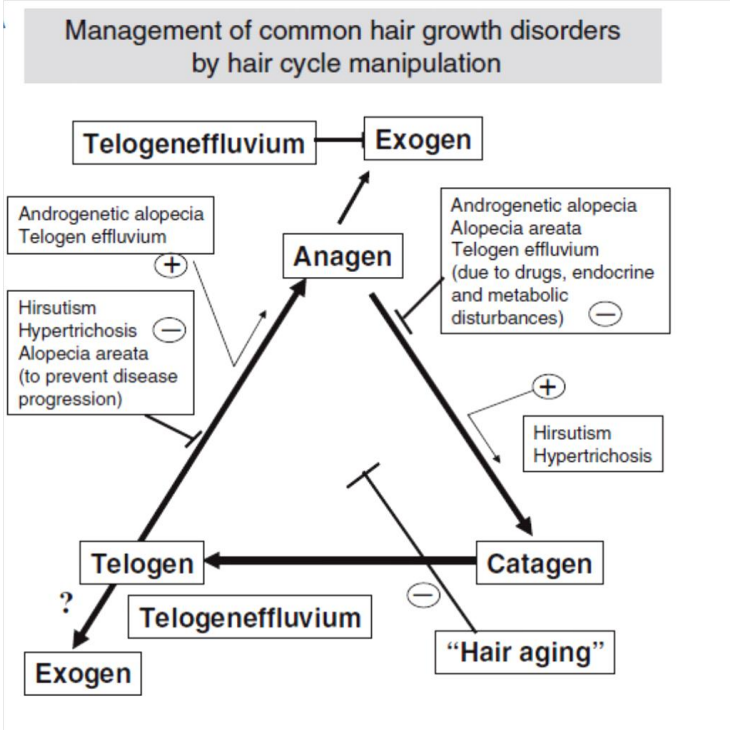

Figure 2.3: Management of common hair disorders by hair cycle manipulation

This figure demonstrates how different points within the hair cycle may be manipulated to treat hair disorders. (+) indicates stimulation and (–) inhibition of the transition from one cycle stage to the next. Figure obtained and reprinted from (Paus and Foitzik, 2004) with permission from Elsevier publishing.

Therefore, understanding how hair cycling is controlled is clinically important as many hair diseases can be attributed to changes in normal hair cycling (Paus and Cotsarelis, 1999, Paus and Foitzik, 2004, Cotsarelis and Millar, 2001, Stenn and Paus, 2001). Indeed, as Albert Kligman stated in 1959:

> "*normal dynamics provide the basis for understanding how the follicle behaves in disease*" (Kligman, 1959).

A patient will notice the problem when HFs are affected as a population rather than in an individual HF. Determining how the hair cycle is controlled and, subsequently, deciphering how to modify this may identify new treatment options and address the clinical need for improved treatment of hair disorders.

2.6 WHAT CONTROLS THE HUMAN HAIR CYCLE?

Here, the literature is reviewed regarding the postulated controls of the human hair cycle. A varied approach has been taken by researchers in this arena and therefore this section is split into two main sections; the first is concerned with the postulated theories of the controller(s) of the hair cycle and the second reviews a small selection of molecular candidates that have been identified as possible regulators of the hair cycle i.e. in the co-ordinated transition of the HF from one stage of the cycle to the next.

2.6.1 Current theories of the hair cycle mechanism

Here we consider the existing proposed theories on how HF cycling may be controlled. Here, mathematical models concerned with hair growth and cycling are not detailed. The reason for this is they do not explicitly consider the internal mechanisms that govern individual HFs through the hair cycle (Nagorcka and Mooney, 1982, Plikus et al., 2011, Halloy et al., 2000, Halloy et al., 2002). These papers are explored further and discussed in Chapters 3 and 5.

2.6.1.1 Inhibition-disinhibition switch theory

Chase led this field when, over half a century ago, he identified that there was a need for the conceptualisation of the hair cycle mechanism as this would enable understanding of hair biology (Chase, 1954). Chase proposed that since "*The hair cycle is clearly only the result of a cycle of follicular activity*" the focus of investigation should be directed to the HF itself and its immediate surrounding environment (Chase, 1954). He described the hair cycle as a dynamic and continuous process and suggested that anagen is initiated by the release of an inhibitory substance i.e. an inhibitor of mitosis is lost in order for anagen to occur. This process involves the HF itself, but this concept of inhibitor-release is extended also to include communication between adjacent skin allowing waves of HF cycling to occur if a threshold is overcome.

The theory offered by Chase is a very brief discussion of hair cycle control, therefore only a few sentences are provided regarding the postulated mechanism. There is no attempt to explain what the inhibitor(s) may be

specifically, nor where they are located exactly, but they are referred to as mitotic inhibitors. An inhibitory-release mechanism for hair cycling control has also been suggested by other authors (Argyris and Trimble, 1964, Argyris, 1972). However, the work they present attempts to explain the propagation and stimulation of populations of HFs rather than the individual control mechanism of the hair cycle in a single follicle. Even Chase overlaps between the two processes and describes his observations regarding mouse hair cycling in waves. He then briefly discusses the release of the inhibitor as being involved in inter-follicular population controls of hair cycling (Chase, 1954). There is experimental evidence for an inhibitor release mechanism being involved in the control of the hair cycle; for example in the function of bone morphogenetic proteins with their antagonist noggin. This will be discussed in the molecular candidates section below.

2.6.1.2 Epithelial theory

Other theories on the mechanism of the hair cycle have been proposed over the years. Some suggest that the epithelial part of the HF is responsible for the initiation of the mature hair cycle.

Stenn proposes that the hair cycle is a regenerative system and compares the HF to the regenerating limb (Stenn in (Stenn et al., 1999)). In this context, the epithelium is known to be essential for regeneration to occur and, therefore, Stenn states that the epithelium is the key component of the hair cycle mechanism with the HF components that represent regenerative tissue being the hair germ and the papilla. The theory states that the signal for anagen initiation is under the control of a unique clock. The reasoning provided for why the clock is thought to be unique is that the HF does not exhibit a rhythm that is in synchronisation with the seasons, or the day-night rhythm and scalp HFs, for example, have a clock lasting years. Stenn proposes that the stem cells of the HF are the providing source for the regeneration of the HF during each cycle and thus are postulated to be the core controllers of the hair cycle. In addition, the stem cells exhibit very slow dividing behaviour in line with the long periodicity seen in the HC. Stenn postulates that the transient amplifying cells are

responsible for determining the anagen duration (Stenn in (Stenn et al., 1999)). As these arise from the stem cells, the clock is therefore hypothesised to be centred in the epithelial stem cells of the HF. The signal for anagen initiation is postulated to arise from the release of an inhibitor and the signal is then carried by a "special" communication between neighbouring epithelial cells. The role of the mesenchymal portion in this explanation is minimal. It is suggested that there is signalling between the mesenchyme and epithelium and that the inhibitory signal arises from the epithelium to the mesenchyme. Stenn then explains HF growth as a mechanical spring that is under inhibitory control. The inhibitory control is likened to a clamp on the spring, and release of this occurs in order for anagen to commence. The nature of what the "special" communication between epithelial cells is not expanded upon here. It is also not clear why only the epithelium is the controller in the HF, particularly when stated by the author himself that the mesenchyme is known to be important. There are parallels draw by Stenn (Stenn in (Stenn et al., 1999)) with Chase's inhibitor release mechanism (Chase, 1954).

2.6.1.3 Resonance theory

Nixon postulates that the hair cycle arises from the tissue as a whole rather than one compartment or cell type that initiates the rhythm of the hair cycle (Nixon in (Stenn et al., 1999)). This has been coined the "Resonance theory" (Stenn and Paus, 2001). Nixon states that the "clock" responsible for the hair cycle may not be located in one place, but arises from the tissue as a whole. Nixon draws upon the well-known pattern formation reaction-diffusion mechanisms and suggests that spatio-temporal oscillations of "morphogen" molecules in the HF set up the changes that occur during the hair cycle. This may be considered a systems biology viewpoint of the hair cycle mechanism (see Chapter 3). The property described as "resonance" by Nixon could be considered as "emergence"; the behaviour that exists when a system is whole and not apparent when the system of interest is taken apart (Huang and Wikswo, 2006).

2.6.1.4 Quartz alarm clock theory

In another postulated theory of the hair cycle, the hair cycle mechanism is suggested to be analogous to an alarm clock (McKay in (Stenn et al., 1999)). An impulse initiates oscillations of the clock and causes the hands to move. Once a trigger is reached the alarm is tripped and this co-ordinates the dissemination of the signal to the surrounding tissue. The author states that this analogy is useful for hypothesis building to aid the thought process into thinking about what the timing mechanism may be within the HF. This has some commonality with the HCC theory below. The offer of how the hair cycle mechanism is controlled is that the alarm trips and the clock moves from telogen into anagen.

This argument thus leads one to predict that a counting mechanism should exist during telogen to allow for the trigger to be tripped. What exactly this may be is not stated for certain, but the author suggests that this may be several things such as accumulation of glucose or the process of shortening of telomers. In addition, the author hints at photoperiod systems involving melatonin also being involved in hair cycling (McKay in (Stenn et al., 1999)). Unfortunately, these processes are not further explored in the explanation. The theory fails to suggest either what the initiating stimulus for the clock to commence oscillations may be, or what the different phases such as anagen-catagen transition are controlled by. There is also no clear explanation as to what exactly the "quartz chip" is within the HF anatomy (Paus and Foitzik, 2004).

2.6.1.5 Morphogenesis theory

In another theory of the hair cycle Jahoda suggests that the "HCC" is established during morphogenesis (Jahoda in (Stenn et al., 1999)). The cyclical nature of the hair cycle is thought to have arisen as an evolutionary result of being capable to regenerate after damage; similar to a regenerating limb in amphibians. Therefore the "clock" driving the hair cycle has been set since morphogenesis. However, there is no explanation as to what the nature of this mechanism is in the proposed theory. Jahoda's theory stands as a contrast to that of both Stenn and Paus (Stenn et al., 1999) who draw a distinction between the process

governing morphogenesis, coined the "morphogenesis clock" (Paus et al., 1999a) and the controls governing the cyclical regeneration of the mature HF: the "HCC". Jahoda supports his proposed morphogenesis theory by stating that rat vibrassae HFs cycle with a pattern that mirrors their sequential embryological appearance in the skin. Although it remains unclear which school of thought is right, in the human hair cycle, it is apparent that the cyclical behaviour of populations of adult HFs differs strikingly after the neonatal period, with previously synchronised HF cycling becoming mosaic (or asynchronous) (Barth, 1987).

2.6.1.6 Bulge activation theory

The bulge activation theory was proposed after epithelial stem cells were localised to the bulge region of the HF experimentally (Cotsarelis et al., 1990). It was previously thought that the matrix cells located in the hair bulb were stem cells prior to this work. The bulge activation theory states that the DP stimulates the stem cells at the end of telogen or the beginning of anagen. This stimulates the proliferation of stem cells which then produce the hair germ and leads to growth of the lower HF. This causes the DP and bulge to no longer be in proximal contact and the authors suggest that this causes the stem cells to return to a less active, slowly dividing state. Another key component suggested by the authors is that during mid-anagen MKs stimulate DP fibroblasts to proliferate. This is supported by experimental evidence of proliferation occurring in the DP in anagen VI and also that MK proliferation precedes events in surrounding mesenchymal HF cells such as the growth of surrounding vasculature. They suggest that this burst of proliferation is key during the hair cycle to ensure the large size of the DP which determines the hair shaft width and bulb size (Cotsarelis et al., 1990). The third essential component of the hair cycle, as detailed in the bulge activation hypothesis, is that MKs determine the length of anagen as they proliferate with a finite duration and this property also explains why anagen length is not easily perturbed (Ebling 1976). The last property essential to the bulge activation theory is the process of upward movement of the DP during catagen as this allows the proximity of the DP to the

bulge and thus activation of stem cells to occur. The authors explicitly note that the activating factor(s) from the DP that stimulates the stem cells is not known, but they postulate that it may be growth factors or cell-cell contact.

The bulge activation theory (Sun et al., 1991) provides a well-constructed account of the possible communication set up between compartments of the HF during the cycle. Spatio-temporal considerations are incorporated into the theory, namely allowing for the altering structure of the HF and thus the changes in proximity of the stem cell population to the DP. This sets up an anatomically orientated account of the control set up within the hair cycle and the theory is supported and inspired by experimental evidence. Indeed, stem cells are the source of cells for reconstruction of the HF during each cycle (Cotsarelis, 2006). As pointed out by the authors, the nature of the "activator(s)" of the stem cells from the DP is not known. In addition, what is the determinant of the proliferative burst seen in mid-anagen of DP fibroblasts and what is the nature of the activation of DP cells by the MKs during anagen? Also, what causes the MKs to cease proliferation at the end of anagen?

Although the bulge activation theory provides a detailed explanation of events that occur during the hair cycle, with some details of direction and timing of "controls" for example by stating that DP activates stem cells at the end of telogen and MKs stimulate DPs in mid-anagen, it is not clear how these events happen to culminate at this point. Also, this theory has been criticised for being unable to convincingly explain all the catagen-associated transformation processes, including HF keratinocyte and HF melanocyte apoptosis, HF basement membrane shrinkage and massive remodelling of the HF mesenchyme (Paus and Foitzik, 2004). The spatio-temporal incorporation of events seems to be a very important aspect of the hair cycle mechanism and is not explicitly adopted by the other theories. There is good evidence of proliferation and changes in stem cell dynamics during the hair cycle. This concept of bulge activation is also very much supported by recent work regarding stem cells, transient amplifying cells and the relationship between these in the HF and during the hair cycle (Hsu et al., 2011). However, the theory

would require to be tested by checking for activation molecules or processes at the points suggested by Cotsarelis and colleagues (Cotsarelis et al., 1990).

2.6.1.7 Papilla morphogen theory

The last theory that we shall discuss in this section is the papilla morphogen theory (Paus and Foitzik, 2004, Paus et al., 1999a, Stenn et al., 1999). The authors involved in the "papilla morphogen" (PM) theory addressed the control of the hair cycle from a distinctive perspective. There was a drive by these colleagues to fully address the need to understand the hair cycle mechanism. By constructing a hypothesis, just as Chase had postulated, and building a theory of the process this would enable clear, hypothesis-driven hair research (Paus et al., 1999a, Paus and Foitzik, 2004, Stenn et al., 1999).

Firstly, when considering the PM theory for the hair cycle, the authors immediately draw upon other chronobiological timing mechanisms and bring the hair cycle mechanism into this context. The hair cycle is firstly likened to a clock and the term "hair cycle clock" to describe the core control mechanism of the hair cycle was coined (Paus et al., 1999a). In this theory, the HCC is thought to have at its centre an oscillator system responsible for the process. The DP is identified as the core component of this suggested theory for the hair cycle control. This is argued to be the case as the DP is necessary for the hair cycle to occur at all: its inductive properties *in vivo* and that it determines the width and size of the hair shaft.

The theory states that the DP fibroblasts secrete PMs exclusively during the G0 and G1 phases of the cell cycle (Paus et al., 1999a, Paus and Foitzik, 2004). Anagen is initiated when the level of PMs exceeds a threshold level. The presence of PM is suggested to be necessary for the initiation and maintenance of anagen. The peak expression of PM occurs at the end of anagen. The PMs are suggested to alter signalling mechanisms that have been postulated to be essential to the mechanism of the hair cycle process. Catagen is heralded by a sudden drop in PM levels below a defined threshold. This arises when the DP fibroblasts enter the S, G2 and M phases of the cell cycle as they are no longer in the secretory phase. It is suggested that the lack of PM causes intra-follicular

apoptosis and all other signalling cascades that are associated with the anagen-catagen transformation, such as termination of melanogenesis, deletion of the HF pigmentary unit, and remodelling of the HF mesenchyme. Anagen re-initiates when the DP cells re-enter G0/G1 and, thus, PM levels reach the threshold level again (Figure 2.4).

In order for PM secretion to be maintained during the long phase of anagen, it is suggested in this theory that only a selection of the fibroblasts are proliferating at once and this crescendos with the greatest level occurring at the end of anagen. Along with the cyclical secretion of PM in line with the cell cycle of DP fibroblasts, this theory also suggests that an "inhibition-disinhibition" system is involved in the hair cycle control. Therefore, also secreted in anti-phase to the papilla morphogens are mitosis inhibitors or "endogenous mitotic inhibitors". These reach peak levels when PMs are commencing their decline in catagen. It is suggested that these may arise from the epithelial HF in response to the PMs.

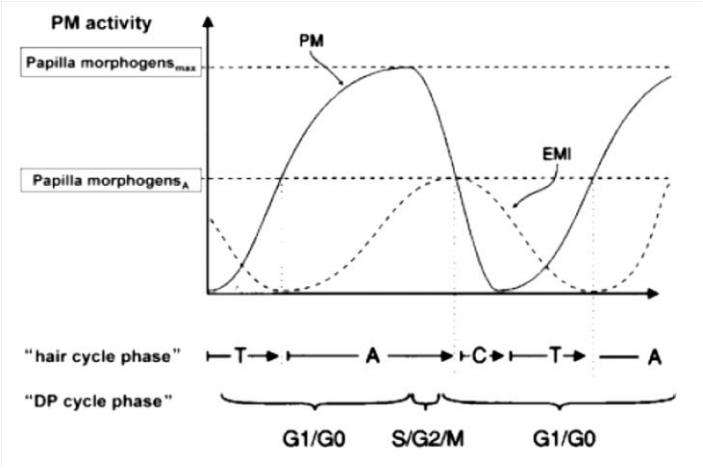

Figure 2.4: The papilla morphogen theory

The figure shows the changes of papilla morphogen and endogenous mitotic inhibitor levels in terms of hair cycle stages and dermal papilla cell cycle stages. PM=papilla morphogen, PM_A/PM_{max} = half maximal and maximum level of PM. EMI=endogenous mitotic inhibitor, DP=dermal papilla, T=Telogen, A= anagen, C= catagen. Figure reproduced with permission from (Paus and Foitzik, 2004).

PM levels should be high in telogen skin, i.e. when hair growth is suppressed. In fact, limited experimental support for this theory has been provided by the demonstration that telogen, but not anagen, epidermis contains

a potent anti-mitotic activity that inhibits anagen development in mice (Paus et al., 1990). Signalling loops are thought to be present between the epithelium and mesenchyme driven by cyclical PM secretion. The inhibition-disinhibition concept is incorporated in the form of anti-phase expression to the papilla morphogens in this theory (Chase, 1954). In addition, the involvement of both the epithelium and mesenchyme is included.

Unfortunately, this theory conflicts with the fact that DP fibroblasts are not known to enter into the cell cycle at the time that has been suggested (i.e. anagen VI) (Paus and Foitzik, 2004). Nevertheless, the exercise in constructing the theory produced a testable hypothesis. Also, as argued by Jahoda (in (Stenn et al., 1999)), it remains possible that PM secretion by DP fibroblasts shows some form of cell cycle-linkage, yet without DP fibroblasts entering mitosis. Positively, the authors identify the need for theoretical consideration of how the hair cycle arises as they realise the importance of this. It brings forward the field by taking a detailed approach to the problem. This is also evident by the production of a thorough discussion and analysis of what the salient features are necessary to be addressed in a theory of the "HCC" (Paus et al., 1999a). The process adopted in trying to answer the question as to the nature of the hair cycle rhythm has been pioneering for the field.

On the negative, this theory tries to identify one region as being the HCC "command centre" (Paus and Foitzik, 2004, Paus et al., 1999a). Whilst this theory does incorporate the epithelial compartment more fully than other theories, the emphasis is placed on the DP as the coordinator. In addition, it is not known that if DP fibroblasts take turns in entering the cell cycle whether the necessary threshold of PMs would be reached. It is difficult to state whether the complex communication set up of inhibitory and excitatory loops detailed by the authors would behave in this way in reality without testing it, for example via mathematical modelling. This critique, however, holds for all the theories postulated above. A positive feature of the theory is that it is unique in that it focuses on the control of catagen as an essential component of the HCC. In addition, it gives a self-perpetuating explanation for the HCC.

In the construction of the "Papilla Morphogen Theory" there was drive for the conceptualisation of the hair cycle mechanism and to determine what exactly a theory of the hair cycle should contain. In addition, the hair cycle is explicitly treated as a chronobiological rhythm. This theory is also unique in that the authors state that the hair cycle needs to be understood from the initiation of catagen rather than the initiation of anagen, whereas the other theories approach the problem from the initiation of anagen.

2.6.1.8 Perspective on the current theories of the hair cycle

A criticism of the current theories of the human hair cycle is that the majority of the theories aim to locate a cell type or region as being the controller of the hair cycle. However, it may be possible for there to be multiple regions involved; in particular regarding the complex multi-cellular composition of the HF. This is the essence of the argument provided in the Resonance Theory (Nixon in (Stenn et al., 1999)). In order for hair cycling to occur, it is apparent that there requires the communication to exist between the epithelial portion of the HF and the mesenchymal HF (Botchkarev and Kishimoto, 2003). This is supported by various studies that have shown the abrogation of the DP stops hair cycling (Stenn and Paus, 2001, Link et al., 1990).

All of the theories manage to incorporate features that the authors feel are essential to the hair cycle. From the summaries and critiques of these theories, it is apparent that there is some discrepancy between individual researchers with respect to the features of HF cycling that are thought salient. The majority of theories are concerned with the control of anagen initiation, although a distinction was drawn between the completion of morphogenesis, which ends in an anagen-like stage, but must not be confused with anagen (Müller-Röver et al., 2001, Paus et al., 1999b). It has been postulated that the anagen-catagen transformation is more important for understanding the control of HF cycling, since at least morphologically, the hair cycle does not commence with anagen, but with catagen (Paus and Foitzik, 2004, Stenn and Paus, 2001).

This literature review shows that the control of HF cycling is a complex issue and that none of the previously proposed theories provide a rigorous, fully

satisfactory explanation for the "HCC". Moreover, none of these hair cycle theories have been tested using mathematical modelling. Given the complexity of the process and the numerous molecular players that are already known to be involved in its regulation (Stenn and Paus, 2001, Schneider et al., 2009) it appears almost mandatory to take a systems biology approach to understanding the regulated, rhythmic changes in HF function during the hair cycle. This is further explored and argued below (see Chapter 3).

2.6.2 Molecular candidates in the human hair cycle

Numerous molecules have been implicated in mediating the hair cycle. See (Schneider et al., 2009, Botchkarev and Kishimoto, 2003, Botchkarev and Paus, 2003, Rendl et al., 2005, Stenn et al., 1994) for comprehensive overviews of the topic. Here, key methods adopted in experimental investigation of the hair cycle are provided and selected molecular candidates for controlling the anagen-to-catagen transition are reviewed. The applicability of these findings to our interest in the human hair cycle is also considered further. More literature reviews are found in the introduction and discussion sections of each manuscript chapter following.

2.6.2.1 Methods of investigating the human hair cycle

The understanding of hair growth and hair cycling has been advanced by the development of molecular biology techniques. In particular, animal models of hair disorders arising via spontaneous or induced mutations have been a central method for advancing the functional roles of genes and their products in hair growth and cycling (Rogers and Hynd, 2001, Stenn and Paus, 2001, Stenn et al., 1994). The murine model remains the most commonly used in hair research with the C5BL/6 type exhibiting colour differences in accordance to the hair cycle stage, thus allowing a readily accessible hair cycle study tool (Rogers and Hynd, 2001, Stenn and Paus, 2001).

With regards to understanding the human hair cycle specifically, HF organ culture, which was developed by Philpott (1990), is a well established laboratory method used to study human HF biology and hair growth without

the need to experiment on human subjects (Randall et al., 2003, Rogers and Hynd, 2001, Kloepper et al., 2010). The ability of human HFs to grow at rates in culture that are almost the same as *in vivo* makes this experimental model useful for the study of hair growth and for investigating the response of human scalp HFs to test compounds added to the organ culture medium (Philpott et al., 1994a, Rogers and Hynd, 2001, Kloepper et al., 2010).

There are several advantages to human HF organ culture as opposed to fresh whole tissue analysis in the study of anagen and catagen HFs. For example, the occurrence rate of telogen and catagen HFs (5-10%) *in vivo* is very low compared to that of anagen HFs (90-95%) (Whiting, 2004). Organ culture allows access to a greater number of catagen HFs as they enter this stage within a few days in culture (Kloepper et al., 2010, Rogers and Hynd, 2001). As mentioned in the hair disorders section, understanding the anagen-catagen transition is of importance in hair disorders and therefore, this provides an instructive assay for investigating anagen-to-catagen transition *in vitro*.

However, it is important to note that extra-follicular surroundings are likely to facilitate and modulate HF cycling. It is known, for example, that human scalp HFs grow in follicular units and that there is better growth of HFs when they are transplanted as a whole unit rather than following separation (Jimenez and Ruifernández, 1999, Avram, 2006). A follicular unit consists of 1 to 4 HFs and therefore one isolated HF, maintained in a well with 2 additional HFs may be a good approximate model for the *in vivo* follicular unit. Also, from studies of murine hair cycle waves, there is increasing appreciation of important extra-follicular inputs that impact within the skin on HF cycling (Plikus et al., 2008, Plikus et al., 2011). In addition, neural inputs into HF cycling, which are also absent in human HF organ culture, must be considered, since the HF is one of the most densely innervated peripheral structures in the mammalian body (Peters et al., 2007, Peters et al., 2006, Botchkarev et al., 2004).

2.6.2.2 Molecular candidates of the hair cycle clock: anagen-to-catagen transition

Numerous candidates have been implicated in regulating the hair cycle. In this section only a few key candidates have been chosen to be discussed. These have been selected as those that affect timing of the hair cycle and anagen to catagen transition.

Insulin-like growth factor-1 (IGF-1) has been identified as a promoter of the anagen phase of the hair cycle. Growth of microdissected human scalp HFs has been shown to be stimulated by the addition of IGF-1 to culture medium and its withdrawal causes HFs to enter catagen (Philpott et al., 1994b). In-situ hybridisation and immunohistochemistry analyses of human skin has shown that IGF-receptor (IGF-R) mRNA and protein is down-regulated during the initiation of catagen, although these changes have not been quantified (Rudman et al., 1997).

The *Fuzzy* phenotype exhibits accelerated hair cycling in mice with reduced proliferation and increased apoptosis of MKs (Mecklenburg et al., 2005). This phenotype has been attributed to a mutation in *Sgk3* (Campagna et al., 2008). Lack of the *Sgk3* gene in mutant mice resulted in impaired maintenance of transiently amplifying matrix cells of the HF (Alonso et al., 2005, Okada et al., 2006). In addition, *Sgk3*-null mice exhibit accelerated hair cycling characterised by a shortened anagen phase and normal catagen and telogen phases (Alonso et al., 2005, Okada et al., 2006). This implicates *Sgk3* as a possible "time-keeper" for the anagen phase in the murine hair cycle. The evidence regarding *Sgk3* and the anagen to catagen transition has been reported in mice experiments. To date, *Sgk3* has not been explored in the human hair cycle.

Another growth factor implicated in the anagen to catagen transition of the hair cycle is hepatocyte growth factor (HGF) which has been investigated in both mice and man (Jindo et al., 1998, Jindo et al., 1995, Lindner et al., 2000). Human scalp HF growth was found to be promoted after the addition of HGF at several concentrations to the media during organ culture. The growth increased

in a dose-related manner when compared to the control group (n=6 in each group). DNA synthesis was also increased in the HGF-treated groups (Jindo et al., 1995). No other parameters, such as hair cycle parameters, were investigated in scalp HFs after HGF treatment.

The expression pattern of HGF in HFs of C5BL/6 mice was found to be hair cycle dependent with HGF protein and gene expressed during anagen and down-regulated in catagen. HGF protein was found to be localised only to the DP of the mice HFs and its receptor Met localised in the follicular epithelium (Jindo et al., 1998). Injection of recombinant HGF in the dorsal skin of C5BL/6 mice, prior to spontaneous catagen onset, caused significant retardation of catagen in the HFs at the site of injection with a gradient effect seen on the periphery of the injection sites (Jindo et al., 1998). The expression profile of HGF in human HFs during the hair cycle is yet to be elicited.

Fibroblast growth factor 5 (*Fgf5*) has been found to induce catagen. Deletion of the *Fgf5* gene causes delayed onset in catagen, prolonged anagen, and produces *angora* phenotype mice which exhibit long hairs with no defect in HF structure (Hebert et al., 1994). In normal mice, total *Fgf-5* mRNA was found to be expressed in the ORS of the HF with expression highest during late anagen (Kawano et al., 2005, Hebert et al., 1994, Rosenquist and Martin, 1996). The splice variant of *Fgf-5*, *Fgf-5S*, blocks the catagen-inducing properties of the complete *Fgf-5* transcript. *Fgf-5S* is expressed in high concentrations during mid anagen and low concentrations during late anagen VI, catagen and telogen. The two variants of *Fgf-5*act together and it seems that communication with the DP may play a role in their function (Suzuki et al., 2000). The importance of *Fgf-5* as a candidate in the anagen to catagen transition is highlighted in the work by Pena *et al* where a short hair phenotype of *Bcl-*x_L transgenic mice was reversed in *Fgf-5* deficient mice (Pena et al., 1999).

Other agents found to promote catagen are neurotrophins (NTs). Multiple members of the NT family have been found to be up regulated in the proximal HF in late anagen and prior to catagen. Neurotrophin receptors have been shown to be expressed in the epidermal keratinocytes of the follicle and also the DP during the anagen to catagen transition (Botchkarev et al., 1998a).

In addition, NT-3 and brain-derived neurotrophic factor (*BDNF*) transgenic mice exhibit premature catagen entry and over-expression of *BDNF* causes shortened hair length; a hallmark of an abrogated anagen phase (Botchkarev et al., 1999b, Botchkarev et al., 1998b).

The transforming growth factor-β (TGFβ)/Bone morphogenetic Protein (BMP) superfamily, consisting of cytokines and growth factors, is thought to be central in the modulation of the hair cycle and notably in the anagen to catagen transition. Transforming Growth Factor-β1 (TGF-β1) inhibits keratinocyte proliferation, induces keratinocyte apoptosis and causes premature catagen entry in isolated human HFs and *in vivo* in murine skin (Soma et al., 2002, Philpott et al., 1994a, Foitzik et al., 2000). TGF-β1 is most highly expressed during late anagen and early catagen in murine experiments (Foitzik et al., 2000). Transforming Growth Factor-β2 (TGF-β2) has also been shown in both mice and man to be a potent catagen inducer. TGF-β1 and TGF-β2 have been localised to the IRS, ORS and CTS of HFs (Soma et al., 2002) and the TGF-β receptors type I and II are expressed in the IRS, ORS and MKs (Paus et al., 1997).

Bone morphogenetic proteins (BMPs) are growth factors whose potent antagonist is noggin. Noggin is known to be mesenchymally derived (Botchkarev et al., 1999a) and acts by binding to BMPs and preventing them from binding to their receptor (Zimmerman et al., 1996). BMPs exert both pro- and anti-apoptotic effects; the pro-apoptotic action of BMPs is mediated by the BMP–MAPK pathway, while the BMP–Smad pathway is implicated in the control of survival (Botchkarev and Paus, 2003). The expression patterns for BMPs, noggin, and BMP receptors in the HF during catagen remain to be elucidated, though data obtained in genetic models suggest a role for BMP signaling in the control of catagen development. Deletion of BMP receptor IA (*BMPR1A*) in HF keratinocytes is accompanied by a markedly delayed entry of the HFs into first catagen (Andl et al., 2004) suggesting the involvement of BMPR1A in the control of the anagen–catagen transition. In addition, BMPs have been shown to have a functional relationship in the murine hair cycle with WNTs (Plikus et al., 2008) exhibiting rhythmical expression of BMP2 and 4 in an asynchronous phase to noggin and β-catenin expression.

In wild-type murine HFs, catagen is accompanied by changes in follicle morphology, including cessation in matrix cell proliferation and apoptosis in the hair bulb. However, in muscle segment homebox2 (*Msx2)* deficient HFs, these events are uncoupled (Ma et al., 2003). There is precocious onset of catagen in *Msx2* knockout mice and this suggests that *Msx2* normally plays a role in maintaining HFs in anagen (Ma et al., 2003). BMPs have been implicated in hair shaft-regulation via a link with *Msx2* as *BmpR1A* mutant HFs exhibit absent or severely decreased expression of the hair-shaft regulatory gene *Msx2* (Andl et al., 2004) thus suggesting that BMPs are upstream of *Msx2*.

Novel candidates have been suggested as hair cycle controllers by time-course gene expression profiling experiments in mice (Lin et al., 2004, Lin et al., 2009). By clustering gene expression profiles by their pattern of expression during the murine hair cycle and subsequently grouping results by their function, novel candidates for regulators of the hair cycle were identified. Circadian genes (those responsible for the circadian rhythm, see Chapter 7 for details) were found to show a hair cycle-dependent oscillatory behaviour in mice (Lin et al., 2009). These novel candidates are thought to mediate their effect by cell cycle mediation as *BMAL1* knockout mice exhibited delayed anagen onset and significant up regulation of p21, which indicates a block at the G1 phase of the cell cycle (Lin et al., 2009). The effect was found mainly during the telogen to anagen transition, however, large oscillations in *Period1* expression, for example, were also noted (but not further investigated) during the anagen to catagen transition (Lin et al., 2009). Circadian genes are thus rather novel candidates for the HCC and have been only briefly studied in the human system.

Circadian genes, thus, are novel and intriguing candidates as components of the "HCC", which have not yet been systematically studied in the human HF. Chapter 7 is concerned with circadian genes and proteins as possible co-ordinators of human hair cycling, and argues why such a chronobiological focus on the problem of human HF cycling is particularly promising, both from a systems biology and from a clinical perspective.

The evidence above relies heavily on murine data, with little or no parallel investigations performed on human HFs. The literature above points

towards several molecules that may coordinate the human hair cycle, however, we do not yet know whether this is the case in the human system.

2.6.2.3 Epithelial-mesenchymal interactions in the control of the hair cycle

The mature HF can be divided into the mesenchymal HF, consisting of the DP and CTS, and the epithelial HF (the remaining portions; including transient amplifying cells of the hair matrix that envelope the DP, hair shaft, IRS and ORS) (Figure 2.1). The communication between epithelium and mesenchyme is vital for understanding the cycling of the HF (Tobin et al., 2003, Paus et al., 1999a, Stenn and Paus, 2001, Rendl et al., 2005, Fuchs et al., 2001, Botchkarev and Kishimoto, 2003). The destruction of the DP, for example, has been shown to cause an inability for hair fibre growth (Cohen, 1961). DP cells in culture have been found to secrete morphogens that stimulate epithelial cells, supporting the notion that the DP cells act to mediate the epithelial compartment of the HF (Rogers and Hynd, 2001). DP cells have been found to exhibit their own molecular signature in comparison to their surrounding cells; the matrix and ORS cells. These contrasting signatures for signalling and transcriptional regulators may be essential for HF biology (Rendl et al., 2005, Botchkarev and Kishimoto, 2003).

During catagen onset, there is down-regulation of factors promoting matrix cell proliferation and differentiation. As described above, promoters of anagen, such as IGF-1 and HGF are secreted by DP fibroblasts and stimulate the matrix cells, of epithelial compartment to proliferate and differentiate (Philpott et al., 1994b, Rudman et al., 1997, Lindner et al., 2000, Jindo et al., 1998, Itami et al., 1995, Shimaoka et al., 1995). HGF is known to function as an important mediator in epithelial-mesenchymal interactions in several systems and has been shown to be expressed solely in the DP and its receptor Met found only in the HF epithelium (Lindner et al., 2000). The interaction of the epithelial and mesenchymal HF is required for HGF-mediated HF growth. FGF-5 is expressed

in the ORS during late anagen and has been suggested to induce catagen by diffusion into the DP (Rosenquist and Martin, 1996). Another example of epithelial-mesenchymal interaction in the HF is that of BMP2, BMP4 and noggin (Kulessa et al., 2000, Plikus et al., 2008). There is evidence that BMP2, BMP4 and noggin exhibit a BMP activity gradient in the HF (Kulessa et al., 2000).

Thus the communication between HF epithelium and mesenchyme is crucial to hair cycle control, and we need to understand the exact mechanisms of these interactions in order to fully grasp the nature of the dynamic regulatory processes that underlie HF cycling.

2.7 SUMMARY: THE BASIS OF THE THESIS

In the hair cycle the HF exhibits a unique chronobiological rhythm, vast regenerative capacity, intricate communication between epidermal and mesenchymal-derived cells and dynamic spatio-temporal behaviour at the cellular and tissue level (Paus et al., 1999a, Schneider et al., 2009).

There is still debate as to what comprises the so-called "HCC". None of the "verbal" hair cycle theories published so far have been tested using mathematical modelling; therefore these models may not predict correctly the effect of certain feedback mechanisms or connections.

On the molecular level, animal models have been central to advancing hair cycling research (Rogers and Hynd, 2001, Schneider et al., 2009). Murine systems such as *balding*, *nude*, *hairless* and *angora* display defects in HF formation and/or cycling through naturally occurring mutations. In addition to spontaneous mutant models, the use of transgenic and knockout mice has allowed further studies of the effect of genetic perturbations on hair cycling (Rogers and Hynd, 2001, Stenn and Paus, 2001, Schneider et al., 2009).

Although numerous molecular pathways have been implicated in the control of HF cycling, the underlying mechanisms regulating its timing remain elusive. Namely, a fully satisfactory theory of HF cycling remains to be

developed, and the molecular nature of the "HCC" has still not been deciphered (Paus and Foitzik, 2004, Paus et al., 1999a, Schneider et al., 2009).

The majority of research has relied on the murine model with gene expression and molecular signatures delineated in line with distinct hair cycle time points (Lin et al., 2004, Schneider et al., 2009, Lin et al., 2009, Rendl et al., 2008). In contrast, the gene and protein expression profile of different stages of human HF cycling remains to be systematically defined. An experimental window exists to study human HFs as they can be isolated from skin and maintained in serum-free medium where they subsequently transit spontaneously from anagen to catagen before degenerating (Randall et al., 2003, Rogers and Hynd, 2001, Philpott et al., 1994a, Kloepper et al., 2010). Fortunately, this hair cycle window is also the clinically most relevant hair cycle switch, whose disturbance underlies most the of the hair growth disorders seen in clinical practice (Paus and Foitzik, 2004).

In light of the above evidence and considerations, it is apparent that there is a disjoint between the phenomena observed at the tissue level and investigations performed at the molecular level. In addition, much of the molecular investigations are performed in rodent species as they allow the study of the whole hair cycle and provide an excellent tool for employing the full power of mouse genomics research. Evidently, it is quite uncertain to what extent the molecular controls of murine HF cycling correspond to those that drive the human hair cycle.

The first basic tenet of the current thesis is that a systems biology approach to human HF cycling holds great promise to make substantial progress in reaching the ultimate goal, i.e. to understand the human "HCC" and to obtain novel pointers as to how it may be therapeutically manipulated more effectively. The above considerations will lead to the exploration of human HF cycling from a systems biology perspective with the focus directed to three key areas a) mathematical modelling, b) HF chronobiology, and c) gene expression profiling.

3 CHAPTER 3: THE CYCLING HAIR FOLLICLE AS AN IDEAL SYSTEMS BIOLOGY RESEARCH MODEL

Authors: **Y. Al-Nuaimi**, G. Baier, R.E. Watson, C.M. Chuong, R. Paus

This is in the format submitted and published in *Experimental Dermatology* 2010

3.1 ABSTRACT

In the post-genomic era, systems biology has rapidly emerged as an exciting field predicted to enhance the molecular understanding of complex biological systems by the use of quantitative experimental and mathematical approaches. Systems biology studies how the components of a biological system (e.g. genes, transcripts, proteins, metabolites) interact to bring about defined biological function or dysfunction. Living systems may be divided into five dimensions of complexity: 1) molecular 2) structural 3) temporal 4) abstraction and emergence and 5) algorithmic. Understanding the details of these dimensions in living systems is the challenge that systems biology approaches aim to address.

Here, we argue that the hair follicle (HF), one of the signature features of mammals, is a perfect and clinically relevant model for systems biology research. The HF represents a stem cell-rich, essentially autonomous mini-organ, whose cyclic transformations follow a hypothetical intra-follicular "hair cycle clock" (HCC). This prototypic neuroectodermal-mesodermal interaction system, at the cross-roads of systems and chronobiology, encompasses various levels of complexity as it is subject to both intra- and extra-follicular inputs (e.g. intra-cutaneous timing mechanisms with neural and systemic stimuli). Exploring how the cycling HF addresses the five dimensions of living systems, we argue that a systems biology approach to the study of hair growth and cycling, in man and mice, has great translational medicine potential. Namely, the easily accessible human HF invites preclinical and clinical testing of novel hypotheses generated with this approach

3.2 INTRODUCTION

"The problem of biology is not to stand aghast at the complexity but to conquer it"

Sidney Brenner, Nobel Laureate (Duncan, 2004)

Systems biology is a fast-evolving life sciences field that aims to establish how the components of a living system combine to cause function (Klipp et al., 2009, 2007). Biological systems can be divided into five levels of complexity: 1) molecular; 2) structural; 3) temporal; 4) abstraction and emergence and 5) algorithmic (Table 3.1) (Huang and Wikswo, 2006).

In the past, cell cultures (particularly yeast) were often used in systems biology research to handle the complexity of living systems (Westerhoff and Palsson, 2004, Bruggeman and Westerhoff, 2006, Sauer et al., 2007, Di Ventura et al., 2006, Klipp et al., 2009). These models are far-removed from the reality of mammalian organisms. Identifying mammalian models that are sufficiently complex to encompass these five dimensions, and approach physiological relevance is an important challenge for systems biology (Klipp et al., 2009, Makarow et al., 2008).

The HF consists of multiple different cell populations of neural crest, ectodermal or mesodermal origin, which are distinct in their location, function and gene and protein expression characteristics (Fuchs, 1998, Schneider et al., 2009, Stenn and Paus, 2001, Paus and Cotsarelis, 1999). Additionally, the HF is a uniquely dynamic mini-organ that undergoes continuous cycling throughout adult life during which elements of its own morphogenesis are recapitulated (Schneider et al., 2009, Fuchs et al., 2001) (Figure 2.2). This process may arise under the dictates of an enigmatic oscillator system (the hair cycle clock (HCC)) (Paus and Foitzik, 2004, Lin et al., 2009, Stenn and Paus, 2001). Hair growth disorders can be attributed, at large, to changes in the normal dynamic behaviour of the HF (Paus and Cotsarelis, 1999, Hadshiew et al., 2004, Paus and Foitzik, 2004, Stenn and Paus, 2001, Cotsarelis and Millar, 2001). Common hair

diseases such as alopecia areata, telogen effluvium, hirsutism and hypertrichosis remain major, unsolved medical problems that call for new approaches in developing effective remedies. The HF is an attractive research model as hair growth; cycling and colour are of profound interest to biological and medical researchers and a vast industry that caters to individuals who wish to manipulate these parameters. The study of HF cycling brings together systems biology, stem cell biology, regenerative medicine, chronobiology and translational medicine (Ito et al., 2004, Yu et al., 2008, Lin et al., 2009, Batista et al., 2007).

Induction, spacing, orientation and morphogenesis of the HF (Schmidt-Ullrich and Paus, 2005) represent classical scenarios of developmental and stem cell systems biology (MacArthur et al., 2009, Vanag and Epstein, 2009, Baker et al., 2009). The hair patterning process is a prototypic neuroectodermal-mesodermal interaction system which is beautifully demonstrated by the pioneering work of Nagorcka and Mooney (Nagorcka and Mooney, 1982, Nagorcka and Mooney, 1985, Mooney and Nagorcka, 1985). Mathematical theory was utilised to explain the spatial patterns of morphogens and thus patterned HF formation. Systems biology research in HF development has been previously covered (Sick et al., 2006, Stark et al., 2007, Baker et al., 2009), therefore here we focus on the cycling adult HF as a systems biology research model.

We argue that the HF, a signature organ of the mammalian species, is optimally suited to address challenges in medical and systems biology research by studying clinically relevant biological phenomena from a comprehensive systems biology perspective.

Table 3.1: The five dimensions of living systems and hair cycle relevance

Dimension	Research objectives	Approach	Challenges	HF (HF) and hair cycle relevance
Dimension 1 **Molecular complexity**	Integrating molecules and pathways to genome-wide networks ("horizontal integration")	Molecular biology, genomics, proteomics, and other "omics," bioinformatics, *applied c*omputer science	Database integration, annotation; high-throughput analysis at higher functional levels; real-time, multiplex measurements of expression profiles	The cycling HF is governed by key molecules; exact drivers are yet to be elicited. As a research tool, the HF can be studied *in vivo* using murine model, or *in vitro* in human HFs. See Dimension 2 also.
Dimension 2 **Structural complexity**	Transcending many size-scales (nanometer to meter): Organelles–cells–tissues–organs–organism ("vertical integration")	Microscopy, nanotechnology, microfabrication, biophysics, biomedical engineering, mechanical engineering, anatomy	Visualization of dynamic protein complexes in cells; cellular compartmentalization; external sensing and actuation of molecular states; bridging the gap between macromolecules and tissues—spanning nanometer to centimetre scales	The HF can be reduced into different structural levels; from cells, to the microdissected and isolated mini-organ, to hair cycle domains, to whole organisms. It provides a mini-system with which to analyze these dimensions. In addition, the structure of the HF changes dramatically during the hair cycle (highlighting the interrelationship between molecular, structural, temporal and emergence dimensions involved in the cycling HF).

Table 3.1 Continued: The five dimensions of living systems and hair cycle relevance

Dimension	Research objectives	Approach	Challenges	Hair follicle and hair cycle relevance
Dimension 3 **Temporal complexity**	Transcending many time scales (nanoseconds to gigaseconds = decades)	System dynamics, nonlinear dynamics, signal processing, biomedical engineering, control theory, time-series analysis, physiology	Noise measurement at various levels; non-linear time series analysis; multi-analyte measurements in nonequilibrium systems—spanning nanosecond to gigasecond time scales	The HF demonstrates various temporal processes and traverses various temporal scales. For example, exhibiting circadian rhythm and hair cycle changes.
Dimension 4 **Abstraction and emergence**	Modelling system-level "emergent" features	System dynamics, pattern-formation, cybernetics, complex system sciences, agent-based models, mathematics	Levels of abstraction, multiscale models and scaling; use of larger-scale effective variables to describe smaller-scale phenomena; "statistical mechanics of biology"	Use of abstraction of the hair cycle, through modelling has proved to be useful in HF cycle research and provides meaningful input to biological understanding and hypothesis generation. The HF is an emergent organ.
Dimension 5 **Algorithmic complexity**	Understanding information coding and computation by the biological medium and developing theoretical models that simulate biological systems	Theoretical computer science, information theory, electrical engineering	Identifying a core system that is computationally irreducible; new syntax for simulation; the integration of hybrid analogue/digital models	HF during cycling will compute problems in the context of the cells, tissue and organism. In addition, the complexity of the models needed to simulate the organisms' computations will need consideration.

3.3 SYSTEMS BIOLOGY IN A NUTSHELL

Systems biology is the study of how the components of a biological system (e.g. genes, transcripts, proteins, metabolites) interact to bring about function (and dysfunction) of that system (Kitano, 2002, Bruggeman and Westerhoff, 2006, Klipp et al., 2009, Di Ventura et al., 2006, Huang and Wikswo, 2006). This discipline rose in the post-genomic era as advances in molecular biology, and the production of high-throughput data such as deciphering the genome in the human genome project (Aderem, 2005, O'Malley and Dupré, 2005, Huang and Wikswo, 2006), still left a gap in our ability to translate the vast amounts of molecular knowledge to understanding biological function (Sauer et al., 2007). Understanding biological systems by a transition from reductionist study on the molecular level to the systems level of life phenomena is systems biology (Kitano, 2002, Bruggeman and Westerhoff, 2006, Noble, 2008b, Westerhoff and Palsson, 2004). In the next section, we provide further details about systems biology, emergence, mathematical modelling in systems biology and a summary of some important successes of systems biology in medical research.

3.3.1 Systems Biology and medical research

An indispensible feature of biological systems is that of emergence. Biological systems are composed of multiple interacting components and involve "communication" at various levels (Table 3.1). For example, individual enzymes do not function in isolation but act within complex pathways. The properties of these pathways *in vivo*, i.e. the systems properties, depend on the interaction of *all* the components and therefore on the molecular properties of each of the involved enzymes. Systems properties only arise in the presence of these interactions. This phenomenon is called emergence (2007, Sauer et al., 2007, Aderem, 2005).

Table 3.2: Summary table of successes of systems biology research in medical studies.

Research Problem	Approach taken	Results	References
Aim to predict the resistance to HER2-targeting receptor tyrosine kinase (RTK) inhibitors (cancer therapies)	An in vitro model of the key pathways involved was made. Predictions were then tested in vivo on human cancer patients	Key resistance factor a tumour suppressor gene (PTEN) was found using the kinetic model. PTEN levels in the clinic were related to resistance to treatment. Enabled patients to be given more personalized treatment for breast cancer.	(Faratian et al., 2009b)
To understand the cause of cardiac arrhythmias in the context of physiology of the heart. To improve drug design and reduce fatal side effects	Virtual human heart models constructed using quantitative data	Use of model led to success in predicting the side-effects of drugs, such as chronic angina medication Ranolazine	(Noble, 2008a)
Establish the dynamic behaviour of HIV virus in response to combination therapy in order to better treat HIV-AIDS	Quantitative data generated to establish the decay of HIV virus following combination therapy. Mathematical models incorporating the data predicted virus decay rates	Decay rates of the virus (both free and in infected cells) were estimated. Prediction of re-emergence of the virus (even at levels below detection) using the model enabled better understanding of the dynamics of HIV virus following therapy and better future therapy approaches	(Perelson et al., 1996, Perelson et al., 1997, Nowak et al., 1996)
To elucidate the relationship between COX inhibitor pain relief and plasma concentrations to improve and predict dose regimes for chronic pain management	A model was developed to assess the factors that correlate to response to COX inhibitors	Modelling endogenous mediators of inflammation helped to elucidate the relation between exposure to the drug and therapeutic response	(Huntjens et al., 2005)
Early studies indicated that gemcabene, a new experimental drug, did not lower lipids as much as statins. Would combination therapy make the drug commercially viable? Could modelling improve this process?	Pfizer undertook a model-based analysis to compare the lipid lowering effects of gemcabene versus ezetimibe in combination with a statin.	Modelling results indicated that gemcabene did not offer superior lipid lowering benefits to ezetimibe when used in combination with a statin. This result contributed significantly to the decision to stop development of the drug. This rapid decision-making reduced drug development time and costs may have been futile	(Mandema Jaap et al., 2005)

In systems biology, the use of mathematical modelling and computational simulation is an important tool for tackling the complex relationships existing between entities in a system (Kell, 2004, Wiley et al., 2003, Di Ventura et al., 2006, Klipp et al., 2009). Mathematical models can bring together the details of linear and non-linear processes, handle numerous variables simultaneously, deduce experimental hypotheses and qualitatively and quantitatively predict behaviour of its components and the system as a whole (Schnell et al., 2007). This iterative process between modelling and experiments is considered a hallmark of systems biology (Kitano, 2002).

Multi-factorial diseases, for example cancer, diabetes and the epilepsies, are brought about by interactions of parts creating higher-level properties or functions that would not be expected via analyses of only the individual entities (Gatenby and Maini, 2003, Faratian et al., 2009a, Schadt, 2009). In order to fully understand multi-factorial diseases they should be considered systems biology diseases (Schadt, 2009). The same argument holds for advancing understanding of normal function. Systems biology is already progressing areas such as cancer research (Faratian et al., 2009a, Faratian et al., 2009b), cell migration in malignancies, regeneration and development (Friedl and Gilmour, 2009) and stem cell dynamics (MacArthur et al., 2009) (See Table 3.2). Thus, systems biology should be considered an important approach in medical research by tackling the complexity of the human system, as shown in Table 3.1 (Faratian et al., 2009a, Gatenby and Maini, 2003, Faratian et al., 2009b, Di Ventura et al., 2006, Makarow et al., 2008, 2007, Hunter et al., 2008). Some successes of systems biology in medicine have already been reported (Table 3.2) and the challenges posed by medical problems are themselves beginning to fertilise systems biology (Makarow et al., 2008, 2007).

3.4 THE HAIR FOLLICLE AS A PROTOTYPIC SYSTEMS BIOLOGY ORGAN

HF cycling displays a number of properties that recommend it for systems biology research. The HF can be investigated at different levels that mirror the five dimensions of living systems (Table 3.1) (Huang and Wikswo, 2006). We discuss some previous studies where this has already been explored in hair cycling research.

3.4.1 Molecular complexity of the hair follicle

Despite the divergent cell types and number of molecular players that interact within a HF, the total number of HF protagonists is finite compared to larger organs. Moreover, the murine HF is among the best-characterized mammalian organs at the gene and protein level (Stenn and Paus, 2001, Rendl et al., 2005, Schneider et al., 2009).

Typically, profiling tools such as metabolomics, proteomics and genomics are used to acquire a systematic analysis of the molecular components in living systems (Huang and Wikswo, 2006). Time-course gene expression profiling of murine skin has led to the identification of novel candidates in hair cycle regulation. This method of eliciting gene expression during the hair cycle also addresses the temporal dimension of living systems (Lin et al., 2009). By clustering gene expression profiles by their pattern of expression during the murine hair cycle and subsequently grouping the clusters by gene function, novel genes and pathways have been identified as candidates in murine hair cycle control. Clock genes (those responsible for the circadian rhythm) have been demonstrated to be hair cycle-dependent and are prominently expressed in the secondary hair germ (SHG) of telogen and early anagen HFs (Panteleyev et al., 2001). *Bmal1* knock-out mice displayed retarded anagen development and lack mitotic cells in the SHG, suggesting that clock genes regulate anagen progression via their effect on the cell cycle. These findings indicate that clock genes can regulate complex non-diurnal organ transformation such as HF

cycling (Lin et al., 2009). Additionally, the systems approach used enabled novel candidates to be identified and allowed understanding of dynamic gene expression during the HF cycle.

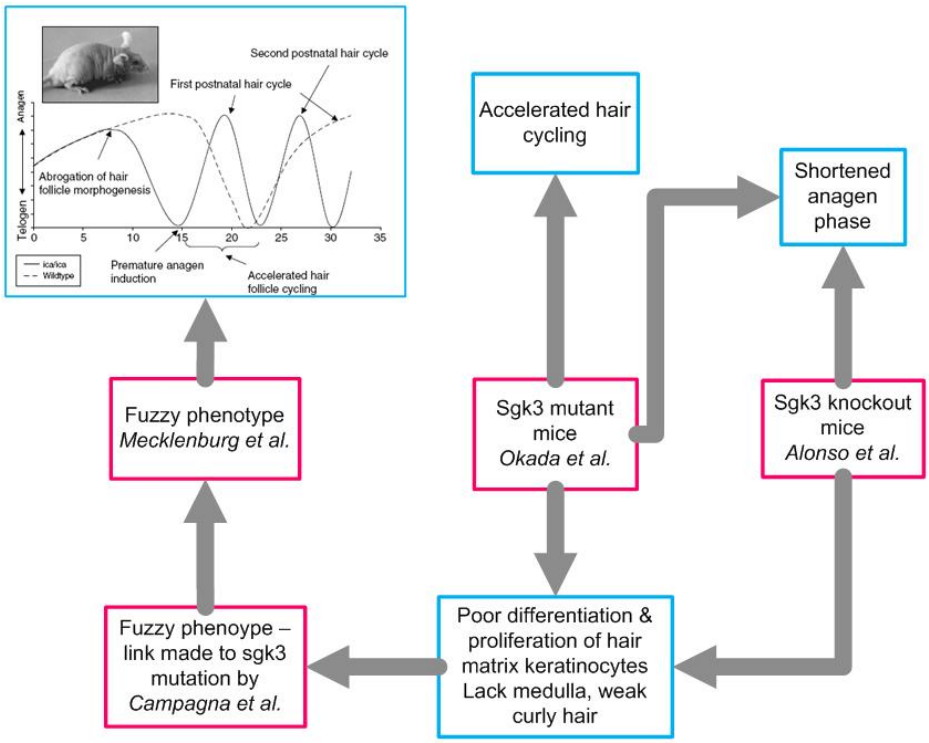

Figure 3.1: Sgk3 mutation and the hair cycle: molecular causes of Fuzzy phenotype

Schema representing the Fuzzy phenotype and the association with the Sgk3 gene mutation. Figure incorporated into the flow diagram is adapted after Mecklenburg, L., et al., Premature termination of hair follicle morphogenesis and accelerated hair follicle cycling in Iasi congenital atrichia (fzica) mice points to fuzzy as a key element of hair cycle control. Experimental Dermatology, 2005. 14(8): p. 561-70. Wiley-Blackwell Publishers

The murine model is diverse as mutations (both natural and engineered) exhibiting defined hair phenotypes can be used to probe the functional importance of molecular players *in vivo* (Schneider et al., 2009, Stenn and Paus, 2001, Schmidt-Ullrich and Paus, 2005, Nakamura et al., 2001). One example, the *fuzzy* phenotype, exhibits strikingly accelerated HF cycling which is linked to a mutation in the gene *Sgk3* (Mecklenburg et al., 2005) (see Figure 3.1). Researchers often investigate one gene or protein of interest, however,

functional overlap of hair cycle candidates (such as via common pathways) exist. For example, Figure 3.2 demonstrates how *Sgk3* and IGF-1 are functionally linked. Anagen HFs express growth factors, such as EGF and IGF-1. These growth factors activate the MAPK and Akt pathways via interacting with tyrosine kinase receptors. IGF-1 is known a catagen-inducer in human HFs *in vitro* (Philpott et al., 1994b). Alonso *et al* showed that loss of *Sgk3* was similar to gaining EGF signalling function. Using cultured primary keratinocytes from *Sgk3*-null and wild-type mice, *Sgk3* was found to negatively regulate phosphatidylinositol-3-kinase (PI3K) signalling and thus antagonise the effects of IGF-1 induced PI3K signalling (Figure 3.2). This work shows the possible function for *Sgk3* in controlling cell fate by modulating tyrosine kinase growth factor signalling pathways. Therefore, the HF exhibits interesting molecular complexity. Full comprehension of how these molecules function with regard to HF cycling would be best achieved using a systems biology approach to identify the common pathways involved and the interactions between molecules, rather than investigating these in isolation (such as those between *Sgk3* and growth factor signalling pathways). A systems biology approach aims to link overlapping pathways and function.

The use of mouse mutants (Nakamura et al., 2001, Schneider et al., 2009, Schmidt-Ullrich and Paus, 2005) represents an ideal systems biology instrument to investigate how the perturbation of a single gene product impacts on the entire HF *in vivo* (Sundberg et al., 2005). This approach can be complemented in the human system via organ-culture of micro-dissected human anagen scalp HFs and perturbing their normal behaviour *in vitro* by utilising and evaluating the impact of defined test agents on hair shaft formation, follicular melanogenesis, catagen transformation, hair MK proliferation and apoptosis and the gene expression profile (Philpott et al., 1994a, Kloepper et al., 2009, Bodo et al., 2005, Bodo et al., 2007). This naturally connects molecular complexity to its structural and temporal complexities by altering HF structure (evident in the hair cycle) and cycle duration (a temporal phenomenon).

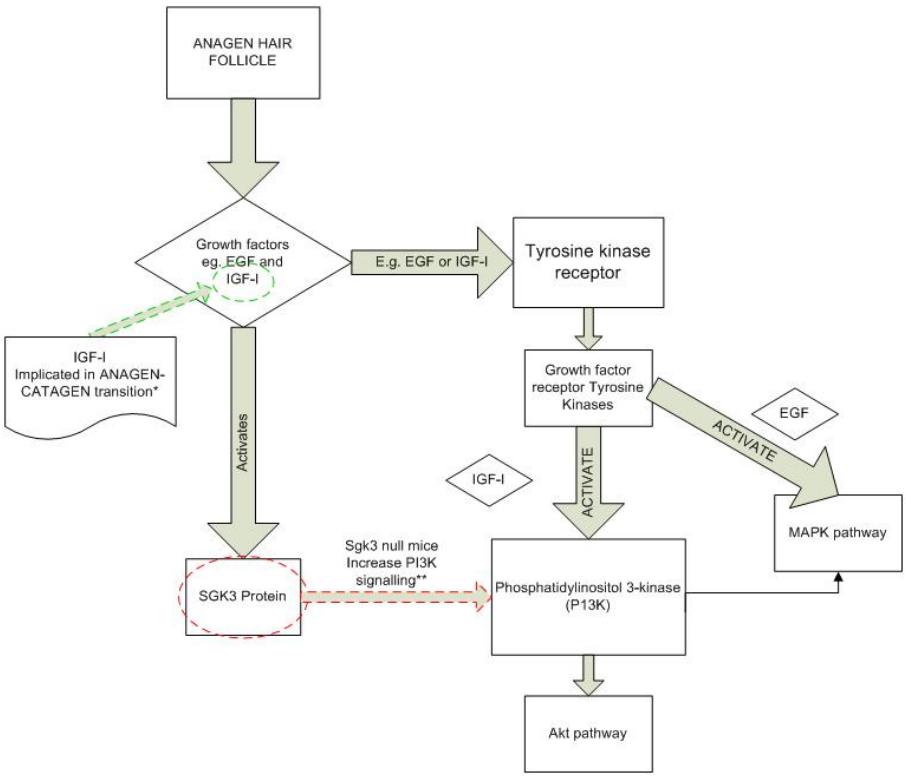

Figure 3.2: The links between SGK3 and growth factor pathways

*Schema of the possible role of the Sgk3 gene in the anagen-catagen switch in hair follicles. *Philpott M., et al. Reference no. (Philpott et al., 1994b), **Alonso et al. Reference (Alonso et al., 2005)*

3.4.2 Structural complexity of the hair follicle

The tissue compartments of the HF are stringently circumscribed and of well-defined composition. This makes the HF a microcosm and an ideal target for systems biology research.

The structure of the HF can directly address the second dimension of living systems that Huang and Wikswo describe (Huang and Wikswo, 2006). HFs are easily accessible for experimentation, observation and perturbation due to their superficial location on the surface of mammalian bodies. This feature makes the HF ideal for systems biology research as access to molecular, structural and phenotypic information is readily available. In addition, the HF can be reduced into different structural levels; from cells (such as stem cells, DP cells, epithelial cells) to isolated mini-organs (e.g. HFs) to whole tissues (e.g.

hair-bearing skin) and organisms (such as humans and mice) (Rogers and Hynd, 2001). Importantly these different structural levels all exhibit systems properties within themselves.

The structural unit of the HF can be considered an essentially autonomous organ as it is able to grow after dissection from its neurovascular supply and transplantation into another part of the integument (Maurer et al., 1998). In addition, isolated human HFs can be maintained in organ culture (Philpott et al., 1990, Philpott et al., 1996). This is an exciting prospect for systems biologists as these mini-organs exhibit emergent properties of great biological relevance: controlled cell proliferation; differentiation; apoptosis and organ regeneration. In addition, the basic autonomous clock driving the HF cycle may reside in the HF itself (Paus et al., 1999a), plus the HF "system" is also sensitive to extra-follicular communication e.g. neurovascular stimuli (Plikus et al., 2008, Plikus et al., 2009), thus increasing the level of system complexity by analysing greater levels of structural complexity.

The mature HF can be divided into the mesenchymal HF, consisting of the DP and CTS, and the epithelial HF (the remaining portions; including transient amplifying cells of the hair matrix that envelope the DP, hair shaft, IRS and ORS). The structural complexity of the HF is intertwined with the molecular complexity of this mini-organ and epithelium and mesenchyme communication is thought to be vital for understanding the hair growth cycling of the HF (Tobin et al., 2003, Paus et al., 1999a, Stenn and Paus, 2001, Rendl et al., 2005, Fuchs et al., 2001, Botchkarev et al., 1999a, Botchkarev and Kishimoto, 2003). The accessibility and exhibition of epithelial and mesenchymal communication in the HF make it an excellent tool for those interested in this type of communication; for example in cancer research (Hu and Polyak, 2008, Faratian et al., 2009a) and molecular communication through time and space in general (Klipp et al., 2009).

3.4.3 Temporal complexity of the hair follicle

Living systems exhibit different temporal properties and scales. For example, in the heart, depolarisation of myocytes takes 1 millisecond; the cardiac cycle, 1 second; and longevity of the organism, gigaseconds (Huang and Wikswo, 2006). The temporal dimension of living systems (Table 3.1) is well-reflected in HF biology since this organ exhibits its own unique temporal cycle; the hair cycle. These cycling events are typical examples of patterns, namely breaks of homogeneity leading to the emergence of new structure (Widelitz et al., 2006). Temporal complexity of HF cycling also relates directly to structural and molecular complexities as these themselves exhibit dramatic hair cycle-dependent changes. During the hair cycle, the HF shows complex, patterned phenomena that are temporo-spatially restricted (Widelitz et al., 2006, Chuong et al., 2006). Despite the large number of molecular candidates implicated in HF cycling control, such as IGF-1 (Rudman et al., 1997), hepatocyte growth factor (*HGF*) (Jindo et al., 1998, Jindo et al., 1995, Lindner et al., 2000) (anagen promoters), fibroblast growth factor-5 (*FGF-5*) (Kawano et al., 2005, Hebert et al., 1994, Rosenquist and Martin, 1996) and neurotrophins (NTs) (catagen inducers) (Botchkarev et al., 1999b, Botchkarev et al., 1998b), the mechanisms regulating its timing remain elusive (Paus and Foitzik, 2004, Stenn and Paus, 2001, Paus et al., 1999a). An integrated, systems, approach to this problem has been lacking with researchers often looking only at one gene or protein of interest (Stenn et al., 1994).

Organ-cultured human HFs are able to synthesize a hair fibre (at rates (Philpott et al., 1994a) and with a keratinisation process (Thibaut et al., 2003) similar to that *in vivo*) and subsequently enter a catagen-like stage i.e. in the absence of extra-follicular tissue, neural, vascular or endocrine signals. A full hair cycle is not exhibited in this *in vitro* model, however, this model has advantages for researching the human anagen-catagen transition as the occurrence rate of catagen HFs *in vivo* is low (Whiting, 2004) compared to the majority of HFs that spontaneously enter catagen with this model (Rogers and Hynd, 2001).

Since oscillatory behaviour is a classical emergent phenomenon (Whittington et al., 2000), the cycling HF is an ideal mammalian system for systems biology studies. The full temporal complexity of HF cycling is evident by the recent discovery that clock genes may play an important role in this "intrinsic" HCC (Lin et al., 2009), thus joining circadian oscillator systems (daily) with the rhythmic organ remodelling process that spans weeks (mice) or even years (man). The HF and skin exhibit circadian rhythms in gene transcription and protein expression (Zanello et al., 2000, Bjarnson et al., 2001, Lin et al., 2009, Bjarnson and Jordan, 2002, Kawara et al., 2002, Mehling and Fluhr, 2006, Tanioka et al., 2009) and therefore this tissue operates on various time-scales simultaneously (Mehling and Fluhr, 2006). To fully understand how these distinct chronobiological systems interact constitutes a systems biology research challenge. Routine hair research approaches cannot hope to master this challenge if hair biologists do not cooperate closely with chronobiologists and systems biologists (Lin et al., 2004, Lin et al., 2009, Mehling and Fluhr, 2006, Schneider et al., 2009).

3.4.4 Abstraction and Emergence

3.4.4.1 The Follicular Automaton

In order to cycle, HFs exhibit oscillations in structural and molecular properties. However, on a high level of abstraction, HF cycling can be studied without explicit reference to the exact molecular mechanisms that produce it. As a starting point to understand HF cycling, a rather abstract mathematical model was proposed; the follicular automaton model (FAM) (Halloy et al., 2000, Halloy et al., 2002). The FAM aimed to establish a model of the dynamics of human scalp hair to predict long-term changes of scalp hair growth and thus understand (and, ideally, predict) the manner by which different balding patterns occur (Figure 3.3).

The FAM has generated useful formation on the dynamics of human hair cycling, with a level of abstraction that may be advantageous (Huang and

Wikswo, 2006). On a population level, the distribution of HFs in the skin provides a striking example of a self-organised spatio-temporal pattern and molecular detail is not required to demonstrate this. In addition, the model simulation of the evolution of hair patterns is hypothesis-stimulating i.e. the pattern of hair growth on the human scalp can be manipulated to elicit male-pattern baldness, diffuse alopecia and "normal" hair growth (Figure 3.3). This provokes hypotheses about HF parameters such as 'heterogeneous distribution of follicular parameters produces a diffuse pattern' whereas 'gradients in mean duration of anagen phase (e.g. from centre to periphery of the scalp) cause a central balding pattern'. The authors also determine that the independence of HFs and variability in the length of the anagen phase are major determinants of collective dynamics of human hair cycling. This model could be advanced, predictions tested, implemented and improved by including molecular signals and further refined by experimental data and hair cycle staging. Despite the limitations (see legend, Figure 3.3); this model is an elegant example of how combined experimental and theoretical methods can be optimally utilized to explore specific scientific problems (here: to provide a basis for long-term prognoses of human scalp hair growth in response to manipulations), make predictions and create new hypotheses. The dynamic behaviour of single HFs and HF populations can be approximated by a simple model (abstraction) and the FAM thus perfectly illustrates a classical systems biology approach to hair research.

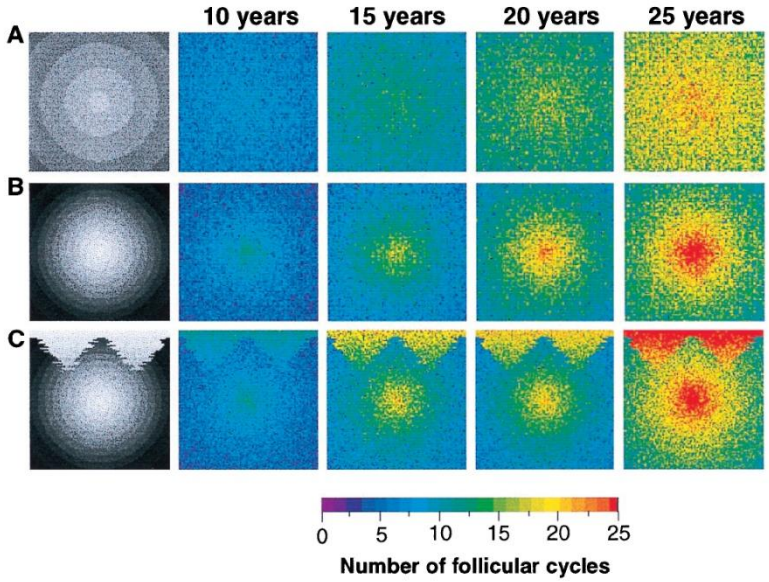

Figure 3.3: Spatiotemporal simulations of the follicular automaton model showing different patterns of hair growth

Experimental (phototrichogram) data collected over 14 years was used to approximate the distribution of durations of hair cycle stages in each HF for each patient by using a log normal distribution. The follicular automaton model of the hair cycle in human scalp hair was defined using the assumptions that (i) each follicle is independent; (ii) each follicle traverses the cycle in the order of anagen-telogen-latency phases; and (iii) after latency the follicle may either enter a new cycle or undergo death or miniaturisation. The figure shows the simulation of human scalp hair growth over "25 years" using the follicular automaton model and various parameters. The model demonstrates how different patterns of alopecia could be achieved by simulating of a population of HFs on a "scalp". Alopecia was achieved by enforcing a limit on the total number of cycles each HF could traverse and by introducing a gradient in the mean anagen duration of HFs across the area of the "scalp". (A) "Hair follicles" were arranged on a grid ("scalp") with hair follicles programmed with different mean durations of the anagen phase across a gradient as shown in left column (decreasing mean from periphery of the "scalp" to the centre). The hair follicles were also programmed to "die" after a set number of cycles. The final hair pattern at 25 years corresponds to a diffuse alopecia commonly seen in women. (B) As in A, but steeper gradient set across the scalp to produce more dramatic balding pattern in the centre. (C) Grid programmed with temporal conditions as well as central gradient to achieve typical male pattern baldness. The final hair pattern at 25 years corresponds to androgenetic alopecia (male pattern baldness) as shown in Figures 4B and 4C. This model has limitations, for example, the method by which data was collected (phototrichogram method) provides only approximate temporal information regarding the durations of hair cycle stages as these durations represent what is observed from the skin's surface and provides no more specific information of the molecular and temporal changes at the HF (rather than scalp) level. The assumption that the results obtained with this method can relate quantitatively to the molecular timings of the human hair cycle is tentative. This is demonstrated, for example, by the fact that catagen (which lasts a few weeks in human scalp hair) is not captured using this method. Adapted after Halloy, J., et al., Modeling the dynamics of human hair cycles by a follicular automaton. Proceedings of the National Academy of Sciences of the United States of America, 2000. 97(15): p. 8328-33. Copyright 2000

3.4.4.2 Intra- and extra-follicular communication in hair follicle dynamics

The HF exhibits emergent properties, i.e. properties that exist in complex systems that are not demonstrated by the components alone and cannot be predicted through understanding the separated parts. For example, understanding the properties of hydrogen and oxygen does not equate to understanding the properties of water (Aderem, 2005). The HF is an emergent organ; the group of cells comprising the HF do not function in the same way when isolated than when operating together within the mini-organ. For example, isolated DP cells will not produce a hair shaft (Tobin et al., 2003, Rendl et al., 2005).

Recently, Plikus *et al*. have shown that adult pelage HFs in mice exhibit hair cycle domains (i.e. spatially distinct HF populations that cycle synchronously within a defined skin territory) (Plikus et al., 2008). These hair cycle domains show the propagation of regenerating HFs as wave patterns (Ma et al., 2003, Suzuki et al., 2003). (Figure 3.4). Through directed experimental techniques, spatial-temporal patterns in HF activity were directly linked to expression levels of the BMPs (*Bmp2* and *Bmp4*) within hair cycle domains (Figure 3.4). Cyclic changes were found in *Bmp2* and *Bmp4* that were asynchronous to hair cyclic changes, WNT/β-catenin signalling and noggin (a BMP antagonist) expression.

On the basis of these studies, the hair cycle was redefined (in the context of a population of HFs and the intra-follicular status of the skin (Plikus et al., 2008)), from the traditional anagen, catagen and telogen stages, into functional phases of propagating anagen, autonomous anagen, refractory telogen and competent telogen (Figure 3.4). This study addresses the population dynamics of cycling murine HFs, i.e. the population behaviour of HFs to either propagate and cycle in waves or not. Human HFs, however, behave differently to murine HFs in that they do not exhibit hair cycle domains and behave independently and stochastically or at the very most, in follicular units (Jimenez and Ruifernández, 1999). This murine study cannot be extrapolated to explain the behaviour of human HFs as yet, however, it could be that a similar mechanism

may exist between follicular units rather than cycle domains, but there is as yet no evidence to support this idea.

The functional phases of the hair cycle proposed in this study, in terms of ability to propagate a wave, can be used to define spatial-temporal relationships and controls within murine skin. Plikus *et al.* (Plikus et al., 2008) demonstrate that stem cell regeneration is subject to control of biological rhythm. This work shows how the intra-follicular clock communicates with intra-cutaneous (but extra-follicular) timing mechanisms and lend themselves to the quantification and mathematical modelling of BMPs, noggin, WNT and β-catenin levels as a function of time and thereby predict and elucidate their function in the hair cycle.

Plikus *et al.* (Plikus et al., 2008) have managed to demonstrate that the emergent properties of HFs within its macro-environment are essential for explaining function. Moreover, this study is a fantastic example of how emergent properties and molecular, structural and temporal complexity are all involved in the process of cycling HFs. This provides yet further evidence that the HF is a classic systems biology tool.

3.4.5 Algorithmic complexity of the cycling hair follicle

Living organisms must be able to "compute" inputs and convert these to outputs. As an example, gene regulatory networks within cells process a signal e.g. hormone level (input) into gene expression patterns and cellular phenotype (outputs) (Table 3.1). The "computational centre" (HCC) that drives the hair cycle in the HF has not been identified (Paus and Foitzik, 2004). The existing theoretical models that simulate hair cycling (Halloy et al., 2000, Halloy et al., 2002, Kolinko and Littler, 2000) do not model the "computations" of the HF during this process. A systems biology approach to hair cycling research should carefully identify the drivers of the hair cycle (internal computer or HCC) whereby inputs to the cycling HF are converted to the outputs; such as a hair shaft formation, regression of the HF, stem cell activation and HF regeneration and so on. In addition, we need to ensure that we have the computational means

to create models that can handle the complexity of such simulations (Huang and Wikswo, 2006).

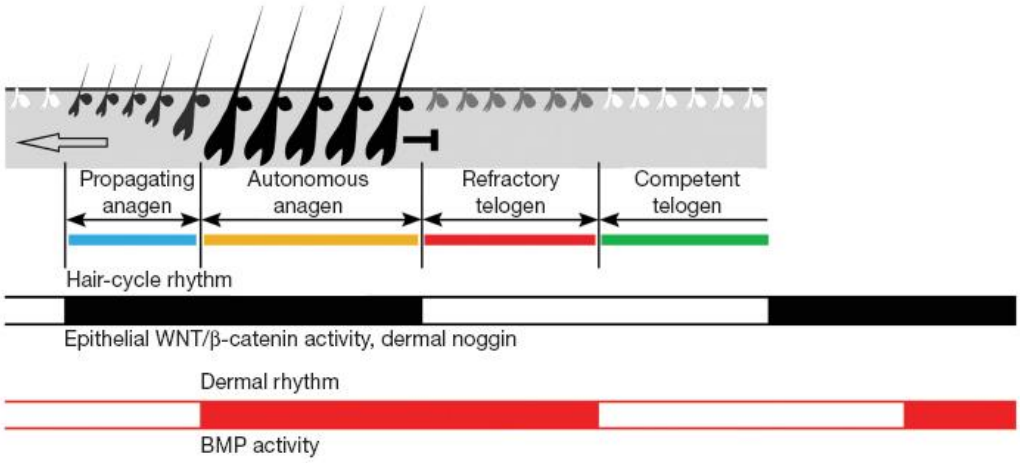

Figure 3.4: Emergent property of murine hair follicles in hair cycling domains and BMP signalling

Employing a technique whereby murine dorsal skin was cut longitudinally and arranged spatially and temporally; in situ-hybridisation was carried out. These spatio-temporal experiments revealed how the propagation of hair cycle waves on the dorsum may arise. Spatio-temporal patterns in HF activity were directly linked to expression levels of the BMPs within hair cycle domains. Cyclic changes were found in Bmp2 and Bmp4 that were asynchronous to hair cyclic changes and that of WNT/β-catenin signalling; which is required for HF stem cell activation and thus hair regeneration. Noggin, a BMP antagonist, was found to be expressed in a similar pattern to WNT signalling. The figure shows the schematic summary of the hair-cycle rhythm (in black) and the dermal rhythm (red) as defined by Plikus et al. Together, they define four new functional stages that correspond to the ability to propagate and respond to hair cycle propagation, these are functional phases of propagating anagen, autonomous anagen, refractory telogen and competent telogen. Refractory telogen is characterised by low noggin, high BMPs and low WNT signalling. Competent telogen is defined by low noggin, low BMPs whereas, during propagating anagen high noggin levels and low BMPs are found. Autonomous anagen is distinguished by the expression of high noggin and high BMPs. Catagen is omitted for simplification.

3.5 PERSPECTIVES – TACKLING THE HUMAN HAIR CYCLE

We have described how the HF is an ideal tool for systems biology research; being a unique mammalian feature, easily accessible, defined in form and function and able to address all the dimensions of living systems as an essentially autonomous mini-organ. It is evident that the dimensions of living systems overlap and are intertwined and the HF demonstrates this flawlessly, for example molecular changes in BMPs are co-ordinated with spatio-temporal changes in the propagation of hair cycle waves and associated structural alterations of HFs as they traverse the hair cycle (Plikus et al., 2008, Plikus et al., 2009).

Human hair cycle research highlights the intertwining pathways that are relevant in the regulation and function of a multi-cellular mini-organ. Interesting recent findings show that circadian genes are differentially expressed in anagen and catagen human HFs (Al-Nuaimi et al., 2009). The cycling HF is thus relevant to regenerative medicine researchers, chronobiologists and stem cell biologists to name but a few (Yu et al., 2008). We would hope that more comprehensive and dynamic analyses of the human hair cycle, via perturbation with siRNAs, for example, and microarray and protein analyses, with the concomitant use of mathematical modelling would be an important direction for human hair research and systems biologists alike and systems biology may make it more possible to unravel the mystery of the enigmatic HCC. This understanding could facilitate the development of novel therapeutic agents for the more effective management of common hair growth disorders.

3.6 CONCLUSIONS

In summary:

- HF cycling in mice and man offers an excellent, clinically relevant, research model for systems biology and also stem cell, chronobiology, regenerative medicine and neuro-endocrinology research;

- The HF model deserves to be fully discovered by dermatological and systems biology research communities;
- We propose that a systems biology approach to human HF cycling via the use of mathematical modelling coupled to experimental work would greatly further hair cycle research.

4 CHAPTER 4: AN INTRODUCTION TO DYNAMICAL SYSTEMS

4.1 ABSTRACT

Dynamical systems theory is a field of applied mathematics used to construct and explore dynamical systems and is used as an important tool in systems biology research. In this chapter we describe essential features of a type of mathematical model used for the description of temporal biological processes; nonlinear ordinary differential equations.

We present a tutorial-style exploration of the basic concepts and definitions of this field that are important in the context of this thesis. In order to demonstrate key principles, we provide a two dimensional non-linear system formulated in the style of apoptosis and proliferation driven cell population dynamics. Using this system we explore its key bifurcation structures and as such demonstrate mechanisms by which oscillations and bistability may arise. This chapter therefore serves as a point of reference for the following chapter detailing a theory of human hair follicle dynamics.

4.2 INTRODUCTION

Dynamical systems theory is an applied mathematical field of study concerned with describing and exploring dynamical systems (Strogatz, 1994). These are mathematical formulations of complex interactions, referred to as *mathematical models* that can be investigated in terms of their evolution from a pre-defined starting point as time progresses. Often, the formulation is in terms of *differential equations*, so that the evolution of important system components (the *variables*) can be expressed as continuous changes with respect to time. Other possibilities are discrete mappings which describe the evolution as discrete updates with respect to time. In both of these cases the systems variables (measurable quantities) are assumed to be continuous, i.e. expressed as real numbers. On a more abstract level of description, when both the time and the variables are updated in a discrete way, one speaks of *cellular automata*. In formulating interactions in these or other ways and examining the behaviour of the models, we learn about the *mechanisms* involved in the real-world counterpart of the mathematical system. This approach has interdisciplinary applications and is an essential tool in understanding and analysing complex systems in systems biology (Klipp et al., 2009). Here, we describe essential features of the most basic type of mathematical models used for the description of temporal biological processes, the nonlinear ordinary differential equations.

4.3 USE OF DYNAMICAL SYSTEMS IN THE THESIS

In the present context, an important feature of the HF is its ability to display characteristic dynamics, which at the macroscopic scale is observed by the rhythmic regeneration and regression of the HF known as the hair cycle. Crucially, most hair disorders of clinical interest are thought to be defined by abnormalities in these dynamics (Paus, 2006, Paus et al., 1999a). In addition, the mechanisms leading to normal or abnormal rhythms in the HF are unknown. The formulation and investigation of a mechanistic mathematical model of the

HF dynamics can therefore inform on the mechanisms underlying these rhythms.

For an expanded motivation of the use of dynamical systems to develop a prototypic model of the HF oscillations the reader is referred to Chapter 5. In what follows, we give a brief overview relating to terminology and concepts used in Chapter 5. The reader may refer to (Strogatz, 1994) for a more comprehensive guide to non-linear dynamics.

4.4 A BRIEF EXPLANATION OF DIFFERENTIAL EQUATIONS AND RELATED DYNAMICS

Ordinary differential equations (ODEs) are concerned with systems' evolution in continuous time, as opposed to discrete-time difference equations. Although HF cycling is often verbally described in terms of distinct stages, the morphological processes and observations are continuous on the macroscopic level. Therefore, we try to capture the dynamics of the HF in continuous time using a model composed of systems of ordinary differential equations. In this framework, key *variables* in the system are identified. These are the components of the system that change within the time scale of interest and that reflect the mechanisms that we are interested in. These are either directly measurable or indirectly related to measurable quantities and as such form the link between model and experimental data. The population of keratinocytes in the human HF is an example of an important variable in relation to the hair cycle (see Chapter 5). A mathematical model is formulated by relating how the selected variables change over time with regards to key interactions between variables (see Equation (1)). Therefore, the model is a formulation of the mechanisms of interest. When the output of the model is compared to data from the real system inference regarding these mechanisms can be made.

$$\frac{dx}{dt} = f(x, \mu) \qquad (1)$$

Equation (1) gives a general formulation for the ODE. Variables are represented by the vector $\boldsymbol{x}$, and one can see in equation (1) that their changes over time (expressed as first-order derivatives with respect to time) at a given temporal instance are defined by some function (**f**) of their respective values at that time. The interactions specified by the ODE also contain static quantities known as parameters (**μ**). These capture quantitative effects that do not vary on the time scale of interest and might include, for example, the rate of increase of a population due to intrinsic, un-modelled processes or the weighting given to the interaction between two variables.

The number of variables in the vector $\boldsymbol{x}$, determines the dimension of the system. $\boldsymbol{f}$ is a function that defines the interactions of the system and its evolution in time. Given the variables, parameters and evolution equations (**f**), the final ingredient of the mathematical model is its *initial condition*. This specifies the value of all variables at t=0 and determines a unique *trajectory* as time evolves. The trajectory is composed of the subsequent values of **x** at all time points, i.e. **x**(t), t>=0. One can visualise the trajectory of the system as a time series plot with time on the abscissa. Alternatively, one can plot values of variables against each other. This gives a view of the *phase space* (or *state space*) of the system (see figures below). The phase space is the set of all points the system can possibly take, and is therefore of dimension equal to that of **x**. A *vector field* describes the direction of flow of the system at each point in space and is usually visualised by arrows pointing in this direction and with size representing the magnitude of velocity (see figures below).

In general, if f was linear, the system could either evolve to a fixed point or blow up to infinity. Fixed points are solutions to $\boldsymbol{f}(\boldsymbol{x}, \boldsymbol{\mu}) = 0$ and therefore represent points at which the trajectory no longer changes over time (hence fixed point or steady state). Describing the number and location of fixed points is an important first step to characterising a dynamical system. In addition, one should know the *stability* of a fixed point. *Stable fixed points* attract nearby

trajectories such that if one is perturbed away from the fixed point, the system will eventually evolve back to that point. *Unstable fixed points* on the other hand are those at which nearby regions of phase space diverge, such that a perturbation of the system away from this point causes the trajectory to evolve to a different region of phase space. Unstable fixed points are thus not observable experimentally. An additional class of (unstable) fixed point is the *saddle,* which has both stable and unstable properties depending on the direction of perturbation away from it.

In addition to fixed points, non-linear dynamical systems (where **f** is a non-linear function of **x**) can display more complex structures to which the trajectory is attracted or repelled from. Stable *limit cycles*, for example, are closed loops in phase space to which the system is attracted and will stay upon as time evolves, resulting in periodic or oscillatory behaviour**.** Similarly as above, unstable limit cycles are oscillations on which the system can evolve, but will deviate from if perturbed by an arbitrarily small amount. They are thus experimentally unobservable as are unstable fixed points. Their knowledge is nevertheless of interest as they play a role in ordering phase space structure.

In general, a dynamical system can be qualitatively described by its number of structures (fixed points and limit cycles, see below) and their stability. In the first instance, we can explore the stable solutions of the model as these will provide an indication of how the equivalent real life system may behave. Stable structures can be found by numerical simulation of the equations using algorithms that approximate **x** given previous values and knowledge of **f** (in this thesis the MATLAB "ODE45" solver is used).

Therefore, an initial pertinent description or exploration of the model dynamics can be found by simulating the system for different values of parameters. When one plots the outcome of these simulations (for example by extracting values of fixed points or the maxima and minima of oscillations) a *bifurcation diagram* is formed. This can be a useful technique in general but is especially important when model parameters cannot be determined

experimentally. This case frequently arises if abstractions of important processes are considered (which is generally the case in biology) or if experimental techniques do not facilitate the quantitative evaluation of their associated parameters. In these cases, the *relative* effect of these processes can be determined by examining the dynamics of the system over changes in its parameters.

As the parameters, $\boldsymbol{\mu}$, vary a *bifurcation* is said to occur if the qualitative characteristics of the system change. A bifurcation point is the point where specific parameter values are seen to produce the change. Thus, bifurcations can model, for example, the emergence of rhythms as a stable fixed point loses stability and forms a stable limit cycle. This is the scenario of a very common bifurcation known as the *Hopf* bifurcation and is a classic way for a dynamical system to generate oscillations.

In order to demonstrate some of these important concepts, we introduce a simplified two dimensional system, which retains some of the properties of the HF model referred to in Chapter 5. The ODE and parameter set are given as follows:

$$\boldsymbol{f_1 = \frac{dx}{dt} = a + \frac{cx}{Km_1 + x} - \frac{(d + C_a y)x}{Km_2 + x^k} - bx} \qquad (2)$$

$$\boldsymbol{f_2 = \frac{dy}{dt} = e(x - y)}$$

Table 4.1: Parameter set for example ODE

Parameter	a	b	c	d	e	k	Km_1	Km_2	C_a
Value	0.1	0.1	Varies	0.7	0.02	2	0.1	0.1	Varies

In relation to the previous notation $\mathbf{x} = (x, y)$, $\boldsymbol{\mu} = (a, b, c, d, e, k, Km1, Km2, Ca)$ and $\mathbf{f} = (f1, f2)$. The system is two dimensional since there are two variables of interest. Seven parameters, the functional form of $\mathbf{f}$ and the set of initial conditions $\mathbf{x}(0)$ specify a solution to this system of ODEs.

In the first line of eq. (1) (variable *x*) there are two terms with positive sign that describe processes leading to the growth of the population (positive rate of change) and two processes with negative sign that describe processes leading to the decay of the population (negative rate of change). One of the growth terms is just a constant and therefore independent of variable ***x***. The other growth term depends on ***x*** in a hyperbolic fashion and is therefore nonlinear. One of the decay terms depends on ***x*** linearly. The other decay term depends on ***x*** in a more complex fashion. The qualitative shape of the function is determined by the value assigned to parameter *k*. The second equation has no specific interpretation, it is meant to represent some other process which depends on the state of the population ***x***. It can also be thought of as a condensed way of representing all other processes that depend on the state of the population.

When C_a =0, the equation for variable *x* only depends on parameters and x itself and is said to be independent of the state of the other variable, y. As the evolution of y is assumed to depend on x (see equation for *y*), whenever one chooses to set C_a >0, the two variables compose a system of interwoven dependencies. Parameter C_a can thus be said to represent the strength of coupling or feedback of *y* on *x*. Mathematically then, one way of investigating the model is to first look at the equation for the population x in isolation (C_a =0), and then compare this to the dynamics of the full model with feedback C_a >0.

With the parameter set described above

Table 4.1) including C_a =0 and c=1.8, our simple system has two fixed points, one stable and one unstable. The stable and unstable fixed points can be seen in the following phase space diagram (Top panel, Figure 4.1):

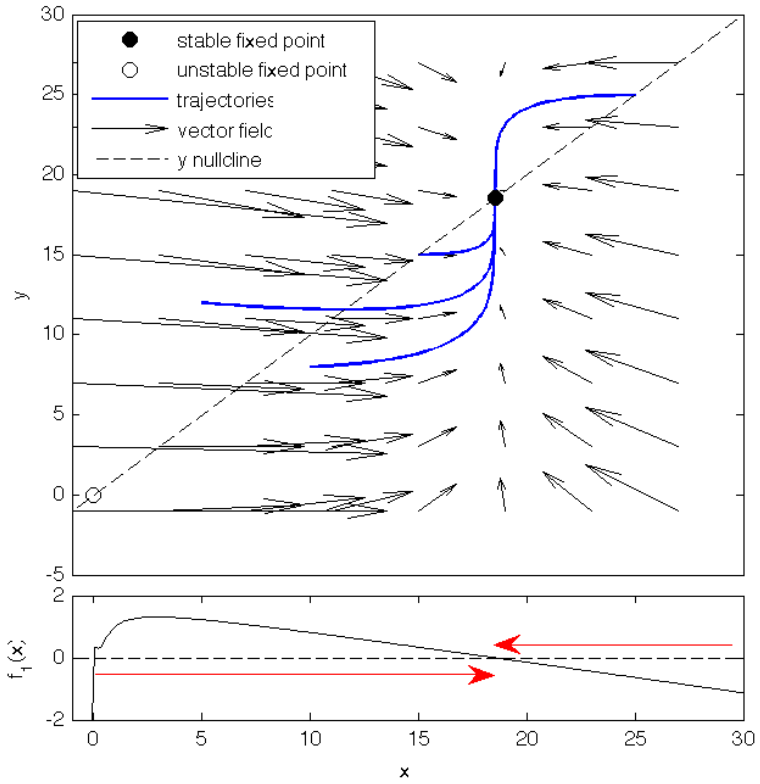

Figure 4.1: Phase space diagram.

Phase space diagram of model as detailed in Equation (2) with C_a=0 and c=1.8. Open circle indicates unstable fixed point and the full circle a stable fixed point. Bottom panel shows a plot of f_1 over a range of x. Red arrows indicate the direction of flow with respect to x.

In Figure 4.1 the two dimensional space is plotted in which the system resides. The arrows indicated on the upper panel of this figure constitute the vector field which describes the magnitude and direction of the change (or flow) of the system at each point in phase space. One can see that the vector field points towards the stable fixed point if approached from any direction. One can extract information regarding the flow in the x and y directions by examining the solutions to f_1=0 and f_2=0. In our simple system, f_2=0 simply requires x=y. This is plotted as a *nullcline* on the figure (dashed line y=x). Information regarding direction of flow with respect to x is extracted from f_1=0 which is plotted in the bottom panel of Figure 4.1. Note that in this case, f_1 is independent

from y since C_a=0. Fixed points are located where both f_1=0 and f_2=0 and can be seen on the figure. The red arrows in the bottom panel indicate that when f_1>0 the direction of travel is in increasing x and *vice versa* for f_2<0.

Some example trajectories are given for different initial conditions as thin blue lines. It can be seen that in each case the system converges to the stable fixed point at (x,y)=(18.5,18.5). This is also demonstrated in the time series of the two variables, as shown in Figure 4.2. Note that the two variables assume identical final values due to the specific construction of the equation for y. In general their final values will differ.

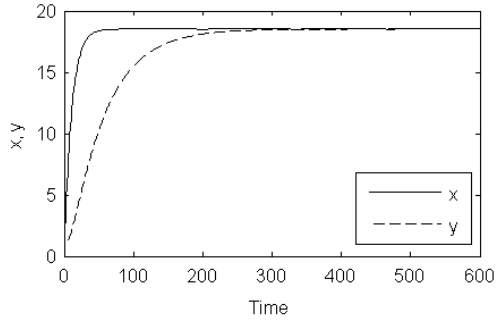

Figure 4.2: Time series of x and y simulated from random initial conditions.

The stability of fixed points in our example were calculated by determining the eigenvalues of the *Jacobian* matrix of the system. The Jacobian is the matrix formed by all partial second derivatives of the system, which in our example gives:

$$J = \begin{pmatrix} \frac{df_1}{dx} & \frac{df_1}{dy} \\ \frac{df_2}{dx} & \frac{df_2}{dy} \end{pmatrix}$$

The eigenvalues, λ, of J are given as solutions to the following equation:

$$J\boldsymbol{v} = \lambda \boldsymbol{v}$$

and in practice are determined using:

$$\det(J - \lambda I) = 0$$

A fixed point is stable when all eigenvalues satisfy Re(λ) <0 and unstable if any of the eigenvalues satisfy Re(λ) >0. Here Re() refers to extracting the real

part of **λ**. When Re(λ)=0, conclusions on stability cannot be drawn from this method. In particular, Re(λ)=0 defines the point of bifurcation where the stability of a fixed point changes.

In Figure 4.3 we demonstrate the presence of stable and unstable fixed points for our system eq. (2) in a bifurcation diagram. In this case, we set C_a =0 and track the system behaviour over changes in *c.* We note that since the variable, *x*, in this system is analogous to a cell population density in Chapter 5, we limit solutions to those satisfying *x* >=0. It can be seen that as parameter *c* changes, the number of stable and unstable fixed points, as well as their value, can change. We note the presence of bistability in this model when $0.4 \leq c \leq 1.4$, which means that the system can evolve to one of two stable fixed points. The fate of the system, in terms of which of these fixed points it is attracted to, is determined by the initial conditions. Each stable fixed point has a *basin of attraction*. Any initial condition within the basin of attraction of a fixed point will evolve towards that fixed point as time progresses. In our case, the boundary between the basins of the two fixed points in the bistable region is given by the unstable fixed point between them (dotted line in Figure 4.3).

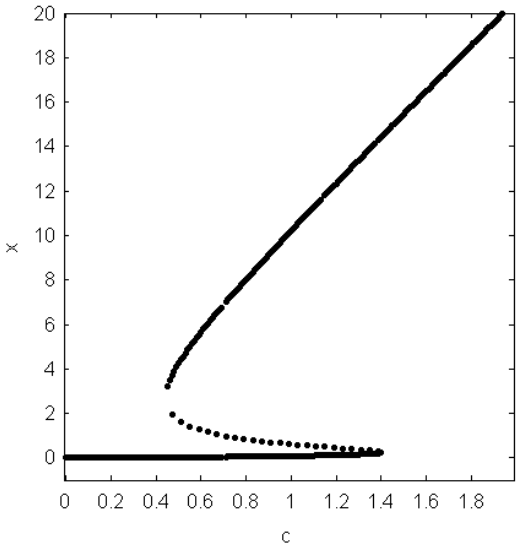

Figure 4.3: Bifurcation diagram showing fixed points in the model with C_a = 0.

Solid lines indicate stable points and dotted line indicates unstable points. There is bistability shown between approx. 0.4 and1.4 (values of c)

When we set C_a to 1 in the model system, oscillations can be produced. We demonstrate this in the bifurcation diagram below (Figure 4.4), again for changes in *c*.

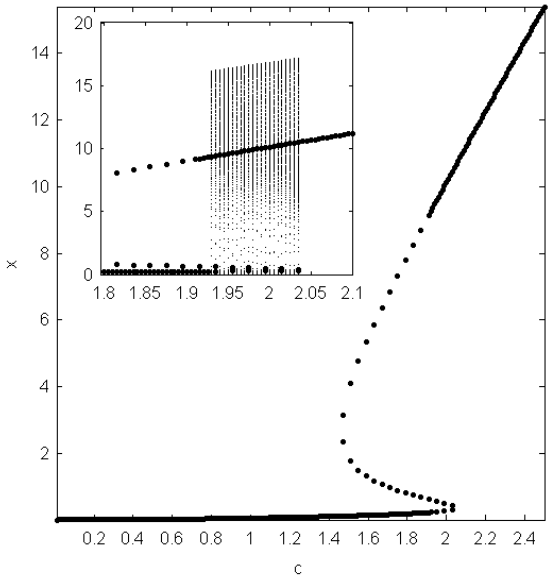

Figure 4.4: Bifurcation diagram for the model with C_a = 1 showing changes over c.

Inset gives a close up of the oscillatory region between c = 1.93 and 2.04

The oscillations are found in the range $1.93 \leq c \leq 2.035$. The two time series of an oscillation at a given value of *c* are shown below (Figure 4.5):

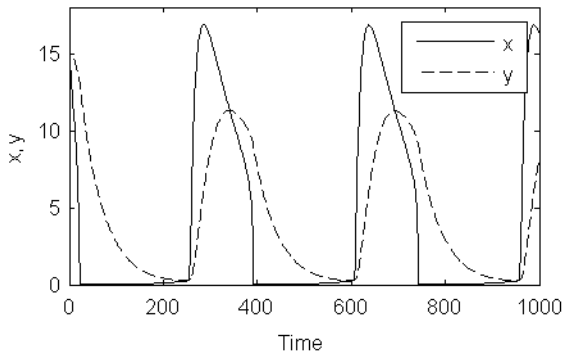

Figure 4.5: Time series for the model where C_a = 1 and c=2.

In the phase space diagram below, we can see that at the parameter set of Figure 4.6, the trajectories of the system converge to the stable limit cycle shown as a thick black line. Thus the system oscillates indefinitely as time progresses. However, the stable fixed point near (10, 10) persists indicating that here the system is bistable between a fixed point and a limit cycle. This will be discussed below.

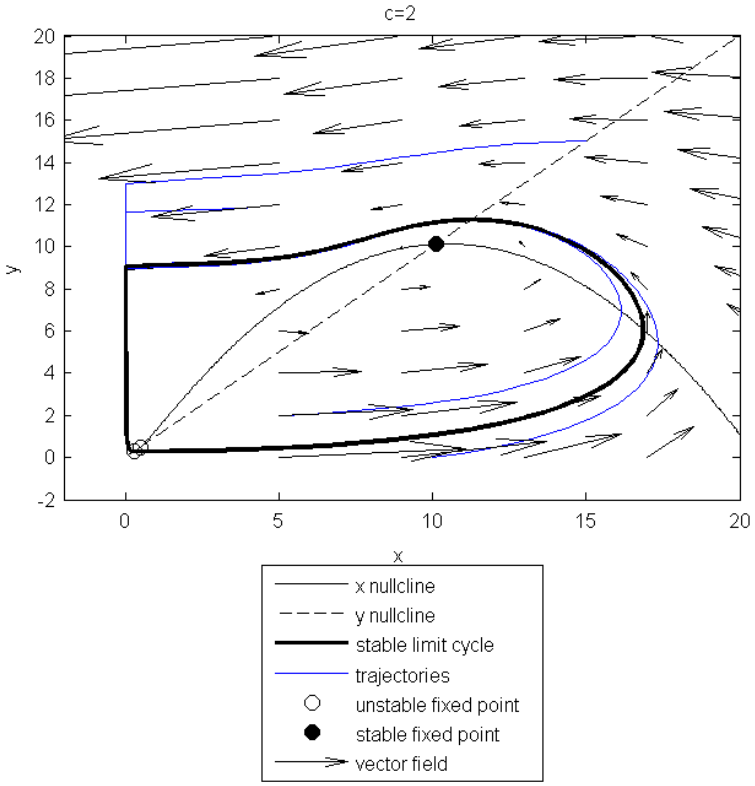

Figure 4.6: Phase space diagram for the model where $C_a = 1$

The details of the dynamics can be understood by considering the bifurcations in the model. As can be seen in Figure 4.4, its dynamics over changes in c present two important branches of fixed points. A contributing factor to the generation of the stable limit cycle, which exists for $1.93 \leq c \leq 2.035$, is the *sub-critical Hopf* bifurcation on the top branch at c=1.91. This bifurcation describes the transition from an *unstable focus* to a *stable focus* as

the real part of the pair of complex eigenvalues becomes negative. The term focus here refers to a fixed point whose eigenvalues have non-zero imaginary part, and leads to damped oscillatory dynamics in the vicinity of the fixed point if the fixed if it is stable. The transition in the eigenvalues of this focus can be seen in Figure 4.7 (the zero-crossing of the real part in the top panel; the transition from empty circles to filled circles in the bottom panel). As the focus gains stability, an unstable limit cycle emerges around it (shown in red in Figure 4.8). The transition thus constitutes a so-called subcritical Hopf bifurcation. (In contrast, in a supercritical Hopf bifurcation a stable limit cycle is generated). Crucially, this unstable limit cycle separates the phase space of the system such that just next to the bifurcation point the two fixed points can now co-exist. The unstable limit cycle is therefore referred to as a *separatrix*, and the system is said to be bistable because one can observe either state for the same setting of parameters. The details of this bistability are shown in Figure 4.8.

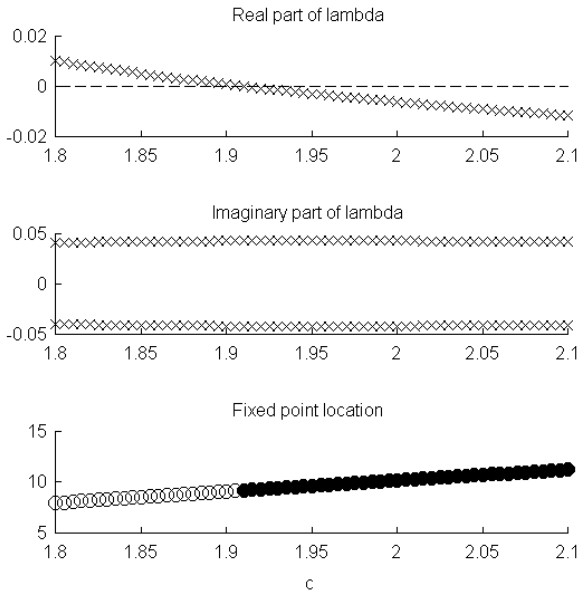

Figure 4.7: Eigenvalues of the fixed point on the top branch over changes in c

(compare to the inset of Figure 4.4). At c=1.91 the fixed point gains stability in a sub-critical Hopf bifurcation as the complex eigenvalues cross the real axis. Top panel: changes in the real part of the eigenvalues over c. The horizontal dashed line is drawn at Re(lambda)=0. Middle panel: the imaginary components do not vary with c. Bottom panel shows the change in stability of the fixed point – open circle is unstable and closed circle is stable.

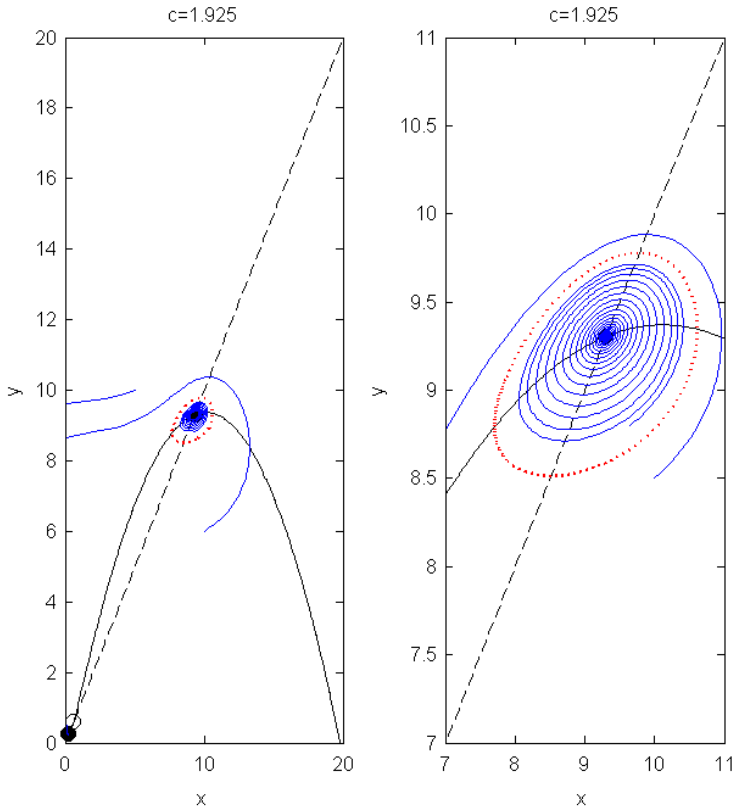

Figure 4.8: Bistability in the model with c=1.925.

The panels show x and y nullclines (solid and broken black lines, respectively), stable and unstable fixed points (solid and open black circles, respectively), unstable limit cycle (broken red line) and example trajectories from different initial conditions (blue lines). The left panel shows all structures of interest, whereas the right panel shows a close-up of the different behaviours at either side of the separatrix.

Then, as c is increased slightly, the stable fixed point on the bottom branch loses stability, as shown in Figure 4.9 (the zero-crossing of the real part in the top panel; the transition from filled to empty circles in the bottom panel).. As the eigenvalues of this fixed point are complex at the moment of transition, this constitutes a supercritical Hopf bifurcation.

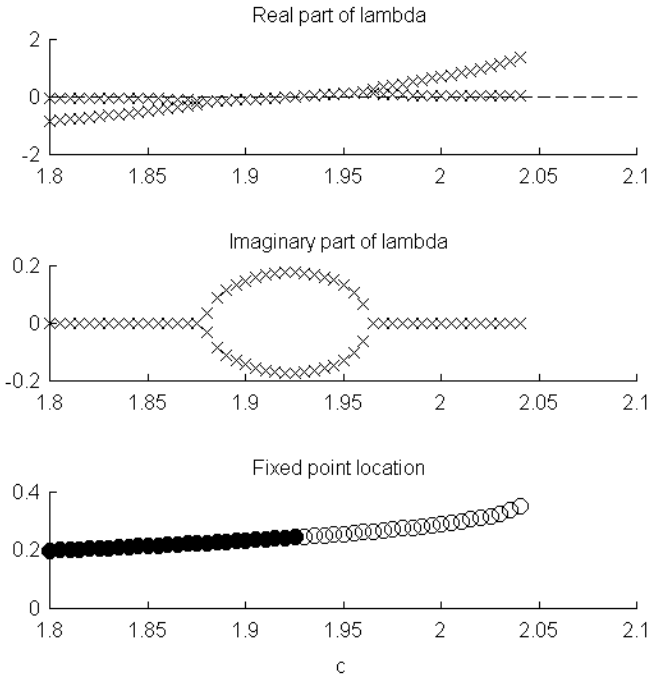

Figure 4.9: Eigenvalues of the stable fixed point on the bottom branch.

Top panel: real part which goes positive at c=1.93, leading to instability of the fixed point. Middle panel: imaginary part of the eigenvalues indicating the node temporarily becomes a focus. Bottom panel: location of the fixed point. Note that the fixed point disappears before c=2.05 (due to collision with the other unstable fixed point)

This loss of stability of the fixed point on the bottom branch means that the two stable structures remaining are the stable limit cycle and the stable fixed point at the centre of the unstable limit cycle.

The offset of oscillations at c=2.035 can also be explained. This is due to a *fold bifurcation of limit cycles.* This is closely related to an important bifurcation of fixed points, known as the *fold bifurcation*, or *saddle-node bifurcation*. This bifurcation occurs when two fixed points, one a *saddle* and one a *node* collide and annihilate each other. Similarly, limit cycles can collide as they grow or shrink with changes in the system parameters. In our system, as c increases, the unstable limit cycle around the stable fixed point on the top branch grows outwards and eventually (at c=2.035) collides with the stable limit cycle. This

annihilates both limit cycles leaving only the stable fixed point on the top branch remaining. This transition is demonstrated in Figure 4.10.

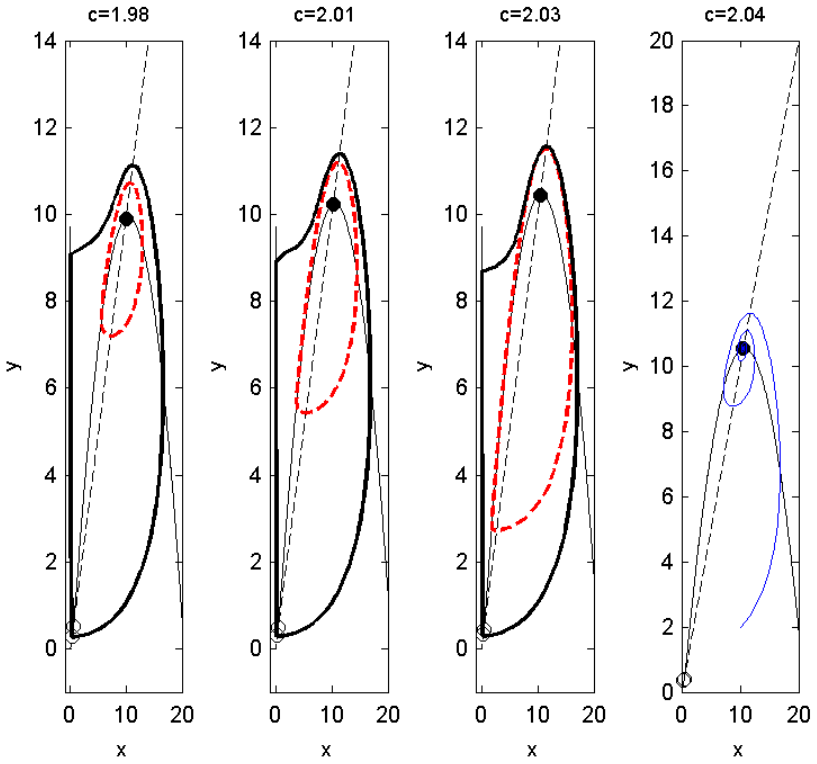

Figure 4.10: Fold bifurcation of limit cycles.

Shown are stable and unstable structures, together with nullclines for increasing c (from left panel to right panel). The stable limit cycle is shown in thick black lines and unstable limit cycle in broken red lines. Stable and unstable fixed points are solid and open black circles, respectively. A trajectory in the right panel is shown as a solid blue line.

In general, a fixed point in the model relates to a stable situation in the real-world analogue, which in our case might be, for example, a keratinocyte population neither growing nor shrinking. In the region of oscillatory behaviour, however, the model predicts a periodically growing and shrinking population. As the analysis shows, this latter behaviour is only possible when one of the model's fixed points becomes unstable. Thus, bifurcation analysis yields the conditions under which cycling (or rhythmic) behaviour can be expected.

Following this brief introduction to dynamical systems we shall in the next chapter present the mathematical model of the human HF cycling.

5 CHAPTER 5: A PROTOTYPIC MATHEMATICAL MODEL OF THE HUMAN HAIR CYCLE

In preparation for submission to the *Journal of Theoretical Biology*

5.1 ABSTRACT

The human hair cycle is a complex, dynamic organ-transformation process during which the hair follicle (HF) repetitively progresses from a growth phase (anagen) to a rapid apoptosis-driven involution (catagen) and finally a relative quiescent phase (telogen) before returning to anagen. At present no theory satisfactorily explains the origin of the hair cycle rhythm. Based on experimental evidence we here propose a prototypic model that focuses on the dynamics of hair matrix keratinocytes. We argue that a plausible feedback-control structure between two key compartments (matrix keratinocytes and dermal papilla) leads to dynamic instabilities in the population dynamics resulting in rhythmic hair growth. The underlying oscillation consists of an autonomous switching between two quasi-steady states. Additional features of the model like bistability and excitability lead to new hypotheses about the impact of interventions on hair growth. We show how *in silico* testing may facilitate testing of candidate hair growth modulatory agents in human HF organ culture or in clinical trials.

5.2 INTRODUCTION

The HF is unique to mammals and displays fascinating dynamic behaviour in the hair cycle. This cutaneous mini-organ undergoes continuous, self-organised, cyclical regeneration and regression events during which a pigmented hair shaft is produced and shed during each cycle. The hair cycle is the only organ transformation event that repeats cyclically for the entire lifetime of the mammalian individual. It represents a unique chronobiological rhythm that encompasses a complex set of changes at the tissue level. In addition, it shows diverse rhythmicity, dependent on where exactly on the integument a HF is located (e.g. scalp versus eyelashes versus eyebrow hair) (Dawber, 1997). The "control" system that governs the hair cycle is proposed to be an autonomous oscillator (Paus and Foitzik, 2004, Paus et al., 1999a). Its exact constituents, however, have essentially remained elusive.

HF cycling commences immediately after HF morphogenesis and consists of three main phases: anagen, a phase of massive epithelial cell proliferation, during which pigmented hair shafts are generated in the anagen hair bulb; catagen, a phase of rapid, apoptosis-driven organ involution; and telogen, an interspersed stage of relative quiescence (Stenn and Paus, 2001, Paus and Foitzik, 2004, Schneider et al., 2009). Active hair shaft shedding occurs during exogen (Higgins et al., 2009, Milner et al., 2002). Each phase in the cycle is of distinct length (e.g. with anagen lasting several years, catagen several weeks, and telogen usually a few months in human scalp HFs). All human HFs show major site-specific variations in the length of each of these phases (Saitoh et al., 1970, Kligman, 1959).

Hair cycling is of clinical relevance as the majority of hair disorders are characterised by a pathological change in normal HF cycling dynamics (Cotsarelis and Millar, 2001, Paus, 2006). If anagen is abrogated and catagen induced prematurely, this will result in hair loss (effluvium). In contrast, when anagen is induced prematurely or lasts overly long, this leads to unwanted hair growth (hirsutism, hypertrichosis). In addition, dramatic transformations in HF size and state can occur during just one hair cycle, which may underlie the HF

transformation events seen when very small (vellus) HFs become large, or very large HF miniaturise during hirsutism, hypertrichosis or androgenetic alopecia, respectively (Tobin et al., 2003, Stenn and Paus, 2001, Paus and Foitzik, 2004, Schneider et al., 2009).

Over the years, a multitude of genes, secreted molecules, enzymes and receptors have been identified that modulate HF cycling, hair shaft growth and hair pigmentation (Stenn et al., 1994, Stenn and Paus, 2001, Schneider et al., 2009, Plikus et al., 2009, Geyfman and Andersen, 2010). It is the general consensus that controlled changes in the expression, secretion or activity of these molecules leads to switches in the local signalling environment, which ultimately drive the HF through its cyclic transformations (Paus and Foitzik, 2004). However, we remain unsure of the "pacemaker(s)" that autonomously govern the coordinated and timely progression of the whole organ through the hair cycle (Paus et al., 1999a, Paus and Foitzik, 2004).

5.3 THE "HAIR CYCLE CLOCK"

The need to explain the origin of hair cycling was first systematically addressed over half a century ago by Chase who proposed an inhibition-disinhibition theory of how the hair cycle rhythm arises (Chase, 1954). More recently, this hair research challenge has been re-examined as an important, as yet unanswered, biological problem of general importance (Stenn et al., 1999, Paus et al., 1999a, Paus and Foitzik, 2004).

Mathematical modelling may be employed to construct and test a theory of where the cyclic transformation activity of the human HF originates and how it is controlled. Unlike other biological cycles, such as the cell cycle and the circadian rhythm, the hair cycle is comparatively unchartered territory in the mathematical modelling arena. However, a small number of mathematical models concerned with hair growth, cycling, or the synchronisation of cycling between larger HF collectives (hair waves) have been proposed (Halloy et al., 2000, Halloy et al., 2002, Nagorcka and Mooney, 1982, Kolinko and Littler, 2000, Golichenkova and Doronin, 2008, Plikus et al., 2011).

Nagorcka and Mooney mathematically modelled the differentiation of wool and mammalian hair shaft during anagen, but did not address the cyclical processing of the human HF (Nagorcka and Mooney, 1982). Similarly, mouse hair shaft growth was modelled with respect to theoretical proliferative activity of MKs (Golichenkova and Doronin, 2008). A cellular automaton model has been adopted to both simulate and predict the dynamics of populations of human (Halloy et al., 2000, Halloy et al., 2002) and mammalian HFs (stem cell activation) (Plikus et al., 2011). A statistical model of human hair cycle laser treatment has been created that was namely concerned with predicting optimal timing for laser hair removal (Kolinko and Littler, 2000).

The existing models either concentrate solely on hair growth (i.e. hair shaft formation) or relate primarily to highly synchronized hair wave pattern formation in rodents. Although it has been shown that the human HF relies most heavily on its intrinsic processes to cycle (Plikus et al., 2011), none of the existing models address the intrinsic processes within the human HF that may explain the fundamental nature of the hair cycle rhythm. As a consequence, a persuasive mechanistic theory of how the human hair cycle is induced and maintained is still missing.

In the current contribution, we aim to outline a dynamical systems theory of the human hair cycle using mathematical modelling. We address the above question from the point of view that a dynamical instability underlies human HF cycling.

5.4 MODEL DESIGN

No molecules, genes or individual cells have as yet been identified as being the "pacemaker(s)" for the hair cycle rhythm. Here, we propose an abstraction from the consideration of the vast number of specific genes, molecules, interlinking pathways and cell-cell interactions that may potentially be involved in HF cycling. We begin by detailing basic criteria that a plausible hair cycle theory should meet and then define the key dynamic features that characterise the hair cycle. This ultimately leads us to a simple but prototypic mathematical model of human HF cycling.

5.5 ESSENTIAL FEATURES OF A GOOD HUMAN HAIR CYCLE THEORY

A satisfactory theory of the human HF cycle should be able to explain, firstly, the autonomy of the cycle. It is particularly apparent that in the human HF the "oscillator system" governing the hair cycle rhythm is located in the HF itself. This is supported, for example, by the maintenance of location specific hair cycle features in transplantation surgery. A second key feature of a hair cycle theory should explain its unique rhythmicity i.e. a long anagen phase, extremely rapid catagen stage and relatively short telogen phase. Thirdly, the central role of the HF mesenchyme (DP and proximal CTS) in hair cycle control must be incorporated and explained (Paus et al., 1999a, Paus and Foitzik, 2004). Another important aspect that the theory should address in human hair cycling is the diverse periodicity seen *in vivo* between different HFs (for example how HFs located in anatomically different sites may come to vary). Lastly, a satisfactory theory of the hair cycle should address or be able to hypotheses as to how HFs might respond to specific treatment and how known hair disorders may arise from the normal healthy HF cycle.

5.6 IDENTIFYING THE KEY PROCESSES AND DYNAMICAL CHANGES IN THE HAIR CYCLE

The HF is a highly dynamic mini-organ in which multiple distinct cell populations that originate from mesoderm or (neuro-)ectoderm intimately interact in a precisely coordinated fashion in order to temporarily and rhythmically generate a (usually pigmented) hair shaft. The HF is predominantly constituted by epithelial cells, whose activities are controlled by specialised mesenchymal cells, i.e. inductive fibroblasts of the DP and the CTS. Jointly, these epithelial and mesenchymal cell populations control the activity of neural crest-derived, specialised melanocytes of the HF pigmentary unit (HFPU) (Schneider et al., 2009, Tobin, 2011). All three interacting cell populations arise from and are replenished by epithelial (or melanocyte) stem cells that are

mainly located in the so-called bulge region or secondary hair germ, or from stem cells located in the HF mesenchyme.

Dramatic structural changes, inextricably linked to a dynamic redistribution of cell populations, occur in the HF as it processes cyclically through the three stages of the hair cycle after morphogenesis (catagen→telogen→anagen →catagen) (Paus and Foitzik, 2004). In order to establish the core events that may be responsible for the hair cycle rhythm, the necessary cell populations, processes and interactions characterising the major cyclical HF transformations must be defined. A summary of these features during each hair cycle phase is provided in Table 5.1. Where available, estimates of population numbers are given. The bulge region and the secondary hair germ of the HF houses epidermal stem cells. Approximately 100-200 stem cells are located in the bulge of mouse pelage HFs. Proliferation of these epithelial stem cells occurs during late telogen and early anagen probably following activation by DP fibroblasts (Zhang et al., 2010, Waghmare et al., 2008, Ito et al., 2004, Greco et al., 2009). The stem cell progeny (transient amplifying cells (TACs)) proliferate to create the ORS, IRS and hair matrix (Ito et al., 2004, Zhang et al., 2009). It is not clear at present whether these processes of proliferation and migration cause the number of stem cells to increase during the hair cycle or whether this activity leads to the production of semi-differentiated cells (TACs) to maintain the stem cell niche at an approximately stable number (Zhang et al., 2009, Wilson et al., 1994, Ito et al., 2004, Lavker et al., 2003) (see Table 5.1 and Figure 5.1) Apoptosis has a negligible role in the stem cell niches and these cells are spared from the extensive apoptosis that characterises catagen. This preserves a cell pool that remains permanently available for HF regeneration (if epithelial HF stem cells get depleted, this results in scarring alopecia) (Harries and Paus, 2010).Therefore, an important tenet for the design of the hair cycle model is the assumption that the stem cell population within its niche remains largely constant and serves as a permanent pool for hair MKs and the HF (Figure 5.1).

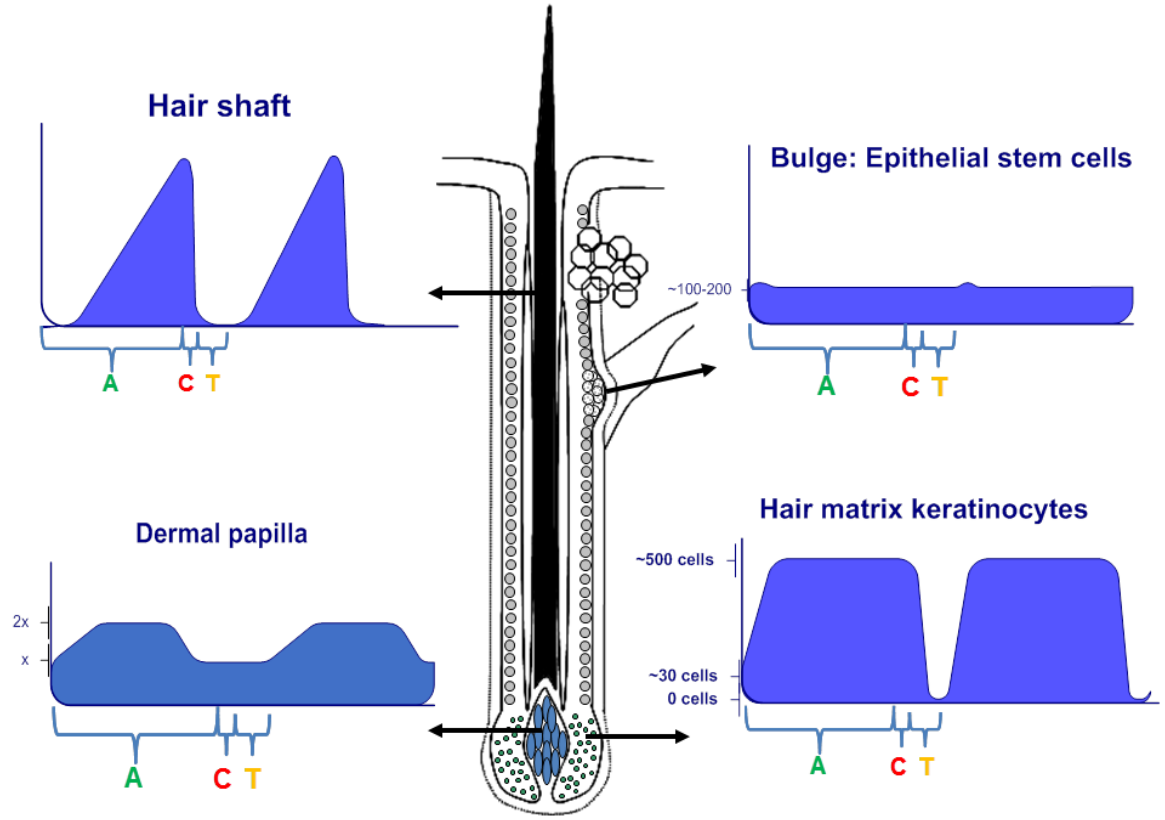

Figure 5.1: Dynamic profiles of populations in the hair follicle

Each cell population exhibits a unique dynamic profile in line with stages of the hair cycle. Anagen (A), catagen (C) and telogen (T). The figure shows an anagen hair follicle. Dynamic profiles are estimates of population dynamics of several core hair follicle cell populations obtained from the available evidence. The schemas depict the size of each population during each cycle stage. This investigation into the hair cycle on the population level summaries the behaviour from a compartmentalised viewpoint. In this model, we focus on the hair matrix keratinocytes (which at numbers close to zero also captures hair germ cells in this compartment). The matrix keratinocytes population is able to capture, in the simplest form, the core events of remodelling, regression and rest during the hair cycle. In addition, the matrix keratinocytes directly supply hair shaft cells (trichocytes).

MKs arise from the differentiation of TACs, which themselves arise from stem cells the number of MKs differs greatly during the hair cycle (Table 5.1). During anagen, MKs undergo rapid proliferation and then terminally differentiate into various epithelial lineages that form the hair shaft and the IRS. The ORS appears to be largely generated by the immediate progeny of the TACs that have arisen from HF epithelial stem cells in the bulge (Panteleyev et al.,

2001, Ito et al., 2004). When MK cells proliferate they do so to replace those that have already undergone terminal differentiation into the hair shaft and IRS Figure 5.1. Thus, another important tenet of our hair cycle theory is that the population size of MKs determines the size cell population available for hair shaft and IRS production.

In adult human scalp skin, hair shaft production follows an approximately linear growth pattern *in vivo*, with the hair shaft thinning at the end of anagen (Ibrahim and Wright, 1982). Even microdissected and amputated hair bulbs of terminal human scalp HFs in anagen VI demonstrate the same hair shaft production speed as the living human scalp (Philpott et al., 1990). In Figure 5.2, we demonstrate the hair shaft elongation rate of anagen scalp HFs isolated from 18 different human individuals, whereby the linearity of hair shaft production is shown. Therefore, our mathematical model proposed below aims to produce a similar, approximately linear, human hair growth pattern. However, while hair shaft formation is linear, HF cycling is not. Each hair cycle phase is of very divergent length (for example, lasting weeks in catagen to years in anagen in human terminal scalp HFs).

Catagen heralds the complete elimination of MK cells via apoptosis. The population remains at or near zero during telogen until the onset of the next anagen phase. When MKs undergo apoptosis in catagen, the supply of cells to the hair shaft is interrupted and hair production ceases. Very early during the anagen-catagen transformation, intrafollicular melanogenesis and all melanosome-based transfer of melanin from HFPU melanocytes into future hair shaft keratinocytes (trichocytes) is abruptly terminated (Slominski et al., 2005, Tobin et al., 1998, Tobin, 2011). As a result, the old hair shaft from the preceding anagen phase is transformed into a so-called “club hair”, whose proximal end is non-pigmented. This club hair is subsequently shed during exogen or is pushed out by the new hair shaft that is generated in the next anagen phase (Higgins et al., 2009).

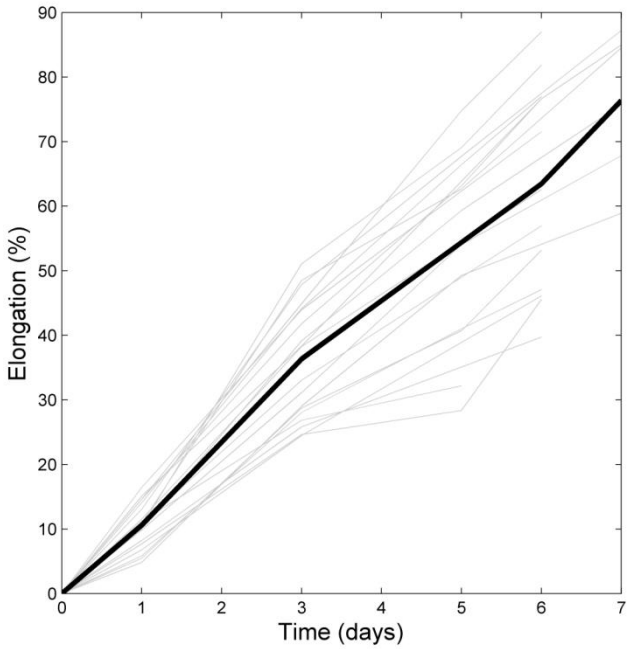

Figure 5.2: Elongation of human hair follicles in organ culture

Human hair follicle elongation data obtained from 18 patients (each patient is shown as the light grey lines) and the average percentage elongation of the 18 patients is shown by the thick black line.

The dynamics of the MK cell population encompasses all key phenomenological cyclical events of a) hair production during anagen, b) cessation of hair production during catagen and telogen, and c) production of a new hair with each anagen phase. MK apoptosis during the catagen phase results in involution of the lower two thirds of the HF whereas MK proliferation during anagen represents a key event of cyclical HF regeneration. Since MKs produce hair via anagen-coupled terminal differentiation, the dynamics of the MK population have a crucial role in abnormalities such as hair loss, which are understood to be pathologies of HF dynamics (Paus et al., 1999a, Paus, 2006). Therefore, the MK population shows the most overt and dramatic changes of cell populations within the HF with proliferation, differentiation and apoptosis identified as key processes dictating these changes (Figure 5.1 and Table 1). In addition, MKs are extremely sensitive to damage (e.g. by drugs, reactive oxygen species, radiation, inflammatory mediators, metabolic and hormonal

abnormalities) and thus play a crucial role in multiple different hair loss disorders (Bodó et al., 2010, Paus, 2006). Therefore, we identify MKs as an excellent cell population to focus on when developing a simple mathematical model of HF cycling that operates at the level of tissue level dynamics.

The CTS and the DP constitute the HF mesenchyme, without which proper HF morphogenesis and cycling are impossible. Indeed, inductive signals from CTS and DP fibroblasts are essential for the epithelial-mesenchymal crosstalk that drives HF cycling (Botchkarev and Kishimoto, 2003, Yang and Cotsarelis, 2010). The DP sits in the centre of the hair bulb and is directly connected to the CTS by the dermal stalk, with MKs enveloping the DP from all sides during anagen (Figure 5.1). A special, dynamically remodelled basement membrane separates MK and DP cells and is needed for proper epithelial-mesenchymal communication in the HF (Link et al., 1990). The unique nature of the bi-directional communication between these two cell populations is evident from the fact that this membrane becomes fenestrated during anagen and that DP fibroblasts have cell processes that protrude into the innermost layer of the hair matrix (Matsuzaki and Yoshizato, 1998, Stenn and Paus, 2001, Nutbrown and Randall, 1995). Without fully functional bi-directional communication between MKs and DP cells HF cycling becomes grossly disturbed and eventually ceases altogether; if the disturbance persists, HFs become dystrophic and eventually disappear.

The dynamics of the DP are mainly determined by bi-directional, hair cycle-dependent fibroblast migration between the DP and the proximal CTS (Table 5.1) (Tobin et al., 2003). Under physiological conditions, there is extremely little, if any apoptosis in the DP during the hair cycle, even in catagen and even under conditions that induce massive MK apoptosis (such as chemotherapy (Lindner et al., 1997)). Also, fibroblast proliferation within the DP is a rare event and may essentially be limited to a narrow window during anagen development (Tobin et al., 2003, Paus and Foitzik, 2004).

Therefore, as MK-DP cell interactions are undoubtedly crucial for normal HF cycling, signals emanating between the two compartments need to be

incorporated in the model. However, for simplicity's sake, DP cell numbers shall not be explicitly modelled.

To summarise, the hair cycle in man (and all other hair-bearing mammals) is underpinned by dynamic changes at the level of defined populations. Among these, MKs are an important cell population on whose analysis a theory of HF cycling can be based. This is since MK dynamics most perfectly reflect all key phenomena that underlie HF cycling, i.e. rhythmic changes in i) proliferation, ii) apoptosis, and iii) differentiation. In addition, since communication between e MK with the mesenchymal HF is essential for hair cycling, our attempt of a dynamical theory of human HF cycling will be based on a mechanistic mathematical description of MK cell numbers (changes in which result from MK proliferation, terminal differentiation or apoptosis) supported by communication with the DP (Figure 5.3). By highlighting the behaviour of selected HF cell populations and understanding the processes that govern the changes in cell numbers, we are able to specify a set of fundamental observations that should be captured in an adequate model for hair cycle dynamics. The most salient of these features is the asymmetric duration of each phase of the hair cycle. Based upon the aforementioned evidence, we now proceed to a mathematical formulation of human HF cycling.

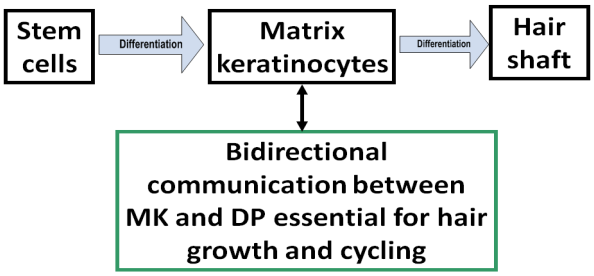

Figure 5.3: Schema representing the mathematical model's core component and links to other cell and compartments within the hair follicle

The core population of matrix keratinocytes are related to epithelial stem cells that supply new cells to the hair follicle (via differentiation). Matrix keratinocytes then differentiate into the hair shaft. The last important compartment involved is the dermal papilla that provides essential communication for hair cycling.

Table 5.1: The population dynamics of distinct cell populations in the hair follicle.

The number of cells in each population may be affected by; proliferation, differentiation, apoptosis and migration and these events are marked as present abundantly (++++) or not present (-) in line with hair cycle stages anagen, catagen and telogen. SC Stem cell, DP Dermal papilla, MK Matrix keratinocytes, CTS Connective tissue sheath, TAC Transient amplifying cell, ORS Outer root sheath, IRS Inner root sheath.

Population		Anagen	Catagen	Telogen	References
SC	**No. of cells**	100-200	100-200	100-200	(Zhang et al., 2010, Waghmare et al., 2008, Hsu et al., 2011)
	Proliferation	++. Early anagen. Slows by late anagen. 2-5 divisions in one hair cycle.	-	-	(Zhang et al., 2009, Wilson et al., 1994, Ito et al., 2004, Hsu et al., 2011, Waghmare et al., 2008)
	Differentiation	+++ stem cell niche/germ transition zone. To TACs and MKs	-	-	(Zhang et al., 2009, Lavker et al., 2003, Hsu et al., 2011)
	Apoptosis	-	-	-	(Ito et al., 2004, Hsu et al., 2011)
	Migration	To hair germ & basal layer ORS (May already be TACs)	Lateral migration in newly generated club hair	Bulge cells leave the niche	(Zhang et al., 2010, Hsu et al., 2011, Zhang et al., 2009, Lavker et al., 2003)
MK	**No. of cells**	100s	0	20-40 cells	(Zhang et al., 2009, Ito et al., 2004).
	Proliferation	++++	-	-	
	Differentiation	++++. Into IRS and HS	-	-	
	Apoptosis	-	+++++	-	(Lindner et al., 1997, Matsuo et al., 1998).
	Migration	-	-	-	(Taylor et al., 2000).

Population		Anagen	Catagen	Telogen	References
HS	**No. of cells**	Proportional to no. of MKs. Fine distal tip, thicker mid-region, narrow proximal club	Ceases in early and mid-catagen	0	(Tobin et al., 2003, Ibrahim and Wright, 1982)
	Proliferation	-	-	-	
	Differentiation	+++	-	-	
	Apoptosis	-	Mid & late catagen	-	(Matsuo et al., 1998, Lindner et al., 1997)
	Migration	-	-	-	
DP	**No. of cells**	Double no. in telogen. Ratio DP:MKs determines hair width	-	½ anagen	(Tobin et al., 2003, Ibrahim and Wright, 1982)
	Proliferation	++++ Greatest anagen IV. Rare at anagen VI	-	-	(Tobin et al., 2003)
	Differentiation	-	-	-	
	Apoptosis	-	-	-	(Lindner et al., 1997, Matsuo et al., 1998, Soma et al., 1998)
	Migration	+++ Into DP from CTS. In anagen VI cells migrate from DP to CTS	Early catagen: (~50% migrate to CTS)	-	

Table 5.1 continued: The population dynamics of distinct cell populations in the hair follicle

The number of cells in each population may be affected by; proliferation, differentiation, apoptosis and migration and these events are marked as present (+) or not present (-) in line with hair cycle stages anagen, catagen and telogen. SC Stem cell, DP Dermal papilla, MK Matrix keratinocytes, CTS Connective tissue sheath, TAC Transient amplifying cells, ORS Outer root sheath, IRS Inner root sheath.

5.7 A PROTOTYPIC HUMAN HAIR CYCLE MODEL

5.7.1 Model formulation

On the basis of the features elaborated above (see Figure 5.4 and Table 5.1) we formulate the following model for human HF cycling. The model focuses on the dynamics of MK cells with respect to the population level processes of proliferation, apoptosis and differentiation. A schematic overview of the model is provided in Figure 5.4.

In general, the dynamics of MK cells, x, under these processes, can be captured mathematically as follows (Equation 1):

$$\frac{dx}{dt} = f(x) - g(x) + (a - b * x) \qquad (1)$$

The two functions, f and g, represent proliferation and apoptosis, respectively, and are in general non-linear. We note that both are assumed to depend on the state of the system, i.e. the size of the MK population. Parameter *a* represents a constant input to the population from stem cells and the term *bx* encompasses all processes leading to a decrease in the number of MKs apart from apoptosis, including differentiation.

We assume saturation in growth, which is modelled with a saturation function e.g. $\frac{p_1.x^n}{p_2 + x^n}$. This assumption is justified as growth of MKs is likely to saturate depending upon factors such as the supply of nutrients (which are not modelled explicitly here). The simplest case is when *n*=1 which leads to a hyperbolic function. The apoptotic function, g, follows a similar form, however we also include the possibility for feedforward inhibition via the parameter, *k*:

$$\frac{dx}{dt} = \frac{p_1.x}{p_2 + x} - \frac{p_4 x}{p_5 + x^k} + (a - bx) \qquad (2)$$

Within this framework, we introduce communication between the MKs and the DP. It is assumed that feedback with the DP affects either proliferation or apoptosis of MKs, for example via papilla morphogens or endogenous inhibitors (Paus et al., 1999a, Stenn and Paus, 2001, Botchkarev and Kishimoto, 2003). These processes enter as additional terms in *f* and *g*, dependent upon a new variable, *z*. Here, we consider negative feedback only, introducing terms for feedback inhibition of the proliferative term and feedback activation of the apoptotic term. This leads to the following form:

$$\frac{dx}{dt} = \frac{p_1 x}{p_2 + x} / (p_3 + C_{prol} * z_1) - \frac{(p_4 + C_{apop} * z_1) * x}{(p_5 + x^k)} + (a - bx) \qquad (3)$$

Here, constants C_{prol} and C_{apop} regulate the strength of feedback of z on the population equation for x. In the present contribution we focus on the role of proliferation control (governed by parameter C_{prol}). We briefly explore the effect of apoptotic control (governed by parameter C_{apop}) on the cycling behaviour but leave a detailed investigation of this term for future research. The index in variable z refers to the two-compartment version described below.

Since communication between the hair matrix and DP are key to the hair cycle these spatial considerations are taken into account in the model (Figure 5.4). We start with the simplest formulation of communication between two compartments, which is assumed to be mediated by signalling molecules. Specifically, we use the following set of differential equations (eq. 4):

Compartment 1:

$$\frac{dx}{dt} = \frac{p_1 . x}{p_2 + x} / (p_3 + C_{prol} . z_1 - \frac{(p_4 + C_{apop} . z_1) . x}{(p_5 + x^k)} + (a - bx)$$

$$\frac{dy_1}{dt} = c_1 . x + D_y (y_2 - \delta_1 . y_1)$$

$$\frac{dz_1}{dt} = D_z (z_2 - \delta_2 . z_1)$$

Compartment 2:

$$\frac{dy_2}{dt} = D_y(y_1 - \delta_3 . y_2)$$

$$\frac{dz_2}{dt} = c_2 . y_2 + D_z(z_1 - \delta_4 . z_2) \quad (4)$$

It is assumed here that the MK population produces a signalling molecule y (at rate c_1) which produces no further direct effect on the population dynamics. However, it diffuses away from the compartment and can thereby either disappear altogether (being degraded or diffuse into compartments where it exerts no effect either) or it can diffuse into compartment 2 (the DP) where it induces the production (or activation) of a regulatory molecule z at rate c_2. This regulator, in turn, exerts no effect in the DP but can diffuse in to either the surroundings or into compartment 1. The diffusion process is modelled by incoming molecules facilitating the production of native intermediaries. The inclusion of δ accounts for the extent to which created the native intermediaries are lost above the rate at which they are created. Thus this accounts for escape and degradation. In compartment 1, control of the keratinocyte population is then performed by the regulator via proliferation inhibition or apoptosis activation as in the model equation (4) above. The diffusion processes take place at two different rates (D_y and D_z) which are the permeation constants in the present model. They would turn into formal diffusion constants in a space-continuous reaction-diffusion model. For all these processes we use first order differential equations as used e.g. for (bio)chemical reactions (see Chapter 4).

5.7.2 Addition of hair shaft growth to the model

Hair shaft production is the most distinctive output of the HF. It can be considered a marker for healthy HF function and normal cycling dynamics. Therefore, hair shaft (h) production was added to the model via an additional variable. A growth rate; dh/dt=αx, is assumed in accordance with the

relationship between the MK cell population size and hair shaft production as discussed in Section 5.6 (Figure 5.2). Without loss of generality, we assume α=1. In order to simulate the termination of hair growth during telogen (relative quiescence) we introduce an algorithm which "wraps" the hair length back to zero during this stage. This is achieved by locating the plateau as a period of small increase in growth and applying a threshold to the derivative of the hair growth variable h. During time periods below this threshold, the hair length is reset to zero; with hair beginning to grow again once the threshold is traversed.

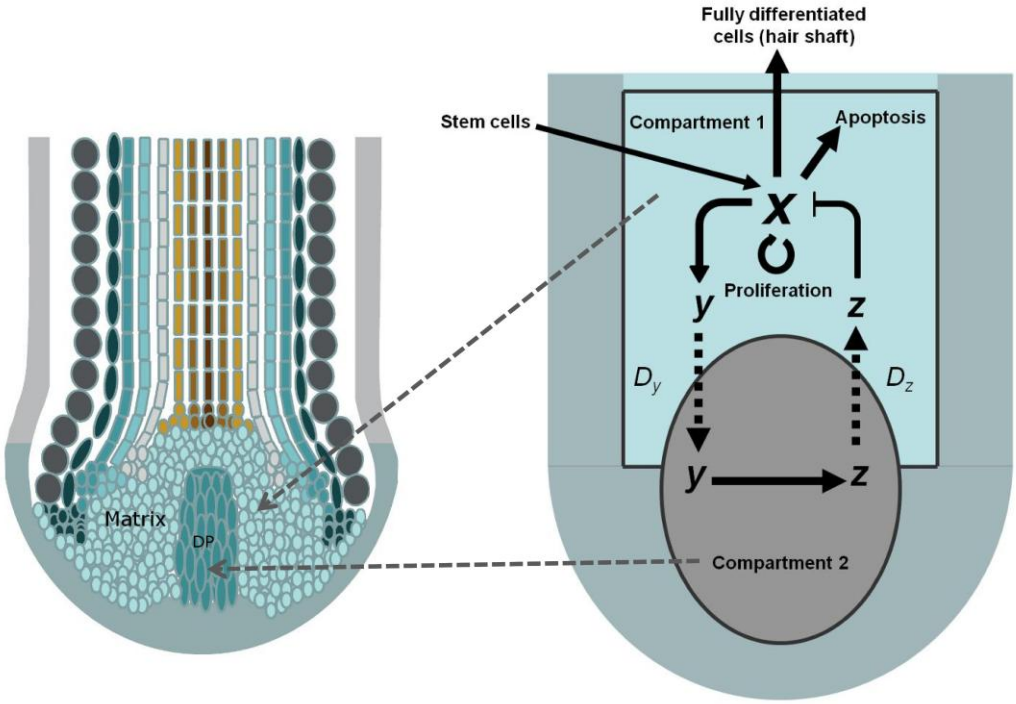

Figure 5.4: Schema of the two compartment model.

x denotes the matrix keratinocyte population in compartment 1 (epithelial hair follicle). Processes affecting the size of x are a constant input a (stem cell input), a proliferation process, an apoptotic process and a constant linear output denoting the differentiation of matrix keratinocytes into the other cell types i.e. layers of the inner root sheath and hair shaft. Bidirectional communication between compartment 1 and 2 is set up by the production of variable y that diffuses into compartment 2 causing the production of z. z diffuses back into compartment 1 where it affects the proliferation and apoptotic processes for x

5.7.3 The unperturbed model

In this section we analyse the model eq. (4) in terms of its key nonlinear components, the power k in the apoptotic term and the influence of feedback in the proliferation term. Using the hair growth variable h as output, we then demonstrate the capability of the model to reproduce key features of the human hair cycle. Since we are ultimately interested in applying the model to hair pathology and its treatment, we also investigate some features of abnormal (non-oscillatory) dynamical behaviour. In the following section we report some results on the model's response to external stimuli.

5.7.4 Steady State for C_{prol}=0 and k=1

Figure 5.5 shows bifurcation diagrams scanning one of the system parameters, namely, the growth rate $p1$, for different values of C_{prol} and k. All other parameters are fixed to the values displayed in Table 5.2. The simplest case is C_{prol}=0 and k=1, i.e. there is no feedback loop in the model and the apoptotic rate is modelled as a hyperbolic function just as the proliferation rate. This reduces the model to a one-dimensional system that can only have steady state solutions. Figure 5.5a shows the corresponding bifurcation diagram. For the values of $p1$ displayed there is only fixed point behavior. At $p1 \approx 0.04$ there is a transcritical bifurcation leading to an abrupt change of slope in the otherwise linear dependence of the steady state value on $p1$. Such a behavior predicts that the dependence of an observed temporally stable keratinocyte population shows different rates of change as a function of the population growth rate. It cannot, however, account for autonomous cycling of the population. Nor does it allow for an interpretation of discrete growth states (anagen and telogen).

5.7.5 Hopf oscillations for C_{prol}=1 and k=1.

When C_{prol}=1, the keratinocyte population is additionally influenced by the regulatory factor z, implying that the model is now composed of 5 dependent variables. Therefore we noe have acontrol loop that results in feedback

inhibition because an increase in the concentration of z reasults in a decrease of the growth rate of the keratinocyte population. Feedback inhibition is implemented in our model via a two-species mechanism involving communication between the two compartments (Figure 5.4).

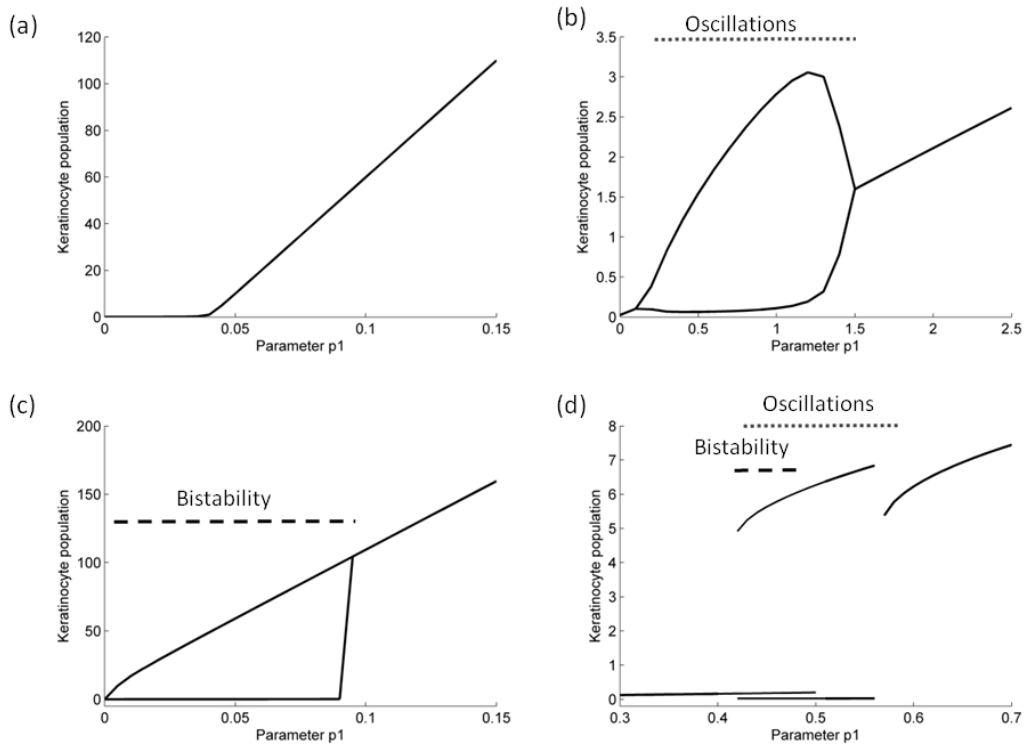

Figure 5.5: Bifurcation diagrams

Each subgraph demonstrates the bifurcations at different values of k and C_{prol}. In subgraph (a) k=1, C_{prol} = 0, in (b) k=1, C_{prol} = 1. (c) demonstrates the results when k=2 and C_{prol} = 0. In (d) k=2, C_{prol} = 1, These graphs demonstrate that the human hair cycle requires feedback inhibition in order to produce cycling behaviour C_{prol}=1, in addition, bistability when k=2 as shown in subgraph (d) this leads to inhibition of apoptotic process when x is large (feed-forward inhibition) and results in the asymmetrical waveform and low frequency oscillations exhibited in the human hair cycle

Such feedback is necessary and in our case sufficient to produce cyclical behaviour (Figure 5.5). The oscillatory behavior is seen for a wide range of parameter p1. Its amplitude depends strongly and nonlinearly on the value

chosen and shrinks to zero as either bifurcation point is approached. A time series of the oscillation is shown in Figure 5.5a (grey) and a phase space representation of the underlying limit cycle is shown in Figure 5.5b(grey). Mathematically, the oscillations result from a dynamical instability of a steady state. The specific instability in equation (4) is a supercritical Hopf bifurcation with the real part of a pair of complex eigenvalues passing from negative to positive. This happens twice and therefore the oscillatory region is bounded by stable fixed point behaviour. All mathematical terms relating to this feedback loop are linear with the exception of the control of the MK population by species *z,* originating in the DP. Therefore, the nonlinearity that causes self-organising instabilities in our model, resides in the equation for the keratinocyte population.

This form of the equation with C_{prol} =1 and k=0 is therefore a variant of the kinetic feedback inhibition oscillator proposed by Goodwin (1963). Here, the delay in the feedback to the keratinocyte population is in part due to transport processes that mediate the feedback. A fast oscillating keratinocyte population is produced by these conditions and thus, feedback is demonstrated to be important to gain cyclical behaviour in the human hair cycle according to this model.

5.7.6 Bistability for C_{prol}=0 and k=2

If instead of switching on the feedback control (as described above) forward inhibition of the apoptotic process by the keratinocyte population is included (i.e. k=2) the dynamics of the keratinocyte population remains independent of other processes but shows a new type of dynamical phenomenon. Figure5.5c shows that this situation generates a region of bistability (compare with Figure5.5a). Two fixed point solutions (represented by black lines) can be observed for a finite range of parameter *p1*.

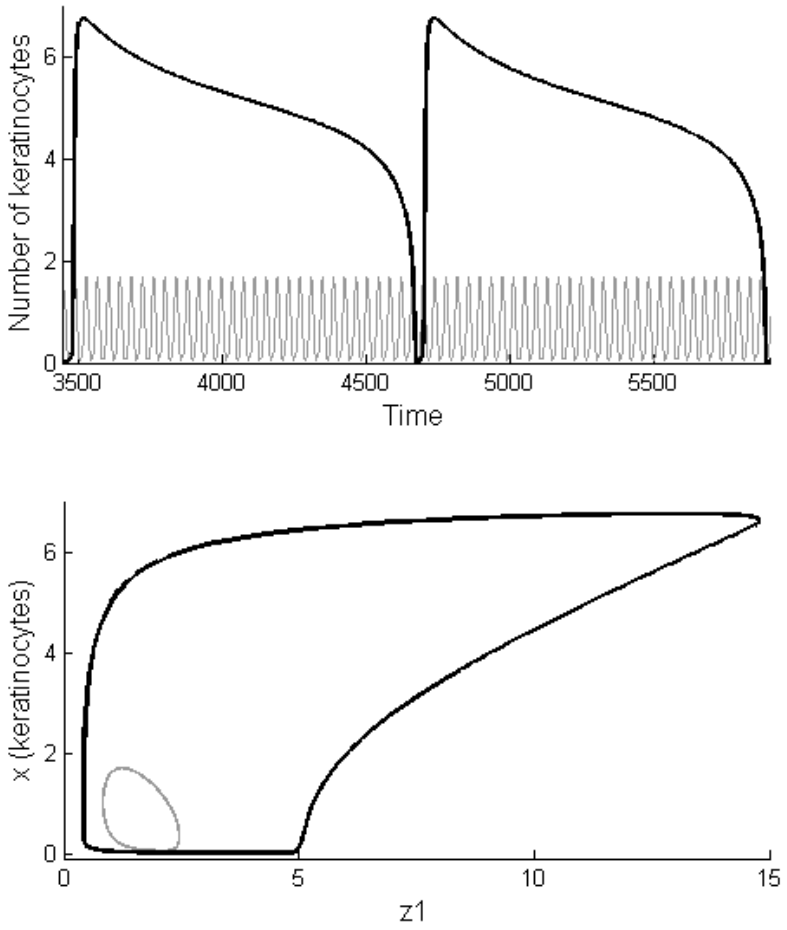

Figure 5.6: Hair cycle model time series and phase space

(a) Time series of the hair cycle model, the output of the model simulates the characteristic dynamic behaviour of the hair matrix keratinocytes during the hair cycle (black line) where k=2. The output is contrasted with the case when k=1 (grey line). (b) The relationship between the level of matrix keratinocytes and z1. The large phase space is contrasted with the small trajectory when k=1 (grey).

This is due to the appearance of three (real) steady state solutions in the fixed point equation for *x* (dx/dt=0). In such a situation, when parameter *p1* is varied across the borders of the region of bistability, the system can be induced to change from one steady state to the other (e.g. switching from a near-zero to large value when *p1* is increased above a value of 0.09 (see Figure 5.5c). We therefore explore a bistable switch as a possible mechanism for HF dynamics.

The lower steady state would represent “telogen” and the upper steady state “anagen”. In our model one possible realisation of switching would be that random fluctuations of the keratinocyte population result in (self-organised) switching between the states. Mathematically, the two stable states are separated by an unstable state which corresponds to a critical population size that lies between the no growth and the growth state (Figure 5.5c). This critical population size presents a decision point. If a random fluctuation of a population in the no growth state exceeds the critical size, the population will continue to grow until it reaches the growth state and then remain there. Switching back happens when a random fluctuation of the population in the growth state reaches a value that lies below the critical state. The population will then keep shrinking until it falls to the “no growth” state. In contrast, if a perturbation leads to a change close to the critical size but not quite reaching it, the population reverts to the original state.

Adding a noise term to the model equation (4) with k=2 and C_{prol} =C_{apop}=0, the amplitude of the noise can be adjusted such that it leads to random variation about a given steady state. When preparing the model in the bistable region near the critical parameter value where the no growth state disappears ($p1$≈0.09), we can adjust the model in the presence of noise perturbations such that the mean duration in anagen is much longer than the duration in telogen as is the case in human hair cycling. However, careful preparation of the parameters of the model is required to reproduce these characteristics. As in the case of Figure 5.5a, the exclusively steady state solutions found do not allow for the explanation of an organised cyclical process.

5.7.7 Relaxation oscillations for C_{prol}=1 and k=2

In light of the above considerations, where neither the supercritical Hopf oscillations nor the bistability alone may fully account for the dynamics of the HF, we further explore the parameters using the combination of both. Now there is a feedback control of the keratinocyte population by variable z and there is a forward inhibition by the population itself, i.e. C_{prol}=1 and k=2. Figure

5.5d shows the corresponding bifurcation diagram where a region of bistability and a limit cycle region are indicated by a dotted bar. In this case, the forward inhibition again generates a region of bistability. However, compared to the situation with C_{prol}=0 (bistability of two fixed points), the bistability now is between a near-zero fixed point and a limit cycle (compare Figures 5.5c and d). The bistable region starts with a fold of limit cycles bifurcation at $p1 \approx 0.415$ and ends with a subcritical Hopf bifurcation at $p1 \approx 0.51$.

The limit cycle is generated in the afore-mentioned fold of limit cycle bifurcation at $p1 \approx 0.415$ and vanishes with a saddle-node on limit cycle bifurcation at $p1 \approx 0.56$. In comparison with the situation in Figure 5.5b (no forward inhibition) the oscillations now start and vanish abruptly, i.e. with finite amplitude at the bifurcation point. The variation of amplitude In this region is much smaller than in the situation with k=1. Further differences between the dynamics of the limit cycles in the cases of Figure 5.5b and 5.5d are shown in Figure 5.6 where time series (Figure 5.6a) and phase space portraits (Figure 5.6b) are plotted for k=1 and k=2. The Hopf cycle (k=1) has a small amplitude, high frequency, and a comparatively harmonic waveform. The cycle with k=2, in contrast, has a large amplitude, low frequency, and strongly asymmetric waveform. Notable generic features of this latter, non-harmonic limit cycle are:

i) Two plateau-like phases where the change of state is comparatively slow. One is near zero and the other has an amplitude between 4 and 6.8 approximately. Both phases can be related to the two respective fixed points in the bistable situation with C_{prol}=0 and k=2 as shown in Figure 5.5c.

ii) Comparatively fast transitions between the two plateau-like states.

iii) Notably, the durations of the two plateau-like states differ strongly with a long upper state and a short lower state being a consistent finding in the present model.

Taken together, features i) and ii) define a type of dynamics classified as relaxation oscillations. The notable properties above directly relate to the dynamics of the HF (Figure 5.1 – matrix keratinocytes). The long upper steady

state is interpreted as anagen, the short lower state telogen and the rapid transition from growth to rest; catagen. Asymmetry in phase durations in each stage is representative of the durations of anagen (long), catagen (very rapid) and telogen (intermediate, but relatively short compared to anagen). The strong asymmetry in the cycle is explained by the vicinity of a saddle-node on limit cycle bifurcation which causes slowing down of the anagen phase but not of telogen. Therefore, the dynamics of the HF model requires both bistability and feedback inhibition, as achieved here with k=2 and C_{prol}=1 to approximate the key features of the HF cycle.

In this version of the hair cycle model; the oscillatory time series of the other variables (y and z) produce, in comparison, a qualitatively similar waveform to the one described for the keratinocyte population. However, at a shorter time scale there are significant phase shifts between oscillations in the two compartments and between the oscillations of the keratinocyte population and the concentration of the feedback species z_1.

So far, we have only considered feedback on the apoptotic term in eq. (4). If the feedback loop to the keratinocyte population is instead closed in the apoptotic component, this results in a similar overall result to the above formulation. Model simulations with a parameter setting of C_{prol}=0 and C_{apop}=1 equally produce relaxation oscillations with an asymmetric waveform and distinct growth and resting phases Figure 5.7. The phase space structure is not identical but qualitatively similar, the only significant difference being the large amplitude in the present case (compare Figure 5.6 and 5.7). The differences are due to the asymmetry of the proliferation and apoptosis terms with k=2. Model settings with both feedback controls switched on (e.g. C_{prol}=, C_{apop}=1) also produces large amplitude low frequency relaxation oscillations.

For simplicity, we only explore feedback on the proliferation term (C_{prol}=1, C_{apop}=0) in all studies below. A detailed exploration of apoptotic control is left for an extended version of the model including greater details of the communication channels between the DP and the keratinocyte compartment.

We finally consider hair production in the model in relation to the state of the matrix keratinocyte population. The near zero-state of the population

defines a no growth phase and the upper state defines a period of strong growth. As a passive output of the oscillatory model in Figure 5.8 hair shaft growth has a saw tooth-like waveform interrupted by brief "no growth" periods (shown in Figure 5.8, middle and right bottom panel). We verified the experimental growth pattern of isolated human HFs (total number of HFs = 347) in organ culture from 18 patients. The growth pattern fits the model output, showing an almost linear Figure 5.2. Human HF organ culture has been shown to grow at approximately the same rate as that *in vivo* (Kwon et al., 2006, Philpott et al., 1990) and therefore the reproduction of this supports the model as an approximation of the hair cycle and hair growth.

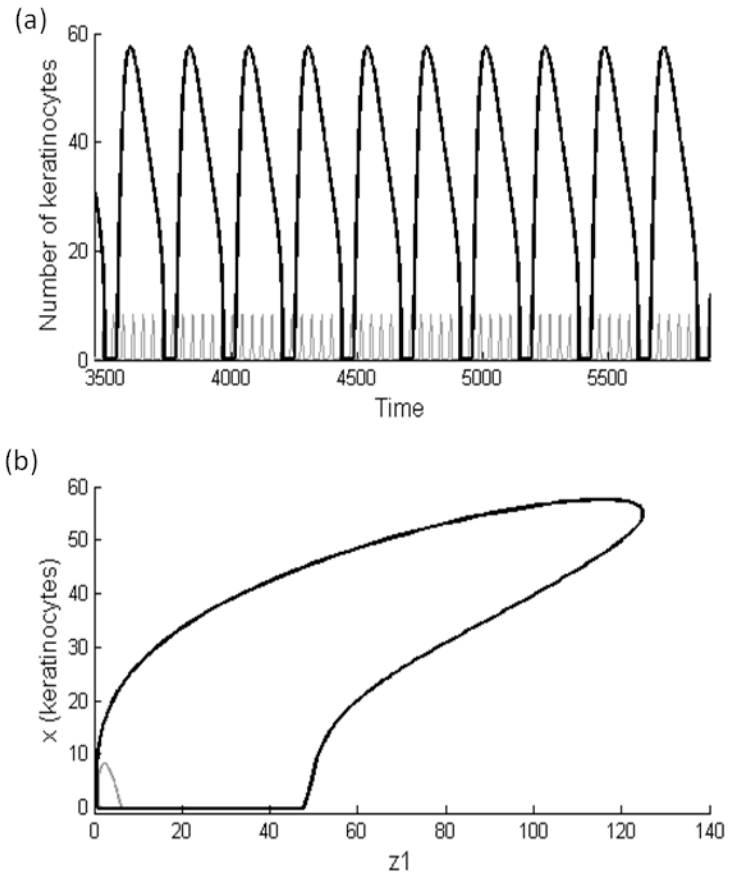

Figure 5.7: Alternative mechanism for the hair cycle where C_{prol}=0 and C_{apop}=1.

(a) Time series showing the model output when k=2 (thinker black line) in contrast to the Hopf oscillations with no Bistability (thin grey line). The frequency is faster when compared to the other mechanism. (b) The relationship between the level of matrix keratinocytes and z1. The large phase space is contrasted with the small trajectory when k=1 (grey).

Table 5.2: Default parameter values used in the hair cycle model. Alterations to the parameter values in the study are listed in the figure legends or in the text in the relevant sections.

Parameter	Value	Parameter	Value
a	0.1	C_{prol}	1
b	0.01	C_{apop}	0
p_1	0.48	C_1	1
p_2	0.1	C_2	1
p_3	0.1	D_y	0.5
p_4	0.5	D_z	0.1
p_5	0.1	α	1
$\delta_1, \delta_2, \delta_3, \delta_4$	2		

5.8 PERTURBATIONS OF THE HAIR CYCLE

We now take the oscillatory model output presented in Section 5.7 as representing healthy hair cycle dynamics and study its properties (as well as the properties of the "no growth" state) under external perturbation. The investigation here aims to realize the impact of i) temporal variation of the environment; ii) external pulses applied during regular growth; and iii) pulse perturbations ("treatment") under abnormal ("no growth") conditions.

5.8.1 Variation of parameters demonstrates a range of dynamics in hair cycling that may account for both normal hair cycling and pathological states

The model predicts different hair cycling lengths depending upon the efficacies of the underlying mechanisms; i.e. different regions of parameter space. The HF does not always cycle and can be arrested in telogen for an abnormally long time period, e.g. in situations of advanced alopecia, and demonstrates transformation in size and dynamic properties depending on skin location or in

the context of hair pathology (Dawber, 1997). HFs are of greatly varying size and produce different types of hair shafts of very divergent length and width, depending on the body region. The model, as evident by the bifurcation diagram Figure 5.5d, is able to reproduce variations in the hair cycle lengths depending on the certain conditions in the model. In Figure 5.8 we demonstrate the output of the model with different values of *p1* on the number of MKs and also the resultant hair shaft. This could potentially explain the various HF sizes and hairs seen *in vivo* and additionally the potential output of no hair growth (Figure 5.8, bottom left panel).

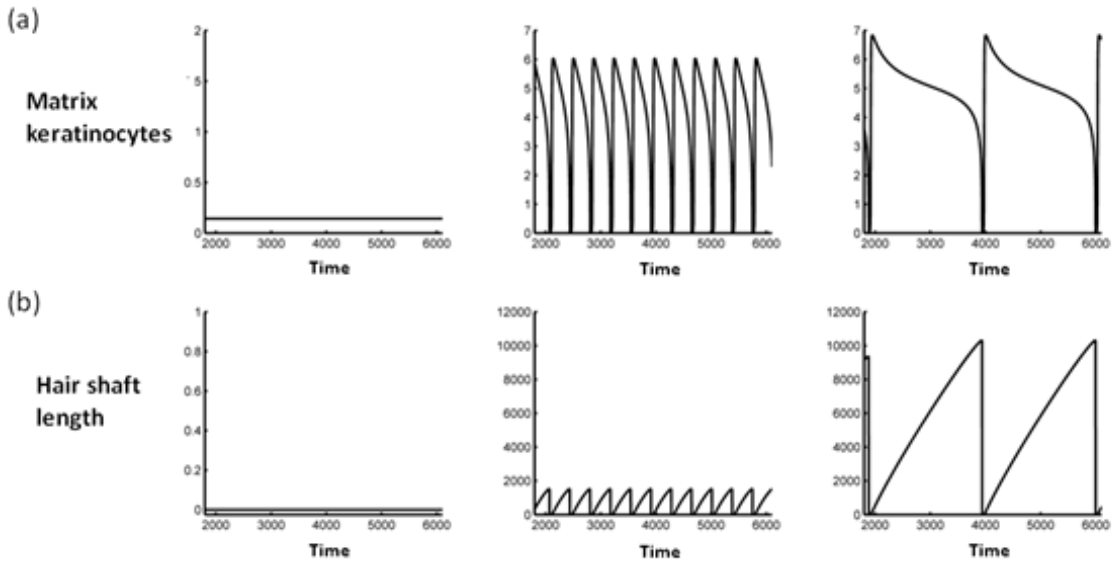

Figure 5.8: Time series of matrix keratinocytes and hair shaft production

Growth of hair can be widely altered depending on the parameter values in the model. Altering one parameter, here p1, demonstrates the "no hair growth" (no cycling, p1=0.35, left panel), small hairs (high frequency hair cycle, p1=0.48, middle panel) and long hairs (very low frequency cycling, p1=0.56, right panel). The transition of the hair follicle in alopecia via the process of miniaturisation may be captured in these transitions whereby the hair follicle shrinks and produces small, ineffective hair (e.g. p1 alters from right to left here). In severe cases of alopecia no visible hair is seen which may be captured by; either short hairs that do not reach the surface (middle panel) or a transition to the no growth situation (left panel).

5.8.2 Pulse perturbation results in changes in normal hair cycling and pathological states

We explored the effect of a pulse perturbation in the key parameters *a* (stem cell supply), *p1* (proliferation rate), and *p4* (apoptosis rate). Initially the time, duration and amplitude of an individual pulse to each of these parameters was fixed. Figure 5.9 shows the result of selected perturbations to the HF oscillator in the standard state (monostable relaxation oscillations). In Figure 5.9a one sees a pulsed increase in parameter *p1* during telogen that leads to a subsequent prolonged anagen phase (in this case approximately a 50% increase compared to the unperturbed phase) and consequently the production of a longer hair shaft.

A similar pulse perturbation of parameter *a* (stem cell input) produced an increase in anagen phase duration (in this case about 90% increase compared to unperturbed phase) and hair length (Figure 5.9b). Since the increase in parameter *a* is proportionally higher than that of *p1* (i.e. 90% increase in parameter value), the effect of this increase is larger and produces a much longer hair shaft.

The administration of a pulse to parameter *p4* within the resting phase produced a prolonged resting phase and also led to greater duration and amplitude of the subsequent growth phase. In contrast, when a pulse in the same parameter was administered during the growth (anagen) phase, anagen duration and the resultant hair length were shortened (Figure 5.9a). Therefore, a phase dependent effect is seen here. Regular maintenance of the change would require regular administrations of pulse perturbations or "treatment" at the correct phase of the hair cycle.

5.8.3 Switching in bistability and excitability as methods to switch from "no hair growth" to the cycling mode

We now explore the model's features outside of the parameter range where the relaxation oscillator is the only solution. The parameters are chosen in the region of bistability where both relaxation oscillations and a lower "no growth"

steady state exist. In this setting we explore the possibility to perturb the system with a pulse to switch behaviour from fixed point to the oscillatory state, i.e. to induce oscillations without permanent change in any parameter.

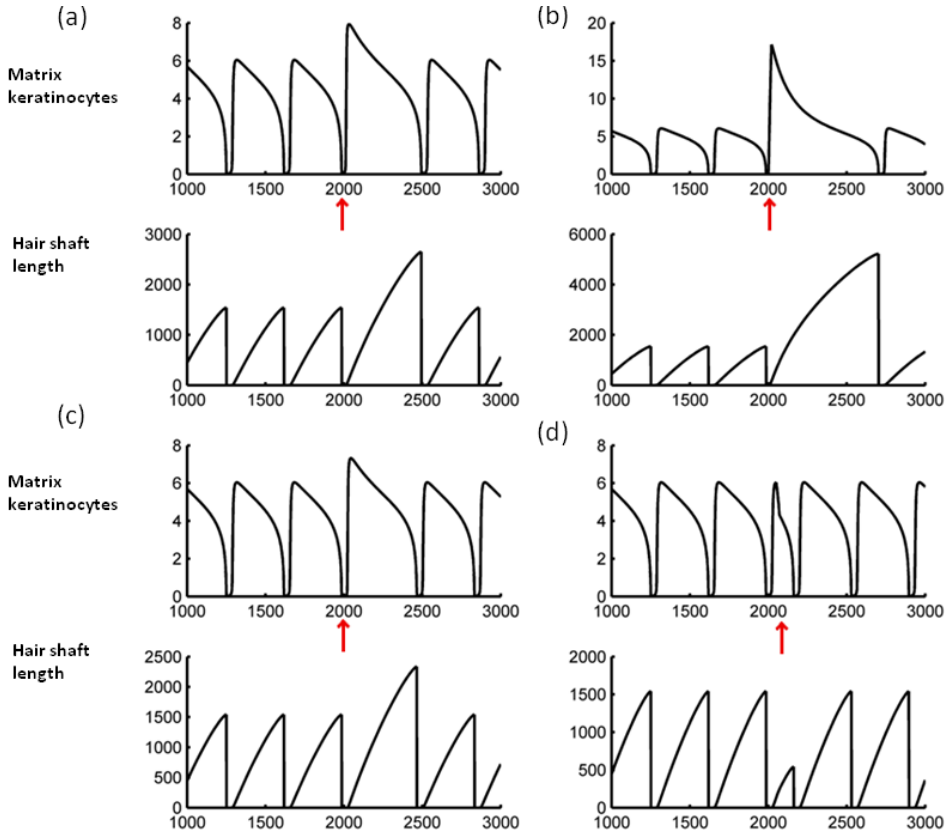

Figure 5.9: Pulse perturbation time series

(a) Pulse in p1 commencing at time t=1995, with a maximum value of a= 1.9. (b) Pulse in a commencing at time t=1995, with a maximum value of a= 1.9, denoted as a red arrow below. (c) and (d) Pulse perturbation of parameter p4 resulted in different effects on the hair cycle and hair growth. The effect was phase dependent with abrogation of anagen if pulsed during anagen (c) or stimulation of a longer hair cycle and hair if perturbation was timed with telogen (resting) phase of the cycle (d). Pulse in p4 at t=2100, with amplitude maximum value of p4=1.9. Pulse timing is marked by red arrow.

The time series (Figure 5.10a) demonstrates a switch from the lower steady state into the oscillatory regime. Oscillations, and consequently hair growth commences as soon as the perturbation has ended. Importantly, as the oscillatory regime is stable, the cycling continues indefinitely in the model. We

test perturbations in all parameters and find parameter *p1* to be the most sensitive in achieving the transition (i.e. inducing permanent oscillations with a minimum of relative change). For example, an 8.8% increase in *p1* achieves the transition. Parameter *c* requires only a slightly larger change (10%) to achieve permanent oscillations.

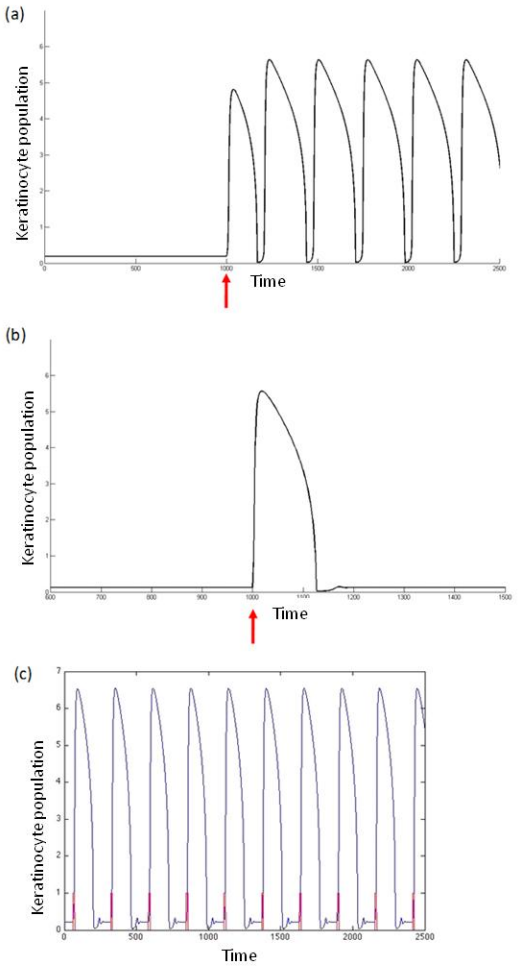

Figure 5.10: The hair cycle model predicts possible mechanisms for the treatment of hair loss.

(a) Demonstrates how switching may be achieved from the lower steady state in the bistable region to the oscillatory state. One pulse in p1 achieved this result. The pulse starts at t=1000 and is of length=5 time points and is a step to a value of p1=0.49. (b) The pulse starts at t=1000 and is length=5 time points and is a step to a value of p1 =0.49. This demonstrates how apparent no hair cycling and thus no hair growth may be perturbed into a whole hair cycle. This is due to excitability demonstrated by the system currently lying outside of the bifurcation point. (c) sinusoidal pulses as in (b) to p1, i.e. regular administered therapy, in this case achieves repeated cycling behaviour.

The fact that the lower fixed point loses stability in a subcritical Hopf bifurcation implies that it might be excitable in the monostable state (Figure 5.5d, p1<0.415), implying that a short pulse (treatment) could start a full cycle. The monostable state would be interpreted as a non-cycling hair (such as occurs in severe alopecia). To test this we apply a pulse perturbation in parameter *p1* to the system prepared in the no growth steady state outside of the bistable region. When the pulse is below a threshold, the effect of the stimulation is negligible and leads to a trivial damped oscillatory return to the no growth state. As such the perturbation can be considered ineffective. If, however, the pulse is suprathreshold as in Figure 5.10b the model produces a large amplitude excursion of nearly the amplitude and rather similar in period to the oscillatory solution (compare with Figure 5.10a). The duration of the pulse was 5 time points, however longer pulses also produce a longer cycle. Therefore, the MK population is in an excitable condition and a comparatively moderate stimulus can induce one full cycle of the HF oscillation. After the one cycle the system returns to the no growth fixed point and remains there, as it is the only stable solution. To maintain cyclical regeneration of hair growth, one must repeat the pulse once the MK population returns to the resting state. This is shown in Figure 5.10c, where a regular pulse of appropriate frequency into the monostable no growth system (with *p1*=0.3) induces "regular" cyclical behaviour. This uses the property that an excitable system performs the full cycle once induced by a suprathreshold stimulus. The period of this induced cyclical behaviour is less than the period in the autonomous cycling, mainly because the system is allowed to settle to the resting state before it is perturbed again. Comparing Figure 5.10b and 5.10c it can be noted that the amplitude of the periodically pulsed system is even slightly bigger than the amplitude of the cycle in the single stimulus simulation Figure 5.10b. If induced regular cycling with full hair growth is desired, the period of the stimuli cannot be decreased above a certain minimum length as a stimulus during the cycle or at the beginning of the resting phase, when the system is refractory, does not lead to a full new cycle. A smaller period than the one chosen in Figure 5.10c leads to irregular hair growth with hairs of different length and decreased average hair

length. Also phenomena like “missed beats” and induction of a full cycle for every second stimulus are observed in these cases.

5.9 DISCUSSION

The human HF exhibits a unique chronobiological rhythm known as the hair cycle. The molecular or cellular “control” mechanism(s) responsible for this regenerative process has not been identified. In this study, we reviewed essential dynamical features of the hair cycle and presented a prototypic mathematical model to advance a theory of the human hair cycle.

The ODE model was constructed from features regarding HF dynamics and interactions derived from the literature and incorporated into the model on the cell population level while specific molecular processes were not included. However, the two compartment model opens the exploration of how human HF dynamics may arise from control processes governing the spatial scale of multi-cellular MK population as a whole.

An important finding in our study is that neither feedback inhibition nor the presence of bistability alone is sufficient to explain the full dynamics of the HF. However, both have been postulated as mechanisms for the hair cycle. Concerning delayed feedback inhibition Chase proposed that the hair cycle is based on an intrinsic inhibition-disinhibition switch (Chase, 1954) and, since then, several theories verbally described the oscillatory nature of the HF as a result of delayed feedback inhibition, although none have led to a mathematical formalisation so far (Paus and Foitzik, 2004, Paus et al., 1999a, Stenn et al., 1999). We show that feedback inhibition indeed allows the production of oscillations in MK numbers and the oscillatory production of hair shafts. In our case part of the delay in feedback arises from transport processes between the two compartments rather than biochemical reactions. This produces oscillations that are described mathematically as the result of a supercritical Hopf bifurcation. Although the frequency of oscillations could be regulated to better fit the low frequency oscillations in the hair cycle via modulation of parameters in the feedback loop; we cannot assume the molecular processes (like synthesis and diffusion) to be much slower than population growth and

decay constants. Therefore, the resultant frequency of oscillations remains on a comparatively fast time scale in the absence of bistability (k=1). Importantly, it is unrealistic that feedback inhibition alone may account for the characteristic profile of the biological process as specified Figure 5.1. The reason for this is that a fast oscillating keratinocyte population would not clearly distinguish between durations of anagen, catagen and telogen phases in terms of periodicity as seen *in vivo* and therefore does not explain the asymmetric low frequency hair cycle profiles observed in human hair cycling.

It is known that a simple linear sequence of biochemical reactions can explicitly produce time delays (see e.g. (Mocek et al., 2005)). The impact of negative feedback modelled by a chain of linear (first-order) reaction terms on the systems dynamics is well-studied, for instance in the Goodwin model (Goodwin, 1963). As the delay mechanism in our model is also described by linear terms, the feedback control (for example of the proliferation) can be expected to have similar impact on the population dynamics. As such the appearance of oscillatory solutions is not unexpected. However, the assumption of a feedback mechanism that involves diffusion between two spatially distinct compartments is a novel mechanism to realize the delay. It depends crucially on the communication between spatially separated compartments.

The presence of a dynamical bistability to explain the two main dynamic "states" (anagen and telogen) of the HF was recently postulated but no mathematical model was provided (Bernard, 2010). The switching between the two states was proposed to be driven by random fluctuations. If we consider bistability alone as a possible mechanism for the hair cycle then this would imply that there is no continuous (monotonous) evolution towards the switching point. In reality, however, catagen HFs cannot transform back into e.g. anagen once they have started to enter catagen; instead, they have to run through telogen in order to re-enter anagen, since this "quiescent" state and its reorganisation of HF architecture appear to be important e.g. for proper reactivation of HF epithelial stem cells in the bulge and secondary hair germ as a prerequisite for anagen development. The *in vivo* situation is that different sub-phases of the hair cycle are defined, but with continuous evolution of

morphological features (Kloepper et al., 2009, Müller-Röver et al., 2001). Therefore, if the mechanism of the hair cycle were to operate only via bistability, the ability to produce the wide range of dynamics typically seen in the HF would be impossible to achieve.

Following these considerations, our theory of the hair cycle therefore requires both bistability and feedback inhibition to produce key dynamical features of the human HCC. When both bistability and inhibitory feedback are present, a cyclical switching occurs between a state of large population with strong growth (anagen), and a subsequent state of near-zero population with no growth (telogen). Anagen is explained as a period in which the proliferation rate and the apoptotic rate change continuously but at two time scales. One in which proliferation dominates over apoptosis such that the population level rises and one in which apoptosis dominates over proliferation and the population level falls. The slow decrease of the population during anagen is due to slow accumulation of the inhibitory feedback species. It continues until a threshold is reached and apoptotic processes take over so the decrease accelerates leading to catagen. The rapid decrease of the keratinocyte population results in abrogation of hair growth and shedding of the hair. The resting period (telogen) then maintains the near-zero population while the impact of the inhibitory species slowly decreases until a second threshold is reached and a new cycle starts leading to the creation and growth of a new hair. Thus, the crucial prerequisite for the switching mechanism is the combination of a bistability between a state of rapid growth and a no growth state with a cyclical process. Autonomous cycling between two pseudo-steady states yields the observed switching. The accumulation of inhibitory signals during anagen is described by Chase and it has been demonstrated experimentally that inhibitory signals are present during telogen in mouse skin (Paus et al., 1990).

The model relies on several assumptions. Firstly, we assume that the behaviour of interest resides at the level of groups of cells; i.e. in the cyclical regeneration of the HF tissue sub-structures during the hair cycle and in the observation of hair growth. Thus, macroscopic cell population considerations form the basis of our theoretical treatment of the HF cycle. Indeed, important

processes will be involved at multiple scales and, in particular, molecular interactions that are often the subject of experimental investigations into the hair cycle will be described on the microscopic scale and here in the model presented we consider the high level of processes that may govern the whole cells and population of cells. This is in line with a current model of interacting populations of HF stem cells in mice (Plikus et al., 2011) and also with the initial dynamical hypothesis of Chase 1954 (Chase, 1954).

Secondly, our population level approach focuses on the cells arising from epithelial stem cells that embody the dynamic changes in HF structure and are directly responsible for hair growth during the hair cycle, namely the MKs. Therefore, we assume that if we understand the controls governing the cyclical regeneration and regression of the MKs then we can understand the hair cycle mechanism. The MK population, at numbers close to zero, is likely to capture the stem cell progenitor population that derive from stem cells and become MKs. For simplicity and to emphasize key dynamic components, we did not explicitly differentiate between these cell types. Similarly, we assumed a simplified constant input of stem cells to the keratinocyte population. Biologically, the system is more complicated and we envisage future models to encompass processes on a multi-scale level. Despite the simplifications here, we have managed to account for a great amount of hair cycling or HF dynamic phenomena.

Thirdly, we assume the process of the human hair cycle is autonomous. This is supported experimentally as described in the introduction and methods, but also by the experimental and modelling work performed by Plikus *et al* who predict the human HF to rely heavily on intrinsic processes in order to cycle (Plikus et al., 2011).

In the model, we are able to observe the strong asymmetry between stage lengths in the human hair cycle caused by the vicinity of a saddle-node on limit cycle bifurcation that leads to slowing down of the anagen phase but not of telogen. The model thus offers an explanation for the unique periodicity of each phase of the hair cycle whereby human scalp hair can grow for some years before it sheds while telogen is typically of the order of a few months. The

previous postulated theories of hair cycling do not address how this salient feature may arise.

Despite the abstraction of the hair biology involved; the model is able to capture the wide variation in dynamics exhibited by the HF and successfully addresses a large proportion of features that are thought essential to a successful theory of the hair cycle (Paus and Foitzik, 2004). The model produces unique asymmetric phases of the hair cycle, and a hair shaft output, as an autonomous process and additionally accounts for varied hair cycle lengths which is dependent on parameter values and even the provides some predictions of how hair disorders such as miniaturization of the HF and severe cases of "no growth" behaviour may arise. We show that the hair cycle and resultant hair may be different lengths by altering parameter values. These parameter differences may reflect the intrinsic properties of HFs located in different body regions or between individuals. This leads to the hypothesis that the intrinsic properties in HFs from one body region to the next (represented by variation in parameters such as *p1*) are the cause of the different hair lengths seen *in vivo*, for example between eyebrow and scalp hairs. Within the present framework, cycle to cycle variation can be accounted for by random fluctuations in model parameters.

Great changes in hair cycle duration and hair growth were demonstrated to occur from one cycle to the next (Tobin et al., 2003) and this can be interpreted as variations of the period (and amplitude) of an autonomous cycling process due to environmental perturbations. In addition, we briefly studied how fluctuations in the lengths of anagen, catagen and telogen from one cycle to the next can be achieved by introducing random fluctuations in the input (supply from stem cells (a)) to the MKs and in the strength of activation of growth of these cells (*p1*) (Supplemental Figures 5.11 and 5.12). Random fluctuations in stem cells and *p1* together seem to be important factors in the model, but for a future sensitivity analysis (to determine the processes that contribute strongest to the variability), estimates of the degree of fluctuations in each parameter are required. This gives a new account of the data presented in relation to the follicular automaton model, which suggests that the hair cycle is

a stochastic switching process assuming two underlying stable states but not an autonomous cycling process (Halloy et al., 2000, Halloy et al., 2002).

As hair disorders are the result of a pathological alteration in normal hair cycle dynamics, the model allows us to capture not only normal variation in hair cycling behaviour, but also that of hair pathologies. The most common of these is androgenetic alopecia (pattern baldness) which is characterized by the miniaturization of the HF, shortening of the hair cycle and diminution of visible hair. This model provides several predictions to explain how these changes may arise. The opposite transition occurs in hirsutism whereby there is an increase in hair cycle length and hair size. For example, timed perturbation (e.g. increase in *p1*) of a short cycling HF can produce a longer hair cycle (Figure 5.10a) and the opposite is a possible mechanism for the terminal to vellus transition seen in pattern baldness (i.e. decrease in parameter such as *p1*). The results of these perturbations are occasionally non-intuitive but can be explained from the bifurcation and phase space structure of the model.

The model predicts, firstly, in the bistable situation where the no growth state coexists with the periodic hair cycling there are possibilities of inducing regular cycling from the no growth state by applying a single, comparatively brief stimulus. Similarly, a single comparatively brief stimulus would be sufficient to switch the process from cyclical growth to no growth. In either case the minimum strength of the perturbation to achieve the transition depends on the critical population size as defined by the separating manifold (see Chapter 4).

This result would for instance predict the possibility that a normally cycling HF could switch to a "permanently" non-cycling follicle due to an accidental environmental stimulus if it is in this particular bistable state. This is a new hypothesis to explain the transition from growth to no growth that occurs, for example, in severe alopecia or in chemotherapy induced alopecia. The model also predicts that there might be effective treatments to cure this problem. Secondly, for the situation where there is a single stable state of no growth, such as may occur in advanced androgenetic alopecia (Cotsarelis and Millar, 2001), the model predicts that there is a potential way to cure. We

predict that the HF exhibits the dynamical property of excitability. Excitability is a generic feature in the vicinity of subthreshold Hopf bifurcation (Chapter 4). If the HF is in an excitable state (near the fold of limit cycle bifurcation in Figure 5.5d), a short pulse (treatment) could start a full cycle. Of course the success of this intervention depends on whether the other model assumptions are fulfilled including, for example, sufficient supply from the bulge stem cells. Indeed, it has recently been shown that androgenetic alopecia arises from the lack of activation of stem cells rather than a lack or depletion in stem cell number, therefore, the possibility that such assumption of stem cell supply may be fulfilled (Garza et al., 2011). In addition, it is known that in advanced alopecia there is a prolonged telogen phase (Cotsarelis and Millar, 2001) and it may be that the HF is in this region and it takes some time for the stimulus to overcome the threshold and thus enter a full cycle again. Lacking a detailed quantitative model the threshold would have to be determined empirically, however, the model provides first hints as to which parameter(s) might be suitable and thus guide us in the means to realise the perturbation.

The notion of HF excitability being an important feature in the dynamics of hair cycling is also reflected in Plikus *et al.* but at a higher spatio-temporal level (Plikus et al., 2011). If the goal of treatment is to maintain a cyclical hair growth in a single follicle under the excitable condition, it is necessary to apply appropriately timed periodic stimuli. In particular, at the end of catagen after shedding there is a refractory period during which a brief perturbation does not induce a new cycle (absolute refractoriness) or induces only a short cycle of small amplitude implying a short hair (relative refractoriness). The notion of refractory telogen had been postulated many years ago and the concept recently supported via experimental work (Plikus et al., 2008, Plikus et al., 2011). Our model further develops this concept in the dynamic behaviour of the single HF. In the future, this modelling approach may be used to dissect the seemingly complex interactions and roles of factors in the hair cycle to better understand the hair cycle mechanism an improve our approach to treating hair cycling abnormalities (Cotsarelis and Millar, 2001, Al-Nuaimi et al., 2010).

A major limitation of the study is the use of arbitrary parameters. The reason for working with arbitrary parameters is that the model is a reduced model and it is still unknown as to the mechanism of the hair cycle. The aim of this study was to conceptualise the hair cycle in terms of dynamics and to implement a theory of the process. The level of abstraction means that there is a lack of experimental data at this higher level. The parameters are likely to therefore represent "lumped" parameters. The use of multi-scale modelling would allow experimental data at the molecular level to marry with this higher tissue level processes that encapsulate the hair cycle. Now that we know some macroscopic properties of the system, we are able to build upon a directed experimental approach. Biologically, an essential component in the hair cycle is the spatial interaction between compartments; in particular, bidirectional communication between the keratinocyte population and the DP. We implemented a two-compartment model assuming two (molecular) species to be involved in the communication. The communication process mathematically represents a feedback loop via coupling of compartments. Possible biological candidates include molecules that are known to diffuse between the DP and the hair matrix such as those interacting in SHH, WNT and BMP signaling (Botchkarev and Kishimoto, 2003).

The autonomy of the HF is a pronounced feature in the human HF. This is demonstrated by the shedding of individual hairs rather than synchronised shedding and is a result of the population of HFs following an asynchronous cycle in relation to each other giving this mosaic pattern. In other mammals, such as mice, the HFs exhibit more synchronised cycling behaviour. This results in a patch of hair simultaneously growing or shedding. The mathematical model concerned with the coupling of HF stem cells in propagating the waves of the murine and rabbit hair cycles demonstrated in principle that human HFs must rely on their intrinsic signals rather than inter-follicular communication in activating each cycle. Our study greatly complements this work providing the missing investigation of the possible intrinsic hair cycle processes (Plikus et al., 2011). We envisage coupling between HFs in our model may provide a model of murine and other mammalian hair cycling dynamics in the future.

The previous proposed theories of the hair cycle were verbally expressed and not tested mathematically. Therefore the present model is an advance from the important work of hair biologists (Paus et al., 1999a, Paus and Foitzik, 2004, Stenn et al., 1999, Chase, 1954, Sun et al., 1991). Likewise, previous mathematical models concerned with hair growth and cycling do not address the intrinsic processes that drive the HF through the cycle (Plikus et al., 2011, Halloy et al., 2000, Halloy et al., 2002). The mathematical model by Plikus *et al* is at a higher level of interest; namely the mechanism of HF coupling in the propagation of hair cycle waves in mice and other mammals (Plikus et al., 2011). Our model complements this. The finding that alopecia may arise by reduction in activation of stem cells is exactly the result of the uncoupled stem cells that is shown to produce the independent HF cycling seen in adult human HFs. Again, the model does not explore what the internal mechanisms may be in the human case (Plikus et al., 2011).

An important direction for the future use of the model would be to characterise hair growth modulators better and within this dynamical systems framework. For example growth factors that are considered to induce growth and proliferation (because they prolong anagen) may in reality act as inhibitors. As shown here an inhibitory effect in our model is predicted to be required at some level to maintain the long growth phase. This may explain why experiments may produce conflicting results depending on their outcome measurements and timing of interventions as the model also predicts that the phase of intervention is important in the result of certain perturbations.

The hair cycle is a complex process involving multi-scale co-ordination of events. Mathematical modelling may play an essential role in dissecting the intricacies of the system (Al-Nuaimi et al., 2010). Here, our dynamical systems construction of the human hair cycle leads to a novel theory that the HF dynamics requires two key dynamical features; feedback inhibition and a bistable switch. The study represents a new approach to deciphering the core components driving the hair cycle and is a first attempt at mathematically modelling the dynamics of the HF. In addition, we predict that hair disorders may be treatable due to the HF exhibiting important dynamical features of

bistability and excitability. We envisage that this important step will be further developed and refined in future work. This will pave the way to exploring this complex system with the aim to understand and predict the systems properties of the HF. The model may be used to establish the key processes that produce the behaviour of interest in order to move towards understanding and eventually finding medical targets.

5.10 CONCLUSION

In this study, we use mathematical modelling to construct a theory of how the human hair cycle, a dynamic regenerative process, may be controlled. Previous proposed theories of the control mechanism of the hair cycle have been verbally expressed and not tested mathematically. Using this original, population based approach; we conclude that the human hair cycle may be explained by an autonomous relaxation oscillator whereby communication between matrix keratinocytes and the dermal papilla are essential to the process.

Supplemental figures

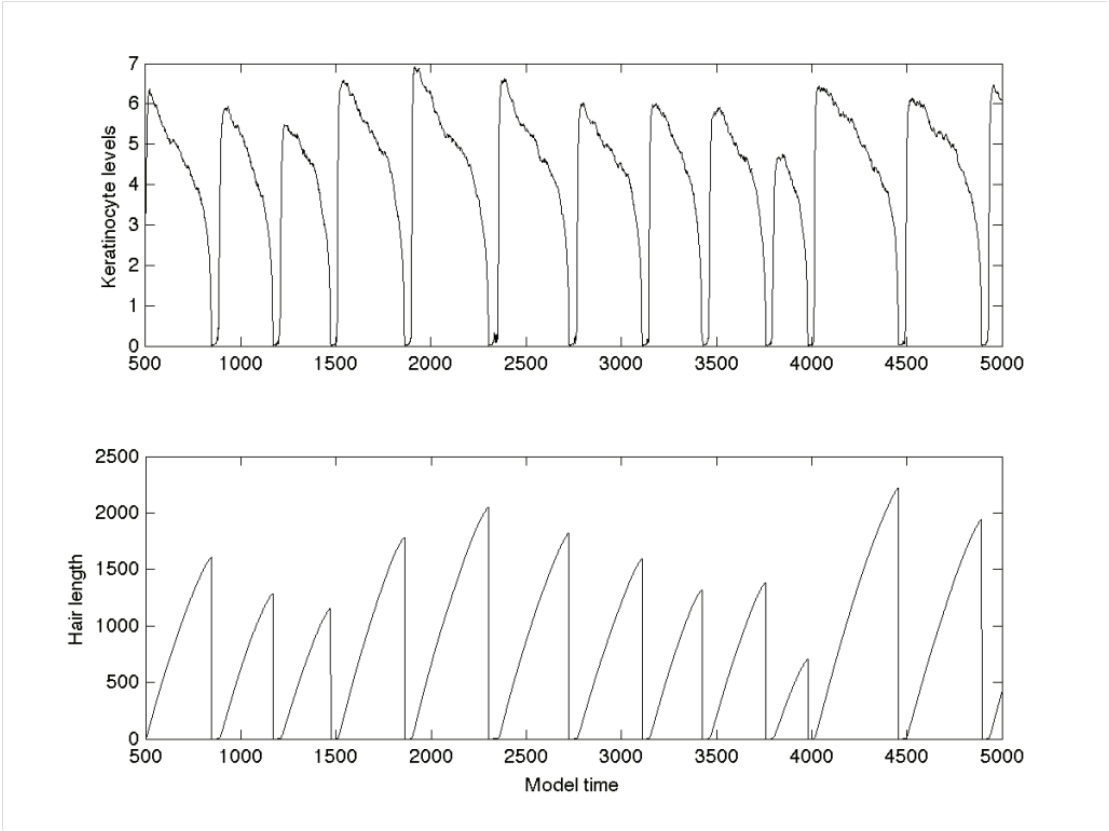

Figure 5.11: Time course of keratinocyte population and hair growth under random fluctuations in parameters a and p1

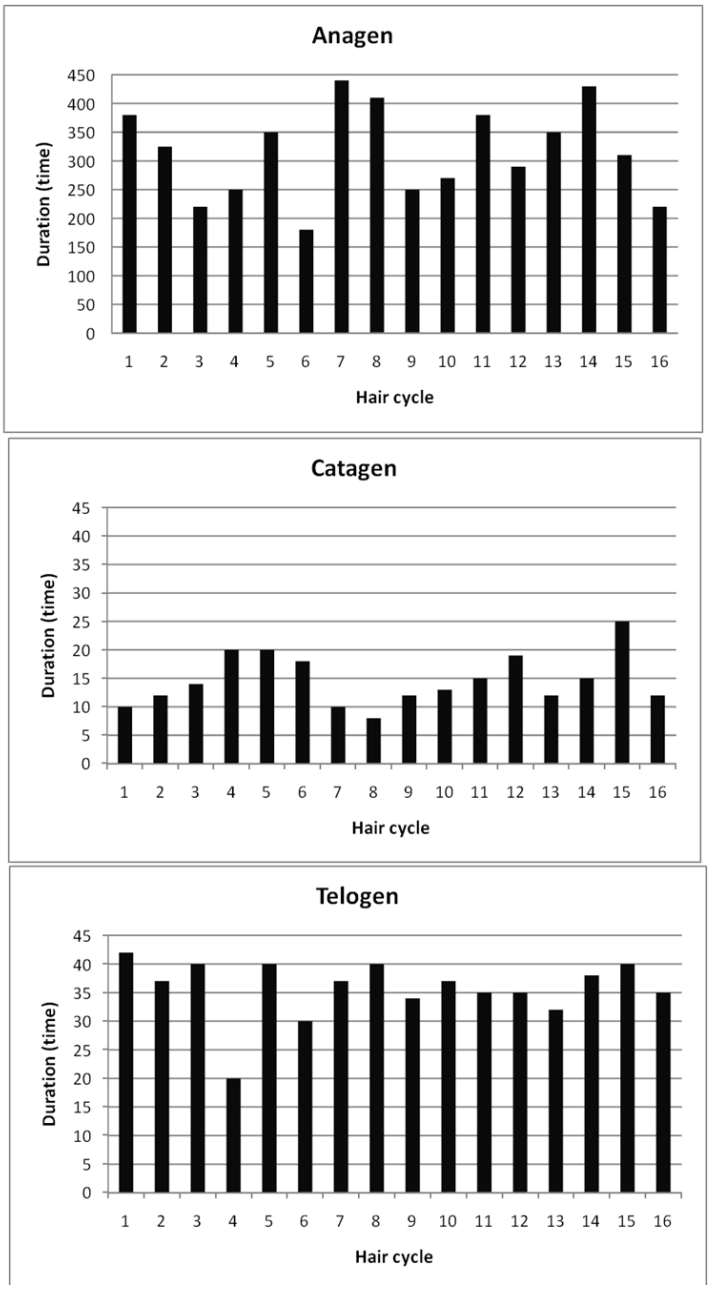

Figure 5.12: Random fluctuations in a and p1

Anagen, catagen and telogen durations vary from one cycle to the next. This is achieved by introducing random fluctuations in parameters a and p1. Durations of each phase of the hair cycle were calculated by measuring the length of time each stage (anagen, catagen or telogen) lasted using the time series output of 16 consecutive hair cycles (i.e. such as in Figure 5.11). The graphs were then plotted for each cycle stage to show the variation achieved as the follicle proceeded through from one cycle to the next.

6 CHAPTER 6: RESEARCH METHODOLOGY

This chapter details the experimental protocols used in the project. The various methods are explained in turn. Where experiments are performed to generate data, the details of methodologies implemented are further detailed in the methods section of the corresponding chapter; this in-keeping with the manuscript style of these chapters.

6.1 HUMAN TISSUE SAMPLE COLLECTION

Human tissue was obtained from two sources following informed consent:

1) Redundant human fronto-temporal and occipital scalp skin from females undergoing facelift surgery (the University of Luebeck, Faculty of Medicine, Germany Ethics Committee approved protocol 06-109.).
2) Redundant human follicular units harvested from the occipital scalp of males undergoing hair transplantation surgery (the University of Manchester, Research Ethics Committee approved reference 09/H1010/10)

Tissue was placed in a universal container in "isolation media"; William's E media (Sigma, Gillingham, UK) supplemented with 100 IU/ml penicillin and 10µg/ml streptomycin (Gibco, Germany, Karlsruhe) and transported to the laboratory at 4°C.

6.2 PROCESSING TISSUE

Once in the laboratory, the tissue was processed as quickly as possible. For whole skin analysis, such as immunofluorescence and immunohistochemistry, whole skin was dissected into small blocks of approximate dimensions 1cm x 0.5cm under the dissection microscope using a scalpel (Figures 6.1a and b). The skin was orientated (Figure 6.1c) and embedded in Shandon Cryomatrix (Pittsburgh, PA, USA). This was snap-frozen in liquid nitrogen and samples were stored at -80ºC until cryosectioned.

Individual HFs were isolated from both whole skin and follicular units by micro-dissection as described below. Isolated HFs were either maintained in

culture (HF culture Section 6.4) or immediately embedded in Shandon Cryomatrix, snap frozen in liquid nitrogen and stored at -80ºC until used for further analyses.

6.3 HAIR FOLLICLE MICRODISSECTION

Human HFs were isolated for further study by the technique of HF microdissection. This is an established technique previously described (Philpott et al., 1990, Sanders et al., 1994). Briefly, this was carried out using aseptic technique under the dissection microscope (Figure 6.1):

1) Tissue was orientated and amputated at the level of the dermis-subcutis junction using a scalpel (Figure 6.1d);
2) The HFs were isolated by gently prising the HF out of surrounding tissue using tweezers(Figure 6.1f);
3) HFs were assessed under a light microscope to ensure they had not been damaged during isolation and that, macroscopically, they appeared to be in anagen stage (Figure 6.1g)

6.4 HAIR FOLLICLE ORGAN CULTURE

Isolated anagen VI HFs were maintained in a 24-well plate; each well containing 500µl serum-free Williams' E medium (Sigma) supplemented with 2mmol/L L-glutamine (Invitrogen, Paisley, UK), 10ng/ml hydrocortisone (Sigma), 10µg/ml insulin (Sigma) and 1% antibiotic/antimycotic mixture (100x, Gibco, Paisley, UK). Culture medium and supplement recipe follows that set up by Philpott *et al* (Philpott et al., 1990, Philpott, 1999, Philpott et al., 1994a). HFs were placed in an incubator at 37°C with 5% CO_2 level. Supplemented media was changed every two days.

This assay was employed as hair growth in culture has been shown to correlate with *in vivo* growth rates (Kwon et al., 2006) and it is considered the best available assay for studying human HFs at present (Rogers and Hynd,

2001). Elongation of hair shafts was measured using a Nikon binocular inverted microscope as previously described (Philpott et al., 1990).

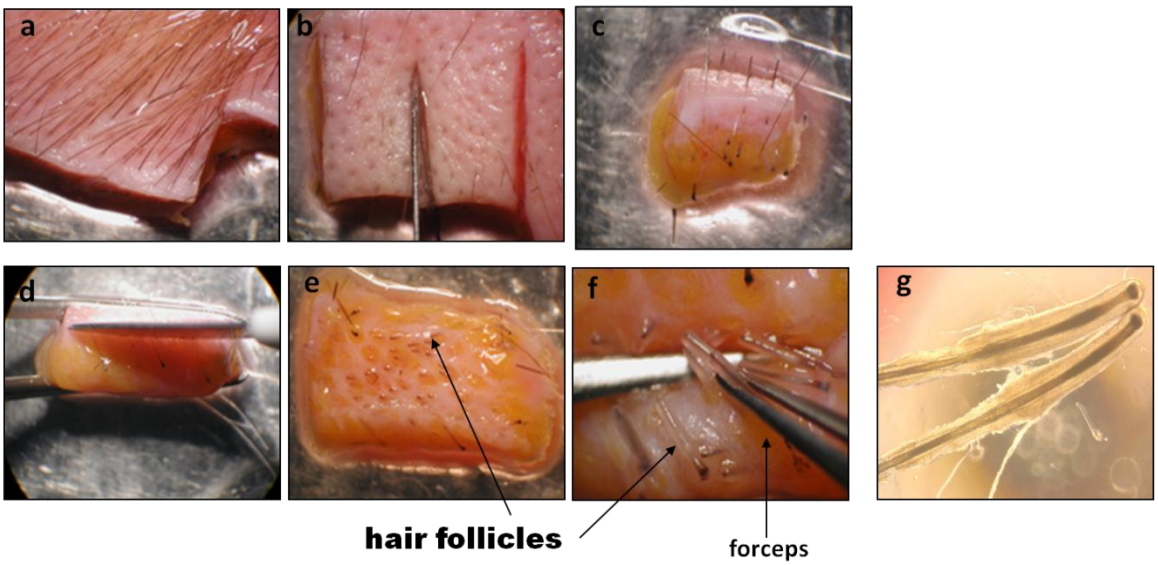

Figure 6.1: Microdissection of anagen VI hair follicles from adult human scalp skin.

Fresh human scalp skin was obtained. In this figure (a) shows frontotemporal scalp skin from a female patient (b) Hair shafts now cut and small sections cut using a scalpel under the microdissecting microscope. (c) skin section orientated ready for either embedding or for amputation at the junction of the dermis and subcutis (d). (d) shows the plane at which the skin is amputated (at the dermis, subcutis junction). (e) The sample, is then orientated with the hair follicles facing upwards. (f) Using forceps, individual hair follicles are dissected out of the surrounding skin and placed in supplemented William's E media (g). (g) Whole hair follicles are assessed under the microscope to ensure they are healthy, intact Anagen VI hair follicles (as shown in g). Figure courtesy of R. Paus.

6.5 ANAGEN AND CATAGEN STAGING OF ISOLATED HUMAN HAIR FOLLICLES IN ORGAN CULTURE

In order to investigate changes in expression of candidate genes and proteins in accordance with the hair cycle, HF organ culture experiments were performed whereby HFs were maintained in culture and assessed daily using light microscopy to determine whether they appeared, macroscopically, to be in anagen or early, mid and late catagen phases (Figure 6.2). The macroscopic characteristics of organ-cultured whole HFs were assessed under the dissection

microscope. Epithelial, mesenchymal and pigmentary characteristics of the HF were used to stage HFs.

Figure 6.2: Macroscopic appearance of isolated whole human hair follicles in different hair cycle stages.

Hair follicles in organ culture. Images taken using bright field microscope magnification x200.

Anagen HFs were characterised by having maximal melanin content, an onion-shaped DP and large hair matrix volume. Early catagen HFs exhibited a thinner, stretched hair matrix, reduced melanin content and an oval shaped DP. Mid-catagen HFs were identified by a smaller, round DP, further decreased hair matrix volume, a pincer-like appearance of the proximal hair matrix and further reduced melanin content. Late catagen HFs can be categorised as they often exhibit a club hair, no melanin in the bulb region, a very small round DP and thin hair matrix. HFs were then placed into anagen, early catagen, mid-catagen and late catagen groups according to these features (Figure 6.2).

Samples of whole human HFs were taken by two methods; 1) once HFs were seen to have entered the correct stage, HFs were immediately embedded in Shandon Cryomatrix and snap frozen in liquid nitrogen or snap frozen for qPCR analyses 2) HFs were staged and once equal amounts of HFs were

identified in either anagen or catagen, then the sample was taken on the same day and embedded or frozen whole as described above.

Microscopic staging of anagen, early, mid and late catagen HFs was performed using the same morphological features as already described above for the macroscopic criteria i.e. shape of the DP and hair matrix volume (this is demonstrated in Figure 6.3). Microscopic staging allows for easier staging of each HF as the anatomy is more readily visible. Therefore, staging relied on morphological appearance for anagen, early, mid and late catagen stages rather than on counting number of proliferative and apoptotic cells. However, cell numbers and number of Ki-67 and TUNEL positive cells were used to distinguish anagen and early catagen. These criteria were published for objectively distinguishing between anagen and early catagen stages in human HFs (Kloepper et al., 2009) (Appendix B).

6.6 VALIDATION STEP FOR MACROSCOPIC STAGING

The original macroscopic stage allocated to whole human HFs in organ culture was compared to the final stage of anagen, early catagen, mid-catagen or late catagen the same HF was allocated to after cryosectioning. Figure 6.3 shows the correlation between macroscopic and microscopic staging when the HFs are in organ culture (Figure 6.3 Top panel) and when they have been cryosectioned (Figure 6.3 Bottom panel).

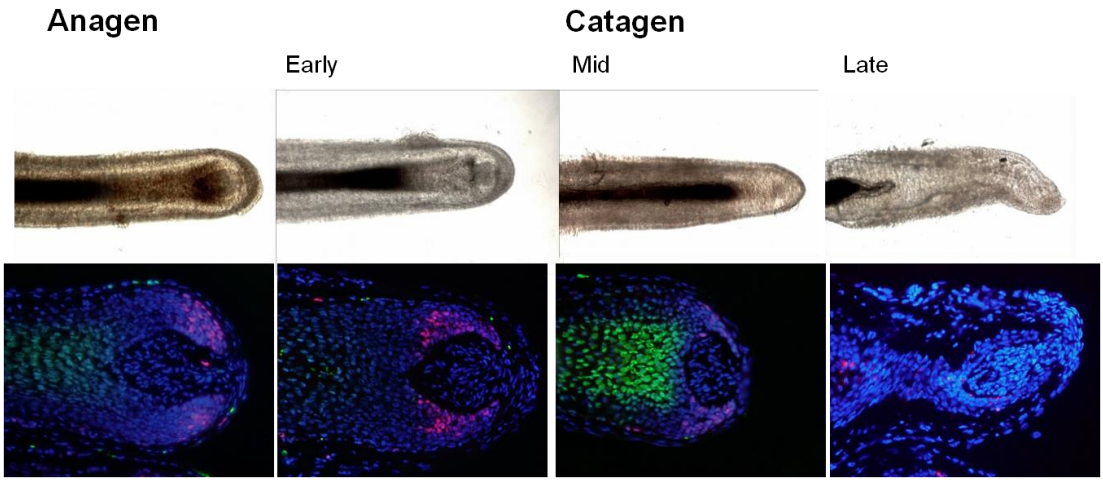

Figure 6.3: Macroscopic and microscopic appearances of anagen and catagen human hair follicles

Top panel shows the macroscopically staged human hair follicles in organ culture. The bottom panel shows the corresponding stage in cryosections of human hair follicles. The morphological appearance of the hair follicles in each stage is assessed in order to stage the hair follicles.

Figure 6.4 shows the accuracy of staging based upon the macroscopic appearance of whole HFs compared to the confirmed stage using microscopic staging methods in the same HF. The data was achieved for this accuracy test by staging whole HFs in organ culture from two separate patient samples. The staging was performed during a "catagen" culture which was performed to collect anagen, early, mid and late catagen HFs for analyses. The sample from Patient 1 sample comprised 42 HFs in total and patient 2 consisted of 45 HFs. The stages allocated to the HFs were documented and the HF identified by its location in a 24 well plate. The HFs were embedded and frozen for subsequent immunofluorescence or immunohistochemisty staining with the HF identifiers also documented. Once the cryosections were used for staining, the slides were blinded and photographs taken of each HF. Microscopic staging was then performed and the results were compared against macroscopic staging (Table 6.1).

6.7 TRH CULTURE EXPERIMENT

In order to investigate the effect of thyrotrophin hormone (TRH) on human HFs in organ culture (see (Gáspár et al., 2010)); anagen VI HFs were isolated from human scalp skin as described above. Isolated HFs were maintained in a 24-well plate supplemented with the following substances which were changed every two days:

- 5 ng/ml, 10 ng/ml and 100 ng/ml of TRH every two days
- control was HFs maintained with no addition of TRH.

HFs were maintained for 6 days in organ culture as previously described (Ackermann et al., 2007, Zanello et al., 2000). Once completed HFs were either frozen whole (5 ng/ml and 100 ng/ml concentrations) for qPCR analysis or embedded for subsequent cryosectioning and immunohistochemistry staining (5 ng/ml and 10 ng/ml concentrations).

Table 6.1: Data for accuracy of macroscopic hair cycle staging

Stage the HF was finally allocated to on microscopic staging of cryosections	**Stage the same HF had been assigned to when in organ culture**				
Anagen	Anagen	Early catagen	Mid catagen	Late catagen	Total
Sample 1	12	0	0	0	12
Sample 2	8	3	0	0	11
Total	20	3	0	0	23
%	86.96%	13.04%	0.00%	0.00%	100.00%
Early Catagen	Anagen	Early catagen	Mid catagen	Late catagen	Total
Sample 1	4	2	0	0	6
Sample 2	0	13	0	0	13
Total	4	15	0	0	19
%	21.05%	78.95%	0.00%	0.00%	100.00%
Mid Catagen	Anagen	Early catagen	Mid catagen	Late catagen	Total
Sample 1	0	6	6	0	12
Sample 2	0	1	11	0	12
Total	0	7	17	0	24
%	0.00%	29.17%	70.83%	0.00%	100.00%
Late Catagen	Anagen	Early catagen	Mid catagen	Late catagen	Total
Sample 1	0	0	0	12	12
Sample 2	0	1	2	6	9
Total	0	1	2	18	21
%	0.00%	4.76%	9.52%	85.71%	100.00%

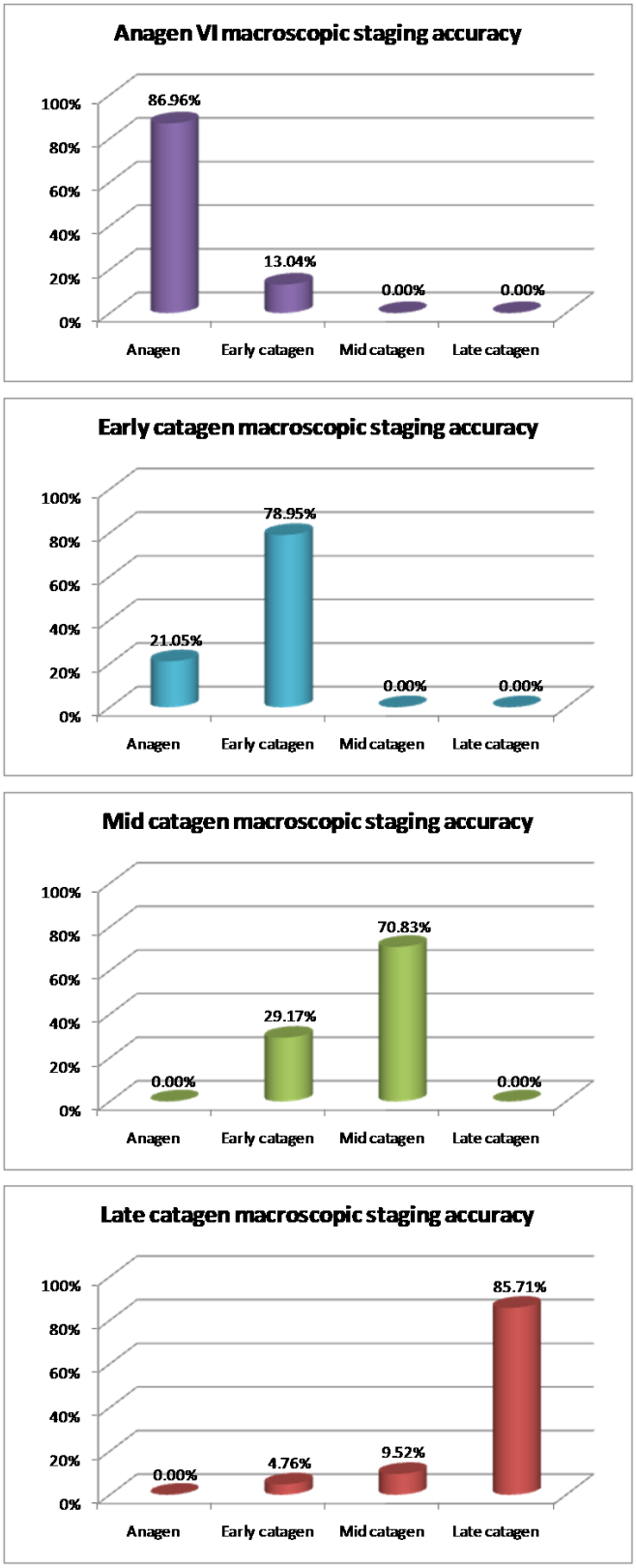

Figure 6.4: Results of the accuracy tests for staging whole human hair follicles

6.8 HAIR FOLLICLE CIRCADIAN CLOCK SYNCHRONISATION AND 24 HOUR TIME SERIES

Dexamethasone (Sigma Alrich D1756) powder was reconstituted in 41.25µl DMSO at 25°C to produce the stock solution 1mg/ml. Serial dilutions were performed with a resultant 100nM Dexamethasone solution.

HFs were obtained and microdissected as described. They were maintained in constant conditions (5% CO_2 at 37°C) in a Petri dish. HFs were incubated in 10mls of 100nM dexamethasone for 30 minutes to establish synchronisation. After 30 minutes, the media with dexamethasone was removed and replaced with normal HF culture media. Collection of samples for 24 hour time series experiments was performed allowing 4 hours following synchronisation prior to collection. Samples were collected for qPCR and stored in RNAlater® or embedded in OCT for cryosectioning for immunohistochemistry/ immunofluoresence analysis.

6.9 IMMUNOHISTOCHEMISTRY AND IMMUNOFLUORESCENCE

Immunohistochemistry staining protocols for localisation and quantification of candidate proteins in human anagen and catagen HFs was established and performed on either; whole human scalp skin cryosections, isolated human scalp HF cryosections or on both whole scalp skin and isolated HFs. The thickness of cryosections was 8µm in whole scalp skin and 6µm for isolated HFs.

Sections that needed direct comparison for quantification were always processed at the same time to ensure that any variation in results were not due to variation in experimental conditions, such as temperature. Negative controls were performed in all experiments by omission of primary antibody. In addition, positive controls; i.e. the use of tissues with known expression of the antigen in question, and blocking peptides (as additional negative control) were used in all experiments where these were available.

Non-specific binding was minimised by treating sections for 20 minutes with serum from the same animal that the secondary antibody had been raised

(all normal serums from DAKO, Denmark). Primary antibodies were incubated overnight at 4°C. Sections were washed in either phosphate buffered saline or Tris-buffered saline between steps. Immunohistochemistry sections were mounted using Pertex and immunofluorescent slides mounted with Fluoromount. Images were captured using the fluorescence microscope Biozero 8000 (Keyence; Osaka, Japan). When intensity of staining or fluorescence was to be measured, the same exposure times were used for sections that were in the same experiment to ensure consistency. Analyses of images was performed using the ImageJ software (Abramoff et al., 2004).

6.10 KI-67/TUNEL STAINING

This established double staining protocol was performed to localise and quantify proliferation and apoptosis concurrently within the human HF. Ki-67 is a marker of proliferation and TUNEL (terminal deoxynucleotidyl transferase dUTP nick end labelling) an apoptosis marker. The methodology has been previously published and the protocol provided below. TUNEL staining was performed using the Apoptag Fluorescein In Situ Apoptosis Detection Kit (Millipore, UK). All washing steps were performed with PBS (phosphate buffered saline). Cryosections were dried at room temperature for 5 minutes. Fixation was performed in 1% paraformaldehyde (PFA) at room temperature for 10 minutes. Following two 5 minute washing steps, the slides were post-fixed in ethanol-acetic acid (2:1) for 5 minutes at -20°C. Following two further washes, equilibration buffer (from the commercial kit) was pipetted on each section and incubated at room temperature for 5 minutes. Subsequently, the sections were incubated in 30% TdT enzyme (in 70% reaction buffer) for 60 minutes at 37°C, followed by 10 minutes in Stop buffer (consisting of 2mls Stop buffer and 68mls distilled water) at 37°C.

Following this step, pre-incubation with 10% normal goat serum in PBS was carried out for 20 minutes at room temperature. This was followed by overnight incubation with the Ki-67 primary antibody mouse anti-human Ki-67 antigen (clone MIB-1, DAKO) at 4°C. The following day, three washes were performed and the fluorescent staining for TUNEL was performed using

fluorescent labelled anti-digoxigenin antibody (commercial kit) at a ratio of 56µl:59µl blocking solution: antibody solution; this was incubated for 30 minutes at room temperature. The secondary antibody for Ki-67 was then applied to the sections following another washing step. Goat anti-mouse rhodamine red (Jackson Immunoresearch) at 1:200 concentration in 2% normal goat serum was applied to the sections and incubated for 45 minutes at room temperature. The sections were counterstained with DAPI for 1 minute after a washing step and then the slides were washed again and mounted with Fluoromount® (Southern Technologies). Negative controls were performed in every experiment whereby the primary steps - 30% TdT enzyme and Ki-67 antibody - were omitted at these points of the procedure.

6.11 MASSON – FONTANA STAINING

Masson Fontana stains argentaffin granules and melanin. Staining was performed on HF cryosections that were fixed with ethanol-acetic acid (2:1) for 10 minutes. Post-fixation was followed by a washing step in TBS and then distilled water for 5 minutes at each step. The cryosections were then heated for 1 hour at 56°C until the resultant black stain was produced. Following a washing step in distilled water for 5 minutes, the sections were placed in 5% sodium thiosulphate solution for 1 minute followed by a wash in distilled water. The sections were then counterstained with haematoxylin for 1 minute and then washed for 5 minutes under tap water. The cryosections were then dehydrated by placement in 70%, 96% and 100% ethanol for 2 minutes at each concentration.

Masson Fontana staining was analysed by taking digital images of all stained sections at using the Biozero 8000 microscope (Keyence) at x20 magnification. All images were taken at the same exposure time to ensure no differences in staining intensities were due to that. ImageJ software (Abramoff et al., 2004) was used to measure the intensity of stains in the three reference areas as shown in Figure 6.5.

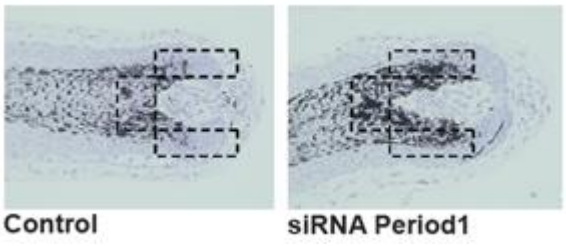

Figure 6.5: Quantification of masson-fontana staining

Images show the reference areas (three rectangular areas) drawn in ImageJ to quantify masson-fontana staining

Analysis of the measured intensity values was performed using Graphpad prism. Statistical analyses performed was the Student's paired t-test with a p value <0.05 was taken as statistically significant.

6.12 PERIOD1 STAINING

PERIOD1 immunofluorescent staining protocol was established during the project. HF cryosections were firstly dried for 10 minutes at room temperature and then fixed in acetone at –20°C for 10 minutes. Following a further 10 minutes of drying at room temperature, the sections were washed in PBS. 10% normal goat serum (DAKO) was used for preincubation for 20 minutes at room temperature and 1:200 primary antibody rabbit anti-human Per1 with 2% normal goat serum was then pipette onto each section and allowed to incubate overnight at 4°C. The following day, the secondary antibody goat anti-rabbit fluorochrome (Jackson Immunoresearch) was applied for 45 minutes following a 5 minute washing step with PBS. The sections were counter stained with DAPI for 1 minute and washed with PBS before being mounted with Fluoromount (Southern Biotechnologies). The stained sample slides were stored at -20°C.

Positive and negative controls were performed with this protocol. Firstly, the use of a blocking peptide was employed. This was prepared by incubating 5 µl blocking peptide per 1 µl of antibody in a separately prepared primary antibody mixture. This was incubated at room temperature for 2 hours prior to commencing the experiment. At the primary antibody step, several sections were incubated with this blocking peptide mixture rather than the primary

antibody, 2% serum mixture. Lastly, two positive controls were used namely HaCaT cells and human pineal gland as they were known to express Period1 protein (Ackermann et al., 2007, Zanello et al., 2000).

6.13 PERIOD1 IMMUNOFLUORESCENCE IN ANAGEN AND CATAGEN HAIR FOLLICLES

Immunofluorescent staining for PERIOD1 protein was performed on isolated anagen and catagen HFs from organ culture. Human HFs were maintained in organ culture and HFs were embedded, frozen and cryo-sectioned. PERIOD1 immunofluorescence was performed and cryosections staged into anagen (n=8), early- (n=15), mid- (n=14) and late catagen (n=9). Sections were photographed using the Biozero 8000 microscope (Keyence). Exposure time and all microscope settings were maintained at the same settings for all photographs of each section to ensure comparisons could be made between the stages. Statistical differences were tested for using Mann Whitney U test and corrections for multiple testing was carried out via Holm-Bonferroni.

6.14 ANALYSES OF IMMUNOHISTOCHEMISTRY IMAGES

Immunolocalisation and intensity analyses were carried out by taking both brightfield and fluorescent images of immunohistochemistry stains using Biozero 8000 microscope (Keyence). The immunofluorescent sections were first assessed to establish the optimal exposure time for analysis of the stains. This ensured that images taken were standardised and would allow accurate assessment and comparison of fluorescent intensity. Images were analysed using ImageJ software whereby a reference area of HFs was outlined in order to take into account the differences in HF area and cell numbers (Figure 6.6).

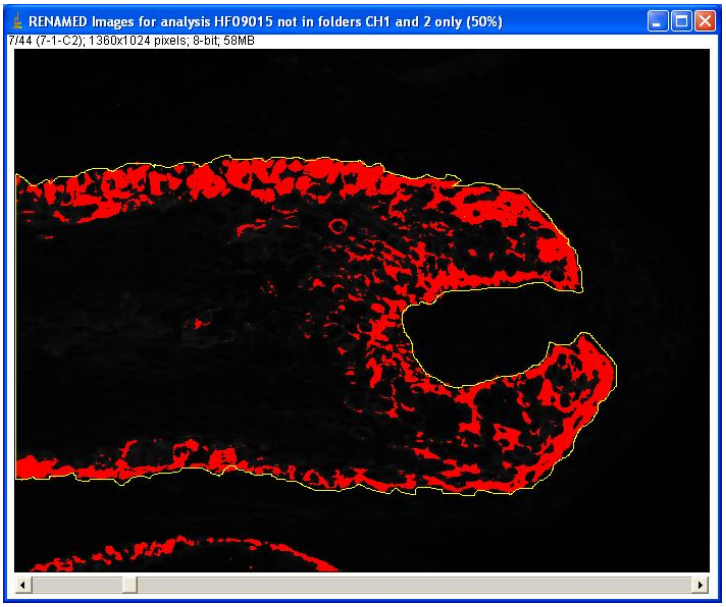

Figure 6.6: Reference area for PERIOD1 immunofluorescent staining analyses

Image showing the reference area chosen for analysis of PERIOD1immunohistochemistry using ImageJ (yellow outline)

6.15 BMAL1 STAINING

The BMAL1 immunofluorescent staining protocol was established during the project. All washes were performed with TBS. HF cryosections were fixed in 1% PFA (in PBS, pH 7.4) for 10 minutes at –20°C. A drying step (room temperature for 10 minutes) both proceeded and followed the fixation step. Sections were washed with TBS before and after endogenous peroxidase activity was blocked with 3% H_2O_2 in TBS for 15 minutes at room temperature. Pre-incubation with 10% normal goat serum (DAKO) in TBS was performed for 20 minutes followed by application of the primary antibody; 1:40 rabbit anti-human BMAL1 (Alpha Diagnostics) with 2% normal goat serum overnight at 4°C. The secondary antibody goat anti-rabbit FITC (Jackson Immunoresearch) with 2% normal goat serum was pipette onto each section at a concentration of 1:200 in TBS. Following 45 minutes incubation time with the secondary antibody, the sections were washed and then counter stained with DAPI for 1 minute. The sections were then embedded in Fluoromount after being washed. The sections were stored at -20°C. The analysis of BMAL1 immunofluorescent staining was identical to that as described for PERIOD1 above.

6.16 ANTIGEN RETRIEVAL

This protocol was used for the positive controls human pineal gland prior to the immunofluorescence protocols for PERIOD1 and BMAL1. Human pineal gland sections were only available embedded in paraffin.

Deparaffinisation was achieved by incubating the paraffin sections in ethanol for 30 minutes at room temperature, followed by dipping the sections into successively less concentrated ethanol; 100%, 95%, 70% and 50% ethanol respectively. The sections were then washed in TBS or PBS (depending on whether the BMAL1 or PERIOD1 staining protocol was going to be used). Citrate buffer (0.01M) was made up at pH 6.0. The sections were heated in the microwave in citrate buffer for 15 minutes. At this stage sections were frequently checked to ensure that the buffer was not evaporating. Citrate buffer was topped up if so to ensure the sections remained wet. After 15 minutes, the sections were cooled at room temperature overnight. The sections were washed and then used following from the fixation steps in the protocols.

6.17 SMALL INTERFERING RIBONUCLEIC ACID (SIRNA) TRANSFECTION OF WHOLE HUMAN HAIR FOLLICLES

This section details the protocol established for the knock-down of genes of interest in microdissected human HFs using siRNA technology (SantaCruz Biotech). The Santa Cruz system was followed according to manufacturer's instructions.

Whole human HFs were obtained by microdissection using the described methodologies detailed in section 6.3. On day 0, the microdissected HFs were placed in supplemented William's E medium in a 6-well plate (15 HFs per well). Solution A and Solution B were prepared under sterile conditions:

Solution A: 6µl siRNA duplex
100µl siRNA transfection medium

Solution B: 6µl siRNA transfection reagent
100µl siRNA transfection medium

Solution A and B were mixed gently with a pipette and incubated for 45 minutes at room temperature. Following the incubation time, HFs were washed with siRNA transfection medium (2ml per well). siRNA transfection medium (800µl) was added to the mixed Solution A and B; 1ml was pipetted into each well of the 6-well plates after the transfection medium had been removed after washing. HFs were incubated with the mixture for 5-7 hrs at 37°C in a 5% CO_2 incubator. Following the incubation period, the transfection mixture was removed and HFs were incubated as normal in supplemented William's E medium.

For every siRNA transfection experiment performed, a parallel control group was run alongside the siRNA transfection. The HFs in the control group were always from the same person as those in the siRNA group so that direct comparisons such as hair cycle stage, mRNA and protein expression could be made. Therefore, half of the HFs obtained from each person were allocated to the siRNA knockdown group and half to the control group. The HFs in the control group were treated by replacing the 6µl siRNA duplex with 6µl scrambled oligonucleotides in Solution A. All other reagents and conditions were the same in the control group as the siRNA treated group.

The siRNA and control samples were taken for qPCR and immunofluorescent staining to confirm knockdown of mRNA and protein after 24 hours. HF cultures were also run for an additional 4 days as detailed in Table 6.2.

Table 6.2: siRNA transfection protocol for human hair follicles

	Day 0	Day 1	Day 2	Day 3	Day 4
siRNA transfection group Half of the total number of HFs obtained from each person placed in this group	Microdissection of HFs Preparation of Solution A and B Incubate with transfection medium After 5-7h remove transfection Medium Incubate HFs for 18-24h in William's E medium + supplements	Take 24 hour samples (confirmation of knock-down by qPCR and IF by comparing expression in the knockdown group with the control group)	Change media		Collection of HFs; whole HFs for qPCR, embed for staining
Control group Half of the total number of HFs obtained from each person placed in this group	Microdissection of HFs Preparation of Solution A (with 6µl scrambled oligonucleotides rather than siRNA duplex with) and solution B Incubate with transfection medium After 5-7h remove transfection Medium Incubate HFs for 18-24h in William's E medium + supplements	Take 24 hour samples (confirmation of knock-down by qPCR and IF by comparing expression in the knockdown group with the control group)	Change media		Collection of HFs; whole HFs for qPCR, embed for staining

6.18 QUANTITATIVE PCR METHODOLOGIES

6.18.1 RNA extraction protocol

Total RNA extractions from whole human HFs were carried out using the PureLink RNA Mini Kit (Invitrogen) and Purelink DNase treatment Kit (Invitrogen). The manufacturer's instructions were followed (Invitrogen). RNA was extracted from whole human HF samples at the same time to ensure comparisons between samples were not due to variations in experimental conditions during RNA extraction.

TRIzol (800µl) was added to each sample of whole HFs and the sample homogenised using a pestle and mortar for 30 seconds followed by an electrical homogeniser for 30 seconds. The lysate was incubated at room temperature for 5 minutes. This was to allow dissociation of nucleoprotein complexes. Chloroform was added to each sample (160µl) and the samples were vigorously shaken for 15 seconds and then incubated at room temperature for 3 minutes. The samples were centrifuged at full speed for 15 minutes and then 400µl of the colourless upper phase was transferred to a fresh RNase free tube by careful pipetting and an equal volume of 70% ethanol was added. After mixing the sample with a vortex, 700µl of the sample was transferred to a spin cartridge and then placed in the centrifuge for 15 seconds. The flow through was discarded and 350µl Wash buffer I was pipette onto the spin column (which contains the bound RNA). After centrifuging the sample again for 15 seconds the flow through was discarded and the spin cartridge inserted into a new collection tube. The samples were then treated with DNase at this step. To each spin cartridge 80µl of the DNase mix was pipette directly onto the surface of the spin cartridge membrane (each mix comprises 8µl DNase reaction buffer, 10µl DNase and 62µl RNase-free water). Following a 15 minute incubation step at room temperature, 350µl Wash Buffer I was added to the spin cartridge and then centrifuged at full speed for 15 seconds. The flow through was discarded and the spin cartridge inserted into a new collection tube. Wash Buffer II with ethanol was then pipette onto the to the spin cartridge (500µl) and the samples centrifuged for 15 seconds. The flow through was discarded and the wash step

plus the centrifuge step was repeated. After discarding the low through, the spin cartridge was dried by a 1 min centrifuge step. The spin cartridge was inserted into a recovery tube and 30µl RNase-free water was added to the centre of the spin cartridge. Following incubation at room temperature for two minutes, the spin cartridge was centrifuged for 1 minute and the resultant RNA was either stored on ice when used immediately or stored at -80°C for long term storage.

Traces of genomic DNA were minimised by the use of DNase treatment steps as described above. Total RNA purity and concentrations were established by analysing the UV absorbance using the Nanodrop ND-1000 (Fisher Scientific, Loughborough, UK).

6.18.2 Reverse transcription

Reverse transcription was carried out using the cloned AMV First Strand cDNA Synthesis Kit (Invitrogen, Paisley, UK) according to the manufacturer's instructions. Total RNA (volume varied as explained below) was added to a maximum volume of 9µl in each reaction with 1 µl oligo (dT) primers, 10mM dNTP mix and DEPC-treated water to make up 12 µl volume. If the total volume of RNA was 9 µl then no DEPC-treated water was added to the reaction mix. A denature step was performed by incubating the RNA and primer at 65°C for 5 minutes and placing the samples on ice. Then, the master reaction mix was prepared and stored on ice; a total volume of 8 µl was added to each reaction on ice; comprising 4 µl 5x cDNA synthesis buffer, 1µl 0.1M DTT (Dithiothreitol), 1µl RNase OUT™, 1µl DEPC-treated water and 1µl Cloned–AMV RT. The reaction tubes were transferred to a pre-heated thermal cycler and incubated. The following temperatures and incubation times were performed; 50°C for 50 minutes followed by 85°C for 5 minutes. The sample was stored at -20°C until used for qPCR experiments.

The volume of RNA added to the reaction mix was adjusted for each sample in each experiment to ensure the same concentration of RNA was loaded in the reverse transcription reactions for each sample set. This was to ensure

that samples whose results were going to be compared by qPCR were subjected to the same conditions and to minimise any variation being due to different RNA amounts included in the reverse transcription reaction rather than true differences. Controls were included for each sample whereby the reverse transcription reaction was carried out without any reverse transcriptase. This was to test for any genomic DNA contamination present in the RNA samples during qPCR.

6.18.3 Assessment of amplification reaction efficiencies (qPCR)

To utilise the delta delta Ct method for relative quantification in the qPCR experiments a standard curve was produced for the housekeeping gene, peptidylprolyl isomerase A (PPIA), and all target genes to check the efficiencies of the amplification reactions for these genes. This is because in order to use the delta delta Ct method, the efficiencies of the PCR amplification reaction for both the gene of interest and normaliser (housekeeper) should be approximately equal to ensure validity of relative quantification. The validations performed here were performed to check what conditions this would be true prior to proceeding to the data generating experiments.

Serial dilutions were performed on cDNA obtained from isolated human HFs. This sample was representative of the samples to be used in later experiments. Quantitative PCR was carried out using the manufacturer's protocol and delta Ct values plotted against template dilutions (relative efficiency plots). A linear line of best fit was plotted and a slope of absolute value <0.1 was determined as acceptable for employing the delta delta Ct method. If the efficiencies of the PCR reactions are equal, the plot of ΔCt against input amount would produce a slope of 0. The dynamic ranges for the assays of interest were established by determining the concentrations of input cDNA that produced a slope of <0.1 in the efficiency plots (Appendix C).

Due to this work, the dynamic ranges were established as summarised in (Table 6.3) and detailed in Appendix C. In light of this analysis, the highest concentrations of cDNA (100ng or 10ng) were used in all qPCR experiments to

ensure the efficiencies between the normaliser and target genes were as equal as possible; minimising any errors in the effect of variation in amplification reactions. This controlled for the variation between target and housekeeper gene efficiencies seen with the lower concentrations of cDNA. Therefore, when performing the delta delta Ct method using these selected dynamic ranges, it was then assumed that the reaction was 100% efficient for analyses.

Table 6.3: Acceptable cDNA concentrations to achieve 100% efficiencies in qPCR reactions

Gene	**Acceptable dynamic range (ng)**
Per1	0.1-100
Bmal1	0.1-100
Clock	0.1-100
Cry1	0.1-100
Cry2	0.1-100
Nr1d1	1-100
Cdkn1a	0.001-100
c-Myc	0.1-100

6.18.4 Real time qPCR

Real time quantitative polymerase chain reaction (qPCR) was performed using human TaqMan® gene expression assays (Applied Biosystems, Warrington, UK) (Table 16). The TaqMan® gene expression assays are detailed in Table 16. The StepOne Plus™ Real-Time PCR system was used (Applied Biosystems). Each reaction well contained 1µl 20x TaqMan® gene expression assay, 10 µl 2X TaqMan® fast advanced master mix, 4 µl cDNA template (equal for all samples in an experimental study) and 5 µl RNase-free water.

Genomic DNA contamination was tested for in the RNA samples by performed qPCR on the control reverse transcription samples as well as the true samples. No PCR amplification product was found with these samples. No

template controls (NTC) were performed for every gene analysed to exclude any contamination of reagents used in the qPCR reactions. Samples were run in triplicate and performed on the same plate.

The conditions for qPCR were as follows; 20 seconds at 95°C, followed by 40 cycles of (denaturation, annealing and extension) 95°C for 1 second; 60°C at 20 seconds respectively. Real-time quantification plots were collected and stored by the StepOne™ software. Relative expression was determined using the delta Ct and delta delta Ct methods against the housekeeper gene PPIA. Results were plotted and analysed using Graphpad prism and excel. Statistical analysis of paired or unpaired Student's t-tests, as appropriate, were performed and results were considered significant if $p<0.05$ (95% confidence interval).

6.19 MICROARRAY EXPERIMENT ON HUMAN ANAGEN AND CATAGEN HAIR FOLLICLES

Redundant human scalp skin was obtained from the scalp of three patients (females, ages 48, 54 and 68) all undergoing facelift surgery following informed consent. Individual HFs were isolated by micro-dissection as described. Anagen VI HFs for each patient were maintained in a 24-well plate in supplemented HF organ culture medium. HFs were placed in an incubator at 37°C with 5% CO_2 level, maintained in culture and assessed daily using light microscopy to determine whether they appeared, macroscopically, to be in anagen or late catagen phases. The supplemented media was changed every two days. Anagen and late catagen samples were taken for microarray analysis to determine gene expression pattern differences between these two distinct cycle points.

Table 6.4: TaqMan® Gene Expression Assays used for qPCR experiments during the project

Gene symbol	Genebank accession number	TaqMan Assay ID	Gene name
CLOCK	NM_004898.2	Hs00231857_m1	clock homolog (mouse)
PER1	NM_001178.4	Hs00242988_m1	period homolog 1 (Drosophila)
BMAL1	NM_002616.2	Hs00154147_m1	aryl hydrocarbon receptor nuclear translocator-like
CRY1	NM_004075.3	Hs00172734_m1	cryptochrome 1 (photolyase-like)
CRY2	NM_021117.1	Hs00323654_m1	cryptochrome 2 (photolyase-like)
Nr1d1	NM_021724.3	Hs00253876_m1	nuclear receptor subfamily 1, group D, member 1
Cdkn1a	NM_000389.4	Hs00355782_m1	cyclin-dependent kinase inhibitor 1A (p21, Cip1)
c-Myc	NM_002467.4	Hs00905030_m1	v-myc myelocytomatosis viral oncogene homolog (avian)
SGK3	NM_013257.4	Hs00179430_m1	Serum glucocorticoid regulated kinase family, member 3
MSX2	NM_002449.4	Hs00741177_m1	msh homeobox 2
BMP2	NM_001200.2	Hs00154192_m1	bone morphogenetic protein 2
BMP4	NM_130850.2	Hs00370078_m1	bone morphogenetic protein 4
NOG		Hs00271352_s1	Noggin
PPIA	NM_021130.3	Hs99999904_m1	peptidylprolyl isomerase A
ACTB	NM_001101.3	Hs99999903_m1	actin, beta

Total RNA was extracted from the anagen VI and late catagen HFs using TRIzol® and the Purelink™ RNA Mini Kit (Invitrogen, UK). The total RNA was extracted at the same time to ensure that the conditions were equal between samples. The quantity and quality of the extracted total RNA was assessed using a BioAnalyzer 2100 (Agilent technologies Ltd., UK) and the samples were submitted to the University of Manchester Genomic Technologies Core Facility.

Total RNA (100ng) from each sample was converted into cDNA used for microarray analysis. Human genome U133A oligonucleotide microarrays were performed following manufacturer's instructions (Affymetrix®, UK). The data was processed firstly, by ensuring quality control using dChip (Li and Wong, 2004) and secondly, by performing background correction, normalisation and expression using the GC-RMA method (Wu et al., 2004).

The baseline or "control" group was taken as anagen and therefore the fold changes were calculated as the expression in catagen compared to anagen per patient. The data was tested for statistical significance by comparing the average expression of the anagen state (average fold change for three patients) against the catagen samples (average fold change for three patients) using paired Student *t*-tests. In addition, subsets of probes were created where probe up or down-regulation was greater or less than 1.5 fold change in all three patients. These subsets were named anagen signatures for the group that were down-regulated in catagen compared to anagen and the catagen signature for the up-regulated group. These sets were separately analysed for over represented gene ontologies (GO) using Database for Annotation, Visualisation and Integrated Discovery version 6.7 (DAVID 6.7) (Huang et al., 2009, Dennis et al., 2003).

Validations experiments for the microarray results was carried out using qPCR, performed in a collaboration with Dr. T. Biró, Department of Physiology, University of Debrecen, Debrecen, Hungary. Analyses of the obtained qPCR results were performed by the candidate. Student's t-test was performed to test for statistically significant differences between groups (anagen versus catagen).

7 CHAPTER 7: CLOCK GENES MODULATE THE HUMAN HAIR CYCLE: A MEETING OF TWO CHRONOBIOLOGICAL SYSTEMS

In preparation for submission to J. Mol. Cell Biol.

AUTHORS

Yusur Al-Nuaimi, Jennifer E. Kloepper, Iain Haslam, Michael Philpott, Balázs I. Tóth, Nilofer Farjo, Bessam Farjo, Gerold Baier, Rachel E.B. Watson, Tamás Bíró, Ralf Paus.

Candidate's contribution:

The candidate has performed the majority of the experimental work for this chapter, contributed to the experimental design, and performed all experiments, analysed and presented and prepared all data for publication (unless stated otherwise below) and wrote the current chapter.

Candidate supervisory team and lab members:

J.K. performed HF staging as second reader, a siRNA transfection experiment in Germany and proof read the chapter. She also has supervised the candidate.

I.H. contributed to experiments; 24 hour sampling for circadian rhythm, RNA extractions and qPCR for siRNA Period1 samples, immunohistochemistry and staining intensity measurements for Masson Fontana and Ki-TUNEL for three siRNA patients.

R.P. was the main supervisor of this project, designed the overall project plan, supervised most of the experimental work, and edited the manuscript.

R.P., R.W and G.B. are the candidate's supervisory team and have directed experimental plans, discussion of results and proof reading, direction and corrections of the text.

Collaborators:

B.T and T.B. performed qPCR for three time point samples of unsynchronised time series and 6 day TRH culture. They have also made suggestions for experiments and corrections of the text.

M.P.'s lab performed the *in situ* hybridisation of clock, Clock immunohistochemistry and has helped to edit the manuscript

N.F and B.F supplied some of the male occipital scalp hair follicles used in the study.

7.1 ABSTRACT

The hair follicle (HF) continuously undergoes cyclic tissue remodelling events controlled by an, as yet unknown, oscillator system. We hypothesised that peripheral circadian clock genes are involved in hair cycle control; namely the anagen-to-catagen transition. Human HF organ culture was used as a clinically relevant model for studying intersecting developmental, chronobiological and growth-regulatory mechanisms in the absence of central clock influences. Isolated, organ-cultured human scalp HFs show circadian expression of core clock genes (*Clock, Bmal1, Period1*) and hair cycle-dependent changes in the expression of *Period1.* Knock-down of *Period1* or *Clock* in human HFs significantly prolonged active hair growth (anagen), stimulated hair matrix keratinocyte proliferation and melanogenesis, and down-regulated clock-controlled genes *Cdkn1a* and *c-Myc*. Thyrotropin-releasing hormone, a hypothalamic regulator of clock gene activity, which promotes human hair growth, modulated clock gene transcription. This provides the first evidence that peripheral clock genes, namely *Period1* and *Clock,* modulate human hair anagen-to-catagen transition. We also show that *Period1* and *Clock* are novel regulators of human pigmentation *in situ*. Therefore, clock gene activity is identified here as an important regulator of human peripheral tissue physiology and remodelling, and constitutes a promising novel target for therapeutic modulation of human hair growth and pigmentation.

7.2 INTRODUCTION

The HF is a unique, highly dynamic mini-organ that, for the entire life-time of mammalian organisms, undergoes a cyclical remodelling process called the hair cycle (Kligman, 1959, Stenn and Paus, 2001, Schneider et al., 2009). In these rhythmic, precisely timed and controlled organ transformations, the HF cyclically recapitulates key aspects of its morphogenesis, undergoes massive cell death, before it regenerates again owing to its rich endowment with several different stem cell populations (Cotsarelis, 2006, Lavker et al., 2003, Fuchs, 2009). The growth stage (anagen) is characterised by long-lasting, intense epithelial proliferation and production of pigmented hair shafts. This is followed by rapid apoptosis-driven organ involution (catagen) where the lower two thirds of the HF regresses, and by a phase of relative quiescence (telogen) (Figure 7.1).

As an archetype of cyclic regenerative events, the hair cycle represents a fascinating system which exhibits its own autonomic, site-dependent periodicity. The HF is an ideal model for studying complex mesodermal-neuroectodermal tissue interactions and lies at the intersection of chronobiology, developmental biology, regenerative medicine and systems biology.

Despite an ever-increasing range of candidates involved in the co-ordination of the timely cyclic activity of the HF, the autonomous oscillator system that drives HF cycling remains essentially unknown, especially in the human HF (Paus & Foitzik Differentiation 2004, Lin et al. 2009, Plikus, Mayer et al. 2008; Schneider, Schmidt-Ullrich et al. 2009, Plikus et al. 2011). Thus, dissecting the regulatory molecules involved in dictating the rhythmic organ regeneration and regression of the HF promises new insights into the molecular mechanisms through which powerful biorhythms impact on mammalian organ regeneration and remodelling. Elucidating the controls that drive human HF

cycling is also of great clinical importance, since the vast majority of hair growth disorders can

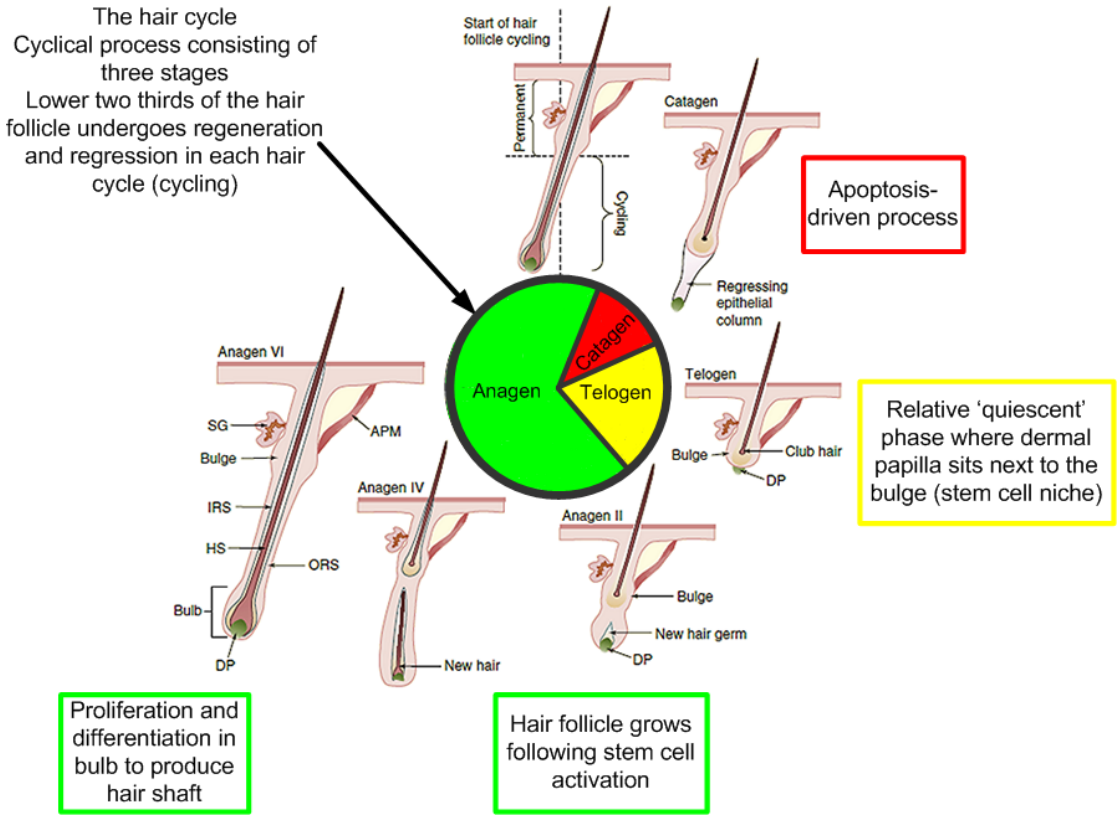

Figure 7.1: The hair cycle

The hair follicle undergoes a continuous cyclical process after morphogenesis involving regression and regeneration of the lower two-thirds of its structure. This process, named the hair cycle, consists of three stages, firstly catagen is initiated (red) involving apoptosis of the epithelial compartment of the hair follicle causing the cessation of hair shaft production and leaving behind an epithelial strand. This stage lasts approximately two weeks in humans. The dermal papilla rests next to the bulge region (epithelial stem cell niche) in the telogen phase (yellow) of the hair cycle and a club hair formed. Shedding of the hair is described as exogen, but is a side path off the cycle stages. After approx. 2-4 months in humans, stem cells are activated and the anagen phase commences (green). This involves the total regeneration of the lower two-thirds of the hair follicle as rapid proliferation and differentiation occurs. Anagen involves the production of a new hair and lasts 2-7 years on the human scalp. DP = dermal (follicular) papilla, HS = hair shaft, ORS = outer root sheath, SG = sebaceous gland. Adapted after Schneider et al, 2009. The Hair Follicle as a Dynamic Miniorgan. Current Biology 19:R132-R142

be attributed to changes in normal HF cycling dynamics, most notably to abnormalities in the anagen-catagen transformation (Cotsarelis and Millar

2001; Paus 2006). Unfortunately, none of the currently FDA-approved major anti-hair loss drugs (e.g. finasteride, minoxidil) counteract undesired anagen shortening at a satisfactory level of efficacy and reliability. Therefore, more effective "hair drugs" that target key components of the human hair cycle are urgently needed.

There is growing consensus that the regulatory mechanisms governing the human hair cycle are based on an autonomous, intra-follicular oscillator system (Al-Nuaimi et al., 2010, Robinson et al., 1997, Paus and Foitzik, 2004, Kwon et al., 2006). Here, we hypothesise that clock genes, responsible for the autonomous oscillatory timing system, that is the circadian rhythm, are core molecular elements of human hair cycle regulation.

Clock genes represent a crucial chronobiological system for the organisation of cyclic changes in the activities of cells, tissues, and organisms (Miller et al., 2007, Lowrey and Takahashi, 2004, Dunlap et al., 2004). The circadian rhythm is brought about by a self-autonomous process driven by transcriptional and translational feedback loops and post-translational processes (Figure 7.2). The result is a timing of approximately 24 hours. The central clock is governed by a central pacemaker ("master clock") in the suprachiasmatic nucleus (SCN) (Dunlap et al., 2004, Dardente and Cermakian, 2007, Langmesser et al., 2008, Shearman et al., 2000, Kume et al., 1999). The molecular components of the core clock mechanism are the PAS (PER-ARNT-SIM) domain transcription factors including Clock, Bmal1,Npas2 and Cry1, Cry2, Period1, Period2 and Period3 (Lowrey and Takahashi, 2004). CLOCK and BMAL1 transcription factors form a heterodimer which bind to the E-box response element for Pers and Crys and induce their transcription making up the positive limb of the feedback process. Translated PER and CRY proteins heterodimerise in the cytoplasm and enter the nucleus to inhibit CLOCK-BMAL1 heterodimerisation via interaction with the PAS domain of CLOCK-BMAL1 forming a negative feedback loop and repress their own transcription (Dardente

and Cermakian, 2007, Langmesser et al., 2008, Shearman et al., 2000, Reppert and Weaver, 2002, Gekakis et al., 1998, Duffield, 2003, Takahashi et al., 2008).

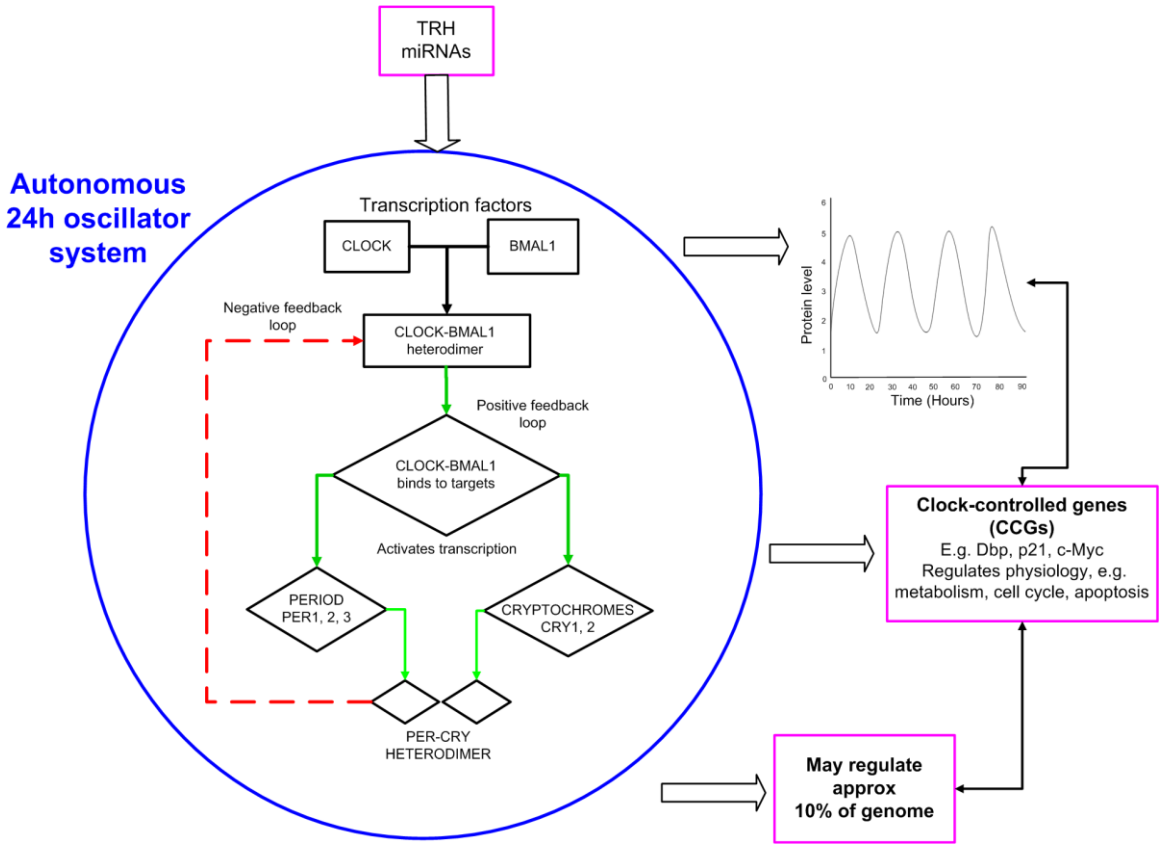

Figure 7.2: Basic core clock mechanism with regulatory inputs and outputs

The mechanism governing the circadian system involves self-sustaining endogenous oscillators which consist of interlocking transcriptional feedback loops synchronised via a central pacemaker ("master clock") in the suprachiasmatic nucleus (SCN) (Dardente and Cermakian, 2007, Langmesser et al., 2008, Shearman et al., 2000, Dunlap et al., 2004, Kume et al., 1999). The molecular components of this core clock mechanism (components within the blue circle represent this at a very simplified level) involve auto-regulated expression of a class of PAS (PER-ARNT-SIM) domain transcription factors including Clock, Bmal1, two Cryptochrome genes (Cry1 and Cry2) and three Period genes Period1, Period2 and Period3 (Lowrey and Takahashi, 2004). CLOCK and BMAL1 proteins form a heterodimer (positive loop, green arrows) which bind to the E-box response element for Per and Cry and induce their transcription. The translated PER and CRY proteins (negative loop, red dashed line) in turn inhibit CLOCK-BMAL1 heterodimerisation via interaction with the PAS domain of CLOCK-BMAL1 (Dardente and Cermakian, 2007, Langmesser et al., 2008, Shearman et al., 2000, Reppert and Weaver, 2002, Gekakis et al., 1998, Duffield, 2003). Other genes that are not involved in the clock mechanism, CCGs, such as D-box binding protein (Dbp), are regulated directly by the CLOCK-BMAL1 heterodimer. These CCGs have been found to be involved in physiological processes with 10% of genes within a tissue found to be CCGs. Importantly the expression of these genes have also shown tissue-specific expression (Duffield, 2003). The resulting

output of the clock mechanism is that mRNA and protein levels within this basic and extended system oscillate as seen in the graph.

A secondary loop exists comprising of orphan nuclear receptor NR1D1 which associates with BMAL1. It is thought that this accessory feedback loop acts to improve the robustness of the circadian mechanism (Takahashi et al., 2008). Recently, it has been shown that peripheral tissues also possess peripheral clocks responsible for implementing local physiology (Dardente and Cermakian, 2007). The core molecular components of both central and peripheral oscillators are preserved. A peripheral clock has been demonstrated in the murine skin (Tanioka et al., 2009).

Other genes that are not involved in the clock mechanism; clock-controlled genes (CCGs), such as *c-Myc* and *Cdkn1a* (also known as *p21*), are regulated directly by the CLOCK-BMAL1 heterodimer (Miller et al., 2007). CCGs have been found to be involved in physiological processes with 10% of genes within a tissue thought to be CCGs. Importantly the expression of these genes have also shown tissue-specific variability (Duffield, 2003).

That clock genes and clock-controlled genes (CCGs) are evident candidates for an involvement in the human hair cycle (Geyfman and Andersen, 2010) is further supported by the fact that clock genes not only exhibit autonomous, self-regulated oscillations (Dardente and Cermakian, 2007, Dunlap et al., 2004, Dibner et al., 2010) but also impact on cell cycle and apoptosis control (Lee, 2005, Chen-Goodspeed and Lee, 2007, Fu et al., 2002, Matsuo et al., 2003, Miller et al., 2007, Takahashi et al., 2008); two key processes occurring during HF cycling. Indeed, CCGs and their encoded proteins are involved in murine HF cycling *in vivo* by interacting with cell cycle control (Lin et al., 2009). Even though it could not be excluded that this reflected the central clock influences on HF cycling, this study suggested that circadian clock genes are involved in cutaneous processes that transcend a 24-hour periodicity (Geyfman and Andersen, 2010). Also, human HF cells from plucked hair shafts have been shown to exhibit circadian rhythmicity in clock genes and CCG expression (Akashi et al., 2010).

The localisation and function of clock genes and proteins in the human HF remain to be characterised, and their impact on human HF cycling awaits clarification. More importantly, previous studies (Lin et al. 2009, Akashi et al. 2010) were not able to distinguish between the central and the peripheral clock in the HF. On this basis, we have addressed the following specific questions:

1. Does the expression of clock genes and proteins in intact human scalp HFs show circadian and/or hair cycle-dependent variations?
2. Does clock gene silencing affect human HF cycling, hair growth and/or pigmentation?
3. Does follicular (i.e. peripheral) clock gene expression underlie neuroendocrine controls that are recognised for the central clock, namely by TRH?

7.3 MATERIALS AND METHODS

7.3.1 Human skin and hair follicle sample collection

Redundant human scalp skin was obtained from the temporal or occipital regions from females undergoing routine facelift surgery (total n=10, 54-71 years) and scalp occipital hair follicular units from males undergoing hair transplantation surgery (total n=6, 28-66 years). Tissue was obtained following ethical approval (Faculty of Medicine, Ethics Committee, University of Lübeck and Translational Medicine, University of Manchester) and informed patient consent. For whole skin analysis, skin was cut into small blocks and either fixed in 10% phosphate buffered formalin and snap frozen in liquid nitrogen or first embedded in Shandon Cryomatrix (Fisher Scientific) prior to snap freezing. For isolated HF analyses, these were isolated by microdissection and then used in HF organ culture experiments or embedded in Shandon Cryomatrix and snap frozen in liquid nitrogen for immunohistochemistry experiments.

7.3.2 Human hair follicle organ culture

Anagen VI HFs were isolated from human scalp skin according to previously described methods (Philpott et al., 1990, Sanders et al., 1994). Using this well-established model, human HFs are able to continue growing in standardised conditions whereby late anagen (anagen VI) HFs will continue to produce a hair shaft exhibiting elongation and eventually enter a catagen-like state spontaneously. The other stages of telogen and early anagen are not captured using this method.

Isolated HFs were maintained in a 24-well plate; each well containing 500 µl serum-free Williams' E medium (Biochrom) supplemented with 2 mmol/L L-glutamine (Invitrogen), 10 ng/ml hydrocortisone (Sigma-Aldrich), 10 µg/ml insulin (Sigma-Aldrich) and 1% antibiotic/antimycotic mixture (100x, GibCo). The supplemented medium was changed every second day.

7.3.3 Time series experiments for temporal gene profiling in anagen human hair follicles

In order to establish the expression pattern of core clock genes and selected CCGs during the circadian cycle, human scalp occipital anagen VI HFs from two patients were obtained. The operations were performed during the time window of 09:30-13:00 GMT. Microdissection of the HFs was performed and the HFs maintained in culture media for 24 hours for two patients and 7 days in the third patient. Synchronisation of the HFs was then performed using 100nM dexamethasone for 30 minutes and whole HFs were harvested every 4 hours following synchronisation for a 24 hour period. The HFs were maintained in constant conditions in a 5% CO_2 incubator at 37ºC. When harvested the HFs were stored in RNAlater and then processed for qPCR analysis (see below) to establish the expression pattern of *Clock*, *Bmal1*, *Period1*, *Nr1d1, Cdkn1a, C-myc*. A further experiment was performed without dexamethasone synchronisation as a comparison using 42 fronto-temporal anagen VI HFs (female, aged 64 years). These HFs were maintained in the same conditions. Time points of 8:00, 14:00 and 21:00 GMT were taken and the HFs snap frozen whole for qPCR analysis of *Clock*, *Bmal1* and *Period1*.

7.3.4 Hair follicle organ culture – "catagen culture"

In order to investigate changes in clock genes and proteins in accordance with the hair cycle, organ cultured anagen VI human HFs were isolated and maintained in organ culture conditions as described. HFs were assessed daily using a Nikon Diaphot inverted binocular microscope to determine whether they appeared, macroscopically, to be in anagen or early, mid- and late catagen phases. Once identified to be in the correct stage (Kloepper et al., 2009, Müller-Röver et al., 2001), HFs were immediately embedded in Shandon Cryomatrix and snap frozen in liquid nitrogen and 6μm thick cryosections cut by cryostat (Model CM 3050S, Leica) and stored at -80°C until required for immunohistochemistry analyses. HF stages (anagen versus catagen) were

assessed by applying carefully defined morphological and immunohistological staging criteria (Kloepper et al., 2009). For qPCR analyses anagen and catagen HFs were stored in RNAlater and then processed as described in the qPCR section (below and Chapter 6). This method was used for collecting HFs that were either maintained in anagen or had spontaneously entered catagen stages (early, mid and late catagen) and frozen for IF PERIOD1 and BMAL1. In addition, anagen and catagen HFs were obtained from one patient to check for any changes in expression between (non-synchronised) anagen and catagen HFs.

7.3.5 Synchronised time series experiment of anagen and catagen hair follicles to determine clock gene expression

Microdissected human scalp HFs were obtained from redundant hair transplantation surgery follicular units. Five patients were used for this experiment (Table 7.1). The first two patient samples for anagen were obtained as described for temporal profiling of anagen HFs. The last three patient samples were obtained after maintaining the HFs in organ culture as described. All HFs were assessed daily and staged according to macroscopic staging criteria (Kloepper et al., 2009). For patient C; once half the HFs had entered anagen and the other catagen, the samples were synchronised using dexamethasone and harvested into two groups anagen and catagen and the six time points for each group. For patients D and E, once all HFs were seen to be in catagen, the synchronisation and harvesting experiment over 24 hours was performed. This took between 7 and 14 days for the HFs to enter the correct stage. The HFs were maintained in RNAlater until processed for qPCR analysis to check the expression of *Clock*, *Bmal1* and *Period1*.

Table 7.1: Patient samples for 24 hour synchronised time series experiment

Patient ID	Age	Gender	Location	Hair cycle stage when samples taken
A	35	M	Occipital	Anagen

B	28	M	Occipital	Anagen
C	40	M	Occipital	Anagen
				Catagen (Both stages harvested on the same day)
D	40	M	Occipital	Catagen
E	40	M	Occipital	Catagen

7.3.6 *Clock* and *Period1* knock-down in organ cultured human hair follicles

Anagen VI HFs were isolated from human scalp skin as described (see above) (Philpott et al., 1990, Sanders et al., 1994). To inhibit the expression of *Clock* and *Period1* genes in human HFs, HFs were transfected with *Clock* siRNA (Clock siRNA (h): sc-35074) and *Period1* siRNA (Per1 siRNA (h): sc-38171) in separate organ culture experiments (see Table 7.2). All reagents were from Santa Cruz Biotechnology, Inc. and the transfections were performed according to manufacturer's gene silencing protocol. HFs were incubated for 5 hours at 37ºC in an atmosphere of 5% CO_2 and 95% air. siRNA Transfection medium was then removed and HFs incubated for either an additional 24 or 96 hours in supplemented William's E Medium. Medium was changed every 48 hours. Control experiments were performed in parallel, using the same patient HFs, with random scrambled oligos (Control siRNA (FITC Conjugate)-A: sc-36869) (Santa Cruz). Whole HFs were collected from the siRNA transfected and control groups for qPCR or immunohistochemical analyses. PERIOD1 (PER1) protein staining, Masson Fontana and double staining for Ki-67/TUNEL were performed to decipher any effect on proliferation and apoptosis, melanin content and PER1 protein production by siRNA treatment at either 24 hours or 96 hours. HFs were allocated into their correct hair cycle stage (either anagen or early, mid-, late catagen) using microscopic staging criteria on all cryosection pictures taken from IHC analyses after 96 hours culture. The results of each stain was analysed

by combining the data from the four patients for the siRNA *Period1* data and the one patient for siRNA *Clock* data. Contingency table analysis (Fisher's Exact test) was performed to test for significant differences in staged groups between the siRNA and control groups. Significant differences were taken as $p<0.05$.

Table 7.2: siRNA transfection experiments – sample demographics and experimental plan

Gene	SiRNA probes used	Patient Age	No. of HFs	Location	Duration of knock-down
Period1	Period1 siRNA (h): sc-38171 and control siRNA	69 yr, female	90	Scalp, occipital	24 hrs
		53 yr, female	70	Scalp, temporal	96 hrs
		47 yr, male	75	Scalp, occipital	96 hrs
		48 yr, male	75	Scalp	96 hrs
		45 yr, male	83	Scalp	96 hrs
Clock	Clock siRNA (h): sc-35074, Control siRNA	71 yr, female	95	Scalp, occipital	24 hrs
		59 yr, female	92	Scalp, temporal	96 hrs

7.3.7 TRH treatment of human hair follicles - 6 day organ culture

To investigate the effect of TRH on human HFs in organ culture, isolated anagen VI HFs were maintained in a 24-well plate for 6 days. 5-100 ng/ml TRH was added to the culture medium every 48 hours as previously described (Gáspár et al., 2010). Once completed, HFs were either frozen whole (5 ng/ml and 100 ng/ml concentrations) for qPCR analysis or embedded for subsequent cryosectioning and immunohistochemical staining (5 ng/ml and 10 ng/ml concentrations). All HFs were maintained in the same conditions in organ culture and all samples were harvested within the same time window (19:00-22:00 h).

7.3.8 Quantitative PCR – Method 1

This method for qPCR was carried out for all experiments apart from those specified in the below section.

Total RNA was extracted from whole HF samples using PureLink RNA Mini Kit (Invitrogen) following the manufacturer's instructions. Samples were all treated with Purelink DNase treatment Kit (Invitrogen) as directed by the instructions. RNA purity and concentrations were established by analysing the UV absorbance using the Nanodrop ND-1000 (Fisher Scientific, Loughborough, UK). Reverse transcription was carried out using the cloned AMV First Strand cDNA Synthesis Kit (Invitrogen, Paisley, UK) according to the manufacturer's instructions. The volume of RNA added to the reaction mix was adjusted for each sample in each experiment to ensure the same concentration of RNA was loaded in the reverse transcription reactions for each sample set. This was to ensure that samples whose results were going to be compared by qPCR were subjected to the same conditions and to minimise any variation being due to different RNA amounts included in the reverse transcription reaction rather than true differences. Controls were included for each sample whereby the reverse transcription reaction was carried out without any reverse transcriptase. This was to test for any genomic DNA contamination present in the RNA samples during qPCR. Real time quantitative polymerase chain reaction (qPCR) was performed using human TaqMan® gene expression assays (Applied Biosystems, Warrington, UK) (Table 7.3). The TaqMan® gene expression assays are detailed in (Table 7.3). The StepOne Plus™ Real-Time PCR system was used (Applied Biosystems). Real-time quantification plots were collected and stored by the StepOne software. Relative expression was determined using the delta Ct and delta delta Ct methods against the housekeeper gene PPIA. Results were plotted and analysed using Graphpad prism and EXCEL (Microsoft®). Statistical analysis of paired or unpaired Student's t-tests were performed or one way ANOVA when appropriate. Results were considered significant if $p<0.05$.

Table 7.3: Taqman® qPCR primers

Gene	GeneBank Accession No.	TaqMan® assay ID	Full gene name
Clock	NM_004898.2	Hs00231857_m1	clock homolog (mouse)
Bmal1	NM_001178.4	Hs00154147_m1	aryl hydrocarbon receptor nuclear translocator-like
Period1	NM_002616.2	Hs00242988_m1	period homolog 1 (Drosophila)
Cry1	NM_004075.3	Hs00172734_m1	cryptochrome 1 (photolyase-like)
Cry2	NM_021117.1, NM_01127457.1	Hs00323654_m1	cryptochrome 2 (photolyase-like)
Cdkn1a	NM_000389.4	Hs00355782_m1	cyclin-dependent kinase inhibitor 1A (p21, Cip1)
c-Myc	NM_002467.4	Hs00905030_m1	v-myc myelocytomatosis viral oncogene homolog (avian)
PPIA	NM_021130.3	Hs99999904_m1	peptidylprolyl isomerase A
ACTB	NM_001101.3	Hs99999903_m1	actin, beta

7.3.9 Quantitative PCR – Method 2

The HF samples; 6 day TRH experiment, non-synchronised anagen and catagen samples, non-synchronised three time point samples and 24 hour knockdown with Period1 and clock confirmation were all performed in the Biro lab, Hungary. The following method was used: Total RNA was isolated using TRIzol (Invitrogen) and 1 µg of total RNA was reverse-transcribed into cDNA by using 15 U of AMV reverse transcriptase (Promega) and 0.025 µg/µl random primers (Promega). Q-PCR was performed on an ABI Prism 7000 sequence detection system (Applied Biosystems) using the 5' nuclease assay as detailed previously (Bodo et al., 2005, Tóth et al., 2009). PCR amplification was performed by using the TaqMan® primers and probes (Table 7.3) and the TaqMan® universal PCR master mix protocol (Applied Biosystems). The internal control gene used to normalise the data for all cases apart from TRH-treated HFs was *peptidylprolyl isomerase A* (*PPIA*). *β-actin* (*ACTB*) was used for the 6 day TRH treated-HFs.

Normalisation was carried out based on the delta Ct method. Experiments were performed in triplicates; the average relative expression levels were calculated and plotted using EXCEL (Microsoft®) or Graphpad prism. Statistical analyses were carried out with SPSS 9.0 statistical software (SPSS Inc.) using independent sample *t*-tests and one-way ANOVA. Pair-wise comparison was performed using both Dunnett and Bonferroni tests in order to compare the means of more than 2 samples.

7.3.10 *In situ* hybridisation for *clock* mRNA

For the *in situ* hybridization, digoxigenin (DIG) labeled *Clock* sense and antisense probes were generated as previously described (Eichberger et al., 2004) (Table 7.4)**.** In brief, 6µm tissue sections were pre-hybridised in pre-hyb-solution (4x saline sodium citrate (SSC), 1x Denhardt's, 50% formamide, 500 mg/ml tRNA and 500 mg/ml salmon testes DNA, denatured at 100 ºC for 10 min and placed on ice before adding to the mix) and incubated at 42 ºC for 3-4 hours. Hybridisation was carried out using fresh pre-hyb-solution containing 80-100ng labelled probe (denatured at 65 ºC for 5 min) at 42 ºC overnight. Sections were washed in 2x SSC for 5 min (two times) and in 2x SSC, 1x SSC, 0.5x SSC, each containing 50% formamide, at 45 ºC – 55 ºC and in 0.1x SSC 50% formamide at 50 ºC – 60 ºC for 20 min. A final wash was in 2x SSC and rinsed in DIG buffer 1 (100mM Tris-HCl, 150mM NaCl pH 7.5). Sections were blocked with 10% normal sheep serum (NSS) in DIG buffer 1 and incubated with an anti-DIG alkaline phosphatase-conjugated antibody (Roche) diluted 1:400 in 1% NSS DIG buffer 1 for 2 hours, followed by washing in DIG buffer 1 (two times) and DIG buffer 2 (100 mM Tris-HCl pH 9.5, 100 mM NaCl, 50 mM $MgCl_2$) for 10 min. The hybrids were visualised by incubating the section with BCIP/NBT (Sigma-Aldrich) liquid substrate in dark at 4 ºC overnight. The colour reaction was stopped by immersing the sections in 10 mM Tris-HCl pH8 1 mM EDTA for 30 min. The developed slides were mounted and examined under a light microscope**.**

Table 7.4: Primer sequences for Clock mRNA in situ hybridisation

Primer	Forward (5' → 3')	Reverse (3' → 5')	Gene bank accession number
Clock (h)	AACAACTTCAGATGGTCCATGGT	GAGTTGTGCCAATGTGTCCAGT	NM_004898.2
GAPDH (h)	TCCCATCACCATCTTCCA	GTCCACCACCCTGTTGCT	NM_002046.3

7.3.11 Quantitative immunohistomorphometry

Immunohistochemistry (IHC) staining for localisation and quantification of clock proteins was established and performed on whole human scalp skin cryosections (8 µm) and isolated human scalp HFs (6 µm). (Table 7.5 provides details of the individual IHC methodologies.) Primary antibodies were incubated overnight at 4°C. Sections were washed in either phosphate-buffered saline or TRIS-buffered saline between steps. Sections that were to be directly compared for quantification were processed at the same time to ensure that any variation in results were not due to different experimental conditions. IHC staining for Masson-Fontana and Ki-67/TUNEL double-immunofluorescence microscopy were carried out as previously described in (Ito et al., 2005b) and (van Beek et al., 2008), respectively. Immunolocalisation and intensity analyses were performed with the Biozero-8000 microscope (Keyence) and analysed using ImageJ software (National Institute of Health). Immunofluorescent images were taken using the same exposure time when using intensity of fluorescent stain for quantitative analyses. To compare staining intensity and positive cell numbers, the mean values from multiple cryosections was taken to allow for variation in sections.

Table 7.5: Protocol summaries for clock protein immunofluorescence and immunohistochemistry experiments

Protein	Primary Antibody	Secondary antibody, detection system	Negative control (besides omission of primary antibody)	Positive control tissue	References
CLOCK	Rabbit anti-human Clock (Clock AB5418P, Chemicon)	Horse anti-rabbit biotinylated (Vector Laboratories). ABC detection system		HaCaT cell line	(Zanello et al., 2000)
BMAL1	Rabbit anti-human MOP3, 1:40 (MOP31-A, Alpha Diagnostics)	Goat anti-rabbit fluorochrome 1:200 (Jackson Immunoresearch)	Primary antibody pre-incubated with blocking peptide (MOP31-P, Alpha Diagnostics)	Human pineal gland	(Ackermann et al., 2007)
PER1	Rabbit anti-human PER1, 1:100 (PER12-A, Alpha Diagnostics)	Goat anti-rabbit fluorochrome 1:200 (Jackson Immunoresearch)	Primary antibody pre-incubated with blocking peptide (PER12-P, Alpha Diagnostics)	Human pineal gland & HaCaT cell line	(Ackermann et al., 2007) (Zanello et al., 2000)

7.4 RESULTS

7.4.1 Expression of the clock genes *Clock, Bmal1*, *Period1* and clock-controlled genes *c-Myc, Nr1d1* and *Cdkn1a* exhibit a circadian rhythm in isolated human scalp anagen hair follicles

In order to establish whether microdissected HFs exhibit a circadian expression pattern, qPCR was performed on isolated human scalp anagen VI HFs. Following dexamethasone synchronisation of clock gene activity, HFs were sampled 4 hourly over a 24-hour period to determine whether *Clock, Bmal1* and *Period1* were expressed.

As shown in Figure 7.3, all three clock genes were expressed with circadian variation expression pattern displayed. The patients show similar expression patterns in terms of their phase distribution and mean overall relative expression values, however some variation was seen between patients (see Table 7.6). In the third patient, the expression patterns were noted to be different; in particular for *Period1* expression (Figure 7.3c) *Period1* mRNA was found to be undetermined in all samples apart from the 8 hours post synchronisation sample. The same patient samples did express *Clock* and *Bmal1* however (Figure 7.3c). This sample was taken after 7 days in culture, in contrast to the results in Figure 7.3a and 7.3b whose samples were harvested within 48 hours of surgery. In the unsynchronised sample, variation in expression levels *Bmal1* and *Period1* mRNA was also seen over the three time points, although this was minimal (Figure 7.4). Human HFs also exhibited circadian rhythmicity of CCGs, *Nr1d1, C-Myc* and *Cdkn1a (p21)* in the patients A and B (Figure 7.5). Patient C was not tested for CCG expression. Subsequent to this analysis, all experiments not involving time series sampling were performed by harvesting HFs within the same time window (7-10 p.m.; see Methods) to control for these dynamic expression changes.

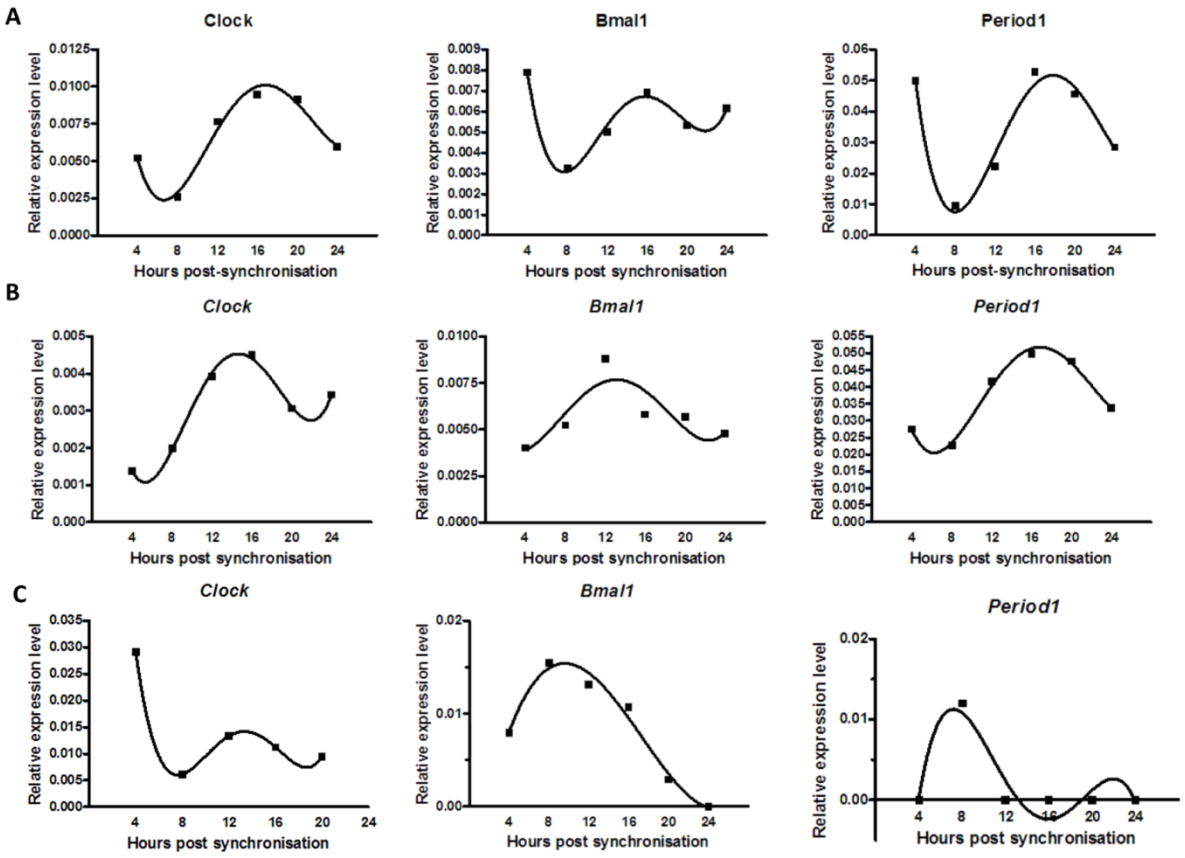

Figure 7.3: Circadian expression profiles of clock transcripts Clock, Bmal1 and Period1 in isolated human hair follicles.

Clock, Bmal1, Period1 mRNA was quantified using qPCR in whole hair follicles synchronised with dexamethasone and sampled at time points 4, 8, 12, 16, 20 and 24 hours post synchronisation. Data shown are the mean relative expression levels for each gene compared to housekeeping gene PPIA in individual patients (A), (B) and (C) (black dots). Fourth order polynomial graphs were fitted to the data to demonstrate the oscillatory pattern of expression over 24 hours (solid black line).

Table 7.6: Summary table of the pattern of clock mRNA expression in anagen hair follicles

Clock, Bmal1, Period1 mRNA was quantified using qPCR in whole hair follicles synchronised with dexamethasone and sampled at time points 4, 8, 12, 16, 20 and 24 hours post synchronisation. Data shown are the mean relative expression levels for each gene over all time points compared to housekeeping gene PPIA in individual patients (A), (B) and (C). S.d = standard deviation.

	Patient	**Amplitude**	**Mean expression**	**s.d.**
Clock	A	0.007	0.007	0.003
	B	0.003	0.003	0.001
	C	0.027	0.012	0.009
Bmal1	A	0.003	0.006	0.001
	B	0.005	0.006	0.002
	C	0.015	0.008	0.006
Period1	A	0.043	0.035	0.017
	B	0.027	0.037	0.011
	C	0.012	0.002	0.005

7.4.2 Clock proteins are expressed in normal human scalp hair follicles

Next, we studied follicular clock gene protein expression and localisation in microdissected human anagen VI HFs. Immunohistochemistry demonstrated that expression of the clock proteins CLOCK, BMAL1 and PER1 was restricted mainly to the HF epithelium, and was most prominent in the human ORS (Figure 7.6). However, BMAL1 immunoreactivity (IR) was also localised to the CTS and the DP of the HF, the key mesenchymal centres of HF biology. Expression of these proteins was confirmed in full-thickness human skin cryosections, using appropriate negative and positive controls (Figure 7.7 and Figure 7.8). These experiments show that human HFs express clock gene transcripts and proteins.

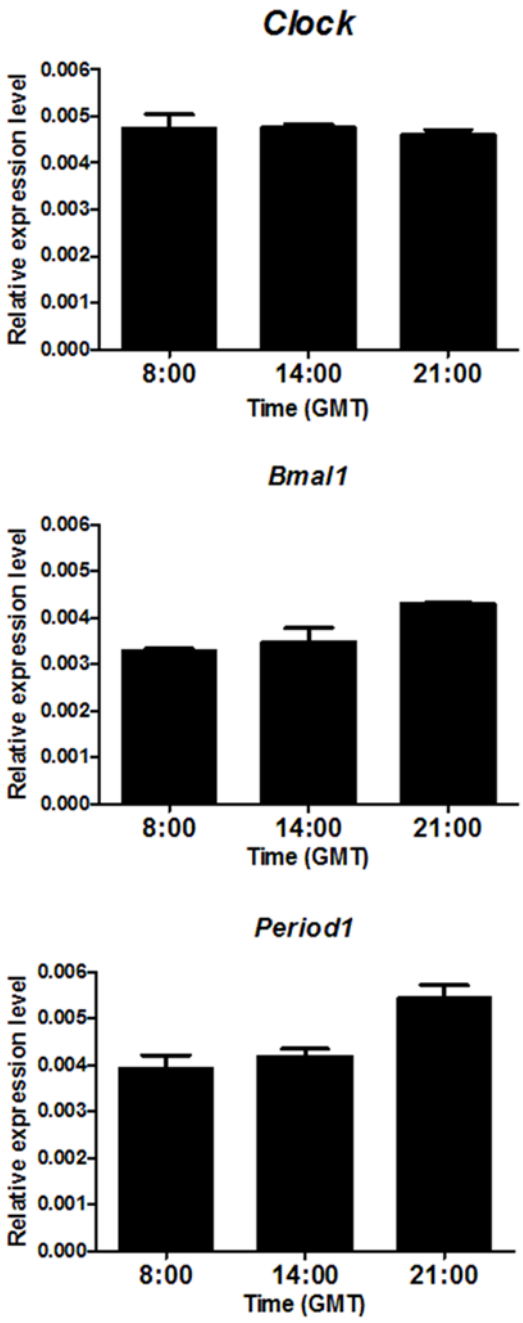

Figure 7.4: Unsynchronised time series of anagen hair follicles in organ culture.

Variation is seen in Bmal1 and Period1. Expression values are relative PPIA expression (housekeeper) calculated by using the delta Ct values. One way ANOVA and Student's t-tests did not find any significant differences between time points. Error bars are standard error of the mean (SEM). GMT = Greenwich Mean Time.

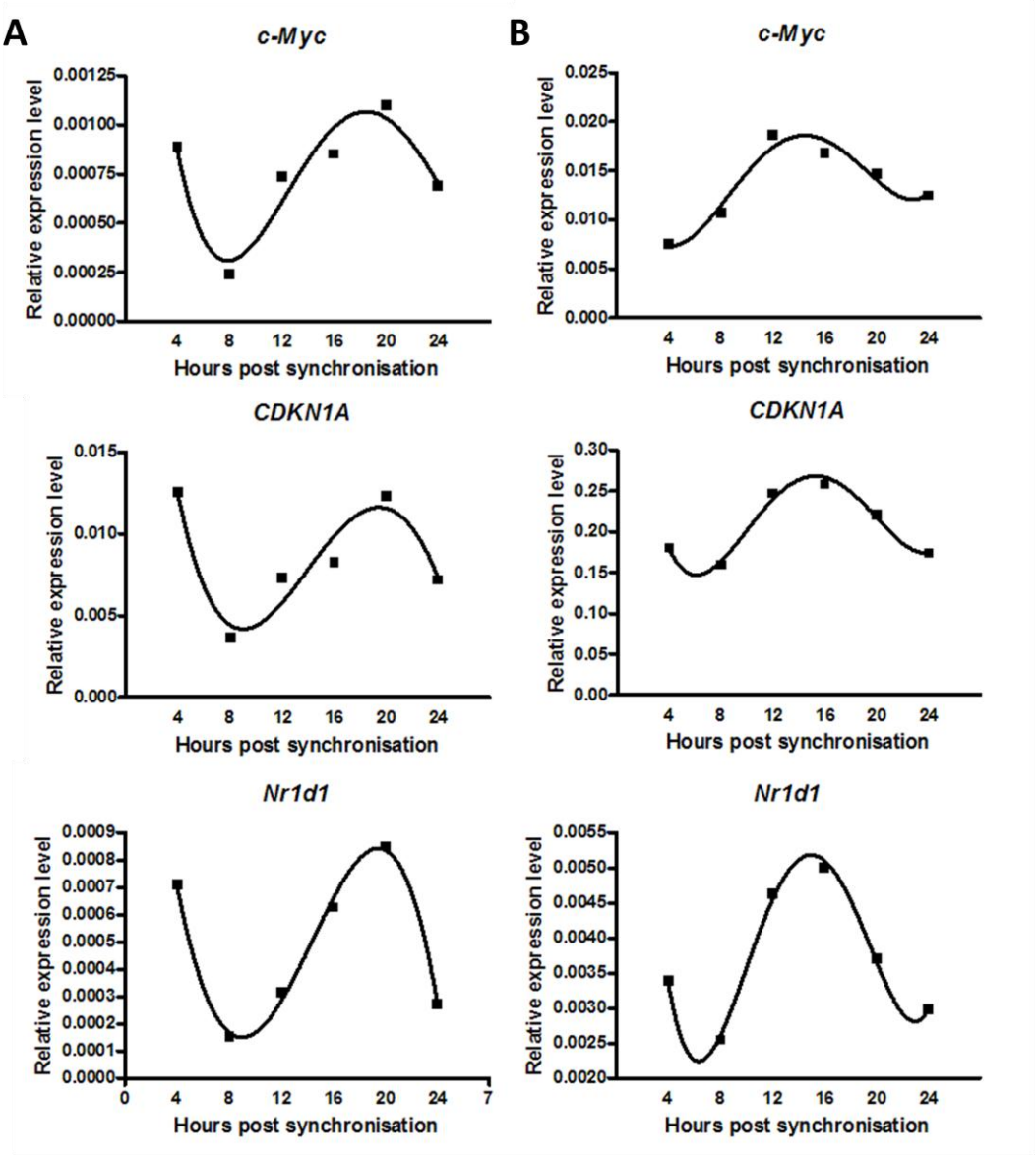

Figure 7.5: Clock controlled genes exhibit circadian expression in human hair follicles.

Two patients (A) and (B) are shown individually. Data is plotted as the mean relative expression value for each time point with PPIA as the housekeeping gene. Fourth order polynomial graphs were fitted to the data to demonstrate the oscillatory pattern of expression over 24 hours (solid black line).

Table 7.7: Immunoreactivity patterns of CLOCK, BMAL1 and PERIOD1 proteins in human hair follicles and skin.

CTS, connective tissue sheath; DP, dermal papilla; ORS, outer root sheath.

Antigen	*Hair follicle IR pattern*	*Skin IR pattern*	*Comments*
CLOCK	**Supra-basal cell layers of the infundibulum and ORS. Not detected in the matrix cells, proximal germinative epithelial cells, DP and CTS.**	**Detected in the epidermis (nuclear and cytoplasmic in the basal cell layer). Dermis: fibroblasts, blood vessels, nerve fibres, eccrine sweat gland, sebaceous gland (suprabasal layers of the sebaceous duct and mature sebocytes)**	Figure 7.6**a and 7.7**
BMAL1	**ORS, hair matrix, DP and CTS**	**Epidermis: all layers and dermis; individual fibroblasts and blood vessels.**	Figure 7.6
PER1	**Whole length of the ORS, matrix keratinocytes (cytoplasm and nucleus). HF mesenchyme (DP, CTS) negative**	**Basal layer of the epidermis and the sebaceous glands**	Figure 7.6 **and 7.8**

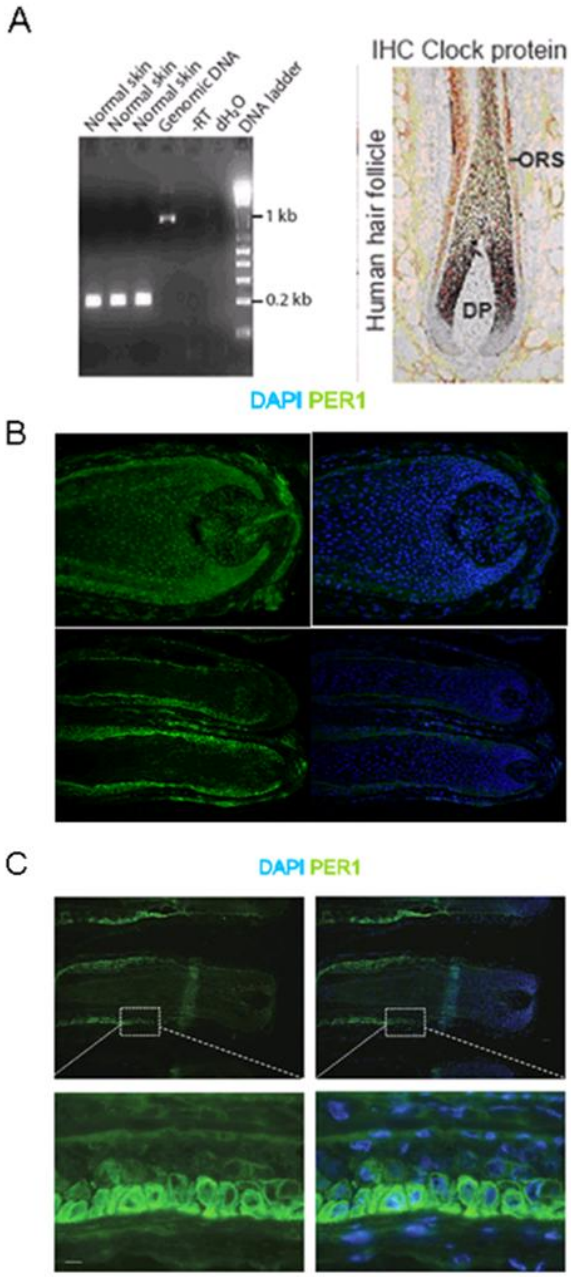

Figure 7.6: Clock, Bmal1 and Period1 expression in human hair follicles

(A) Clock protein and mRNA expression in human hair follicles. *RT-PCR gel showing Clock expression in normal human skin. IHC detected CLOCK protein in the hair follicle (ORS and supra-basal cell layers of the infundibulum) and in the basal and supra-basal layers of the epidermis in skin. (B)* ***Immunofluorescence human BMAL1 protein in*** *isolated micro-dissected human hair follicles. BMAL1 localised to the ORS and CTS. Expression did not significantly change between anagen and catagen stages using quantitative immunohistochemistry analyses of staining intensity (C)* ***PERIOD1 (PER1) protein expression in isolated human hair follicle cryosections****. PER1 is localised to the nucleus and cytoplasm (green). Cell nuclei are counterstained with DAPI (blue). PER1 is found in the ORS and MKs of the hair follicle.*

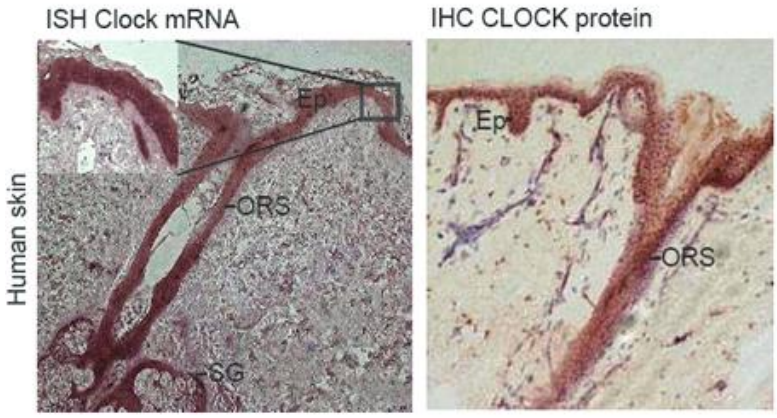

Figure 7.7: Clock mRNA and protein expression in human skin cryosections

Clock *mRNA localisation in the human skin and hair follicle was confirmed by in situ hybridisation (ISH) of whole human scalp skin cryosections (Red staining, left panel). Immunohistochemistry for CLOCK protein (red/bown staining, right panel) detected in the outer root sheath and supra-basal cell layers of the infundibulum in the hair follicle and in the basal and supra-basal layers of the epidermis in skin.*

7.4.3 Period1 and *Clock* expression increase in catagen hair follicles

To further test our working hypothesis that clock genes are implicated in the regulation of human hair cycling, we assessed whether the transcription and protein expression of clock genes was altered during the anagen-to-catagen transformation of organ-cultured HFs.

PER1 protein expression was found in the ORS and bulb MKs of anagen (A), early (EC), mid catagen (MC) and late (LC) catagen HFs Figure 7.9. In most analysed HFs, PER1 immunoreactivity was negative to minimal in the matrix during anagen, became increasingly positive during catagen stages, and was maximal in late catagen, as assessed by quantitative immunohistomorphometry (Figure 7.9). This expression difference in BMAL1 immunoreactivity between anagen and catagen HFs was not found (data not shown).

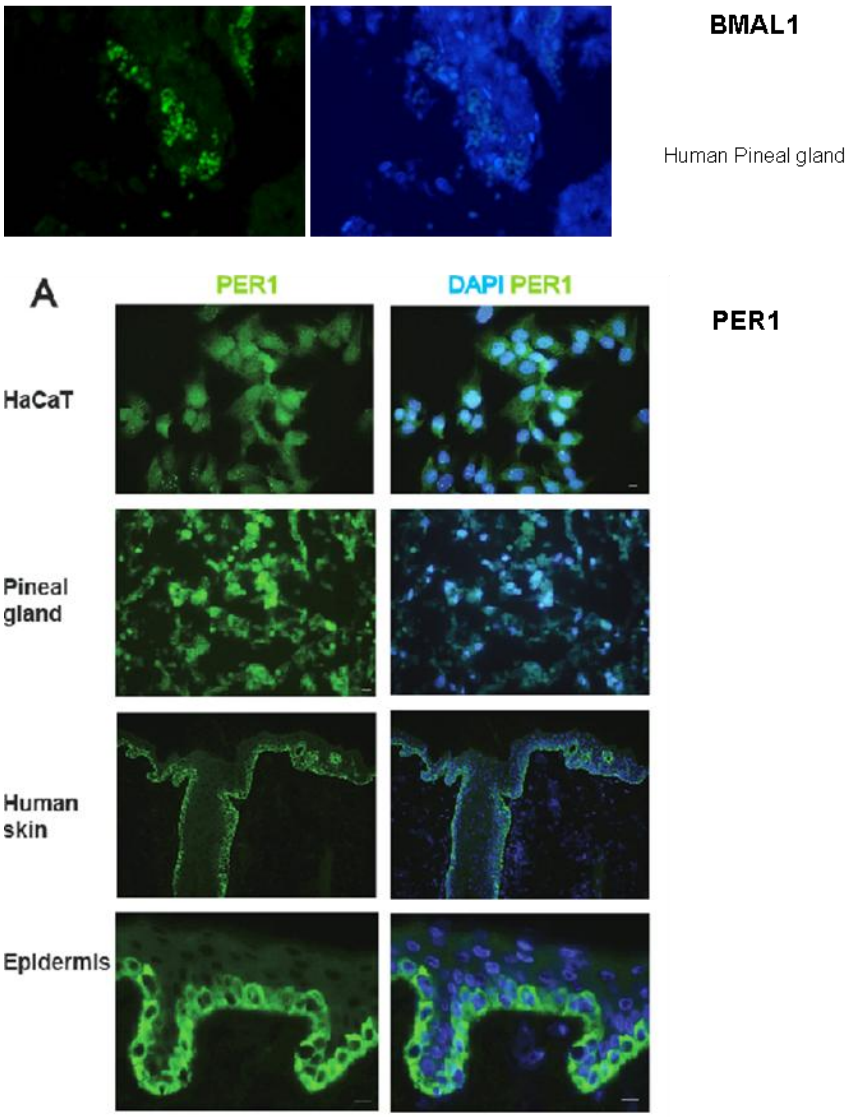

Figure 7.8: Immunofluorescent staining of BMAL1 and PER1 in positive control tissue and skin cryosections

Top panel displays BMAL1 immunofluorescent staining (green) in positive control tissue pineal gland. The right side picture shows the use of blocking peptide as a negative control. PER1immunofluorescent staining (lower picture set, green fluorescence) is localised to the nucleus and cytoplasm. Cell nuclei are counterstained with DAPI (blue). Basal cell expression of PER1 is found in the epidermis of whole human skin and in nuclei and cytoplasm of positive control tissues HaCaT cells and human pineal gland.

The protein expression data was also followed up on the transcriptional level (Figure 7.10). Synchronised samples comparing the expression of *Clock, Bmal1* and *Period1* in anagen and catagen HFs over 24 hours was obtained

(Figure 7.10). It was found that *Clock* exhibited a significantly higher mean expression in anagen when compared to catagen (mean anagen 0.007 (SEM 0.001), mean catagen 0.004 (SEM 0.0005) unpaired Student's t-test, p=0.046). There was no significant difference in mean expression values between anagen and catagen samples for both *Bmal1* and *Period1.* On qualitative assessment of the data: the wave form appeared to be different between the two cycle stages in all three genes (Figure 7.10) therefore, amplitude of expression was calculated by subtracting the minimum expression level for each gene in each state from its maximum (Figure 7.11). Compared to anagen VI there was a significantly increased amplitude of *Period1* mRNA expression in the catagen HFs (unpaired Student's t-test; $p<0.05$) (Figure 7.11). No phase shift effect was noted in the *Clock* and *Bmal1* samples between the anagen and catagen samples. In the *Period1* sample, there appeared to be some phase shifting, but the main difference noted in the amplitude of expression in catagen compared to anagen here.

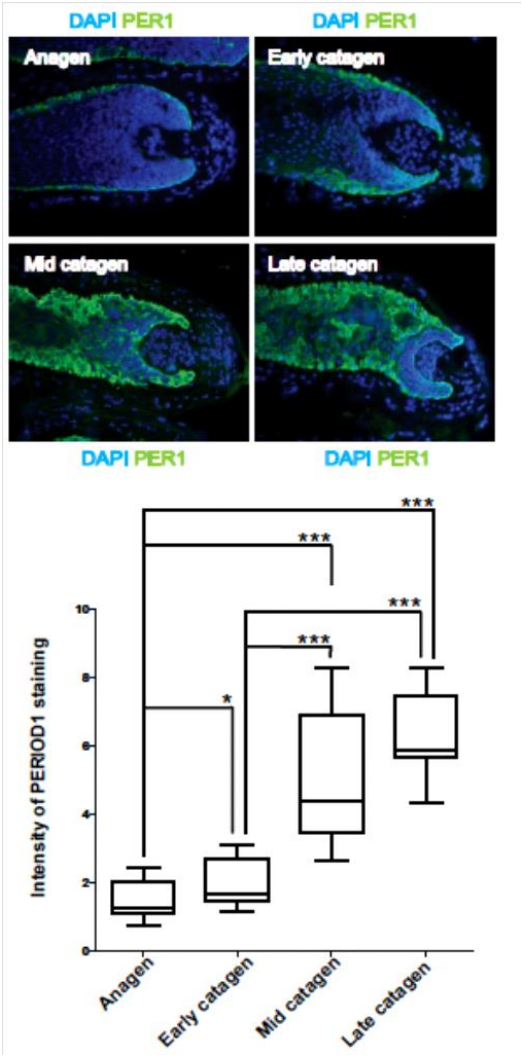

Figure 7.9: Differential expression of Period1 in human organ cultured hair follicles during anagen and catagen

*PER1 immunofluorescence on human anagen and catagen HFs. The HFs had been assigned to defined hair cycle stages on the basis of morphological criteria (Kloepper et al., 2009). As HFs were maintained in organ culture and a proportion spontaneously entered catagen. The time for this to occur varied between patients and is usually 4-9 days. PER1expression increased from anagen to late catagen with greatest expression in late catagen. Fluorescent images were analysed using ImageJ software. Intensity of fluorescent staining (FITC) was measured in reference area of interest (only the epithelial hair follicle) and average intensity in the reference area recorded. Intensity/area was calculated and results tested for statistical significance using Mann-Whitney U tests to compare two groups and p values were corrected for multiple testing using the Holm-Bonferroni test (*p <0.05,***p<0.001). Abbreviations: CTS, connective tissue sheath; ORS, outer root sheath; IRS, ORS, outer root sheath; DP, dermal papilla; MK, matrix keratinocytes.*

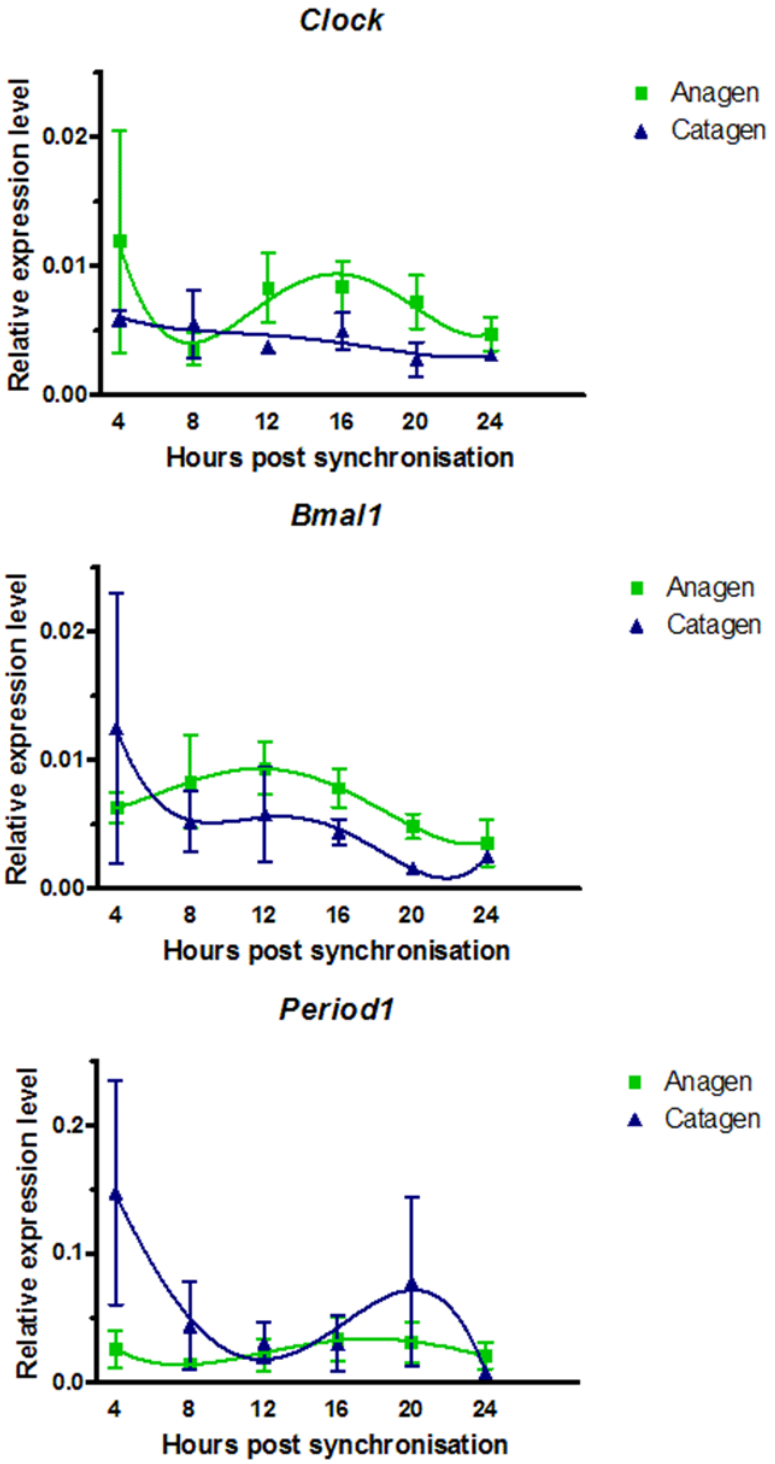

Figure 7.10: Time series expression of clock mRNA in anagen and catagen human hair follicles

The average relative expression levels (from three patients in each group – anagen (green) and catagen (green)) (determined by the delta Ct method against housekeeping gene PPIA) for each time point are displayed in the graphs. Error bars shown are SEM.

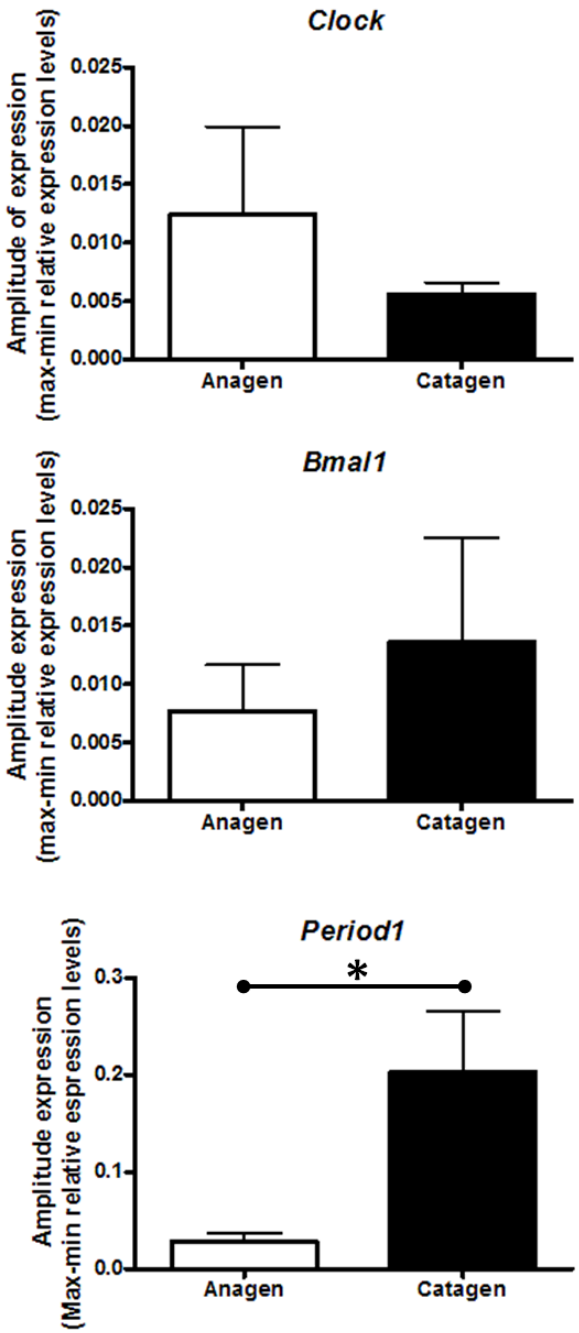

Figure 7.11: Amplitudes of clock mRNA expression in anagen versus catagen hair follicles

Difference in amplitude of expression was calculated by obtaining the maxima and minima expression levels for each gene (Figure 7.10). The plotted values show the means with SEM as error bars. Statistical significance was tested for using unpaired Student's t-test. Period1 amplitude in catagen was significantly greater than the anagen sample with $p<0.05$. Error bars shown are SEM.

7.4.4 *Period1* silencing in human hair follicles significantly prolongs anagen

In light of these data, we went on to functionally investigate the possible role of *Period1* and *Clock* in the anagen-to-catagen transition. Given that *Period1* expression was low in anagen and sharply rose during catagen, we hypothesised that silencing of *Period1* would prolong anagen duration. To test this hypothesis, human scalp HFs from four patients, were transfected with a *Period1*-specific siRNA probe. Success of the technique in human anagen HF organ culture was demonstrated on the mRNA and protein level (Figure 7.12).

Human HFs transfected with *Period1* siRNA showed a significantly greater proportion of anagen HFs (71.4%) than the control group (4.3%) 96 hours following *Period1* knock-down ($p<0.05$, Fisher's exact test) (see Figure 7.13 and (Table 7.8). In addition, the test group also showed a higher number of Ki-67 positive (i.e. proliferating) hair MKs compared to the scrambled oligonucleotide-treated HFs (three patients, total number of HFs in siRNA group= 10, control group = 12, non-significant) (Figure 7.14a). Since HF melanogenesis is tightly coupled to anagen (Tobin et al., 1999, Slominski et al., 2005), HF pigmentation was assessed as another independent marker for anagen prolongation. As shown by quantitative histochemistry (Masson-Fontana), 96 hours after Period1 knockdown, the melanin content of silenced HFs was higher than that of control HFs, but the difference did not reach statistical significance (three patients, total number of HFs in siRNA group= 12, control group = 10, Student's t-test $p=0.07$) (Figure 7.14b).

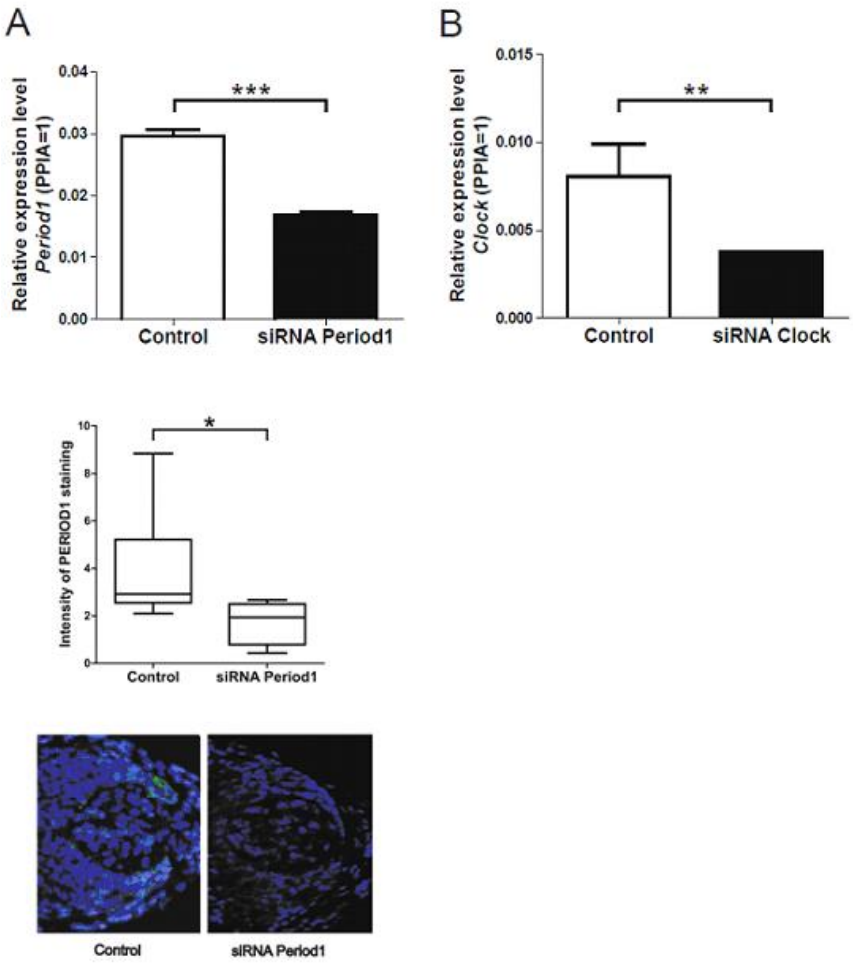

Figure 7.12: Period1 and Clock mRNA knock-down in human scalp hair follicles

*(A) Relative expression of Period1 mRNA in human hair follicles transfected with Period1 siRNA (n=24, mean 0.018) and corresponding control (n=24, mean 0.03). Housekeeping gene PPIA. Quantitative immunohistomorphometry of PER1 immunofluorescent staining 96 hours following Period1 knock-down compared to the control (random oligonucleotides). Hair follicles in the same hair cycle stage (mid catagen) were compared in the two groups to ensure that any differences in protein expression were not connected to the cycle stage differences in the two groups. (C) shows a box plot of the intensity of PER1 fluorescent staining in the matrix keratinocytes (reference area below Auber's line). The hair follicles transfected with siRNA Period1 showed a statistically significant reduction in the expression of PER1 protein. Mann-Whitney U test, * p<0.05 (B) Relative expression of Clock mRNA following Clock knock-down (n=26, mean expression 0.0003) and corresponding control (n=25, mean expression 0.007). Housekeeping gene PPIA. The difference between knock-down and control groups for each knock-down experiment was tested statistically using Student's t-test. ** p<0.01, ***p<0.001.*

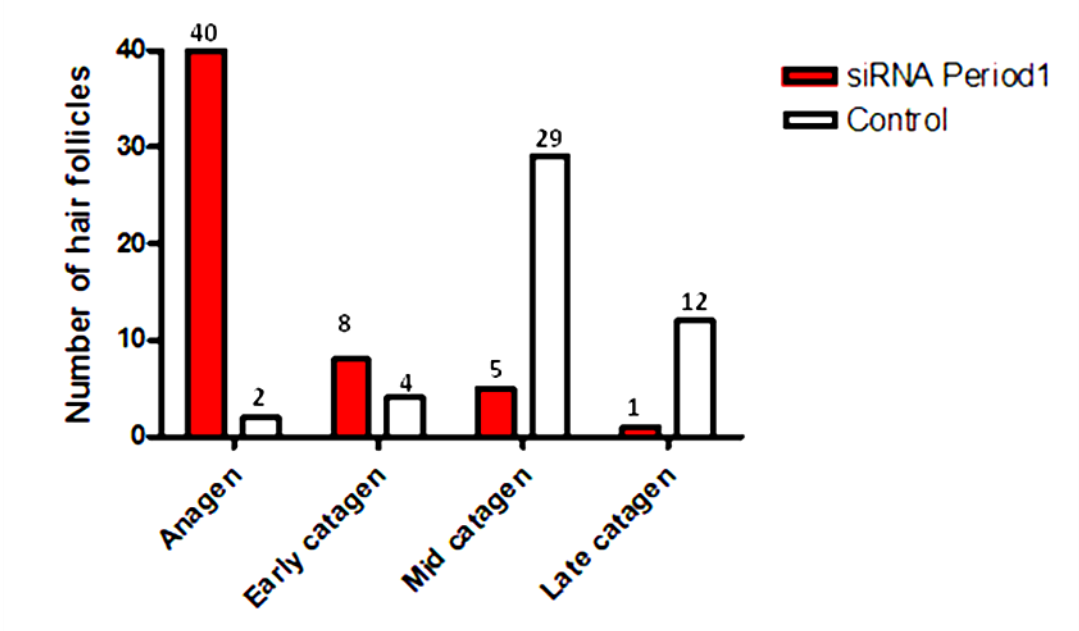

Figure 7.13: Hair cycle stages in Period1 knock-down hair follicles and controls

Graph displays the number of hair follicles found to be in each hair cycle stage 96 hours post-Period1 knock-down. This graph combines the staging results from 4 Period1 knock-down experiments performed for 96 hours on separate patients. 40 hair follicles were still in anagen in the Period1 knock-down group compared to only 2 hair follicles in the control group (treated with scrambled oligonucleotides). (p<0.05, Fisher's exact test).

7.4.5 *Period1* inhibits human HF melanogenesis

In order to check whether *Period1* has a hair cycle-independent effect on human HF pigmentation, only anagen VI HFs were compared between silenced and control groups in one patient. The melanin content of *Period1*-silenced anagen HFs was significantly increased (p=0.034, Figure 7.15).

	Anagen **n (%)**	**Catagen** **n (%)**	Total
siRNA Period1	40 (74.1)	14 (25.9)	54 (100)
Control	2 (4.3)	45 (95.7)	47 (100)

Table 7.8: Hair cycle stages in Period1 knockdown hair follicles and control

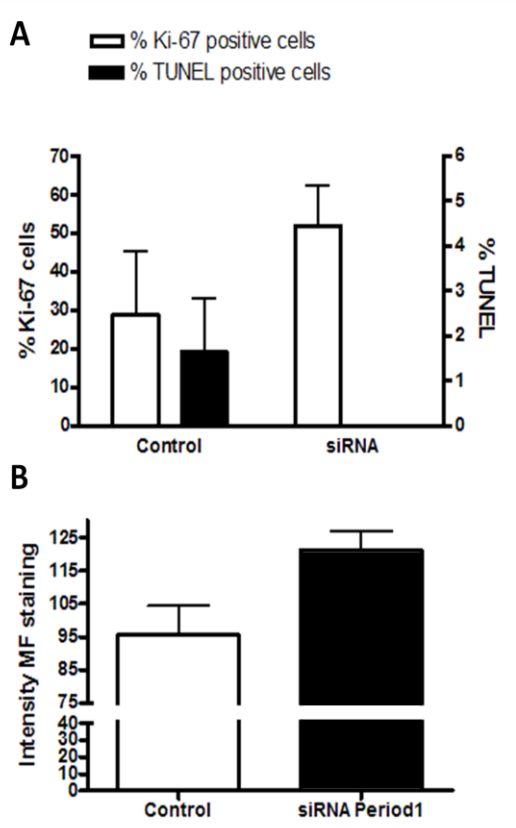

Figure 7.14: Period1 knockdown in human hair follicles - effect on proliferation, apoptosis and melanin content

In the 3 patients, 96 hours following Period1 knock-down, there was increased ki-67 positive cells and a decrease in TUNEL positive cells in the Period1 knockdown group These differences were not statistically significant. (B) An increased melanin content was also observed. (three patients, total number of HFs in siRNA group n= 12, control group n= 10, Student's t-test p=0.07). Error bars shown are SEM.

7.4.6 Clock knock-down prolongs anagen and increases both melanin content and hair matrix keratinocyte proliferation

We assessed whether *Clock* silencing also prolonged anagen. In the *Clock* knock-down group, 21.1% of HFs remained in anagen compared to 5.4% in the control group (Figure 7.16a). In addition, keratinocyte proliferation in the hair matrix was significantly increased after *Clock* silencing (p=0.017) (Figure 7.16b). As shown by quantitative histochemistry, when only anagen VI HFs were

compared between silenced and control groups, the melanin content of *Clock*-silenced anagen HF was significantly increased (Figure 7.16c).

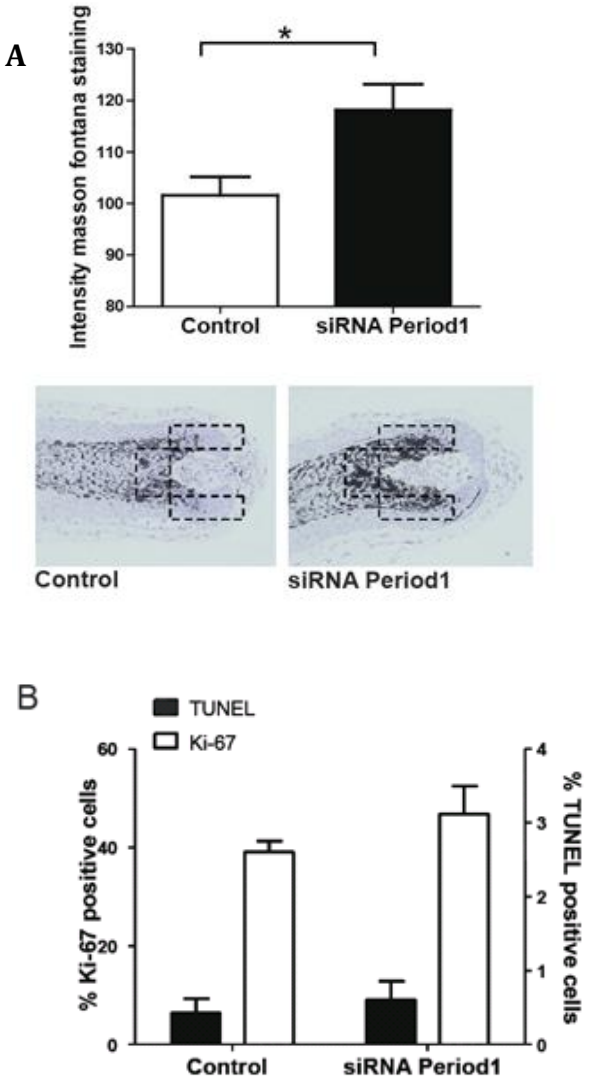

Figure 7.15: Modulation of melanin content in anagen hair follicles following Period1 knockdown

A. Period1 *knock-down increases melanin content in human anagen scalp hair follicles 24 hours following transfection. Images show Masson Fontana staining (Mann-Whitney U test, p=0.016). Average intensities were obtained over multiple cryosections to ensure un-biased quantification of sections. (B)* Period1 *knock-down in human hair follicles resulted in an increase in proliferation of human HFs 24 hours following transfection. Double immune-staining for Ki-67/TUNEL was performed on hair follicles following* Period1 *knock-down and the control group. An increased percentage of Ki-67 positive matrix keratinocytes were found in* Period1 *knock-down hair follicles (46.7%) when compared to control group (36.0%) (transfected with random oligos). This difference was found to be non-significant (Mann-Whitney U test, p=0.2). Error bars are SEM.*

7.4.7 Period1 may regulate anagen to catagen transition via CCGs genes some of which are already implicated in the hair cycle control

As a first attempt towards exploring the unknown mechanism by which clock genes may impact on human HF biology, we assessed by qPCR how *Period1* silencing affects the transcription of selected clock-controlled gene (CCG) expression, with emphasis on classical CCGs that are recognised as regulators of cell cycling and the apoptotic machinery. This revealed that *Period1* knock-down down-regulated the expression of c-*Myc* and *p21(CDKN1A)*, although this is the result of a preliminary study (Figure 7.17).

7.4.8 TRH may regulate the intrafollicular expression of clock-related transcripts

We wanted to determine whether TRH may regulate clock genes in the human HF. By qPCR we show that, compared to vehicle control HFs, TRH-treatment significantly up-regulated the transcription of Clock and Bmal1, while it significantly down-regulated Period1 expression (at the lower concentration of TRH) (Figure 7.18). Moreover, by quantitative immunohistomorphometry, PER1 protein expression was down-regulated by TRH, when only anagen VI TRH-treated and control HFs were compared.

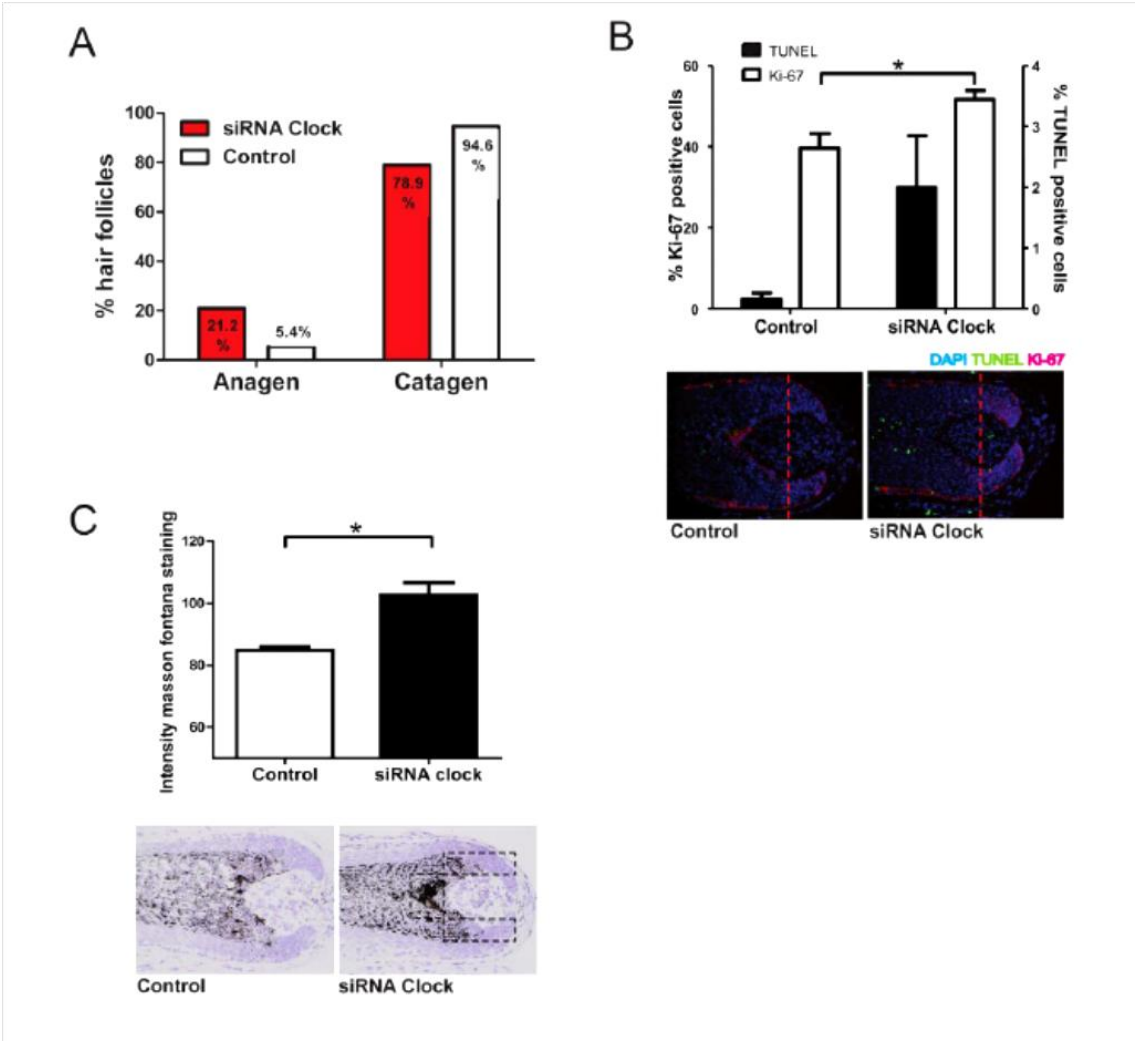

Figure 7.16: Clock knock-down in human hair follicles resulted in increased number of anagen hair follicles, melanin content and proliferation in human scalp hair follicles.

(A) 96 hours Clock *knock-down, 21.1% of hair follicles were found to still be in anagen as compared to 5.4% of hair follicles in the control group (using scrambled oligonucleotides). (B) Significantly increased melanin content was found in human hair follicles after* Clock *knockdown compared to the control (p=0.034). Average intensities were obtained over multiple cryosections to ensure un-biased quantification of sections. The intensity of the stains were measured in the reference areas as shown in B. (C) Double staining for Ki-67/TUNEL following* Clock *knock-down and the control group. The number of DAPI, Ki-67 (C) and TUNEL positive cells were counted within the reference area (C shows the reference area; this was the region bound by the epithelial hair follicle and below Auber's line (red line)). The percentage of Ki-67 positive and TUNEL positive cells was calculating using the number of DAPI positive cells as the total number of cells. Mann-Whitney U test compared* Clock *knockdown and control for differences.* Clock *knockdown resulted in a significant increase in the percentage of Ki-67 positive cells (p=0.017) after immunohistochemistry double staining for Ki-67 and TUNEL. The percentage of TUNEL positive cells also increased but this was not statistically significant. * p<0.05. Error bars shown are SEM.*

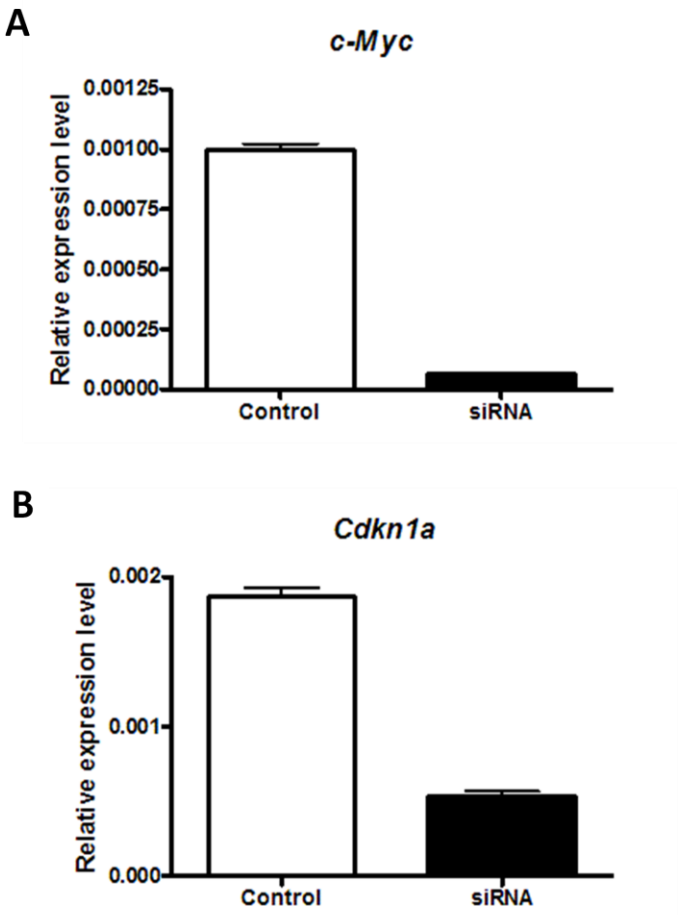

Figure 7.17: Expression of clock-controlled genes c-Myc and Cdkn1a following Period1 knockdown

qPCR was performed on one patient sample and relative expression levels determined of target genes against housekeeper gene PPIA. Both CCGs are down-regulated in the knock-down group. Statistical analysis was not performed as a greater patient number is awaited. Error bars shown are SEM.

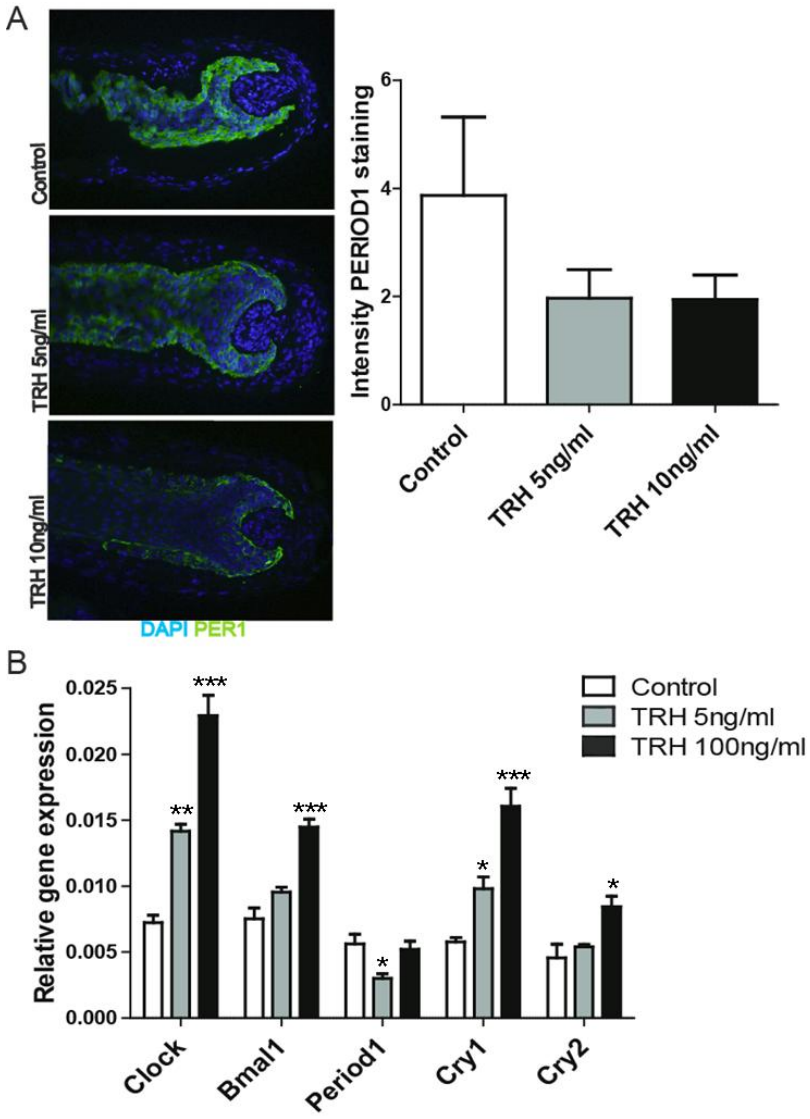

Figure 7.18: Thyrotropin-releasing hormone treatment - modulation of clock gene expression and PER1 protein expression.

PER1 protein expression decreases in intensity with thyrotropin-releasing hormone treatment. (B) Clock, Bmal1, Cry1 and Cry2 mRNA expression increases in a dose-dependent manner with thyrotropin-releasing hormone treatment. Expression was determined relative to housekeeper ACTB. The effect of TRH on CLOCK expression was significant at p<0.01 at 5ng/ml and p<0.001 at concentration 100ng/ml. The effect of TRH on Bmal1 was significant at higher TRH concentration when compared to control HFs (p<0.001). Cry1 expression was found to be significantly higher (p<0.001) in hair follicles treated with 100ng/ml of TRH compared to the control group. Period1 gene expression decreased compared to control hair follicles, but the trend was not dose-dependent. Period1 transcription was highest in the control group, lowest in the group treated with 5ng/ml of TRH (p<0.05) and increased in the 100ng/ml TRH treated group. Hair follicles in the same stage were compared to each other. Error bars shown are SEM.

7.5 DISCUSSION

The molecular control mechanisms that coordinate the human hair cycle have not been identified (Stenn and Paus, 2001, Paus and Foitzik, 2004, Paus et al., 1999a). In this study the role of clock genes and proteins, as potential candidates in controlling the human hair cycle, have been investigated. This study implicates circadian clock genes as regulators of infradian tissue remodelling events i.e. the human hair cycle. Importantly, we show that peripheral clock genes are not only expressed in a circadian and hair cycle dependent manner, but also actively modulate human anagen-to-catagen transition in the absence of influences from the central clock. Specifically, we identify *Period1* and *Clock* as functionally important anagen-terminating signals in the human HF. Although not established here, we present preliminary work that suggests that the mechanism may be via modulating the activity of cell- and hair cycle modulatory CCGs such as *p21* or *c-Myc*. In addition, we report the novel finding that *Period1* and *Clock* modulate HF pigmentation *in situ*. Finally, we explore the possibility that intra-follicular activity of clock gene activity in human HFs may be modulated by the neuroendocrine hormone TRH.

Evidence of a functional peripheral circadian clock is demonstrated in both anagen and catagen isolated human HFs. Both core clock and clock-controlled mRNAs were found to be expressed in a circadian manner (clock-controlled mRNA expression was investigated in anagen HFs only). The experimental assay of healthy micro-dissected human scalp HFs was used so as to eliminate any extra-follicular inputs on HF cycling (including central clock influences). Therefore, from our results, organ-cultured human scalp HFs seem to exhibit a functional circadian clock when removed from any central clock influences.

These results are in line with previous work on mammalian skin and cultured skin cell populations that show circadian expression of clock genes in these samples (Bjarnson et al., 2001, Balsalobre, 2002, Gachon et al., 2004, Lee, 2006,

Gréchez-Cassiau et al., 2008, Duguay and Cermakian, 2009, Lin et al., 2009, Akashi et al., 2010, Spörl et al., 2011).

We also demonstrate that human scalp HFs differentially transcribe the core clock mRNA (*Period1*) and its protein product (PER1) in a hair cycle-dependent manner; with up-regulation in catagen. In addition, knock-down of *Period1* significantly promoted anagen maintenance. Interestingly, we saw that in Patient C, the anagen HFs exhibited very minimal *Period1* mRNA expression (Figure 7.3c). The HFs had been maintained in organ culture for 7 days and both anagen and catagen HFs were harvested on the same day. Although, this was only reported in one patient, this fits into the hypothesis that *Period1* promotes catagen. The anagen HFs may have remained in anagen as they had a "*Period1* repression" (or knock-down) status. Of course, this can be confirmed or refuted by repeating the experiment for greater patient numbers in the future.

Our data also suggests that *Clock* promotes catagen, with knock-down promoting the anagen state. Our human data complements the previously documented role for *Clock* in the HF switch from telogen to anagen in mice *in vivo* with knock-out mice exhibiting delayed anagen entry (unfortunately, this switch cannot yet be studied in human HF organ culture as HFs do not enter telogen from catagen in organ culture) (Lin et al., 2009). Also, the Period1 protein and mRNA expression differences between anagen and catagen reported here are mirrored in the murine hair cycle: *Period1* mRNA expression in mouse skin increased during the anagen-catagen transformation of the HF (Lin et al., 2009), though less dramatically than seen during the human anagen-catagen transformation here. While this murine *in vivo* study could not exclude a major influence of the central clock on HF cycling, our current study excludes the central clock from playing a role in our isolated human HFs and therefore suggests that the peripheral clock is important for HF cycling, at least in the human system. This would need to be further examined in future experimental work.

While clock gene expression has already been reported in isolated, cultured human melanocytes (Zanello et al. 2000), we demonstrate here that *Period1* and *Clock* may be novel, endogenous inhibitors of human HF pigmentation, namely in the HF pigmentary unit (Tobin, 2011). This makes *Period1* and *Clock* the first clock genes to be potentially important modulators of normal human pigmentation *in situ*. Therefore, the current study extends upon previously published work by demonstrating circadian and hair cycle-dependent clock gene activity in intact human HFs (not just hair shafts (Akashi et al., 2010)) in the *absence* of central clock influences, and by demonstrating that clock gene silencing impacts human HF cycling and pigmentation.

The major hair growth- and proliferation-modulatory effects of clock gene silencing seen here are in line with the established concept that clock gene and CCGs directly control cell cycling (Lowrey and Takahashi, 2004, Miller et al., 2007). In fact, we demonstrate, in preliminary data performed on one patient, that selected genes involved in cell cycling are modulated by a knock-down of *Period1.* For example, the effect of *Period1* on the anagen-catagen transformation of human HFs may be via CCGs. The crucial cell cycle regulator and CCG, C-Myc, which is under direct circadian regulation (Lee, 2006, Fu et al., 2002) and also controls murine HF cycling (Bull et al., 2005), is affected by *Period1* knock-down. Thus, *Period1* may regulate the human hair cycle via modulating the cell cycle machinery of HF keratinocytes, very similar to the CCGs investigated in the murine hair cycle study by Lin et al. 2009 (Lin et al., 2009).

Namely, we show that the cell cycle regulator, *p21* (CDKN1A), acts as a CCG in isolated human HF and that *Period1* knock-down reduces *p21* expression. This fits nicely to the findings of Lin *et al*. who have shown an up-regulation of *p21* in the secondary hair germ of *Bmal1* knockout mice which display *delayed* anagen induction (Lin et al., 2009). Intriguingly, *Period1* is implicated in tumour suppression: *Per1* and *Per2* knockout mice exhibit neoplastic and hyperproliferative phenotypes, and deregulation of cell cycle

genes such as *c-Myc* and *Cyclin D1 are* found in *mPer2* mutants (Lee, 2005, Lee, 2006). Therefore, it is reasonable to propose that *Period1* controls the anagen-catagen transformation of human HFs by balancing apoptosis and proliferation in the hair matrix via CCG pathways as a hypothesis for future work. Among these classical *Period1* target genes, c-Myc and *p21* are recognised as important hair cycle-regulatory genes (Bull et al., 2005, Bull et al., 2001, Mitsui et al., 2001, Ohtani et al., 2007). Therefore, while this remains to be demonstrated, it is conceivable that *Period1* regulates the anagen-to-catagen transition via its impact on CCGs genes that subsequent execute this HF transformation.

It has been the experience in some laboratories that siRNA transfection induces apoptosis in human hair follicles in organ culture. To further delineate the role of *Period1* and *Clock* in the human hair follicle, it would be prudent to check the hair growth, hair cycle, melanin content, proliferation and apoptosis effect of siRNA transfection compared to untransfected HF controls also. This would indicate whether the changes seen in the *Period1* and *Clock* knock-down groups compared to the scrambled oligonucleotides controls was an effect that was over and above performing no transfection at all. This shall be performed in future experiments.

Since our organ-cultured human HFs did not contain the bulge region and its epithelial and melanocyte stem cells (Philpott et al., 1994a, Ito et al., 2004), the observed catagen inhibition and stimulation of HF pigmentation must have occurred independent of bulge epithelial and melanocyte stem cells. Using a recently developed model of keratin 15-promoter-driven GFP expression in human HF epithelial progenitor cells (Tiede et al., 2009), we hope to dissect, next, how *Period1* or *Clock* silencing impact on adult human epithelial stem cell biology *in situ*. A future question is therefore: How did clock genes and related CCGs impact on the progeny of these stem cells (i.e. transit amplifying cells) that constitute the hair bulb cells that have been studied in the current human HF organ culture assay?

The impact of thyrotropin-releasing hormone (TRH), a hypothalamic clock gene regulator (Gary et al., 1996, Gary et al., 2003) on human HF clock gene and PER1 protein expression was assessed here. This was particularly interesting in the current context, since it has been shown that TRH is expressed in human HFs and promotes human hair shaft growth and prolongs anagen duration *in vitro* (Gáspár et al., 2010). We found that TRH stimulated *Clock, Bmal1, Cry1* and *Cry2* mRNA expression, while its effect on *Period1* mRNA was variable according to dose, but decreased PER1 protein expression in human HFs. This suggests that TRH may modulate clock gene activity within the human HF. It is not clear, however, whether these differences may be secondary to phase shifting effects. We are currently performing further experiments to confirm these results following acute treatment with TRH. Human HFs have recently been recognised as an extra-hypothalamic site of TRH expression on the gene and protein level. In addition, TRH has been shown to inhibit catagen and stimulates hair MK proliferation (Gáspár et al., 2010). Therefore, TRH may serve as an intra-follicular neuroendocrine input signal for the regulation of human hair cycling. This is in line with the recognition that TRH centrally modulates clock-related biological rhythms (Gary et al., 2003). Therefore, regulatory feedback loops between TRH expression and clock gene activity can be envisioned and this will require further analyses.

This study extends upon previously published work by demonstrating circadian and hair cycle-dependent clock gene activity in intact human HFs in the absence of central clock influence. In addition, we demonstrate functional effects of clock gene silencing on human HF growth, cycling and pigmentation. Moreover, our data support the working hypothesis that spontaneous or neuroendocrinologically induced fluctuations in intra-follicular clock gene activity are an integral component of the proposed human "HCC" (Paus & Foitzik 2004). This begs the question of how the molecular machinery that governs circadian events (i.e. a 24 hour rhythm) may also be responsible for co-coordinating infradian processes such as the human hair cycle (which lasts

several months to years). Our findings are in line with a growing body of evidence that circadian clock genes regulate multiple physiological processes including infradian rhythms, such as the cell cycle (Khapre et al., 2010, Matsuo et al., 2003), tumour suppression (Fu et al., 2002, Yang et al., 2009, Chen-Goodspeed and Lee, 2007), seasonal rhythms (Hazlerigg and Loudon, 2008), breeding patterns (Miller et al., 2004), and the reproductive cycle. The control of infradian events by "circadian" clock genes may even extend to disease states such as diabetes and depression (Takahashi et al., 2008, Ando et al., 2009). Therefore, the concept that clock genes are part of the autonomous oscillator system that drives infradian HF cycling is in line with an evolving paradigm shift in our understanding of so-called "circadian" clock functions (Geyfman and Andersen, 2010).

The activity of two core clock genes (*Period1, Clock*) modulate human HF growth, cycling and pigmentation. Our findings suggest a new mechanism for how human HF cycling may be autonomously and rhythmically controlled. Therefore *Period1* activity is particularly highlighted here as a promising novel target for therapeutic hair growth modulation. Antagonising the activity of *Period1, Clock* and selected down-stream CCGs may serve to counteract various forms of hair loss characterised by premature catagen induction and subsequent telogen effluvium. Promotion of these targets may be exploited for treating unwanted hair growth (hirsutism) (Cotsarelis and Millar, 2001, Paus, 2006). Furthermore, the novel inhibitory role of *Period1* and *Clock* in human hair pigmentation identified here invites the speculative question whether excessive *Period1* and *Clock* activity may in any way be related to hair greying.

In summary, we show that the human HF offers a clinically relevant model for studying how two distinct chronobiological systems, i.e. "circadian" system and the oscillator system that drives non-diurnal, cyclic organ transformation intersect (Schneider et al., 2009, Plikus et al., 2008). Finally, human HF organ culture may facilitate dissection of the role of *peripheral* clock genes in peripheral human tissue physiology and remodelling.

8 CHAPTER 8: TOWARDS DEFINING A MOLECULAR SIGNATURE OF HUMAN ANAGEN AND CATAGEN BY TRANSCRIPTOME PROFILING

Chapter under preparation for submission as “Patterns of Expression” article to *Experimental Dermatology*

8.1 CHAPTER SUMMARY

In the previous chapters, we presented two hypothesis-driven modes to investigate the human hair cycle (in particularly the controls that drive the anagen-to-catagen transition) from a systems biology perspective. The first approach used mathematical modelling to address the nature of the human hair cycle rhythm, and the second explored a chronobiological hypothesis regarding the role of circadian transcription factors as potential regulators of the anagen-to-catagen transition.

In the current chapter, these research strategies are complemented with a third "unbiased" experimental approach by exploring the global gene expression (transcriptome) profile of the human anagen and catagen states. This final component of the thesis was intended as an important step towards defining the molecular signature of human HF cycling, namely towards establishing an extended data base for future systems biology research into important genes and signalling pathways that participate in regulating the anagen-catagen transformation of human HFs.

8.2 ABSTRACT

The human hair cycle represents a complex, dynamic systems process that is based on interconnected networks of molecules and signalling pathways. These are recruited to drive the hair follicle (HF) through its cyclic transformations from organ growth (anagen) via organ regression (catagen) to resting (telogen). Despite great advances in our understanding of the hair cycling process, for example with the use of mouse mutants, there are large gaps in the knowledge of how these candidates are expressed in the human hair follicle, and their impact on human HF cycling. Therefore, the global gene expression (transcriptome) profile of the human anagen and catagen states was explored by microarray and qPCR analysis of microdissected, organ-cultured anagen and catagen HFs from three female patients. Fold changes were calculated using anagen as the baseline sample. This gene profiling approach revealed that similar genes and pathways that had been shown to control the murine hair cycle *in vivo*, such as *Sgk3*, *Msx2* and the *BMP* pathway, are also differentially regulated during the anagen-catagen transformation of human hair follicles. In addition, novel genes including *AKR1C2* and *Dsg4* were found to be significantly up-regulated in catagen and anagen respectively. This study contributes to the identification of important key and novel genes in human hair cycle control and suggests targets for therapeutic hair growth regulation. In addition, this anagen-catagen transcriptome analysis allows future refinements of mathematical hair cycle models by integrating concrete molecular candidates into these models.

8.3 INTRODUCTION

The HF undergoes dramatic structural and molecular changes in a cyclical manner during the hair cycle. This process represents dynamic, spatio-temporal changes at multiple scales. It has been suggested that changes in local signalling cause the transition from one cycle to the next (Stenn and Paus, 2001, Botchkarev and Kishimoto, 2003, Schneider et al., 2009). However, much of the data we have on the hair cycle relies on murine data. Previous studies have not looked at hair cycle associated gene profile changes in the human system.

Hair cycle dependent changes in the transcription of individual genes and gene products during selected hair cycle stages has been identified, mostly in mice (see (Schneider et al., 2009, Stenn and Paus, 2001, Paus and Foitzik, 2004)). Schlake *et al* published one of the first investigations of global hair cycle expression profiles using microarray analysis. The authors used murine dorsal skin, therefore, the HFs were synchronised in the murine hair cycle (Schlake et al., 2004). The work was limited by the fact that the HF itself was not extracted from the skin, thus results were confounded by hair cycle-associated transcriptional changes in peri- and inter-follicular skin cell populations. A similar temporal expression experiment on RNA extract from total skin was performed on the murine hair cycle by Lin *et al* (Lin et al., 2004). Again, synchronised hair cycling in the neonatal and juvenile mice was utilised in the microarray analyses. Unfortunately, the "first hair cycle" investigated in this analysis actually represented the end of postnatal HF morphogenesis. Therefore, this study did not allow one to distinguish clearly between morphogenesis and hair cycle associated transcriptional changes.

To-date there is no published microarray analysis that has compared human anagen VI HFs and catagen HFs from the same patient. Previous global expression analyses of microdissected human HFs has focussed on identifying gene expression profile changes in human anagen VI HFs in response to defined test agents, such as hormones, polyamines or chemotherapy (Bodo et al., 2007, Langan et al., 2010, Gáspár et al., 2010, Ramot et al., 2010, Ramot et al., 2011). Another study has compared the transcriptome expression profiles between

white and grey human HFs (Choi et al., 2011). In addition, previous studies have investigated extracted human HF compartments, which also allow site specific expression profiles to be identified, such as human HF DP cells (Park et al., 2007, Iino et al., 2007) and the CTS (de Schellenberger et al., 2011).

Establishing changes in the global gene expression profile between human anagen and catagen states may provide important indications as to which genes: a) may be involved in regulating the human anagen to catagen transformation, and b) may serve as specific molecular markers of human anagen VI versus catagen.

As argued before, understanding the complex systems changes that occur in the human HF in the normal anagen and catagen stages may aid in tackling the disease process (Al-Nuaimi et al., 2010, Paus, 2006, Paus and Foitzik, 2004). Human HFs, although possessing many similarities with murine hair, also exhibit important differences in their temporal and spatial cycling properties (Al-Nuaimi et al., 2010, Plikus et al., 2011). Moreover, definition of the human anagen-catagen transcriptome may facilitate future refinements of mathematical hair cycle models, since this could allow one to by integrate key molecular players into such models.

In this pilot study, we aim to explore the human anagen and catagen states using microarray analysis and to establish whether important hair cycle-regulatory candidate genes known from the murine hair cycle also are differentially regulated during the human anagen-catagen transformation.

8.4 METHODS

8.4.1 Hair follicle isolation and culture for microarray analysis

Redundant human scalp skin was obtained from the scalp of three patients (all females, ages 48, 54 and 68) undergoing facelift surgery following informed consent (Table 8.1). Individual HFs were isolated by micro-dissection as previously described (Philpott et al., 1990, Sanders et al., 1994).

The HFs were assessed under the dissection microscope to ensure they had not been damaged during isolation and that they appeared to be in anagen VI (Kloepper et al., 2010). Isolated, exemplary reference HFs were examined histologically, following published hair cycle staging criteria (Kloepper et al., 2010) and using the hair staging accuracy investigation (Chapter 6.7) as validations for whether the "macroscopic" hair cycle staging had been accurate. The investigation presented in Chapter 6.7 and previous comparisons in the Paus lab (University of Luebeck), revealed a reasonable congruence between "macroscopic" and histomorphometric human hair cycle staging results. The HFs were assessed to ensure they had not been damaged during isolation and that, macroscopically, they appeared to be in anagen VI (Kloepper et al., 2009).

Anagen VI HFs for each patient were maintained in a 24-well plate; each well contained 500µls serum-free Williams' E medium (Biochrom, Cambridge, UK) supplemented with 2mmol/L L-glutamine (Invitrogen, Paisley, UK), 10ng/ml hydrocortisone (Sigma-Aldrich, Taufkirchen, Germany), 10µg/ml insulin (Sigma-Aldrich) and 1% antibiotic/antimycotic mixture (100x, Gibco, Germany, Karlsruhe). The supplemented media was changed every two days. HFs were placed in an incubator at 37°C with 5% CO_2 level, maintained in culture and assessed daily using light microscopy to determine whether they appeared, macroscopically, to be in anagen or late catagen phases. Once HFs were seen to have entered the appropriate stage for experimentation, HFs were immediately snap frozen in liquid nitrogen. Anagen and late catagen samples were taken for microarray analysis to determine gene expression pattern differences between these two distinct cycle points.

8.4.2 RNA extraction for microarray analyses

Anagen VI and late catagen HF samples for three female patients were taken for total RNA extraction (Table 8.1). The extractions were performed together in one run to ensure consistent experimental conditions and subsequent microarray analyses. Total RNA was extracted following the manufacturer's protocols using TRIzol® and the Purelink™ RNA Mini Kit (Invitrogen, UK) (homogenisation was performed by adding 800µl TRIzol® to each sample and using a pestle and mortar for 1 minute followed by 30 seconds with a homogeniser). The quantity and quality of the extracted total RNA was assessed using a BioAnalyzer 2100 (Agilent technologies Ltd., UK).

Table 8.1: Summary of the patient samples used for microarray and qPCR experiments

Patient	Gender	Location	Stage	Samples	Microarray	qPCR
1	Female	Fronto-temporal	Anagen	30HFs	✓	
			Late catagen	10 HFs	✓	
2	Female	Fronto-temporal	Anagen	28 Hfs	✓	✓
			Late catagen	28 Hfs	✓	✓
3	Female	Fronto-temporal	Anagen	20HFs	✓	
			Late catagen	20 HFs	✓	
4	Male	Occipital	Anagen	30 HFs		✓
			Late catagen	30 HFs		✓
5	Male	Occipital	Anagen	25 HFs		✓
			Late catagen	37 HFs		✓

8.4.3 Microarray analysis

Human genome U133A oligonucleotide microarrays were performed by the University of Manchester Genomic Technologies Core Facility following the manufacturer's instructions (Affymetrix®, UK). Technical quality control was performed using dChip (Li and Wong, 2004) followed by background correction, normalisation and expression using the GC-RMA method (Wu et al., 2004). Anagen state was taken as the baseline and fold changes were calculated as the expression in catagen compared to anagen for each patient. Differential expression between anagen and catagen samples was tested using paired Student's t-tests. The data was filtered by creating a subset of probes whereby up or down-regulation was greater or less than 1.5 fold change in all three patients. Genes were subsequently analysed for over represented gene ontologies (GO) using the online tool Database for Annotation, Visualisation and Integrated Discovery version 6.7 (DAVID 6.7) (Huang et al., 2009, Dennis et al., 2003).

8.4.4 Additional hair follicle cultures for validation by real-time qPCR

Two additional HF cultures were performed in exactly the same way as described above (see Table 8.1), however, in these samples the HFs were harvested on the same day when half the HFs in culture were in anagen and the other half were in catagen.

8.4.5 Real-time qPCR

In order to validate the results from the microarray experiment, total RNA extracted from three patients (Table 8.1) was used to perform qPCR on a sub-selection of genes identified from the microarray. Total RNA isolations, reverse transcriptions and qPCR experiments were performed by University of Debrecen Physiology Department, Biro lab, Hungary. Taqman® (Applied Biosystems) gene expression assays were obtained for msh homeobox 2 ((Msx2) Assay ID Hs00741177_m1, RefSeq: NM_002449.4, Amplicon length

130bp), serum/glucocorticoid regulated kinase family, member 3 ((Sgk3) Assay ID Hs00179430_m1, RefSeq: NM_013257.4, Amplicon length 88 bp), bone morphogenetic protein 2 ((Bmp2), Assay ID Hs00154192_m1, RefSeq : NM_001200.2, Amplicon length 60 bp), bone morphogenetic protein 4 ((Bmp4), Assay ID Hs00370078_m1, RefSeq: NM_130850.2, Amplicon length 58 bp), secreted phosphoprotein 1 ((Spp1), Assay ID Hs00959010_m1, RefSeq: NM_001040058.1, Amplicon length 84 bp), frizzled homolog 10 (Drosophila) ((Fzd10, Assay ID Hs00273077_s1, RefSeq: NM_007197.3, Amplicon length 116bp), desmoglein 4 ((Dsg4), Assay ID Hs00698286_m1, RefSeq: NM_177986.3, Amplicon length 154 bp), FK506 binding like protein (FKBPL, Assay ID Hs00276690_g1, RefSeq NM_022110.3, Amplicon length 75 bp), BMP and activin membrane-bound inhibitor homolog (Xenopus laevis) ((Bambi), Assay ID Hs03044164_m1, RefSeq: NM_012342.2, Amplicon length 52 bp). The relative expression was obtained against the endogenous control peptidylprolyl isomerase A (cyclophilin A) ((PPIA), Assay ID Hs99999904_m1, RefSeq: NM_021130.3, Amplicon length 98 bp)), because previous analysis in the Biró lab had shown this housekeeping gene to undergo only minimal hair cycle-dependent expression changes during the human anagen-catagen transformation (data not shown).

Total RNA was isolated using TRIzol (Invitrogen) and then 1 µg of total RNA was reverse-transcribed into cDNA by using 15 U of AMV reverse transcriptase (Promega; Madison, WI, USA) and 0.025 µg/µl random primers (Promega). Quantitative PCR was performed on an ABI Prism 7000 sequence detection system (Applied Biosystems; Foster City, CA, USA) using the 5' nuclease assay as detailed in our previous reports (Tóth et al., 2009, Bodo et al., 2005) and the TaqMan® universal PCR master mix protocol (Applied Biosystems). Experiments were performed in triplicates; the average relative expression levels were calculated using delta Ct method and relative fold change in catagen compared to anagen was calculated using the delta delta Ct method. The normalised relative expressions obtained via delta Ct method for anagen

and catagen was tested statistically using the paired Student's *t*-test. Statistical analysis was performed using GraphPad prism 5.

8.5 RESULTS

8.5.1 Microarray results

Of the 54613 probe sets arrayed, 29244 (53.55%) were up-regulated and 25269 (46.27%) down-regulated in catagen compared to anagen (Table 8.2 and Figure 8.1). This global result represents the average expression of each probe set across the three patients. However, in order to establish the "transcriptional signature" in anagen, we selected genes that were down-regulated by a fold change of ≤1.5 in all three patients as an "anagen signature" subset. Likewise genes up-regulated with ≥1.5 fold change in all three patients were considered to provide the "catagen signature" (Figure 8.2). Each of these signature groups reassuringly contained genes associated with each state. For example, multiple hair keratins were seen to be differentially expressed in the anagen subset and several extracellular matrix genes in the catagen subset. Comprehensive lists of the genes in each subset can be found in Table 8.3 and 8.4. Of these subset genes, very few genes were up- or down-regulated by greater than 2 fold in all three patients. Twenty-four genes were down-regulated (by a fold change of <2 in all three patients) in catagen compared to anagen (Table 8.3). Only three genes were up-regulated by >2x in all three patients in catagen compared to anagen (Table 8.4). These were secreted phosphoprotein 1, disabled homolog 1 and aldo-ketoreductase family 1, member C2.

***Table 8.2: Table detailing the numbers of genes in each subset selected for further analysis* (corresponds to red data values in Figure 8.2)**

	Probe sets	**Genes**
Total number of probe sets on the microarray	54613	-
Up-regulated in catagen	29244	-
Down-regulated in catagen	25269	-
≥1.5 in all three patients (catagen signature)	26	20
≤-1.5 in all three patients (anagen signature)	118	100

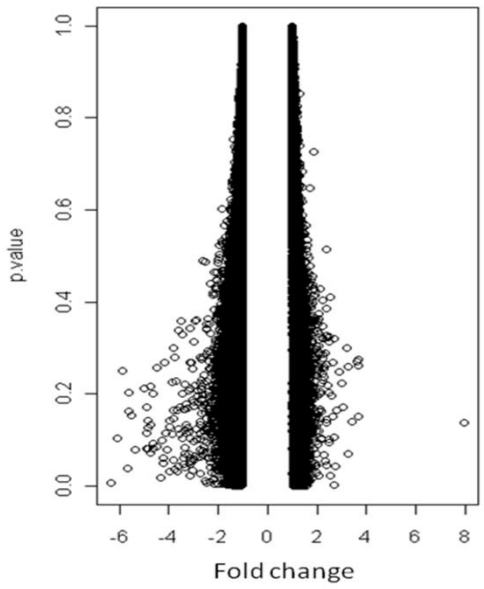

Figure 8.1: Scatter plot of the microarray results

Fold change values of catagen samples compared to the anagen samples and the p-values obtained from paired Student's t-test.

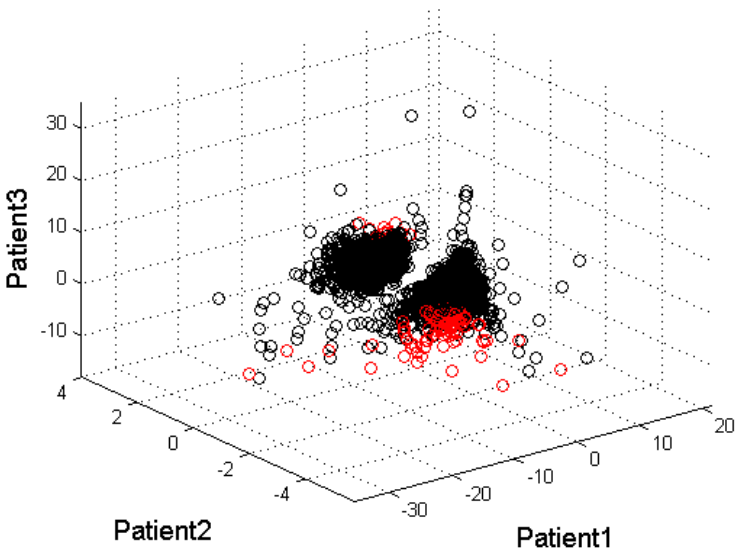

Figure 8.2: 3D scatter plot of the fold change values for each probe set in three patients.

Red indicates the subsets taken for further analyses.

Table 8.3: Genes selected as "anagen signature"

Average fold change across three patients is displayed ordered by the greatest fold change. Bold indicates those that were significant - paired Student's t-test ($p<0.05$). The gene names presented in bold were those taken for verification with qPCR

Genes	Average Fold change	*p* value	Genes	Average Fold change	*p* value
KRT33A	-13.3	0.20	**MSX2**	-2.7	0.17
KRT81	-11.0	0.16	RARRES1	-2.7	0.12
GPRC5D	-10.3	0.27	WNT3	-2.7	0.09
KRTAP4-5	-8.8	0.17	MSX1	-2.6	0.07
KRTAP4-3	-8.5	0.10	KIF26A	-2.6	0.06
KRTAP4-4	-6.8	0.13	SHROOM3	-2.5	**0.01**
KRT34	-6.6	0.08	GPR37	-2.5	**0.01**
LY6G6D	-6.5	**0.01**	NALCN	-2.5	**0.01**
KRTAP1-3	-6.4	0.11	PPM1H	-2.4	0.05
KRTAP2-4	-6.3	**0.04**	CYP26B1	-2.4	0.15
KRTAP2-1	-5.9	0.08	PSORS1C2	-2.4	0.15
DSG4	-5.8	0.08	NPR3	-2.4	**0.04**
KRTAP1-1	-5.8	0.08	CAMK2N1	-2.3	0.06
KRTAP9-4/ 9-9	-5.7	0.09	LONRF2	-2.3	**0.01**
KRTAP2-2	-5.6	0.07	HHIP	-2.3	**0.03**
KRTAP2-4	-5.4	0.09	H2AFJ	-2.3	0.10
KRTAP4-2	-5.3	0.10	XK	-2.2	0.11
KRTAP3-1	-4.9	0.11	MT4	-2.2	**0.01**
KRTAP4-6	-4.8	0.06	CKMT1A/B	-2.2	0.07
KRTAP4-9	-4.7	0.08	IFRD1	-2.2	0.08
KRTAP4-7	-4.7	0.05	ILVBL	-2.2	**0.04**
RNF182	-4.6	0.12	DLX1	-2.2	0.07
SELENBP1	-4.5	**0.02**	TC2N	-2.2	**0.02**
CRNN	-4.3	0.06	PCYOX1	-2.2	**0.03**
KRT31	-4.2	0.19	QPCT	-2.2	**0.005**
KRTAP3-3	-4.2	**0.03**	GPR37	-2.1	0.05
FAM126B	-4.1	0.10	SMAD6	-2.1	**0.04**
FZD10	-4.0	**0.04**	GAS2L3	-2.1	0.06
BAMBI	-3.9	**0.03**	DLX3	-2.1	**0.04**
KRT73	-3.9	**0.04**	KRT73	-2.1	0.09
C8orf44/ SGK3	-3.8	0.08	TDH	-2.1	0.06
DLX2	-3.7	0.06	LOC100131317	-2.1	**0.03**
KRT86	-3.7	0.07	SAMD8	-2.0	**0.03**
P2RY5	-3.6	0.05	OCA2	-2.0	0.05
LONRF2	-3.6	**0.04**	KCNK7	-2.0	**0.04**
KRTAP3-2	-3.5	0.07	SNHG3	-2.0	**0.04**
MUC15	-3.4	0.06	AXIN2	-1.9	**0.03**
KIF5C	-3.4	0.05	MUCL1	-1.9	**0.02**
DYNC1I1	-3.4	0.05	FBXO8	-1.9	**0.03**
LOC100131317	-3.3	0.05	PAG1	-1.9	**0.03**
MYCN	-3.3	0.10	VPS8	-1.8	0.05
MSX2	-3.2	**0.02**	EFHD1	-1.8	**0.01**
PPP2R1B	-3.2	0.06	MAP3K7IP3	-1.8	**0.005**
KIF5C	-3.2	0.06	ID3	-1.8	**0.01**
MYB	-3.2	**0.03**	EEA1	-1.7	**0.01**
GAS2L3	-3.1	0.06	**FKBPL**	-1.7	**0.04**
NCRNA00084	-3.0	0.08	DPY30	-1.7	**0.004**
SGK3	-2.9	0.06	TTC9	-1.6	**0.01**
PPP2R1B	-2.9	0.10	NAV2	-1.6	**0.001**
FAM49A	-2.8	0.08	PRKAG2	-1.6	**0.005**
KRT37	-2.8	0.08	RNF149	-1.6	**0.02**
NCRNA00084	-2.8	0.07	SLC6A15	-1.6	**0.01**
KRT85	-2.8	**0.03**	ARHGAP29	-1.5	**0.001**

Table 8.4: Genes selected as "catagen signature"

Fold change >1.5 in all three patients. Here the average fold changes across the three patients is provided and ordered by the greatest fold change. Bold indicates probes that were significant by paired Student's t-test p<0.05. The gene names presented in boldwere those taken for verification with qPCR

Gene	**Fold change**	***p* value**
SPP1	3.7	0.07
TNFAIP6	3.1	0.11
COL14A1	2.7	0.10
DAB1	2.7	**0.002**
AKR1C2	2.6	**0.02**
CCDC3	2.5	0.05
MMP16	2.5	0.05
NEFL	2.4	0.07
COL27A1	2.1	**0.02**
FHL1	2.0	**0.04**
C18orf1	2.0	**0.03**
AKR1C1	2.0	**0.05**
NFATC1	2.0	**0.04**
KCND3	1.8	**0.04**
LOC143381	1.8	0.05
PARD6G	1.7	**0.01**
LOC100130097	1.7	**0.01**
PARVA	1.7	**0.01**
TANC2	1.6	**0.01**
ANKRD6	1.6	**0.01**

Using the DAVID online tool (Dennis et al., 2003), over-represented gene ontology (GO) categories were identified in the two subsets of anagen signature and catagen signature. The functional categories are provided in Figure 8.3 and 8.4 and Table 8.5. The significantly over-represented groups in the catagen group were found to be: cell adhesion, steroid dehydrogenase activity, regulation of cellular component size, collagen, cell projection and cell division. In anagen the significantly over-represented categories were: keratin filament, pattern specification process, skeletal system development, cell fate commitment, embryonic morphogenesis, response to protein stimulus, serine/threonine kinase signalling pathway, neuron differentiation and BMP signalling pathway. These are considered key biological processes that

significantly distinguish anagen and catagen states in these three patients. The full lists of functional categories are found in Appendices D and E.

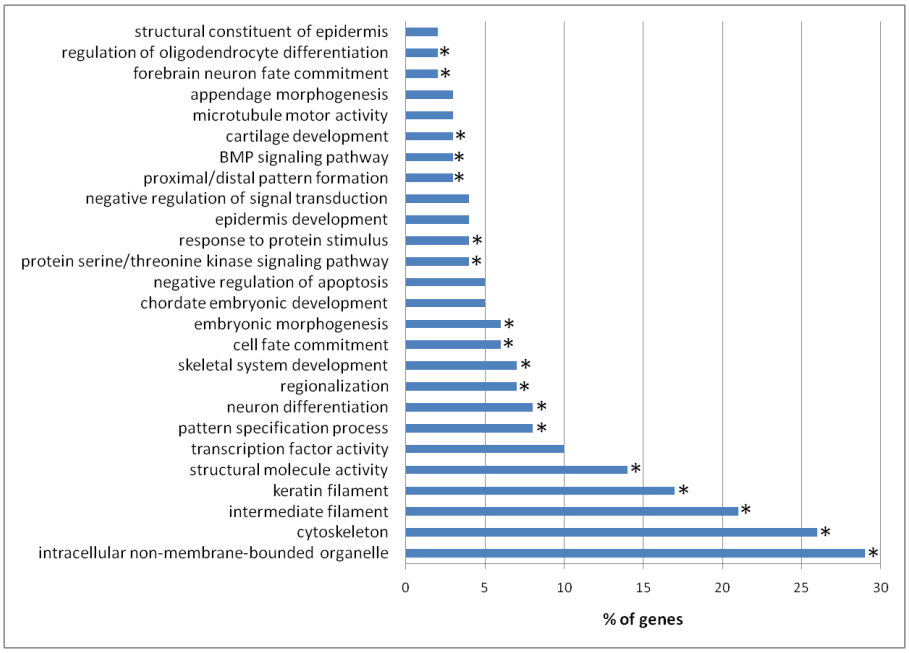

Figure 8.3: GO functional categories for the anagen signature

*(Genes down-regulated in catagen compared to anagen) *indicates significant increase in biological representation when compared to the background genome expression (this is provided by DAVID).*

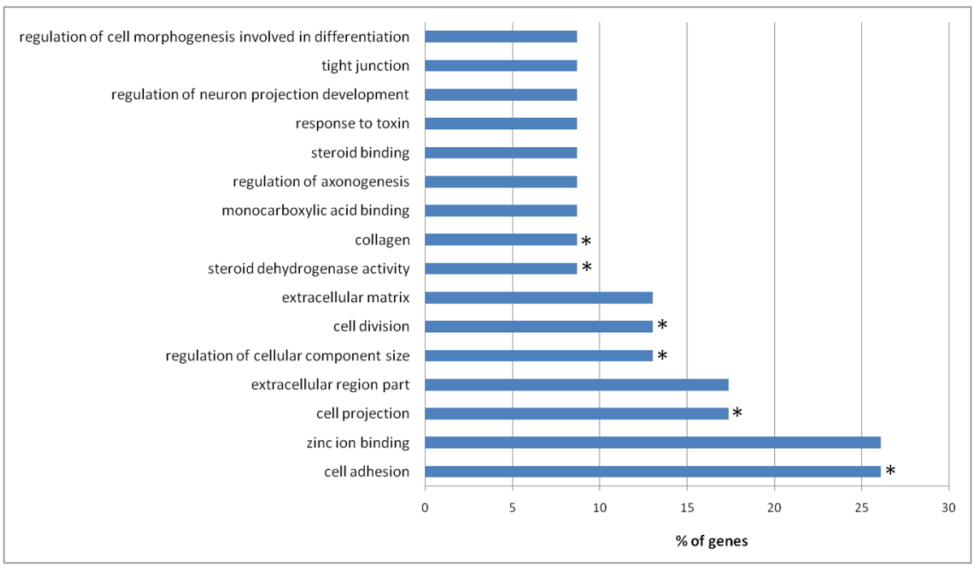

Figure 8.4: GO functional categories of genes up-regulated in catagen

*(compared to anagen) *indicates significant increase in representation over the background genome expression.*

Table 8.5: Significantly overrepresented functional categories in anagen and catagen states

*Functional categories determined by DAVID analysis to be significantly over-represented compared to background genome expression. Gene abbreviations are according to the NCBI listings. *indicates genes that have been previously shown to be involved in hair growth, development, cycling or hair disorders.*

Functional category	Catagen	Anagen
Cell adhesion	SPP1*, COL27A1 COL14A1*, TNFAIP6 (*TNFalpha)	
Steroid dehydrogenase activity	AKR1C2, AKR1C1	
Regulation of cellular component size	SPP1*, FHL1, NEFL	
Collagen	COL27A1, COL14A1*	
Cell projection	SPP1*, KCND3, NEFL, PARVA	
Cell division	PARD6G	
Keratin filament		KRTAP2-2, KRTAP1-3, KRT85*, KRTAP3-2*, KRT86*, KRTAP4-7, KRTAP4-9, KRTAP4-3, KRTAP3-1, KRTAP2-4, KRTAP4-6, KRT73, KRTAP4-5, KRTAP4-2, KRTAP3-3, KRT81*, KRTAP1-1*, KRTAP9-4/9-9, KRTAP4-4, KRTAP2-1
Pattern specification process		AXIN2, SMAD6, DLX1*, WNT3*, HHIP, SHROOM3, DLX2*, CYP26B1
Cell fate commitment		DLX1*, WNT3*, IFRD1, DLX2*, CYP26B1
Skeletal system development		MSX2*, AXIN2, DLX1*, MSX1*, NPR3, DLX2
Neuron differentiation		KIF5C, EFHD1, DLX1*, ID3*, DLX2*
Serine/threonine kinase signaling pathway		MSX2*, SMAD6, BAMBI, MSX1*
Response to protein stimulus		MSX2*, ID3*, MSX1*, LY6G6D
Embryonic morphogenesis		WNT3*, MSX2*, SHROOM3, MSX1*, DLX2*, CYP26B1
BMP signalling pathway		MSX2*, SMAD6, MSX1*

Table 8.6: Microarray results for BMP2 and BMP4 in anagen and catagen hair follicles

Gene	Patient 1	Patient 2	Patient 3	Average	*p* value
Bmp2	-5.1	-1.9	-1.1	-2.7	0.22
Bmp4	-1.50138	-1.0495	-1.01651	-1.2	0.34

8.5.2 Quantitative PCR verification results

To verify the microarray findings, qPCR was performed on nine genes selected from the anagen and catagen subsets. In addition, due to the DAVID gene

ontology analyses finding BMP signalling as a significant biological process, *Bmps 2* and *4* were also included in the qPCR analysis, even though the genes *Bmp2* and *Bmp4* were not identified from the microarray analyses as being differentially expressed (Table 8.6).

The qPCR results revealed large differences in average relative expressions of the target genes between the anagen and catagen samples (Table 8.7, Figure 8.5 and Figure 8.6). The differences were, however, not significant at the 0.05 level.

Statistically significant differences were found on comparing the anagen and catagen relative expression levels for each gene by individual patients (Figures 8.7 and 8.8). *Spp1* was not up-regulated in catagen compared to anagen apart from in the individual patient 2 (Figure 8.8) and therefore, the trend and fold change difference were not confirmed in this transcript.

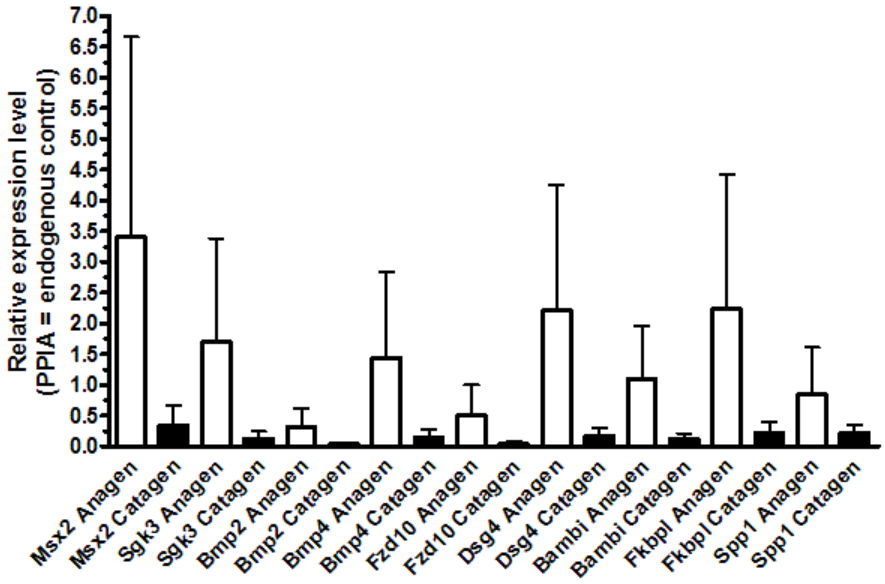

Figure 8.5: qPCR results from three patients' anagen and catagen samples.

Relative expressions of candidate gene targets are provided and obtained from the delta Ct normalisation method. Large fold change differences are seen, however none are statistically significant on p<0.05 level.

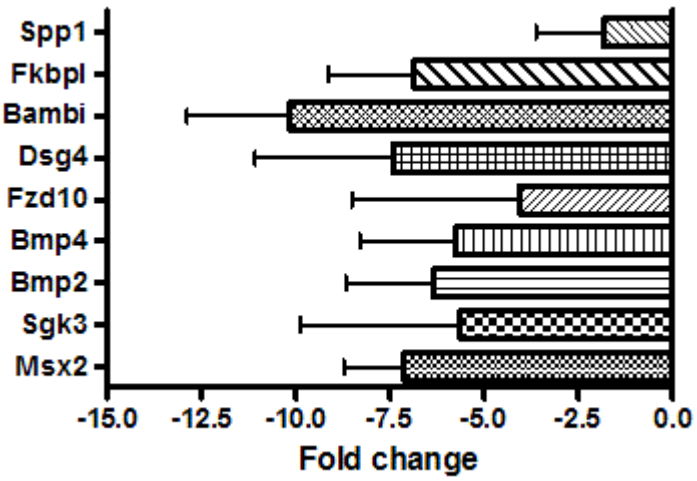

Figure 8.6: Validations of microarray results using the nine selected target genes in qPCR.

The average fold change in expression in catagen compared to anagen is shown here and was obtained using the delta delta Ct normalisation method (n=3, Error bars: SEM).

Table 8.7: Fold changes in candidates mRNA in catagen compared to anagen determined by qPCR

Performed on anagen and catagen for three patients. Fold changes were obtained using the delta delta Ct method.

	Fold change (Catagen compared to Anagen)								
Patient	**Msx2**	**Sgk3**	**Bmp2**	**Bmp4**	**Fzd10**	**Dsg4**	**Bambi**	**Fkbpl**	**Spp1**
2	-6.3	-1.1	-5.7	-4.8	0	-4.3	-5.7	-3.0	1.0
4	-4.9	-1.7	-2.7	-1.9	0.7	-3.3	-15.1	-6.6	-1.3
5	-10.2	-14.1	-10.7	-10.5	-12.9	-14.7	-9.8	-10.9	-5.2
Average	**-7.1**	**-5.6**	**-6.3**	**-5.8**	**-4.1**	**-7.4**	**-10.2**	**-6.9**	**-1.8**

8.6 DISCUSSION

In this pilot study, we report the transcriptome profile of the human anagen and catagen state in microdissected, organ-cultured anagen and catagen HFs from three female patients. This gene profiling approach revealed that similar genes and pathways that had been shown to control the murine hair cycle *in vivo*, such as *Sgk3, Msx2* and the BMP pathway, are also differentially regulated during the anagen-catagen transformation of human hair follicles.

Although this transcriptome analysis of the human anagen-catagen transformation needs to be extended to additional individuals before definitive conclusions can be drawn, it already points to both recognised and novel key players in human hair cycle control and suggests additional targets for therapeutic hair growth regulation. In addition, this anagen-catagen transcriptome analysis allows future refinements of mathematical hair cycle models by integrating concrete molecular players into these models.

Bone morphogenetic protein (BMP) signalling was identified as having a significant representation in human anagen compared to catagen follicles. BMP signalling has been shown to be involved in murine HF biology and cycling regulation (Andl et al., 2004, Kulessa et al., 2000, Plikus et al., 2008, Botchkarev and Sharov, 2004, Botchkarev, 2003, Guha et al., 2004, Kobielak et al., 2007, Kwan et al., 2004, O'Shaughnessy et al., 2004, Rendl et al., 2008, Sharov et al., 2006, Zhang et al., 2006).

Here, we show, for the first time, that the BMP pathway is significantly over-represented in human anagen HFs, in particular genes that have been intimately associated with BMP signalling, such as *Msx1* and *Msx2*, *Bambi* and *Smad6* were significantly up-regulated in this microarray investigation. The results from the microarray for *Bambi* and *Msx2* were verified by qPCR and we additionally checked the expressions of *Bmp2* and *Bmp4* in the qPCR experiments and these were significantly up-regulated in anagen compared to catagen. Additionally, we found that there was an anagen-associated expression of *Bambi*, a BMP pathway inhibitor. This was verified by qPCR. These results are complimented by a microarray analysis on depilation-induced hair cycling in rats whereby *Bambi* was identified as being up-regulated during the hair cycle (Umeda-Ikawa et al., 2009). In addition, miRNA-3 has been shown to regulate *Bambi* in the murine HF (Mardaryev et al., 2010). In addition, we found that the gene *ID3* is significantly up-regulated in anagen. This gene has also been shown to be controlled by BMP in murine HFs (O'Shaughnessy et al., 2004). Therefore, in light of the evidence, BMP functioning is an important anagen process in the human HF.

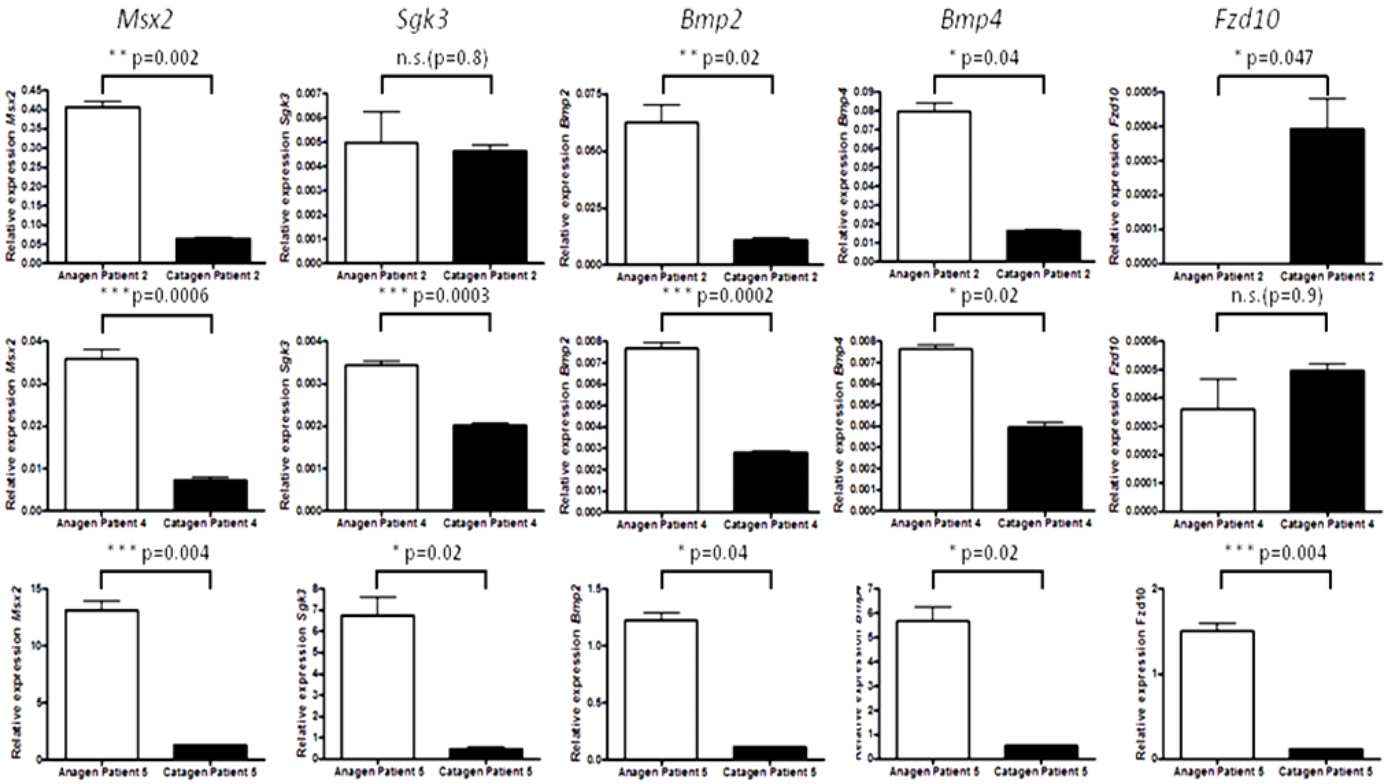

Figure 8.7: qPCR results for Msx2, Sgk3, Bmp2, Bmp4 and Fzd10 in anagen and catagen hair follicles in each individual patient.

** p<0.05, ** p<0.01, p<0.001. Error bars shown are SEM.*

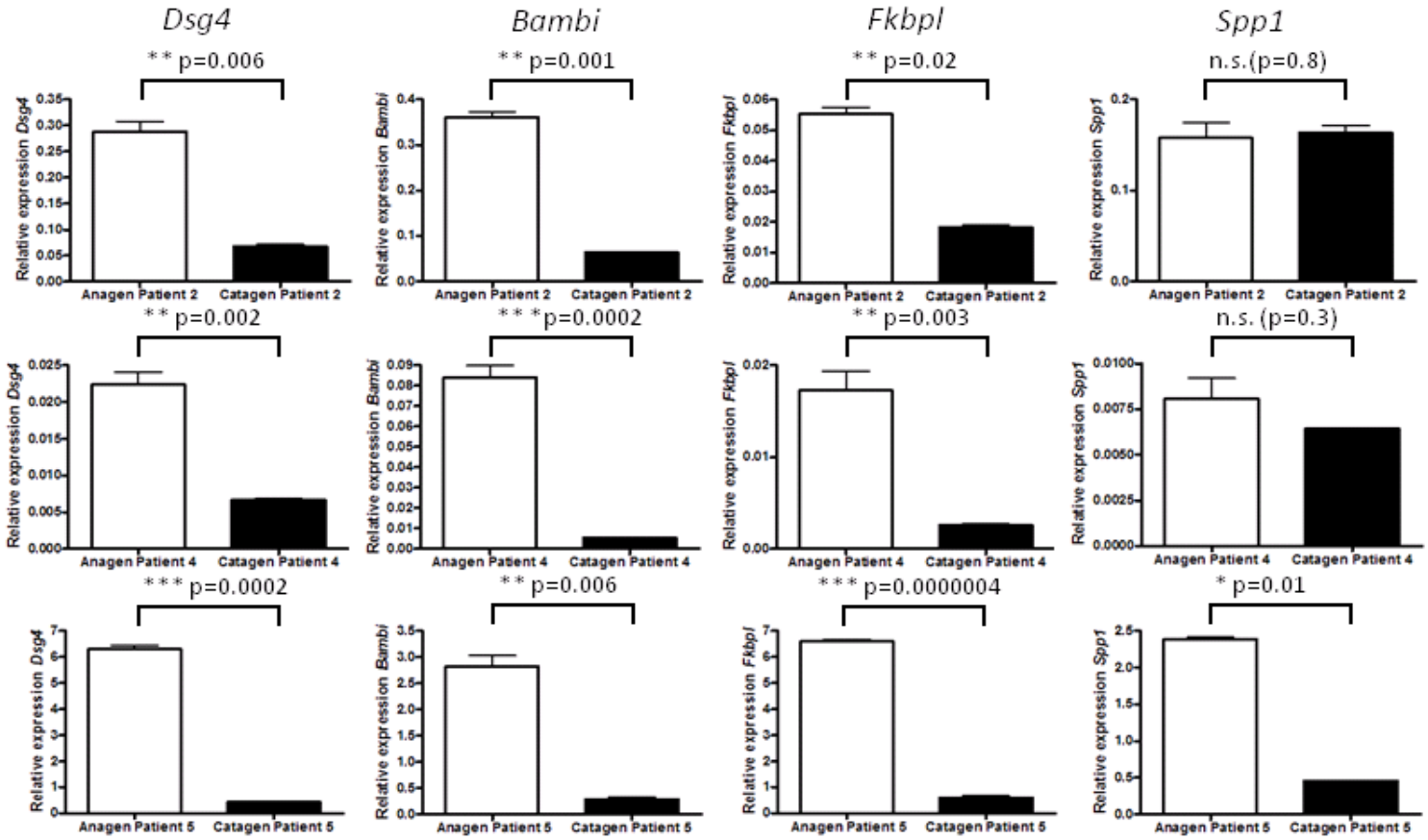

Figure 8.8: qPCR results for the expression of Dsg4, Bambi, Fkbpl and Spp1 in anagen and catagen hair follicles for three individual patients

** p<0.05, ** p<0.01, *** p<0.001. All results were significant apart from Spp1 where we see conflicting results. Patients 2 and 4 have similar change between anagen and catagen whereas patient 5 shows that there is actually a decrease in Spp1 in catagen compared to anagen. Error bars shown are SEM.*

This study has also identified possible novel genes in the physiology of the anagen and catagen state. Interestingly, the genes *AKR1C2* and *AKR1C1* were significantly up-regulated in catagen compared to anagen. These genes are members of the aldo-keto reductase (AKR) superfamily and code for enzymes responsible for steroid metabolism (Arthur and Reichardt, 2010, Penning et al., 2004). *AKR1C1* and *AKR1C2* encode for the proteins; 20α-HSD and Type 3α-HSD respectively. 20α-HSD eliminates progesterone and Type 3α-HSD eliminates 5α-dihydrotestosterone (Jin and Penning, 2007). These enzymes not only metabolise steroids but also regulate androgen receptors (Penning et al., 2004) and *AKR1C1* is involved in the metabolism of prostaglandin (Colombe et al., 2007).

Skin and the HF are known to metabolise and produce steroids (Hoffmann, 2003, Ito et al., 2005a) and androgens play a key role in the pathogenesis of hair disorders such as androgenetic alopecia and hirsutism (Eicheler et al., 1998, Chen et al., 2002, Steiner et al., 2008, Riedel-Baima and Riedel, 2008, Naito et al., 2008). However, there is comparatively little research specifically concerning the AKR superfamily in the physiology of skin and particularly HF function (Hoffmann, 2003). One study has shown that *AKR1C2* is implicated in hirsutism (Steiner et al., 2008). Here we show that these genes are also important as catagen markers, which has not been reported previously (Zouboulis et al., 2007).

In addition, a previous study has shown that increased *AKR1C1 and AKR1C2* expression occurs following UV treatment of human skin with concomitant expression of apoptosis markers (Marín et al., 2009). These authors suggest a role in keratinocyte survival and protection of keratinocytes from apoptosis. This is highly interesting as this information and our findings that these two genes are significantly up-regulated in catagen (a hair cycle stage heralded by apoptosis), provides a novel hypothesis that they are important in HF cycling and function and may even be the important factors in the pathogenesis of hormone related hair disorders, namely androgenetic alopecia.

Another gene identified as differentially expressed in catagen was *Spp1* (secreted phosphoprotein 1) commonly known as osteopontin (*OPN*)). It is

known to be expressed in human DP cells (Chermnykh et al., 2010), however, there are limited reports on osteopontin and its role in the HF.

In the skin, osteopontin has been implicated in psoriasis, skin cancer (Chang et al., 2008) and has been shown to have anti-apoptotic effects (Buback et al., 2009). *Spp1* has been shown to protect cells from environmental insults (Wang and Denhardt, 2008, Denhardt et al., 2001) and may function to protect surviving HF cells during catagen. One report in rat HFs shows that osteopontin is expressed specifically in catagen (Yu et al., 2001). Yu *et al* showed that the expression of osteopontin was specific to the DP and the catagen stage in rat DP cells (Yu et al., 2001). Our study shows inconclusive results regarding the expression of *Spp1* as the qPCR validations did not show up-regulation in catagen. The report in rat DP cells supports our microarray finding that *Spp1* is a catagen-specific gene in human HFs, but the exact expression profile will need to be clarified further.

Desmoglein 4 (*Dsg4*) mutations lead to hypotrichosis (Kljuic et al., 2003, Meyer et al., 2004, Schaffer et al., 2006, Bazzi et al., 2009). Here this was identified as an anagen associated transcript via microarray and qPCR analyses. *Dsg4* is specifically expressed in the HF (Bazzi et al., 2006) and therefore may be a suitable anagen marker.

Loss of muscle segment homeobox 2 (*Msx2*) causes major defects in hair cycling and hair shaft differentiation resulting in "cyclic alopecia" in mutant mice (Ma et al., 2003). Here, *Msx2* was significantly up-regulated in human anagen HFs compared to catagen. *Msx2* has been reported, to be expressed in human skin (Stelnicki et al., 1997). The microarray and qPCR results presented here are the first human hair cycle-dependent findings concerning this gene. *Msx2* is also linked to BMPs as a downstream target (Cai et al., 2009) and has functional connections to another anagen-to-catagen regulatory gene, i.e. *Dlx2* (Distal less homeobox 2) as shown in gene ontology analyses. Interestingly *Dlx3* has been postulated to play a role in normal HF cycling (Hwang et al., 2008). The current transcriptome analysis identifies *Dlx2* and *Dlx1*, but not *Dlx3,* as candidates for maintaining anagen in human HFs.

Another gene that has been prominently implicated in timing of the murine hair cycle was identified as a member of the human anagen transcript

profile here. *Sgk3* is responsible for the *fuzzy* phenotype (Campagna et al., 2008, Alonso et al., 2005, Okada et al., 2006) (see Chapters 2 and 3 also). Again, there are no reports on *Sgk3* expression in the human HF. *Sgk3* has been shown to affect cell survival and beta catenin expression; which are also known to be important in hair cycling (McCormick et al., 2004). Therefore, this gene may play an important role in human hair cycling.

Other candidate human hair cycle-regulatory genes identified via the current microarray analysis are *Wnt3* and *Smad6*. *Wnt3* has already been shown to affect murine HF morphogenesis and cycling (Millar et al., 1999, Charpentier et al., 2000). In addition, *Wnt* has been demonstrated to maintain the anagen-like expression properties of DP cells *in vitro* (Kishimoto et al., 2000).

Frizzled 10 (*Fzd10*) is a cell surface receptor for *Wnts* and is known to be expressed in the matrix, ORS and DP of postnatal murine HFs (Reddy et al., 2004). There is evidence that *Bmp2* modulates several Wnts and Frizzled proteins including *Fzd10* (Yang et al., 2006). The results of the microarray analysis here showed that there was up-regulation in anagen; however, this was not confirmed by the qPCR analysis. This is the first report of *Fzd10* expression in the human HF. Since the results were conflicting between qPCR and the microarray, this is best followed-up in additional patients and on the protein level, before one reaches conclusions.

Fkbpl (*fk506*) was chosen as an interesting new candidate to verify the microarray date with. This was chosen as *Fkbpl* (otherwise known as Tacrolimus) is important in treating many dermatological conditions. In addition, it has been shown to induce anagen (Iwabuchi et al., 1994). *Fkbpl* decreases the expression of VEGF and IGF-1 in human skin, while no hair growth effect was found (Wang et al., 2009). However, in mice, *Fkbpl* is a very potent anagen-inducing and catagen-suppressing agent (Maurer et al., 1997, Paus et al., 1996).

Since we used isolated human HFs maintained in organ culture, one must consider the possibility that the human HF *in vitro* does not utilise the same signals for controlling its cyclic anagen-catagen transformation as it does *in vivo*. This is thought to be unlikely, since the "HCC" is an intra-follicular mechanism and should be preserved even after HF microdissections, culture, and

transplantation (Paus and Foitzik, 2004). Another limitation of the work is that we present mainly microarray data, which could be followed-up only very selectively within the temporal confines of this thesis. In order to fully investigate the current pilot observations further, we would now expect to systematically compare the transcriptome results on the translational level, namely by immunohistology. Indeed a thorough investigation of these processes should now include protein analyses as transcription changes may not be reflected on the protein level (White and Salamonsen, 2005).

We attempt to explore these issues by establishing immunohistochemistry protocols for some of the most interesting gene products, namely MSX2 and SGK3. In addition, we also plan to perturb these genes and the BMP pathway by using RNA interference technology; using the simple, small-interfering RNA silencing strategies that we had successfully employed for intra-follicularly expressed circadian genes (see Chapter 6).

To further dissect the complex interactions that exist in the HF, namely epithelial-mesenchymal interactions, future work should entail isolated cell compartments of the HF, such as by laser capture microdissection to obtain the expression profiles of these HF compartments (Rogers and Koike, 2009). Also, we only investigated the proximal HF, thus excluding e.g. hair cycle-dependent gene expression changes in the HF's epithelial stem cell compartment, the bulge. Thus future transcriptome analyses should explicitly include this region, using full-length scalp HFs, as they become available e.g. during routine hair transplant surgery.

A major limitation of the study is the low number of patients that was available for transcriptome analysis. A larger patient set, which should also include HFs from male donors, would ensure that confidence can be placed on the dissected human anagen and catagen signature, and may reveal gender-specific gene expression differences. Due to the severe limitation of available human skin and HFs, the microarray arrays were performed on female patients, while and the additional patients for qPCR validations (patients 4 and 5) were male. The majority of results agreed between the female patient in qPCR (patient 2) and the male results (patients 4 and 5).

While constitutive gender differences in the gene expression patterns of human HF have not yet been systematically studied, it is already known that there are substantial gender-dependent differences in the transcriptional response of male versus female scalp HFs when these are exposed to oestrogen (Ohnemus et al., 2006) or prolactin in HF organ culture (Langan et al., 2010). This makes the future search for gender-dependent differences in the human anagen and catagen gene expression profile both interesting and important.

One study performed on plucked human HFs (Kim et al., 2006) aimed at to use HFs as a clinical diagnosis tool. Therefore, the study design differed to the needs of our study. The limitations of that study were that only hair shafts were plucked and analyses were performed in ignorance of the exact hair cycle stage. Also, only a portion of the proximal epithelial HF would have been analysed, excluding much of the hair matrix and the entire HF mesenchyme (Botchkarev and Kishimoto, 2003).

To conclude, previous studies have either looked at the transcriptome changes in RNA extracts from total skin between different murine hair cycle states or have investigated transcriptional changes in human anagen HFs in response to defined test agents. However, there are no previous publications which systematically compare the transcriptome of spontaneously developed human anagen and catagen HFs in organ culture. Therefore, despite its evident limitations, the current pilot study provides novel pointers to the transcriptional changes that may be functional important during the anagen-catagen transformation.

This suggests important new molecular targets for therapeutic intervention in common human hair growth disorders. Working hypotheses generated on the basis of the current transcriptome analyses can be tested functionally in human HF organ culture, e.g. by antagonising signalling mediated by the identified target genes (such as *Msx2*).

In addition, this work may be used to develop future mathematical models of the signalling pathways involved in human hair cycle control.

9 CHAPTER 9: SUMMARY OF THE THESIS AND FUTURE PERSPECTIVES

The human hair cycle has been investigated in this thesis using both theoretical and experimental approaches. This final chapter summarises the main conclusions drawn from the work presented in this thesis, and develops perspectives for future work on human hair cycle research from a systems biology viewpoint (for more extensive discussion and future perspectives of the individual results generated in this thesis, see the Discussion sub-chapters of Chapters 5 to 8).

After introducing the general field of research (Chapter 1), the relevant literature regarding our current understanding of the molecular mechanisms that drive human HF cycling was reviewed (Chapter 2). This analysis established that the molecular nature of the "HCC", both in man and in mice, is still unknown and that fully convincing theoretical models of HF cycling remain to be developed.

In Chapter 3, the HF was presented as a complex, multilevel, systems biology problem, which deserves to be fully discovered as a unique and clinically relevant research model by mainstream system biology researchers. In addition, it was concluded that in order to understand the human hair cycle, systems biology approaches (i.e. integration of experimental data complemented by the construction of a mathematical model) should be employed.

In Chapter 4 non-linear dynamics was introduced in the thesis with the principles and important terminologies explained. In Chapter 5, these general principles were then applied to the human hair cycle via the construction of a mathematical model that captures key features of human HF dynamics. In this model, the human hair cycle was portrayed as a multi-cellular dynamical system. It is argued that the hair cycle controls act on a tissue level which act to coordinate distinct cell populations through the cycle. To conclude, we have presented a simple mathematical model that captures the dynamics of the human HF. Using a dynamical systems approach we provide the first mathematically formulated theory of the intrinsic components of the "HCC". Our prototypic two compartment model is based on the key cell populations responsible for hair growth; MKs with communication set up by a second

compartment; the DP. The key conclusion is that HF dynamics requires two essential features; a *bistable switch* and *feedback inhibition*. Importantly, this simple model not only captures normal cyclical behaviour of the HF, but other essential features of HF dynamics as seen *in vivo* and may be a future tool for experimental and treatment predictions. The model is a novel contribution to the field and accounts for both the dynamics of the normal cycling human HF and pathological states. This is an important feature of the model as its behaviour, depending upon parameter values and initial conditions, can account for both the normal cycling dynamics of the human HF and pathological behaviour. This is in line with the concept of "dynamical disease" in that disease is a pathological alteration of normal dynamics (Glass and Mackey, 1988).

After detailing the experimental methodology employed in the current thesis (Chapter 6), Chapter 7 turns to another hypothesis-driven application of systems biology to studying the problem of human HF cycling. It is argued that clock and clock target genes represent a classical systems biology paradigm. These "circadian" genes control and coordinate very complex processes on both the cell and tissue level, while their own activities are also subject to multiple external controls. Specifically, we test in Chapter 7 the working hypothesis that selected clock and clock target genes are functionally important in the control of the anagen-catagen transformation.

We show that circadian genes and proteins, responsible for autonomously coordinating the circadian rhythm, are involved in human HF cycling. *In vitro*, isolated human HFs exhibit both a circadian rhythm and hair cycle-dependent expression changes independently from central clock influences (such as from the suprachiasmic nucleus). By adopting siRNA technology for gene silencing purposes, *Period1* and *Clock* are identified as modulators of the anagen-catagen transition in human scalp HFs in organ culture. *Period1* and *Clock* also affect melanin content in anagen HFs, which produces new hypotheses regarding the role of these molecules in melanogenesis.

This work is novel as circadian clock genes have not previously been implicated in human hair cycle control. This work establishes that the human

HF exhibits multiple chronobiological rhythms on several levels. The exact mechanisms by which the circadian clock system affects the infradian hair cycle remain to be elucidated. It is hypothesised firstly, that the effector mechanisms may be via clock-controlled genes such as *c-Myc* and *Cdkn1a*. Secondly, intra-follicular clock gene activity may be under hormonal controls such as regulation by the intra-follicularly generated (hair growth and pigmentation modulating) neurohormone, TRH.

In Chapter 8, the transcriptome profiles of isolated, organ-cultured human scalp anagen and catagen HFs is established. Significantly over-represented gene functional categories in catagen were cell adhesion, steroid dehydrogenase activity, regulation of cell compartment size, collagen, cell projection and cell division. Anagen was characterised by the over-representation of keratin filament, BMP signalling, patterning, development, differentiation, serine/theorine kinase signalling and morphogenesis genes compared to background genome expression. This unbiased human transcriptome analysis not only identifies many genes that were known to be important in the control of murine HF cycling, but also demonstrates differential expression of novel candidate marker genes between anagen and catagen human HF.

This pilot study suggests that anagen and catagen in human organ culture HFs have distinct gene expression profiles. The identified marker genes could be used in the future to: verify human hair cycle staging, develop novel hair therapeutic targets and be factored into mathematical models of human HF cycling. The study remains to be complemented by additional systematic analyses on the protein level.

In the experimental components of this thesis, anagen and catagen human scalp organ cultured HFs were utilised for study. The organ culture model is currently the best available assay for studying human HF cycling *in vitro*, however, this needs to be complemented on the *in vivo* level. Feasible future experiments include corresponding clinical trials, using e.g. the phototrichogram technique (Dhurat and Saraogi, 2009) and analysis of fresh samples of whole human skin. Unfortunately, this is severely limited by the fact

that usually only 5-10% of human scalp HFs are not in the anagen stage at one time. Therefore, such *in vivo* analyses will require many months or years to collect enough catagen and telogen human HFs for analyses.

The distinct, but complementary research approaches employed in this thesis underscore that there is a challenge in dealing with the complexity in scales that one faces in hair biology i.e. both microscopic and macroscopic processes are involved in the hair cycle. A logical next step towards this challenge would be to integrate the novel molecular hair cycle control mechanisms (such as circadian clock genes or newly identified anagen/catagen marker genes) into the existing mathematical model of human HF cycling. The aim would be to then understand how such fast oscillators (circadian clock and cell cycle oscillators) may function *together* to regulate the slow human HF oscillator in a coordinated manner. This will require multi-scale modelling.

Complementary experimental investigations would involve laser capture microdissection to gain compartmentalised expression of mRNA and proteins of interest. This will elegantly complement the compartmentalised mathematical model proposed here and thus build a spatio-temporal expression edifice of the anagen and catagen states. In addition, siRNA technologies may be implemented to further probe the functional role of candidate genes in human hair cycle control and to dissect the underlying mechanisms of action.

To conclude, this thesis constitutes a first major step towards human hair research from a systems biology perspective. The thesis demonstrates that human HF cycling provides a most intriguing and clinically relevant systems biology problem. The current work raises the hope that the application of classical tools of system biology to human hair research will improve our understanding of human hair biology and pathology.

In summary, the key findings of the thesis are:

a. The human hair follicle is a dynamic organ whose cyclical activity may be controlled at the tissue level in the form of an autonomous relaxation oscillator. The mechanism requires delayed feedback between two

compartments (the MKs and DP). This presents a new theory of the human 'hair cycle clock'.

b. Knock-down of core circadian clock components; *Clock* and *Period1,* prolongs anagen phase in isolated human hair follicles.

c. Human isolated hair follicles in anagen and catagen have differential transcriptome signatures which may utilised to develop markers for human hair anagen and catagen states

Finally, the thesis is presented in a graphical abstract below.

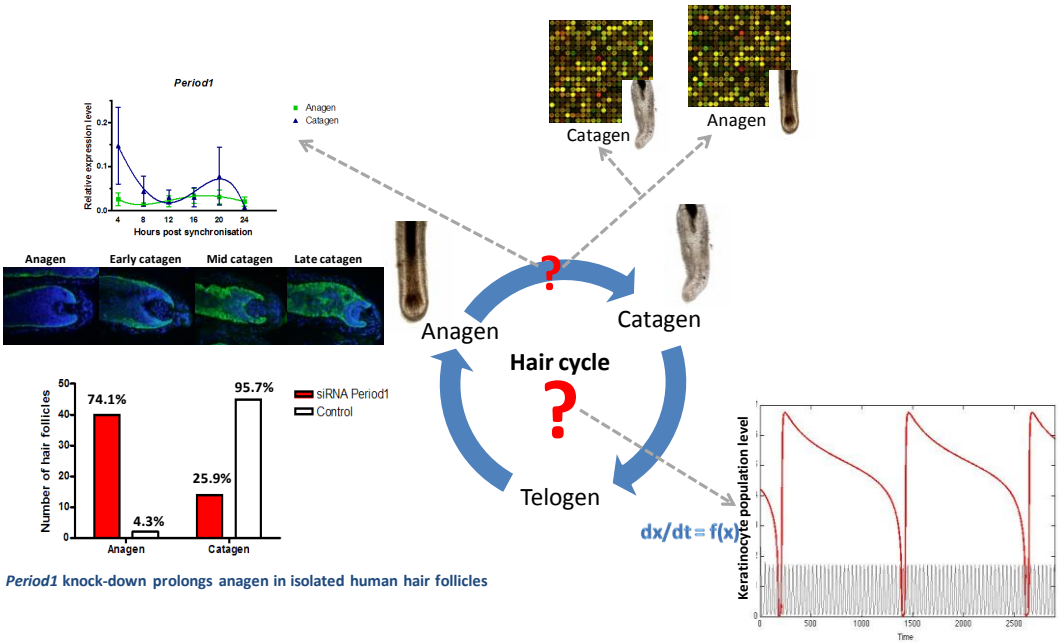

Figure 9.1: Graphical abstract of the thesis

Microarray chip image obtained from http://www.nchu.edu.tw/~ibms/ibms1/JJW/microarray%20lab%20index.htm

10 REFERENCES

2007. **Systems Biology: a vision for engineering and medicine.** A report from the Academy of Medical Sciences and The Royal Academy of Engineering. London: Academy of Medical Sciences and The Royal Academy of Engineering.

ABRAMOFF, M. D., MAGALHAES, P. J. & RAM, S. J. 2004. Image Processing with ImageJ. *Biophotonics International,* 11**,** 36-42.

ACKERMANN, K., DEHGHANI, F., BUX, R., KAUERT, G. & STEHLE, J. H. 2007. Day-night expression patterns of clock genes in the human pineal gland. *Journal of Pineal Research,* 43**,** 185-194.

ADEREM, A. 2005. Systems Biology: Its Practice and Challenges. *Cell,* 121**,** 511–513.

AKASHI, M., SOMA, H., YAMAMOTO, T., TSUGITOMI, A., YAMASHITA, S., YAMAMOTO, T., NISHIDA, E., YASUDA, A., LIAO, J. K. & NODE, K. 2010. Noninvasive method for assessing the human circadian clock using hair follicle cells. *PNAS,* 107**,** 15643–15648.

AL-NUAIMI, Y., BAIER, G., WATSON, R. E., CHUONG, C. M. & PAUS, R. 2010. The cycling hair follicle as an ideal systems biology research model. *Experimental Dermatology,* 19**,** 707-13.

AL-NUAIMI, Y., PHILPOTT, M., KLOEPPER, J., TÓTH, B., MCKAY, I., BIRO, T. & PAUS, R. 2009. A role for clock-related genes in human hair growth control? *Journal of Investigative Dermatology,* 129**,** S67.

ALONSO, L., OKADA, H., PASOLLI, H. A., WAKEHAM, A., YOU-TEN, A. I., MAK, T. W. & FUCHS, E. 2005. Sgk3 links growth factor signaling to maintenance of progenitor cells in the hair follicle. *The Journal of Cell Biology,* 170**,** 559–570.

ANDL, T., AHN, K., KAIRO, A., CHU, E. Y., WINE-LEE, L., REDDY, S. T., CROFT, N. J., CEBRA-THOMAS, J. A., METZGER, D., CHAMBON, P., LYONS, K. M., MISHINA, Y., SEYKORA, J. T., CRENSHAW, E. B. & MILLAR, S. E. 2004. Epithelial Bmpr1a regulates differentiation and proliferation in postnatal hair follicles and is essential for tooth development. *Development,* 131**,** 2257-2268.

ANDO, H., TAKAMURA, T., MATSUZAWA-NAGATA, N., SHIMA, K. R., ETO, T., MISU, H., SHIRAMOTO, M., TSURU, T., IRIE, S., FUJIMURA, A. & KANEKO, S. 2009. Clock gene expression in peripheral leucocytes of patients with type 2 diabetes. *Diabetologia,* 52**,** 329–335.

ARGYRIS, T. S. 1972. Chalones and the Control of Normal, Regenerative and Neoplastic Growth of the Skin. *Am Zoologist,* 12**,** 137-149.

ARGYRIS, T. S. & TRIMBLE, M. E. 1964. In the Mechanism of Hair Growth Stimulation in Wound Healing. *Developmental Biology,* 9**,** 230-254.

ARTHUR, J. W. & REICHARDT, J. K. V. 2010. Modeling Single Nucleotide Polymorphisms in the Human AKR1C1 and AKR1C2 Genes: Implications for Functional and Genotyping Analyses. *PLoS One,* 5 e15604.

AVRAM, M. R. 2006. Hair Transplantation for Men and Women. *Seminars in Cutaneous Medicine & Surgery,* 25**,** 60-64.

BAKER, R. E., SCHNELL, S. & MAINI, P. K. 2009. Waves and patterning in developmental biology: vertebrate segmentation and feather bud formation as case studies. *International Journal of Developmental Biology,* 53**,** 783-794.

BALSALOBRE, A. 2002. Clock genes in mammalian peripheral tissues. *Cell Tissue Research,* 309**,** 193-199.

BARTH, J. H. 1987. Normal hair growth in children. *Pediatric Dermatology,* 4**,** 173-184.

BATISTA, R. T. B., RAMIREZ, D. B., SANTOS, R. D., DEL ROSARIO, M. C. I. & MENDOZA, E. R. 2007. EUCLIS--An information system for circadian systems biology. *IET Systems Biology,* 1**,** 266-273.

BAZZI, H., DEMEHRI, S., POTTER, C. S., BARBER, A. G., AWGULEWITSCH, A., KOPAN, R. & CHRISTIANO, A. M. 2009. *Desmoglein 4* is Regulated by Transcription Factors Implicated in Hair Shaft Differentiation. *Differentiation,* 75**,** 292–300.

BAZZI, H., GETZ, A., MAHONEY, M. G., ISHIDA-YAMAMOTO, A., LANGBEIN, L., WAHL III, J. K. & CHRISTIANO, A. M. 2006. Desmoglein 4 is expressed in highly differentiated keratinocytes and trichocytes in human epidermis and hair follicle. *Differentiation,* 74**,** 129–140.

BERNARD, B. A. 2010. The hair follicle, a bistable biological system. *Experimental Dermatology,* 19**,** 017.

BJARNSON, G. A. & JORDAN, R. 2002. Rhythms in Human Gastrointestinal Mucosa and Skin. *Chronobiology International,* 19**,** 129-140.

BJARNSON, G. A., JORDAN, R. C. K., WOOD, P. A., LI, Q., LINCOLN, D. W., SOTHERN, R. B., HRUSHESKY, W. J. M. & BEN-DAVID, Y. 2001. Circadian Expression of Clock Genes in Human Oral Mucosa and Skin *Association with Specific Cell-Cycle Phases*. *American Journal of Pathology,* 158**,** 1793-1801.

BODO, E., BIRO, T., TELEK, A., CZIFRA, G., GRIGER, Z., TOTH, B. I., MESCALCHIN, A., ITO, T., BETTERMANN, A., KOVACS, L. & PAUS, R. 2005. A hot new twist to hair biology: involvement of vanilloid receptor-1 (VR1/TRPV1) signaling in human hair growth control. *American Journal of Pathology,* 166**,** 985-98.

BODÓ, E., KANY, B., GÁSPÁR, E., KNÜVER, J., KROMMINGA, A., RAMOT, Y., BÍRÓ, T., TIEDE, S., VAN BEEK, N., POEGGELER, B., MEYER, K. C., WENZEL, B. E. & PAUS, R. 2010. Thyroid-Stimulating Hormone, a Novel, Locally Produced Modulator of Human Epidermal Functions, Is Regulated by Thyrotropin-Releasing Hormone and Thyroid Hormones. *Endocrinology,* 151**,** 1633-1642.

BODO, E., TOBIN, D. J., KAMENISCH, Y., BIRO, T., BERNEBURG, M., FUNK, W. & PAUS, R. 2007. Dissecting the impact of chemotherapy on the human hair follicle: a pragmatic in vitro assay for studying the pathogenesis and potential management of hair follicle dystrophy. *American Journal of Pathology,* 171**,** 1153-67.

BOTCHKAREV, V. A. 2003. Bone Morphogenetic Proteins and Their Antagonists in Skin and Hair Follicle Biology. *Journal of Investigative Dermatology,* 120**,** 36-47.

BOTCHKAREV, V. A., BOTCHKAREV, N. V., ALBERS, K. M., VAN DER VEEN, C., LEWIN, G. R. & PAUS, R. 1998a. Neurotrophin-3 involvement in the regulation of hair follicle morphogenesis. *Journal of Investigative Dermatology,* 111**,** 279-85.

BOTCHKAREV, V. A., BOTCHKAREVA, N. V., PETERS, E. M. & PAUS, R. 2004. Epithelial growth control by neurotrophins: leads and lessons from the hair follicle. *Progress in Brain Research,* 146**,** 493-513.

BOTCHKAREV, V. A., BOTCHKAREVA, N. V., ROTH, W., NAKAMURA, M., CHEN, L.-H., HERZOG, W., LINDNER, G., MCMAHON, J. A., PETERS, C., LAUSTER, R., MCMAHON, A. P. & PAUS, R. 1999a. Noggin is a mesenchymally derived stimulator of hair-follicle induction. *Nature Cell Biology,* 1**,** 158-164.

BOTCHKAREV, V. A., BOTCHKAREVA, N. V., WELKER, P., METZ, M., LEWIN, G. R., SUBRAMANIAM, A., BULFONE-PAUS, S., HAGEN, E., BRAUN, A., LOMMATZSCH, M., RENZ, H. & PAUS, R. 1999b. A new role for neurotrophins: involvement of brain-derived neurotrophic factor and neurotrophin-4 in hair cycle control. *FASEB J,* 13**,** 395-410.

BOTCHKAREV, V. A. & KISHIMOTO, J. 2003. Molecular control of Epithelial-Mesenchymal Interactions During Hair Follicle Cycling. *Journal of Investigative Dermatology Symposium Proceedings,* 8**,** 46-55.

BOTCHKAREV, V. A. & PAUS, R. 2003. Molecular Biology of Hair Morphogenesis: Development and Cycling. *Journal of Experimental Zoology,* 298B**,** 164–180.

BOTCHKAREV, V. A. & SHAROV, A. A. 2004. BMP signaling in the control of skin development and hair follicle growth. *Differentiation,* 72**,** 512–526.

BOTCHKAREV, V. A., WELKER, P., ALBERS, K. M., BOTCHKAREVA, N. V., METZ, M., LEWIN, G. R., BULFONE-PAUS, S., PETERS, E. M. J., LINDNER, G. & PAUS, R. 1998b. A New Role for Neurotrophin-3. Involvement in the Regulation of Hair Follicle Regression (Catagen). *American Journal of Pathology,* 153**,** 785-799.

BRUGGEMAN, F. J. & WESTERHOFF, H. V. 2006. The Nature of Systems Biology. *Trends in Microbiology,* 15**,** 45-50.

BUBACK, F., RENKL, A. C., SCHULZ, G. & WEISS, J. M. 2009. Osteopontin and the skin: multiple emerging roles in cutaneous biology and pathology. *Experimental Dermatology,* 18**,** 750–759.

BULL, J. J., MULLER-ROVER, S., PATEL, S. V., CHRONNELL, C. M., MCKAY, I. A. & PHILPOTT, M. P. 2001. Contrasting localization of c-Myc with other Myc superfamily transcription factors in the human hair follicle and during the hair growth cycle. *Journal of Investigative Dermatology,* 116**,** 617-22.

BULL, J. J., PELENGARIS, S., HENDRIX, S., CHRONNELL, C. M., KHAN, M. & PHILPOTT, M. P. 2005. Ectopic expression of c-Myc in the skin affects the hair growth cycle and causes an enlargement of the sebaceous gland. *British Journal of Dermatology,* 152**,** 1125-33.

CAI, J., LEE, J., KOPAN, R. & MA, L. 2009. Genetic interplays between *Msx2* and *Foxn1* are required for *Notch1* expression and hair shaft differentiation. *Developmental Biology,* 326**,** 420-430.

CAMPAGNA, D. R., CUSTODIO, A. O., ANTIOCHOS, B. B., CIRLAN, M. V. & FLEMING, M. D. 2008. Mutations in the serum/glucocorticoid regulated kinase 3 (Sgk3) are responsible for the mouse fuzzy (fz) hair phenotype. *Journal of Investigative Dermatology,* 128**,** 730-2.

CHANG, P.-L., HARKINS, L., HSIEH, Y.-H., HICKS, P., SAPPAYATOSOK, K., YODSANGA, S., SWASDISON, S., CHAMBERS, A. F., ELMETS, C. A. & HO, K.-J. 2008. Osteopontin Expression in Normal Skin and Non-melanoma Skin Tumors. *Journal of Histochemistry and Cytochemistry,* 56**,** 57-66.

CHARPENTIER, E., LAVKER, R. M., ACQUISTA, E. & COWIN, P. 2000. Plakoglobin Suppresses Epithelial Proliferation and Hair Growth In Vivo. *The Journal of Cell Biology,* 149**,** 503-519.

CHASE, H. B. 1954. Growth of the hair. *Physiol. Rev.,* 34**,** 113–126.

CHEN-GOODSPEED, M. & LEE, C. C. 2007. Tumor Suppression and Circadian Function. *Journal Biological Rhythms,* 22**,** 291-298.

CHEN, W., THIBOUTOT, D. & ZOUBOULIS, C. C. 2002. Cutaneous Androgen Metabolism: Basic Research and Clinical Perspectives. *Journal of Investigative Dermatology,* 119**,** 992-1007.

CHERMNYKH, E. S., VOROTELYAK, E. A., GNEDEVA, K. Y., MOLDAVER, M. V., YEGOROV, Y. E., VASILIEV, A. V. & TERSKIKH, V. V. 2010. Dermal papilla cells induce keratinocyte tubulogenesis in culture. *Histochemistry and Cell Biology,* 133**,** 567–576.

CHOI, H. I., CHOI, G. I., KIM, E. K., CHOI, Y. J., SOHN, K. C., LEE, Y., KIM, C. D., YOON, T. J., SOHN, H. J., HAN, S. H., KIM, S., LEE, J. H. & LEE, Y. H. 2011. Hair greying is associated with active hair growth. *British Journal of Dermatology*.

CHUONG, C. M., DHOUAILLY, D., GILMORE, S., FOREST, L., SHELLEY, W. B., STENN, K. S., MAINI, P., MICHON, F., PARIMOO, S., CADAU, S., DEMONGEOT, J., ZHENG, Y., PAUS, R. & HAPPLE, R. 2006. What is the biological basis of pattern formation of skin lesions? *Experimental Dermatology,* 15**,** 547-564.

COHEN, J. 1961. The transplantation of individual rat and guniea pig whisker papillae. *J Embrol Exp Morphol,* 9**,** 117-127.

COLOMBE, L., VINDRIOS, A., MICHELET, J.-F. & BERNARD, B. A. 2007. Prostaglandin metabolism in human hair follicle. *Experimental Dermatology,* 16**,** 762–769.

COTSARELIS, G. 2006. Epithelial Stem Cells: A Folliculocentric View. *Journal of Investigative Dermatology. Symposium Proceedings,* 126**,** 1459-1468.

COTSARELIS, G. & MILLAR, S. E. 2001. Towards a molecular understanding of hair loss and its treatment. *Trends in Molecular Medicine,* 7**,** 293-301.

COTSARELIS, G., SUN, T.-T. & LAVKER, R. M. 1990. Label-Retaining Cells Reside in the Bulge Area of Pilosebaceous Unit: Implications for Follicular Stem Cells, Hair Cycle, and Skin Carcinogenesis. *Cell,* 61**,** 1329-1337.

DARDENTE, H. & CERMAKIAN, N. 2007. Molecular circadian rhythms in central and peripheral clocks in mammals. *Chronobiology International,* 24**,** 195-213.

DAWBER, R. (ed.) 1997. *Diseases of the hair and scalp,* Oxford: Blackwells.

DE SCHELLENBERGER, A. A., HORLAND, R., ROSOWSKI, M., PAUS, R., LAUSTER, R. & LINDNER, G. 2011. Cartilage oligomeric matrix protein (COMP) forms part of the connective tissue of normal human hair follicles. *Experimental Dermatology,* 20**,** 361-266.

DENHARDT, D. T., NODA, M., O'REGAN, A. W., PAVLIN, D. & BERMAN, J. S. 2001. Osteopontin as a means to cope with environmental insults: regulation of inflammation, tissue remodeling, and cell survival. *The Journal of Clinical Investigation,* 107**,** 1055-1061.

DENNIS, G. J., SHERMAN, B. T., HOSACK, D. A., YANG, J., GAO, W., LANE, H. C. & LEMPICKI, R. A. 2003. DAVID: Database for Annotation, Visualization, and Integrated Discovery. *Genome Biology,* 4**,** P3.

DHURAT, R. & SARAOGI, P. 2009. Hair Evaluation Methods: Merits and Demerits. *International Journal of Trichology,* 1**,** 108-119.

DI VENTURA, B., LEMERLE, C., MICHALODIMITRAKIS, K. & SERRANO, L. 2006. From in vivo to in silico biology and back. *Nature,* 443**,** 527-533.

DIBNER, C., SCHIBLER, U. & ALBRECHT, U. 2010. The Mammalian Circadian Timing System: Organization and Coordination of Central and Peripheral Clocks. *Annual review of physiology,* 72**,** 517–549.

DUFFIELD, G. E. 2003. DNA microarray analyses of circadian timing: the genomic basis of biological time. *Journal of Neuroendocrinology,* 15**,** 991-1002.

DUGUAY, D. & CERMAKIAN, N. 2009. The crosstalk between physiology and circadian clock proteins. *Chronobiology International,* 26**,** 1479-1513.

DUNCAN, D. E. 2004. Discover Dialogue: Sydney Brenner. *Discover Science, Technology and the Future* [Online].

DUNLAP, J. C., LOROS, J. J. & DECOURSEY, P. J. 2004. *Chronobiology Biological Timekeeping,* Sunderland, Massachusetts, Sinauer Associates.

EICHBERGER, T., REGL, G., IKRAM, M. S., NEILL, G. W., PHILPOTT, M. P., ABERGER, F. & FRISCHAUF, A.-M. 2004. FOXE1, A New Transcriptional Target of GLI2 Is Expressed in Human Epidermis and Basal Cell Carcinoma. *The Journal of Investigative Dermatology,* 122**,** 1180-1187.

EICHELER, W., HAPPLE, R. & HOFFMANN, R. 1998. 5α-Reductase activity in the human hair follicle concentrates in the dermal papilla. *Archives of Dermatology Research* 290**,** 126–132.

FARATIAN, D., CLYDE, R. G., CRAWFORD, J. W. & HARRISON, D. J. 2009a. Systems pathology—taking molecular pathology into a new dimension. *Nature reviews Clinical Oncology,* 6**,** 455–464.

FARATIAN, D., GOLTSOV, A., LEBEDEVA, G., SOROKIN, A., MOODIE, S., MULLEN, P., KAY, C., UM, I. H., LANGDON, S., GORYANIN, I. & HARRISON, D. J. 2009b. Systems Biology Reveals New Strategies for Personalizing Cancer Medicine and Confirms the Role of PTEN in Resistance to Trastuzumab. *Cancer Research,* 69**,** 6713–6720].

FOITZIK, K., LINDNER, G., MUELLER-ROEVER, S., MAURER, M., BOTCHKAREVA, N., BOTCHKAREV, V., HANDJISKI, B., METZ, M., HIBINO, T., SOMA, T., DOTTO, G. P. & PAUS, R. 2000. Control of murine hair follicle regression (catagen) by TGF-beta1 in vivo. *FASEB J,* 14**,** 752-60.

FRIEDL, P. & GILMOUR, D. 2009. Collective cell migration in morphogenesis, regeneration and cancer. *Nature Reviews Molecular Cell Biology,* 10**,** 445-457.

FU, L., PELICANO, H., LIU, J., HUANG, P. & LEE, C. C. 2002. The Circadian Gene Period2 Plays an Important Role in Tumor Suppression and DNA Damage Response In Vivo. *Cell,* 111**,** 41–50.

FUCHS, E. 1998. Beauty is skin deep: the fascinating biology of the epidermis and its appendages. *Harvey Lectures,* 94**,** 47-77.

FUCHS, E. 2009. The Tortoise and the Hair: Slow-Cycling Cells in the Stem Cell Race. *Cell,* 137**,** 811-819.

FUCHS, E., MERRILL, B. J., JAMORA, C. & DASGUPTA, R. 2001. At the roots of a never-ending cycle. *Developmental Cell,* 1**,** 13–25.

GACHON, F., NAGOSHI, E., BROWN, S. A., RIPPERGER, J. & SCHIBLER, U. 2004. The mammalian circadian timing system: from gene expression to physiology. *Chromosoma,* 113**,** 103-112.

GARY, K. A., SEVARINO, K. A., YARBROUGH, G. G., PRANGE JR., A. J. & WINOKUR, A. 2003. The Thyrotropin-Releasing Hormone (TRH) Hypothesis of Homeostatic Regulation: Implications for TRH-Based Therapeutics. *The Journal of Pharmacology and Experimental Therapeutics,* 305**,** 410-416.

GARY, K. A., SOLLARS, P. J., LEXOW, N., WINOKUR, A. & PICKARD, G. E. 1996. Thyrotropin-releasing hormone phase shifts circadian rhythms in hamsters. *Neuroreport,* 7**,** 1631-1634.

GARZA, L. A., YANG, C.-C., ZHAO, T., BLATT, H. B., LEE, M., HE, H., STANTON, D. C., CARRASCO, L., SPIEGEL, J. H., TOBIAS, J. W. & COTSARELIS, G. 2011. Bald scalp in men with androgenetic alopecia retains hair follicle stem cells but lacks CD200-rich and CD34-positive hair progenitor cells. *The Journal of Clinical Investigation,* 121**,** 613-622.

GÁSPÁR, E., HARDENBICKER, C., BODÓ, E., WENZEL, B., RAMOT, Y., FUNK, W., KROMMINGA, A. & PAUS, R. 2010. Thyrotropin releasing hormone (TRH): A new player in human hair growth control. *The FASEB Journal,* 24**,** 393-403.

GATENBY, R. A. & MAINI, P. K. 2003. Cancer summed up. *Nature,* 421**,** 321.

GEKAKIS, N., STAKNIS, D., NGUYEN, H. B., DAVIS, F. C., WILSBACHER, L. D., KING, D. P., TAKAHASHI, J. S. & WEITZ, C. J. 1998. Role of the CLOCK Protein in the Mammalian Circadian Mechanism. *Science,* 280**,** 1564-1569.

GEYFMAN, M. & ANDERSEN, B. 2010. Clock genes, hair growth and aging. *Aging,* 2**,** 122-128.

GLASS, L. & MACKEY, M. 1988. *From Clocks to Chaos: The Rhythms of Life,* Guildford, Princeton University Press.

GOLICHENKOVA, P. D. & DORONIN, Y. K. 2008. Reconstruction of Proliferative Activity of Hair Follicle Cells Based on the Geometric Parameters of the Hair Shaft. *Moscow University Biological Sciences Bulletin,* 632**,** 77-79.

GOODWIN, B. C. 1963. *Temporal Organization of Cells,* New York, Academic Press.

GRÉCHEZ-CASSIAU, A., RAYET, B., GUILLAUMOND, F., TEBOUL, M. & DELAUNAY, F. 2008. The Circadian Clock Component BMAL1 Is a critical Regulator of $p21^{WAF1/CIP1}$ Expression and Hepatocyte Proliferation. *Journal of Biological Chemistry,* 283**,** 4535-4542.

GRECO, V., CHEN, T., RENDL, M., SCHOBER, M., PASOLLI, H. A., STOKES, N., CRUZ-RACELIS, J. D. & FUCHS, E. 2009. A Two-Step Mechanism for Stem Cell Activation during Hair Regeneration. *Cell Stem Cell,* 4**,** 155-169.

GUHA, U., MECKLENBURG, L., COWIN, P., KAN, L., O'GUIN, W. M., D'VIZIO, D., PESTELL, R. G., PAUS, R. & KESSLER, J. A. 2004. Bone Morphogenetic Protein Signaling Regulates Postnatal Hair Follicle Differentiation and Cycling. *American Journal of Pathology,* 165**,** 729–740.

HADSHIEW, I. M., FOITZIK, K., ARCK, P. C. & PAUS, R. 2004. Burden of Hair Loss: Stress and the Underestimated Psychosocial Impact of Telogen Effluvium and Androgenetic Alopecia. *Journal of Investigative Dermatology,* 123**,** 455–457.

HALLOY, J., BERNARD, B. A., LOUSSOUARN, G. & GOLDBETER, A. 2000. Modeling the dynamics of human hair cycles by a follicular automaton. *Proceedings of the National Academy of Sciences of the United States of America,* 97**,** 8328-33.

HALLOY, J., BERNARD, B. A., LOUSSOUARN, G. & GOLDBETER, A. 2002. The follicular automaton model: effect of stochasticity and of synchronization of hair cycles. *Journal of Theoretical Biology,* 214**,** 469-79.

HARRIES, M. J. & PAUS, R. 2010. The pathogenesis of primary cicatricial alopecias. *American Journal of Pathology,* 177**,** 2152-2162.

HAZLERIGG, D. & LOUDON, A. 2008. New Insights into Ancient Seasonal Review Life Timers. *Current Biology,* 18**,** R795–R804.

HEBERT, J. M., ROSENQUIST, T., GOTZ, J. & MARTIN, G. R. 1994. FGF5 as a regulator of the hair growth cycle: evidence from targeted and spontaneous mutations. *Cell,* 78**,** 1017-25.

HIGGINS, C. A., WESTGATE, G. E. & JAHODA, C. A. B. 2009. From Telogen to Exogen: Mechanisms Underlying Formation and Subsequent Loss of the Hair Club Fiber. *Journal of Investigative Dermatology,* 129**,** 2100–2108.

HOFFMANN, R. 2003. Steroidogenic Isoenzymes in Human Hair and Their Potential Role in Androgenetic Alopecia. *Dermatology,* 206**,** 85–95.

HORNBERG, J. J., BRUGGEMAN, F. J., WESTERHOFF, H. V. & LANKELMA, J. 2006. Cancer: A Systems Biology disease. *BioSystems,* 83**,** 81-90.

HSU, Y. C., PASOLLI, H. A. & FUCHS, E. 2011. Dynamics between stem cells, niche, and progeny in the hair follicle. *Cell,* 144**,** 92-105.

HU, M. & POLYAK, K. 2008. Molecular characterisation of the tumour microenvironment in breast cancer. *European Journal of Cancer,* 44**,** 2760–2765.

HUANG, D. W., SHERMAN, B. T. & LEMPICKI, R. A. 2009. Systematic and integrative analysis of large gene lists using DAVID Bioinformatics Resources. *Nature Protoc.,* 4**,** 44-57.

HUANG, S. & WIKSWO, J. 2006. Dimensions of systems biology. *Reviews of Physiology Biochemistry and Pharmacology.* Berlin: Springer Berlin Heidelberg.

HUNTER, P. J., CRAMPIN, E. J. & NIELSEN, P. M. F. 2008. Bioinformatics, multiscale modeling and the IUPS Physiome Project. *Briefings in bioinformatics,* 9**,** 333-343.

HUNTJENS, D. R. H., DANHOF, M. & DELLA PASQUA, O. E. 2005. Pharmacokinetic–pharmacodynamic correlations and biomarkers in the development of COX-2 inhibitors. *Rheumatology,* 44**,** 846–859.

HWANG, J., MEHRANI, T., MILLAR, S. E. & MORASSO, M. I. 2008. Dlx3 is a crucial regulator of hair follicle differentiation and cycling. *Development* 135**,** 3149-3159.

IBRAHIM, L. & WRIGHT, E. A. 1982. A quantitative study of hair growth using mouse and rat vibrissal follicles. *J. Embryol. exp. Mor,* 72.

IINO, M., EHAMA, R., NAKAZAWA, Y., IWABUCHI, T., OGO, M., TAJIMA, M. & ARASE, S. 2007. Adenosine Stimulates Fibroblast Growth Factor-7 Gene Expression Via Adenosine A2b Receptor Signaling in Dermal Papilla Cells. *Journal of Investigative Dermatology,* 127**,** 1318–1325.

ITAMI, S., KURATA, S. & TAKAYASU, S. 1995. Androgen induction of follicular epithelial cell growth is mediated via insulin-like growth factor-I from dermal papilla cells. *Biochemical & Biophysical Research Communications,* 212**,** 988-94.

ITO, M., KIZAWA, K., HAMADA, K. & COTSARELIS, G. 2004. Hair follicle stem cells in the lower bulge form the secondary germ, a biochemically distinct but functionally equivalent progenitor cell population, at the termination of catagen. *Differentiation,* 72**,** 548-57.

ITO, N., ITO, T., KROMMINGA, A., BETTERMANN, A., TAKIGAWA, M., KEES, F., STRAUB, R. H. & PAUS, R. 2005a. Human hair follicles display a functional equivalent of the hypothalamic-pituitary-adrenal axis and synthesize cortisol. *FASEB Journal,* 19**,** 1332-4.

ITO, T., ITO, N., SAATHOFF, M., BETTERMANN, A., TAKIGAWA, M. & PAUS, R. 2005b. Interferon-gamma is a potent inducer of catagen-like changes in cultured human anagen hair follicles. *British Journal of Dermatology,* 152**,** 623-31.

IWABUCHI, T., MARUYAMAB, T., SEI, Y. & ADACHICYD, K. 1994. Effects of immunosuppressive peptidyl-prolyl cis-trans isomerase (PPIase) inhibitors, cyclosporin A, FK506, ascomycin and rapamycin, on hair growth initiation in mouse: immunosuppression is not required for new hair growth. *Journal of Dermatological Science,* 9**,** 64-69.

JIMENEZ, F. & RUIFERNÁNDEZ, J. M. 1999. Distribution of Human Hair in Follicular Units. *Dermatological Surgery,* 25**,** 294-298.

JIN, Y. & PENNING, T. M. 2007. Aldo-Keto Reductases and Bioactivation/Detoxication. *Annual Review of Pharmacology and Toxicology,* 47**,** 263–92.

JINDO, T., TSUBOI, R., IMAI, R., TAKAMORI, K., RUBIN, J. S. & OGAWA, H. 1995. The effect of hepatocyte growth factor/scatter factor on human hair follicle growth. *Journal of Dermatological Science,* 10**,** 229-32.

JINDO, T., TSUBOI, R., TAKAMORI, K. & OGAWA, H. 1998. Local injection of hepatocyte growth factor/scatter factor (HGF/SF) alters cyclic growth of murine hair follicles. *Journal of Investigative Dermatology,* 110**,** 338-42.

KAWANO, M., KOMI-KURAMOCHI, A., ASADA, M., SUZUKI, M., OKI, J., JIANG, J. & IMAMURA, T. 2005. Comprehensive analysis of FGF and FGFR expression in skin: FGF18 is highly expressed in hair follicles and capable of inducing anagen from telogen stage hair follicles. *Journal of Investigative Dermatology,* 124**,** 877-85.

KAWARA, S., MYDLARSKI, R., MAMELAK, A. J., FREED, I., WANG, B., WATANABE, H., SHIVJI, G., TAVADIA, S. K., SUZUKI, H., BJARNASON, G. A., JORDAN, R. C. K. & SAUDERN, D. N. 2002. Low-dose Ultraviolet B Rays Alter the mRNA Expression of the Circadian Clock Genes in Cultured Human Keratinocytes. *Journal of Investigative Dermatology,* 119**,** 1220-1223.

KELL, D. B. 2004. Metabolomics and systems biology: making sense of the soup. *Current Opinion in Microbiology,* 7**,** 296–307.

KHAPRE, R. V., SAMSA, W. E. & KONDRATOV, R. V. 2010. Circadian regulation of cell cycle: Molecular connections between aging and the circadian clock. *Annals of Medicine,* 42**,** 404–415.

KIM, S. J., DIX, D. J., THOMPSON, K. E., MURRELL, R. N., SCHMID, J. E., GALLAGHER, J. E. & ROCKETT, J. C. 2006. Gene Expression in Head Hair Follicles Plucked from Men and Women. *Annals of Clinical & Laboratory Science,* 36**,** 115-126.

KISHIMOTO, J., BURGESON, R. E. & MORGAN, B. A. 2000. Wnt signaling maintains the hair-inducing activity of the dermal papilla. *Genes and Development,* 14**,** 1181-1185.

KITANO, H. 2002. Systems Biology: A brief overview. *Science,* 295**,** 1662-1664.

KLIGMAN, A. M. 1959. The Human Hair Cycle. *The Journal of Investigative Dermatology***,** 307-316.

KLIPP, E., LIEBERMEISTER, W., WIERLING, C., KOWALD, A., LEHRACH, H. & HERWIG, R. 2009. *Systems Biology: A textbook,* Weinheim, Wiley-VCH.

KLJUIC, A., BAZZI, H., SUNDBERG, J. P., MARTINEZ-MIR, A., O'SHAUGHNESSY, R., MAHONEY, M. G., LEVY, M., MONTAGUTELLI, X., AHMAD, W., AITA, V. M., GORDON, D., UITTO, J., WHITING, D. A., OTT, J., FISCHER, S., GILLIAM, T. C., JAHODA, C. A. B., MORRIS, R. J., PANTELEYEV, A. A., NGUYEN, V. T. & CHRISTIANO, A. M. 2003. Desmoglein 4 in Hair Follicle Differentiation and Epidermal Adhesion: Evidence from Inherited Hypotrichosis and Acquired Pemphigus Vulgaris. *Cell,* 113**,** 249–260.

KLOEPPER, J. E., SUGAWARA, K., AL-NUAIMI, Y., GÁSPÁR, E., VAN BEEK, N. & PAUS, R. 2009. Methods in hair research: how to objectively distinguish between anagen and catagen in human hair follicle organ culture. *Experimental Dermatology*.

KLOEPPER, J. E., SUGAWARA, K., AL-NUAIMI, Y., GÁSPÁR, E., VAN BEEK, N. & PAUS, R. 2010. Methods in hair research: how to objectively distinguish between anagen and catagen in human hair follicle organ culture. *Experimental Dermatology,* 19**,** 305-312.

KOBIELAK, K., STOKES, N., DE LA CRUZ, J., POLAK, L. & FUCHS, E. 2007. Loss of a quiescent niche but not follicle stem cells in the absence of bone

morphogenetic protein signaling. *Proceedings of the National Academy of Sciences of the United States of America,* 104**,** 10063–10068.
KOLINKO, V. & LITTLER, C. M. 2000. Mathematical modeling for the prediction and optimization of laser hair removal. *Lasers in Surgery & Medicine,* 26**,** 164-76.
KRAUSE, K. & FOITZIK, K. 2006. Biology of the hair follicle: the basics. *Seminars in Cutaneous Medicine & Surgery,* 25**,** 2-10.
KULESSA, H., TURK, G. & HOGAN, B. L. M. 2000. Inhibition of Bmp signaling affects growth and differentiation in the anagen hair follicle. *The EMBO Journal,* 19**,** 6664-6674.
KUME, K., ZYLKA, M. J., SRIRAM, S., SHEARMAN, L. P., WEAVER, D. R., JIN, X., MAYWOOD, E. S., HASTINGS, M. H. & REPPERT, S. M. 1999. mCRY1 and mCRY2 Are Essential Components of the Negative Limb of the Circadian Clock Feedback Loop. *Cell,* 98**,** 193-205.
KWAN, K. M., LI, A. G., WANG, X.-J., WURST, W. & BEHRINGER, R. R. 2004. Essential Roles of BMPR-IA Signaling in Differentiation and Growth of Hair Follicles and in Skin Tumorigenesis. *Genesis,* 39**,** 10–25.
KWON, O. S., OH, J. K., KIM, M. H., PARK, S. H., PYO, H., K., KIM, K. H., CHO, K. H. & EUN, H. C. 2006. Human hair growth ex vivo is correlated with in vivo hair growth: selective categorization of hair follicles for more reliable hair follicle organ culture. *Archives of Dermatological Research,* 297**,** 367-371.
LANGAN, E. A., RAMOT, Y., GOFFIN, V., GRIFFITHS, C. E. M., FOITZIK, K. & PAUS, R. 2010. Mind the (Gender) Gap: Does Prolactin Exert Gender and/or Site-Specific Effects on the Human Hair Follicle? *Journal of Investigative Dermatology,* 130**,** 886-891.
LANGBEIN, L. & SCHWEIZER, J. 2005. Keratins of the Human Hair Follicle. *International Review of Cytology,* 243**,** 1-78.
LANGMESSER, S., TALLONE, T., BORDON, A., RUSCONI, S. & ALBRECHT, U. 2008. Interaction of circadian clock proteins PER2 and CRY with BMALI and CLOCK. *BMC Molecular Biology,* 9.
LAVKER, R. M., SUN, T. T., OSHIMA, H., BARRANDON, Y., AKIYAMA, M., FERRARIS, C., CHEVALIER, G., FAVIER, B., JAHODA, C. A., DHOUAILLY, D., PANTELEYEV, A. A. & CHRISTIANO, A. M. 2003. Hair follicle stem cells. *J Investig Dermatol Symp Proc,* 8**,** 28-38.
LEE, C. 2005. The Circadian Clock and Tumor Suppression by Mammalian Period Genes. *Methods in Enzymology,* 393**,** 852-861.
LEE, C. C. 2006. Tumor supression by the mammalian *period* genes. *Cancer Causes Control,* 17**,** 525-530.
LEGUÉ, E. & NICOLAS, J.-F. 2005. Hair follicle renewal: organisation of stem cells in the matrix and the role of stereotyped lineages and behaviors. *Development,* 132**,** 4143-4154.
LI, C. & WONG, W. H. 2004. Model-based analysis of oligonucleotide arrays: Expression index computation and outlier detection. *Proceedings of the National Academy of Sciences of the United States of America,* 98**,** 31-36.
LIN, K. K., CHUDOVA, D., HATFIELD, G. W., SMYTH, P. & ANDERSEN, B. 2004. Identification of hair cycle-associated genes from time-course gene

expression profile data by using replicate variance. *Proceedings of the National Academy of Sciences of the United States of America,* 101**,** 15955-60.

LIN, K. K., KUMAR, V., GEYFMAN, M., CHUDOVA, D., IHLER, A. T., SMYTH, P., PAUS, R., TAKAHASHI, J. S. & ANDERSEN, B. 2009. Circadian Clock Genes Contribute to the Regulation of Hair Follicle Cycling. *PLOS Genetics,* 5**,** e1000573.

LINDNER, G., BOTCHKAREV, V. A., BOTCHKAREVA, N. V., LING, G., VAN DER VEEN, C. & PAUS, R. 1997. Analysis of apoptosis during hair follicle regression (catagen). *American Journal of Pathology,* 151**,** 1601-17.

LINDNER, G., MENRAD, A., GHERARDI, E., MERLINO, G., WELKER, P., HANDJISKI, B., ROLOFF, B. & PAUS, R. 2000. Involvement of hepatocyte growth factor/scatter factor and met receptor signaling in hair follicle morphogenesis and cycling. *FASEB Journal,* 14**,** 319-32.

LINK, R. E., PAUS, R., STENN, K. S., KUKLINSKA, E. & MOELLMANN, G. 1990. Epithelial growth by rat vibrissae follicles in vitro requires mesenchymal contact via native extracellular matrix. *Journal of Investigative Dermatology,* 95**,** 202-207.

LOWREY, P. L. & TAKAHASHI, J. S. 2004. Mammalian Circadian Biology: Elucidating Genome-wide Levels of Temporal Organisation. *Annu. Rev. Genomics Hum. Genet.,* 5**,** 407-41.

MA, L., LIU, J., WU, T., PLIKUS, M., JIANG, T. X., BI, Q., LIU, Y. H., MULLER-ROVER, S., PETERS, H., SUNDBERG, J. P., MAXSON, R., MAAS, R. L. & CHUONG, C. M. 2003. 'Cyclic alopecia' in Msx2 mutants: defects in hair cycling and hair shaft differentiation. *Development,* 130**,** 379-89.

MACARTHUR, B. D., MA'AYAN, A. & LEMISCHKA, I. R. 2009. Systems biology of stem cell fate and cellular reprogramming. *Nature Reviews Molecular Cell Biology,* 10**,** 672-681.

MAKAROW, M., HOJGAARD, L. & CEULEMANS, R. 2008. European Science Foundation. Setting Science Agendas for Europe: Advancing Systems Biology for Medical Applications. *ESF Science Policy Briefing,* 35**,** 1-12.

MANDEMA JAAP, W., HERMANN, D., WANG, W., SHEINER, T., MILAD, M., BAKKER-ARKEMA, R. & HARTMAN, D. 2005. Model-Based Development of Gemcabene, a New Lipid-Altering Agent. *The AAPS Journal.,* 7**,** Article 52.

MARDARYEV, A. N., AHMED, M. I., VLAHOV, N. V., FESSING, M. Y., GILL, J. H., SHAROV, A. A. & BOTCHKAREVA, N. V. 2010. Micro-RNA-31 controls hair cycle-associated changes in gene expression programs of the skin and hair follicle. *The FASEB Journal,* 24**,** 3869–3881.

MAR'IN, Y. E., SEIBERG, M. & LIN, C. B. 2009. Aldo-keto reductase 1C subfamily genes in skin are UV-inducible: possible role in keratinocytes survival. *Experimental Dermatology,* 18**,** 611–618.

MATSUO, K., MORI, O. & HASHIMOTO, T. 1998. Apoptosis in murine hair follicles during catagen regression. *Archives of Dermatological Research,* 290**,** 133-136.

MATSUO, T., YAMAGUCHI, S., MITSUI, S., EMI, A., SHIMODA, F. & OKAMURA, H. 2003. Control Mechanism of the Circadian Clock for Timing of Cell Division in Vivo. *Science,* 302**,** 255-259.

MATSUZAKI, T. & YOSHIZATO, K. 1998. Role of hair papilla cells on induction and regeneration processes of hair follicles. *Wound Repair and Regeneration,* 6**,** 526-530.

MAURER, M., HANDJISKI, B. & PAUS, R. 1997. Hair Growth Modulation by Topical Immunophilin Ligands. *American Journal of Pathology,* 150**,** 1433-1441.

MAURER, M., PETERS, E. M. J., BOTCHKAREV, V. A. & PAUS, R. 1998. Intact hair follicle innervation is not essential for anagen induction and development. *Archives of Dermatological Research,* 290**,** 574–578.

MCCORMICK, J. A., FENG, Y., DAWSON, K., BEHNE, M. J., YU, B., WANG, J., WYATT, A. W., HENKE, G., GRAHAMMER, F., MAURO, T. M., LANG, F. & PEARCE, D. 2004. Targeted Disruption of the Protein Kinase SGK3/CISK Impairs Postnatal Hair Follicle Development. *Molecular Biology of the Cell,* 15**,** 4278–4288.

MECKLENBURG, L., TOBIN, D. J., CIRLAN, M. V., CRACIUN, C. & PAUS, R. 2005. Premature termination of hair follicle morphogenesis and accelerated hair follicle cycling in Iasi congenital atrichia (fzica) mice points to fuzzy as a key element of hair cycle control. *Experimental Dermatology,* 14**,** 561-70.

MEHLING, A. & FLUHR, J. W. 2006. Chronobiology: Biological Clocks and Rhythms of the Skin. *Skin Pharmacol Physiol,* 19**,** 182-189.

MEYER, B., BAZZI, H., ZIDEK, V., MUSILOVA, A., KURTZ, T. W., NURNBERG, P., PRAVENEC, M. & CHRISTIANO, A. M. 2004. A spontaneous mutation in the desmoglein 4 gene underlies hypotrichosis in a new *lanceolate hair* rat model. *Differentiation,* 72**,** 541–547.

MILLAR, S. E., WILLERT, K., SALINAS, P. C., ROELINK, H., NUSSE, R., SUSSMAN, D. J. & BARSH, G. S. 1999. WNT Signaling in the Control of Hair Growth and Structure. *Developmental Biology,* 207**,** 133–149.

MILLER, B. H., L., M. E., PANDA, S., HAYES, K. R., ZHANG, J., ANDREWS, J. L., ANTOCH, M. P., WALKER, J. R., ESSER, K. A., HOGENESCH, J. B. & TAKAHASHI, J. S. 2007. Circadian and CLOCK-controlled regulation of the mouse transcriptome and cell proliferation. *PNAS,* 104**,** 3342-3347.

MILLER, B. H., OLSON, S. L., TUREK, F. W., LEVINE, J. E., HORTON, T. H. & TAKAHASHI, J. S. 2004. Circadian *Clock* Mutation Disrupts Estrous Cyclicity and Maintenance of Pregnancy. *Current Biology,* 14**,** 1367-1373.

MILNER, Y., SUDNIK, J., FILIPPI, M., KIZOULIS, M., KASHGARIAN, M. & STENN, K. S. 2002. Exogen, Shedding Phase of the Hair Growth Cycle: Characterization of a Mouse Model. *Journal of Investigative Dermatology,* 119**,** 639-644.

MITSUI, S., OHUCHI, A., ADACHI-YAMADA, T., HOTTA, M., TSUBOI, R. & OGAWA, H. 2001. Cyclin-dependent kinase inhibitors, p21waf1/cip1 and p27kip1, are expressed site- and hair cycle-dependently in rat hair follicles. *Journal of Dermatological Science,* 25**,** 164-169.

MOCEK, W. T., RUDNICKI, R. & VOIT, E. O. 2005. Approximation of delays in biochemical systems. *Mathematical Biosciences,* 198**,** 190-216.

MOONEY, J. R. & NAGORCKA, B. N. 1985. Spatial patterns produced by a reaction-diffusion system in primary hair follicles. *Journal of Theoretical Biology,* 115**,** 299-317.

MÜLLER-RÖVER, S., HANDJISKI, B., VAN DER VEEN, C., EICHMÜLLER, S., FOITZIK, K., MCKAY, I. A., STENN, K. S. & PAUS, R. 2001. A Comprehensive Guide for the Accurate Classification of Murine Hair Follicles in Distinct Hair Cycle Stages. *Journal of Investigative Dermatology,* 117**,** 3-15.

NAGORCKA, B. N. & MOONEY, J. R. 1982. The role of a reaction-diffusion system in the formation of hair fibres. *Journal of Theoretical Biology,* 98**,** 575-607.

NAGORCKA, B. N. & MOONEY, J. R. 1985. The role of a reaction-diffusion system in the initiation of primary hair follicles. *Journal of Theoretical Biology,* 114**,** 243-72.

NAITO, A., SATO, T., MATSUMOTO, T., TAKEYAMA, K., YOSHINO, T., KATO, S. & OHDERA, M. 2008. Dihydrotestosterone inhibits murine hair growth via the androgen receptor. *British Journal of Dermatology,* 159**,** 300-305.

NAKAMURA, M., SUNDBERG, J. P. & PAUS, R. 2001. Mutant laboratory mice with abnormalities in hair follicle morphogenesis, cycling, and/or structure: annotated tables. *Experimental Dermatology,* 10**,** 369-390.

NOBLE, D. 2008a. Computational Models of the Heart and Their Use in Assessing the Actions of Drugs. *journal of Pharmacological Sciences,* 107**,** 107-117.

NOBLE, D. 2008b. Prologue: Mind Over Molecule: Activating Biological Demons. *Annals of the New York Academy of Sciences,* 1123**,** xi-xix.

NOWAK, M. A., ANDERSON, R. M., BOERLIJST, M. C., BONHOEFFER, S., MAY, R. M. & MCMICHAEL, A. J. 1996. HIV-1 evolution and disease progression. *Science,* 274**,** 1008–1011.

NUTBROWN, M. & RANDALL, V. A. 1995. Differences Between Connective Tissue-Epithelial Junctions in Human Skin and the Anagen Hair Follicle. *Journal of Investigative Dermatology,* 104.

O'MALLEY, M. A. & DUPRÉ, J. 2005. Fundamental issues in systems biology. *BioEssays,* 27**,** 1270-1276.

O'SHAUGHNESSY, R. F. L., CHRISTIANO, A. M. & JAHODA, C. A. B. 2004. The role of BMP signalling in the control of ID3 expression in the hair follicle. *Experimental Dermatology,* 13**,** 621–629.

OHNEMUS, U., UENALAN, M., INZUNZA, J., GUSTAFSSON, J.-Å. & PAUS, R. 2006. The Hair Follicle as an Estrogen Target and Source. *Endocrine Reviews,* 27**,** 677–706.

OHTANI, N., IMAMURA, Y., YAMAKOSHI, K., HIROTA, F., NAKAYAMA, R., KUBO, Y., ISHIMARU, N., TAKAHASHI, A., HIRAO, A., SHIMIZU, T., MANN, D. J., SAYA, H., HAYASHI, Y., ARASE, S., MATSUMOTO, M., NAKAO, K. & HARA, E. 2007. Visualizing the dynamics of p21Waf1/Cip1 cyclin-dependent kinase inhibitor expression in living animals. *Proceedings of the National Academy of Sciences of the United States of America,* 104**,** 15034–15039.

OKADA, T., ISHII, Y., MASUJIN, K., YASOSHIMA, A., MATSUDA, J., OGURA, A., NAKAYAMA, H., KUNIEDA, T. & DOI, K. 2006. The Critical Roles of

Serum/Glucocorticoid-Regulated Kinase 3 (SGK3) in the Hair Follicle Morphogenesis and Homeostasis. *American Journal of Pathology,* 168**,** 1119-1133.

PANTELEYEV, A. A., JAHODA, C. A. B. & CHRISTIANO, A. M. 2001. Hair follicle predetermination. *Journal of Cell Science,* 114**,** 3419-3431.

PARK, S. Y., KWACK, M. H., CHUNG, E. J., IM, S. U., HAN, I. S., KIM, M. K., KIM, J. C. & SUNG, Y. K. 2007. Establishment of SV40T-transformed human dermal papilla cells and identification of dihydrotestosterone-regulated genes by cDNA microarray. *Journal of Dermatological Science,* 47**,** 201-208.

PAUS, R. 2006. Therapeutic strategies for treating hair loss. *Drug Discovery Today,* 3**,** 101-110.

PAUS, R., BÖTTGE, J.-A., HENZ, B. M. & MAURER, M. 1996. Hair growth control by immunosuppression. *Archives of Dermatological Research,* 288**,** 408-410.

PAUS, R. & COTSARELIS, G. 1999. The Biology of Hair Follicles. *The New England Journal of Medicine,* 341**,** 491-497.

PAUS, R. & FOITZIK, K. 2004. In search of the ''hair cycle clock'': a guided tour. *Differentiation,* 72**,** 489-511.

PAUS, R., FOITZIK, K., WELKER, P., BULFONE-PAUS, S. & EICHMŰLLER, S. 1997. Transforming Growth Factor-β Receptor Type I and Type II Expression During Murine Hair Follicle Development and Cycling. *Journal of Investigative Dermatology,* 109**,** 518-526.

PAUS, R., MULLER-ROVER, S. & BOTCHKAREV, V. A. 1999a. Chronobiology of the hair follicle: hunting the " hair cycle clock". *Journal of Investigative Dermatology. Symposium Proceedings,* 4**,** 338-45.

PAUS, R., MÜLLER-RÖVER, S., VAN DER VEEN, C., MAURER, M., EICHMÜLLER, S., LING, G., HOFMANN, U., FOITZIK, K., MECKLENBURG, L. & HANDJISKI, B. 1999b. A Comprehensive Guide for the Recognition and Classification of Distinct Stages of Hair Follicle Morphogenesis. *Journal of Investigative Dermatology,* 113**,** 523-532.

PAUS, R., STENN, K. S. & LINK, R. E. 1990. Telogen skin contains an inhibitor of hair growth. *British Journal of Dermatology,* 122**,** 777-784.

PENA, J. C., KELEKAR, A., FUCHS, E. V. & THOMPSON, C. B. 1999. Manipulation of outer root sheath survival perturbs the hair growth cycle. *The EMBO Journal,* 18**,** 3596-3603.

PENNING, T. M., JINA, Y., STECKELBROECK, S., LANIŠNIK RIŽNER, T. & LEWIS, M. 2004. Structure–function of human 3α-hydroxysteroid dehydrogenases: genes and proteins. *Molecular and Cellular Endocrinology* 215**,** 63–72.

PERELSON, A. S., ESSUNGER, P., CAO, Y., VESANEN, M., HURLEY, M., SAKSELA, K., MARKOWITZ, M. & HO, D. D. 1997. Decay Characteristics of HIV-1 infected compartments during combination therapy. *Nature,* 387**,** 188-191.

PERELSON, A. S., NEUMANN, A. U., MARKOWITZ, M., LEONARD, J. M. & HO, D. D. 1996. HIV-1 Dynamics in vivo: Virion Clearance Rate, Infected Cell Life-Span, and Viral Generation Time. *Science,* 271**,** 1582–1586.

PETERS, E. M. J., LIOTIRI, S., BODO, E., HAGEN, E., BIRO, T., ARCK, P. C. & PAUS, R. 2007. Probing the Effects of Stress Mediators on the Human Hair Follicle.

Substance P Holds Central Position. *American Journal of Pathology,* 171**,** 1872-1886.
PETERS, E. M. J., STIEGLITZ, M. G., LIEZMAN, C., OVERALL, R. W., NAKAMURA, M., HAGEN, E., KLAPP, B. F., ARCK, P. & PAUS, R. 2006. p75 Neurotrophin Receptor-Mediated Signaling Promotes Human Hair Follicle Regression (Catagen). *American Journal of Pathology,* 168**,** 221-234.
PHILPOTT, M. 1999. In vitro maintenance of isolated hair follicles: current status and future development. *Experimental Dermatology,* 8**,** 317-9.
PHILPOTT, M. P., GREEN, M. R. & KEALEY, T. 1990. Human hair growth in vitro. *J Cell Sci,* 97**,** 463-471.
PHILPOTT, M. P., SANDERS, D., WESTGATE, G. E. & KEALEY, T. 1994a. Human hair growth in vitro: a model for the study of hair follicle biology. *Journal of Dermatological Science,* 7 Suppl**,** S55-72.
PHILPOTT, M. P., SANDERS, D. A. & KEALEY, T. 1994b. Effects of insulin and insulin-like growth factors on cultured human hair follicles: IGF-I at physiologic concentrations is an important regulator of hair follicle growth in vitro. *Journal of Investigative Dermatology,* 102**,** 857-61.
PHILPOTT, M. P., SANDERS, D. A. & KEALEY, T. 1996. Whole hair follicle culture. *Dermatologic Clinics,* 14**,** 595-607.
PLIKUS, M. V., BAKER, R. E., CHEN, C.-C., FARE, C., DE LA CRUZ, D., ANDL, T., MAINI, P. K., MILLAR, S. E., WIDELITZ, R. B. & CHUONG, C.-M. 2011. Self-Organizing and Stochastic Behaviors During the Regeneration of Hair Stem Cells. *Science,* 332**,** 586-589.
PLIKUS, M. V., MAYER, J. A., DE LA CRUZ, D., BAKER, R. E., MAINI, P. K., MAXSON, R. & CHUONG, C. M. 2008. Cyclic dermal BMP signalling regulates stem cell activation during hair regeneration. *Nature,* 451**,** 340-4.
PLIKUS, M. V., WIDELITZ, R. B., MAXSON, R. & CHUONG, C. M. 2009. Analyses of regenerative wave patterns in adult hair follicle populations reveal macro-environmental regulation of stem cell activity. *The International Journal of Developmental Biology,* 53**,** 857-868.
PORTER, R. M. 2006. The New Keratin Nomenclature. *Journal of Investigative Dermatolology,* 126**,** 2366–2368.
RAMOT, Y., BÍR'O, T., TIEDE, S., T'OTH, B. I., LANGAN, E. A., SUGAWARA, K., FOITZIK, K., INGBER, A., GOFFIN, V., LANGBEIN, L. & PAUS, R. 2010. Prolactin—a novel neuroendocrine regulator of human keratin expression *in situ*. *The FASEB Journal,* 24**,** 1768–1779.
RAMOT, Y., TIEDE, S., B'IR'O, T., ABU BAKAR, M. H., SUGAWARA, K., PHILPOTT, M. P., HARRISON, W., PIETILÄ, M. & PAUS, R. 2011. Spermidine Promotes Human Hair Growth and Is a Novel Modulator of Human Epithelial Stem Cell Functions. *PLoS One,* 6**,** e22564.
RANDALL, V. A., SUNDBERG, J. P. & PHILPOTT, M. P. 2003. Animal and in vitro models for the study of hair follicles. *Journal of Investigative Dermatology. Symposium Proceedings,* 8**,** 39-45.
REDDY, S. T., ANDL, T., LU, M.-M., MORRISEY, E. E. & MILLAR, S. E. 2004. Expression of *Frizzled* Genes in Developing and Postnatal Hair Follicles. *Journal of Investigative Dermatology,* 123**,** 275 –282.

RENDL, M., LEWIS, L. & FUCHS, E. 2005. Molecular Dissection of Mesenchymal–Epithelial Interactions in the Hair Follicle. *PLOS Biology,* 3**,** e331.

RENDL, M., POLAK, L. & FUCHS, E. 2008. BMP signaling in dermal papilla cells is required for their hair follicle-inductive properties. *Genes and Development,* 22**,** 543-557.

REPPERT, S. M. & WEAVER, D. R. 2002. Coordination of circadian timing in mammals. *Nature,* 418**,** 935-941.

RIEDEL-BAIMA, B. & RIEDEL, A. 2008. Female pattern hair loss may be triggered by low oestrogen to androgen ratio. *Endocrine Regulations,* 42**,** 13-16.

ROBINSON, M., REYNOLDS, A. J. & JAHODA, C. A. 1997. Hair cycle stage of the mouse vibrissa follicle determines subsequent fiber growth and follicle behavior in vitro. *J Invest Dermatol,* 108**,** 495-500.

ROGERS, G. & KOIKE, K. 2009. Laser capture microdissection in a study of expression of structural proteins in the cuticle cells of human hair. *Experimental Dermatology,* 18**,** 541-547.

ROGERS, G. E. & HYND, P. I. 2001. Animal Models and Culture Methods in the Study of Hair Growth. *Clinics in Dermatology,* 2001**,** 105-119.

ROGERS, M. A., LANGBEIN, L., WUNDER, S. P., WINTER, H. & SCHWEIZER, J. 2006. Human Hair Keratin-Associated Proteins (KAPs). *International Review of Cytology,* 251**,** 209-263.

ROSENQUIST, T. A. & MARTIN, G. R. 1996. Fibroblast growth factor signalling in the hair growth cycle: expression of the fibroblast growth factor receptor and ligand genes in the murine hair follicle. *Developmental Dynamics,* 205**,** 379-86.

RUDMAN, S. M., PHILPOTT, M. P., THOMAS, G. A. & KEALEY, T. 1997. The role of IGF-I in human skin and its appendages: morphogen as well as mitogen? *Journal of Investigative Dermatology,* 109**,** 770-7.

SAITOH, M., UZUKA, M. & SAKAMOTO, M. 1970. Human hair cycle. *Journal of Investigative Dermatology,* 54**,** 65-81.

SANDERS, D. A., PHILPOTT, M. P., NICOLLE, F. V. & KEALEY, T. 1994. The isolation and maintenance of the human pilosebaceous unit. *British Journal of Dermatology,* 131**,** 166-76.

SAUER, U., HEINEMANN, M. & ZAMBONI, N. 2007. Getting Closer to the Whole Picture. *Science,* 316**,** 550-551.

SCHADT, E. E. 2009. Molecular networks as sensors and drivers of common human diseases. *Nature,* 461**,** 218-223.

SCHAFFER, J. V., BAZZI, H., VITEBSKY, A., WITKIEWICZ, A., KOVICH, O. I., KAMINO, H., SHAPIRO, L. S., AMIN, S. P., ORLOW, S. J. & CHRISTIANO, A. M. 2006. Mutations in the Desmoglein 4 Gene Underlie Localized Autosomal Recessive Hypotrichosis with Monilethrix Hairs and Congenital Scalp Erosions. *Journal of Investigative Dermatology,* 126**,** 1286–1291.

SCHLAKE, T., BEIBEL, M., WEGER, N. & BOEHM, T. 2004. Major shifts in genomic activity accompany progression through different stages of the hair cycle. *Gene Expression Patterns,* 4**,** 141-152.

SCHMIDT-ULLRICH, R. & PAUS, R. 2005. Molecular principles of hair follicle induction and morphogenesis. *Bioessays,* 27**,** 247–261.

SCHNEIDER, M. R., SCHMIDT-ULLRICH, R. & PAUS, R. 2009. The Hair Follicle as a Dynamic Miniorgan. *Current Biology,* 19**,** R132-R142.

SCHNELL, S., GRIMA, R. & MAINI, P. K. 2007. Multiscale Modeling in Biology. *American Scientist,* 95**,** 134-142.

SCHWEIZER, J., LANGBEIN, L., ROGERS, M. A. & WINTER, H. 2007. Hair follicle-specific keratins and their diseases. *Experimental Cell Research,* 313**,** 2010-2020.

SHAROV, A. A., SHAROVA, T. Y., MARDARYEV, A. N., TOMMASI DI VIGNANO, A., ATOYAN, R., WEINER, L., YANG, S., BRISSETTE, J. L., DOTTO, G. P. & BOTCHKAREV, V. A. 2006. Bone morphogenetic protein signaling regulates the size of hair follicles and modulates the expression of cell cycle-associated genes. *Proceedings of the National Academy of Sciences of the United States of America,* 103**,** 18166–18171.

SHEARMAN, L. P., SRIAM, S., WEAVER, D. R., MAYWOOD, E. S., CHAVES, I., ZHENG, B., KUMA, K., LEE, C. C., VAN DER HORST, G. T. J., HASTINGS, M. H. & M., R. S. 2000. Interacting Molecular Loops in the Mammalian Circadian Clock. *Science,* 288**,** 1013-1019.

SHIMAOKA, S., TSUBOI, R., JINDO, T., IMAI, R., TAKAMORI, K., RUBIN, J. S. & OGAWA, H. 1995. Hepatocyte growth factor/scatter factor expressed in follicular papilla cells stimulates human hair growth in vitro. *Journal of Cellular Physiology,* 165**,** 333-8.

SICK, S., REINKER, S., TIMMER, J. & SCHLAKE, T. 2006. WNT and DKK determine hair follicle spacing through a reaction-diffusion mechanism.[see comment]. *Science,* 314**,** 1447-50.

SLOMINSKI, A., WORTSMAN, J., PLONKA, P. M., SCHALLREUTER, K. U., PAUS, R. & TOBIN, D. J. 2005. Hair Follicle Pigmentation. *Journal of Investigative Dermatology. Symposium Proceedings,* 124**,** 13-21.

SOMA, T., OGO, M., SUZUKI, J., TAKAHASHI, T. & HIBINO, T. 1998. Analysis of apoptotic cell death in human hair follicles in vivo and in vitro. *Journal of Investigative Dermatology,* 111**,** 948-54.

SOMA, T., TSUJI, Y. & HIBINO, T. 2002. Involvement of Transforming Growth Factor-β2 in Catagen Induction During the Human Hair Cycle. *Journal of Investigative Dermatology,* 118**,** 993-997.

SPÖRL, F., SCHELLENBERG, K., BLATT, T., WENCK, H., WITTERN, K.-P., SCHRADER, A. & KRAMER, A. 2011. A Circadian Clock in HaCaT Keratinocytes. *Journal of Investigative Dermatology,* 131**,** 338-348.

STARK, J., ANDL, T. & MILLAR, S. E. 2007. Hairy Math: Insights into Hair-Follicle Spacing and Orientation. *Cell,* 128**,** 17-20.

STEINER, A. Z., CHANG, L., JI, Q., OOKHTENS, M., STOLZ, A., PAULSON, R. J. & STANCZYK, F. Z. 2008. 3α-Hydroxysteroid Dehydrogenase Type III Deficiency: A Novel Mechanism for Hirsutism. *The Journal of Clinical Endocrinology and Metabolism,* 93**,** 1298–1303.

STEINERT, P. M., PARRY, D. A. D. & MAREKOV, L. N. 2003. Trichohyalin Mechanically Strengthens the Hair Follicle. *The Journal of Biological Chemistry,* 278**,** 41409-41419.

STELNICKI, E. J., KÖMÜVES, L. G., HOLMES, D., CLAVIN, W., HARRISON, M. R., ADZICK, N. S. & LARGMAN, C. 1997. The human homeobox genes MSX-1,

MSX-2, and MOX-1 are differentially expressed in the dermis and epidermis in fetal and adult skin. *Differentiation,* 62**,** 33–41.
STENN, K. S., NIXON, A. J., JAHODA, C. A. B., MCKAY, I. A. & PAUS, R. 1999. What controls hair follicle cycling? *Experimental Dermatology,* 8**,** 229-236.
STENN, K. S. & PAUS, R. 2001. Controls of Hair Follicle Cycling. *Physiological Reviews,* 81**,** 449-494.
STENN, K. S., PROUTY, S. M. & SEIBERG, M. 1994. Molecules of the cycling hair follicle - a tabulated review. *Journal of Dermatological Science,* 7 (Suppl)**,** S109-S124.
STROGATZ, S. H. 1994. *Nonlinear dynamics and chaos: With applications to Physics, Biology, Chemistry, and Engineering,* Cambridge, MA, Perseus books publishing.
SUN, T.-T., COTSARELIS, G. & LAVKER, R. M. 1991. Hair Follicular Stem Cells: The Bulge Activation Hypothesis. *Journal of Investigative Dermatology,* 96**,** 77s-78s.
SUNDBERG, J. P., PETERS, E. M. J. & PAUS, R. 2005. Analysis of Hair Follicles in Mutant Laboratory Mice. *Journal of Investigative Dermatology Symposium Proceedings,* 10**,** 264-270.
SUZUKI, N., HIRATA, M. & KONDO, S. 2003. Traveling stripes on the skin of a mutant mouse. *PNAS,* 100**,** 9680-9685.
SUZUKI, S., OTA, Y., OZAWA, K. & IMAMURA, T. 2000. Dual-mode regulation of hair growth cycle by two Fgf-5 gene products. *Journal of Investigative Dermatology,* 114**,** 456-63.
TAKAHASHI, J. S., HONG, H.-K., KO, C. H. & MCDEARMON, E. L. 2008. The genetics of mammalian circadian order and disorder: implications for physiology and disease. *Nature Reviews,* 9**,** 764-775.
TANIOKA, M., YAMADA, H., DOI, M., BANDO, H., YAMAGUCHI, Y., NISHIGORI, C. & OKAMURA, H. 2009. Molecular Clocks in Mouse Skin. *Journal of Investigative Dermatology,* 129**,** 1225-1232.
TAYLOR, G., LEHRER, M. S., JENSEN, P. J., SUN, T.-T. & LAVKER, R. M. 2000. Involvement of Follicular Stem Cells in Forming Not Only the Follicle but Also the Epidermis. *Cell,* 102**,** 451-461.
THIBAUT, S., COLLIN, C., LANGBEIN, L., SCHWEIZER, J., GAUTIER, B. & BERNARD, B. A. 2003. Hair keratin pattern in human hair follicles grown in vitro. *Experimental Dermatology,* 12**,** 160-164.
TIEDE, S., KLOEPPER, J. E., WHITING, D. A. & PAUS, R. 2007. The 'follicular trochanter': an epithelial compartment of the human hair follicle bulge region in need of further characterisation. *British Journal of Dermatology,* 157**,** 1013-1016.
TIEDE, S., KOOP, N., KLOEPPER, J., FÄSSLER, R. & PAUS, R. 2009. Nonviral in Situ Green Fluorescent Protein Labeling and Culture of Primary, Adult Human Hair Follicle Epithelial Progenitor Cells. *Stem cells,* 27**,** 2793–2803.
TOBIN, D. J. 2011. The cell biology of human hair follicle pigmentation. *Pigment Cell Melanoma Research* 24**,** 75–88.
TOBIN, D. J., GUNIN, A., MAGERL, M., HANDIJSKI, B. & PAUS, R. 2003. Plasticity and cytokinetic dynamics of the hair follicle mesenchyme: implications

for hair growth control. *Journal of Investigative Dermatology,* 120**,** 895-904.

TOBIN, D. J., HAGEN, E., BOTCHKAREV, V. A. & PAUS, R. 1998. Do hair bulb melanocytes undergo apoptosis during hair follicle regression (catagen)? *Journal of Investigative Dermatology,* 111**,** 941-947.

TOBIN, D. J., SLOMINSKI, A., BOTCHKAREV, V. & PAUS, R. 1999. The fate of hair follicle melanocytes during the hair growth cycle. *Journal of Investigative Dermatology. Symposium Proceedings,* 4**,** 323-32.

TÓTH, B. I., GÉCZY, T., GRIGER, Z., ANIKÓ DÓZSA3, SELTMANN, H., KOVÁCS, L., NAGY, L., ZOUBOULIS, C. C., PAUS, R. & BÍRO, T. 2009. Transient Receptor Potential Vanilloid-1 Signaling as a Regulator of Human Sebocyte Biology. *Journal of Investigative Dermatology,* 129**,** 329–339.

TROTTER, M. 1924. The life cycle of hair in selected regions of the human body. *Am. J. Phys. Anthrop.,* 7**,** 427-437.

UMEDA-IKAWA, A., SHIMOKAWA, I. & DOI, K. 2009. Time-Course Expression Profiles of Hair Cycle-Associated Genes in Male Mini Rats after Depilation of Telogen-Phase Hairs. *International Journal of Molecular Sciences,* 10**,** 1967-1977.

VAN BEEK, N., BODÓ, E., KROMMINGA, A., GÁSPÁR, E., MEYER, K., ZMIJEWSKI, M. A., SLOMINSKI, A., WENZEL, B. E. & PAUS, R. 2008. Thyroid Hormones Directly Alter Human Hair Follicle Functions: Anagen Prolongation and Stimulation of Both Hair Matrix Keratinocyte Proliferation and Hair Pigmentation. *J Clin Endocrinol Metab,* 93**,** 4381–4388.

VANAG, V. K. & EPSTEIN, I. R. 2009. Pattern formation mechanisms in reaction-diffusion systems. *International Journal of Developmental Biology,* 53**,** 673-681.

WAGHMARE, S. K., BANSAL, R., LEE, J., ZHANG, Y. V., MCDERMITT, D. J. & TUMBA, T. 2008. Quantitative proliferation dynamics and random chromosome segregation of hair follicle stem cells. *The EMBO Journal,* 27**,** 1309–1320.

WANG, K. X. & DENHARDT, D. T. 2008. Osteopontin: Role in immune regulation and stress responses. *Cytokine & Growth Factor Reviews,* 19**,** 333–345.

WANG, Y., YANG, S., WU, L. & TU, P. 2009. Topical tacrolimus suppresses the expression of vascular endothelial growth factor and insulin-like growth factor-1 in late anagen. *Clinical and Experimental Dermatology,* 34**,** e937-e940.

WESTERHOFF, H. V. & PALSSON, B. O. 2004. The evolution of molecular biology into systems biology. *Nature,* 22**,** 1249-1252.

WHITE, C. A. & SALAMONSEN, L. A. 2005. A guide to issues in microarray analysis: application to endometrial biology. *Reproduction,* 130**,** 1-13.

WHITE, G. M. & COX, N. H. 2006. *Diseases of the skin,* Philadelphia, Elsevier, Mosby.

WHITING, D. A. 2004. ***The Structure of the Human Hair Follicle.*** *Light Microscopy of Vertical and Horizontal Sections of Scalp Biopsies,* Fairfield, Canfield Publishing.

WHITTINGTON, M. A., TRAUB, R. D., KOPELL, N., ERMENTROUT, B. & BUHL, E. H. 2000. Inhibition-based rhythms: experimental and mathematical

observations on network dynamics. *International Journal of Psychophysiology,* 38**,** 315-336.
WIDELITZ, R. B., BAKER, R. E., PLIKUS, M., LIN, C.-M., MAINI, P. K., PAUS, R. & CHUONG, C. M. 2006. Distinct Mechanisms Underlie Pattern Formation in the Skin and Skin Appendages. *Birth Defects Research,* 78**,** 280–291.
WILEY, H. S., SHVARTSMAN, S. Y. & LAUFFENBURGER, D. A. 2003. Computational modeling of the EGF-receptor system: a paradigm for systems biology. *Trends in Cell Biology,* 13**,** 43-50.
WILSON, C., COTSARELIS, G., WEI, Z.-G., FRYER, E., MARGOLIS-FRYER, J., OSTEAD, M., TOKAREK, R., TUNG-TIEN, S. & LAVKER, R. M. 1994. Cells within the bulge region of mouse hair follicle transiently proliferate during early anagen: heterogeneity and functional differences of various hair cycles. *Differentiation,* 55**,** 127-136.
WU, Z., IRIZARRY, R. A., GENTLEMAN, R., MURILLO, F. M. & SPENCER, F. 2004. A Model Based Background Adjustment for Oligonucleotide Expression Arrays. *Johns Hopkins University Department of Biostatistics Working Papers* [Online]. Available: http://www.bepress.com/jhubiostat/paper1.
YANG, C.-C. & COTSARELIS, G. 2010. Review of hair follicle dermal cells. *Journal of Dermatological Science,* 57**,** 2–11.
YANG, L., YAMASAKI, K., SHIRAKATA, Y., DAI, X., TOKUMARU, S., YAHATA, Y., TOHYAMA, M., HANAKAWA, Y., SAYAMA, K. & HASHIMOTO, K. 2006. Bone morphogenetic protein-2 modulates Wnt and frizzled expression and enhances the canonical pathway of Wnt signaling in normal keratinocytes. *Journal of Dermatological Science,* 42**,** 111-119.
YANG, X., WOOD, P. A., ANSELL, C. M., QUITON, D. F. T., OH, E.-Y., DU-QUITON, J. & HRUSHESKY, W. J. M. 2009. The circadian clock gene Per1 supresses cancer cell proliferation and tumor growth at specific times of day. *Chronobiology International,* 26**,** 1323-1339.
YU, B. D., MUKHOPADHYAY, A. & WONG, C. 2008. Skin and hair: models for exploring organ regeneration. *Human Molecular Genetics,* 17**,** R54-9.
YU, D.-W., YANG, T., SONODA, T., GONG, Y., CAO, Q., GAFFNEY, K., JENSEN, P. J., FREEDBERG, I. M., LAVKER, R. M. & SUN, T.-T. 2001. Osteopontin Gene is Expressed in the Dermal Papilla of Pelage Follicles in a Hair-Cycle-Dependent Manner. *Journal of Investigative Dermatology,* 117**,** 1554-1558.
ZANELLO, S. B., JACKSON, D. M. & HOLICK, M. F. 2000. Expression of the Circadian Clock Genes *clock* and *period1* in Human Skin. *The Journal of Investigative Dermatology,* 115**,** 757-760.
ZHANG, J., HE, X. C., TONG, W.-G., JOHNSON, T., WIEDEMANN, L. M., MISHINA, Y., FENG, J. Q. & LI, L. 2006. Bone Morphogenetic Protein Signaling Inhibits Hair Follicle Anagen Induction by Restricting Epithelial Stem/Progenitor Cell Activation and Expansion. *Stem Cells,* 24**,** 2826–2839.
ZHANG, Y. V., CHEONG, J., CIAPURIN, N., MCDERMITT, D. J. & TUMBAR, T. 2009. Distinct Self-Renewal and Differentiation Phases in the Niche of Infrequently Dividing Hair Follicle Stem Cells. *Cell Stem Cell,* 5**,** 267-278.
ZHANG, Y. V., WHITE, B. S., SHALLOWAY, D. I. & TUMBAR, T. 2010. Stem cell dynamics in mouse hair follicles. *Cell Cycle,* 9**,** 1504-1510.

ZIMMERMAN, L. B., JESÚS-ESCOBAR, J. M. D. & HARLAND, R. M. 1996. The Spemann Organizer Signal noggin Binds and Inactivates Bone Morphogenetic Protein 4. *Cell,* 86**,** 599-606.

ZOUBOULIS, C. C., CHEN, W. C., THORNTON, M. J., QIN, K. & ROSENFIELD, R. 2007. Sexual Hormones in Human Skin. *Hormone and metabolic research,* 39**,** 85-95.

11 APPENDIX

APPENDIX A FRONT PAGE REPRINT OF THE CYCLING HAIR FOLLICLE AS AN IDEAL SYSTEMS BIOLOGY RESEARCH MODEL

DOI:10.1111/j.1600-0625.2010.01114.x
www.blackwellpublishing.com/EXD

Viewpoint

The cycling hair follicle as an ideal systems biology research model

Yusur Al-Nuaimi[1,2], Gerold Baier[1], Rachel E. B. Watson[2], Cheng-Ming Chuong[3] and Ralf Paus[2,4]

[1]Doctoral Training Centre in Integrative Systems Biology, Manchester Interdisciplinary Biocentre, University of Manchester, Manchester, UK;
[2]Epithelial Sciences, School of Translational Medicine, Manchester Academic Health Sciences Centre, University of Manchester, Manchester, UK;
[3]Department of Pathology, Keck School of Medicine, University of Southern California, Los Angeles, USA;
[4]Department of Dermatology, University of Lübeck, Lübeck, Germany
Correspondence: Ralf Paus, University Hospital Schleswig-Holstein, Campus Lübeck, Department of Dermatology, Lübeck 23538, Germany, Tel.: +49 451 500 2543, Fax: +49 451 500 6595, e-mail: ralf.paus@uk-sh.de

Accepted for publication 23 March 2010

Abstract: In the postgenomic era, systems biology has rapidly emerged as an exciting field predicted to enhance the molecular understanding of complex biological systems by the use of quantitative experimental and mathematical approaches. Systems biology studies how the components of a biological system (e.g. genes, transcripts, proteins, metabolites) interact to bring about defined biological function or dysfunction. Living systems may be divided into five dimensions of complexity: (i) molecular; (ii) structural; (iii) temporal; (iv) abstraction and emergence; and (v) algorithmic. Understanding the details of these dimensions in living systems is the challenge that systems biology aims to address. Here, we argue that the hair follicle (HF), one of the signature features of mammals, is a perfect and clinically relevant model for systems biology research. The HF represents a stem cell-rich, essentially autonomous mini-organ, whose cyclic transformations follow a hypothetical intrafollicular "hair cycle clock" (HCC). This prototypic neuroectodermal-mesodermal interaction system, at the cross-roads of systems and chronobiology, encompasses various levels of complexity as it is subject to both intrafollicular and extrafollicular inputs (e.g. intracutaneous timing mechanisms with neural and systemic stimuli). Exploring how the cycling HF addresses the five dimensions of living systems, we argue that a systems biology approach to the study of hair growth and cycling, in man and mice, has great translational medicine potential. Namely, the easily accessible human HF invites preclinical and clinical testing of novel hypotheses generated with this approach.

Key words: anagen – BMP – chronobiology – clock genes – hair cycle – telogen – WNT

Please cite this paper as: The cycling hair follicle as an ideal systems biology research model. Experimental Dermatology 2010; **19**: 707–713.

Introduction

"*The problem of biology is not to stand aghast at the complexity but to conquer it*" *Sidney Brenner, Nobel Laureate* (1)

Systems biology is a fast-evolving life sciences field that aims to establish how the components of a living system combine to cause function (2,3). Biological systems can be divided into five levels of complexity: (i) molecular; (ii) structural; (iii) temporal; (iv) abstraction and emergence; and (v) algorithmic (Table S1) (4).

In the past, cell cultures (particularly yeast) were often used in systems biology research to handle the complexity of living systems (2,5–8). These models are far removed from the reality of mammalian organisms. Identifying mammalian models that are sufficiently complex to encompass these five dimensions, and approach physiological relevance is an important challenge for systems biology (2,9).

The hair follicle (HF) consists of multiple different cell populations of neural crest, ectodermal or mesodermal origin, which are distinct in their location, function and gene and protein expression characteristics (10–13). Additionally, the HF is a uniquely dynamic mini-organ that undergoes continuous cycling throughout adult life during which elements of its own morphogenesis are recapitulated (11,14) (Fig. 1). This transformation process arises under the dictates of an enigmatic oscillator system [the hair cycle clock (HCC)] (12,15,16). Hair growth disorders can be attributed, at large, to changes in the normal dynamic behaviour of the HF (12,13,15,17,18). Common hair diseases such as alopecia areata, telogen effluvium, hirsutism and hypertrichosis remain major, unsolved medical problems that call for new approaches in developing effective remedies. The HF is an attractive research model as hair growth, cycling and colour are of profound interest to biological and medical researchers, and a vast industry that caters to individuals who wish to manipulate these parame-

APPENDIX B REPRINT METHODS IN HAIR RESEARCH: HOW TO OBJECTIVELY DISTINGUISH BETWEEN ANAGEN AND CATAGEN IN HUMAN HAIR FOLLICLE ORGAN CULTURE

DOI:10.1111/j.1600-0625.2009.00939.x
www.blackwellpublishing.com/EXD

Methods in hair research: how to objectively distinguish between anagen and catagen in human hair follicle organ culture

Jennifer Elisabeth Kloepper[1]*, Koji Sugawara[1]*, Yusur Al-Nuaimi[2], Erzsébet Gáspár[1], Nina van Beek[1] and Ralf Paus[1,2]

[1]Department of Dermatology, Allergology and Venerology, University of Luebeck, Luebeck, Germany;
[2]School of Translational Medicine, University of Manchester, Manchester, UK
Correspondence: R. Paus, Department of Dermatology, Allergology and Venerology, University of Luebeck, Luebeck, Germany,
Tel.: +49 (0)451 500-2543, Fax: +49 (0)451 500-5092, e-mail: ralf.paus@uk-sh.de
**These authors contributed equally to this work.*

Accepted for publication 5 June 2009

Abstract: The organ culture of human scalp hair follicles (HFs) is the best currently available assay for hair research in the human system. In order to determine the hair growth-modulatory effects of agents in this assay, one critical read-out parameter is the assessment of whether the test agent has prolonged anagen duration or induced catagen *in vitro*. However, objective criteria to distinguish between anagen VI HFs and early catagen in human HF organ culture, two hair cycle stages with a deceptively similar morphology, remain to be established. Here, we develop, document and test an objective classification system that allows to distinguish between anagen VI and early catagen in organ-cultured human HFs, using both qualitative and quantitative parameters that can be generated by light microscopy or immunofluorescence. Seven qualitative classification criteria are defined that are based on assessing the morphology of the hair matrix, the dermal papilla and the distribution of pigmentary markers (melanin, gp100). These are complemented by ten quantitative parameters. We have tested this classification system by employing the clinically used topical hair growth inhibitor, eflornithine, and show that eflornithine indeed produces the expected premature catagen induction, as identified by the novel classification criteria reported here. Therefore, this classification system offers a standardized, objective and reproducible new experimental method to reliably distinguish between human anagen VI and early catagen HFs in organ culture.

Key words: classification – eflornithine – gp100 – hair follicle cycle – melanin – Philpott assay

Please cite this paper as: Methods in hair research: how to objectively distinguish between anagen and catagen in human hair follicle organ culture. Experimental Dermatology 2010; 19: 305–312.

Introduction

Hair follicles (HFs) undergo cycles of organ transformation, in which stages of rapid growth and hair shaft formation (anagen) alternate with stages of apoptosis-driven HF regression (catagen) and relative HF quiescence (telogen), (1–4). In basic and applied human hair research, the serum-free organ-culture of microdissected normal human scalp HFs (anagen VI), which was pioneered by Philpott et al. (5), has become the most important experimental tool for preclinical hair research. This method has been employed by numerous laboratories world-wide (6–10) and has allowed major progress in our understanding of various aspects of human HF biology.

Given the clinical importance of the anagen–catagen transformation for human hair growth disorders (1,4), one crucial parameter to be assessed, when this assay is employed, is to determine whether the assayed test agent prolongs the duration of anagen VI or promotes catagen development, compared to appropriate vehicle controls. In the former case, the test agent can credibly be claimed to be a candidate hair growth promoter, while in the latter case it becomes a convincing candidate inhibitor of human hair growth. The ability to accurately and sensitively recognize the anagen-to-catagen transformation of HFs *in vitro*, therefore, is a vital methodological challenge one faces when employing human HF organ culture.

Numerous potent anagen promoters and catagen inducers have been tested and identified in this manner in many different laboratories, using human HF organ culture (11–14). For example, hepatocyte growth factor (HGF) has been found to promote hair shaft elongation of cultured human HFs (8,9) whereas testosterone (15) and oestrogen (15) were found to inhibit hair growth *in vitro*. Epidermal

growth factor (EGF) (16) and transforming growth factor-beta2 (TGF-β2) (6,7) have an inhibitory effect on cultured human HFs as well. Importantly, Philpott et al. showed that insulin, insulin-like growth factor I (IGF-I) and IGF-II prevent the entry of human HFs *in vitro* into a catagen-like state (17).

Catagen is the transitional phase and a process of bulbar involution that immediately follows anagen VI. Morphological signs of catagen development are rapid terminal differentiation of keratinocytes and apoptosis within the regressing hair bulb (1–3,6,10,16). With the onset of catagen, melanin production stops (18–20), and the proximal portion of the hair shaft becomes club-shaped. However, organ-cultured human HFs routinely do not show the complete, classical sequence of catagen transformation events seen in scalp HFs *in vivo*. Also, catagen transition *in vitro* develops much faster, and sooner or later is overshaddowed by HF degeneration before catagen transformation has been completed (6,16,17).

Since there is little published literature on how to reliably distinguish a human anagen VI HF from one that is in early catagen (i.e. catagen I–IV), previously published HF organ culture studies were forced to rely on drawing parallels to the existing, well-defined recognition and classification criteria for identifying the various stages of murine HF cycling *in vivo* (21) and to draw pointers from the much more limited information available on the morphological characteristics of human catagen HFs (22,23). Thus, investigators have relied on personal experience to ensure that the assignment of an organ-cultured HF to a distinct hair cycle stage was really accurate and no standardized or objective system for doing so existed. However, distinguishing an early catagen HF in culture from an anagen VI HF, which can look very similar under the microscope, can be quite challenging.

To address this significant methodological shortcoming in basic and applied human hair research, we have attempted in this *Methods paper* to develop a standardized, objective and reproducible system for human HF classification in organ culture. For this purpose, we have defined objective qualitative and quantitative criteria (see Table 1) whose systematic application allows one to distinguish

Table 1. Qualitative morphological and quantitative morphometric criteria to distinguish between early catagen and anagen VI hair follicles

Criterion	Compartment	Marker	Anagen VI	Early catagen	Figure
Qualitative morphological criteria					
1	Entire hair bulb	Hair matrix, Dermal papilla, Melanin content	Larger volume, More onion-shaped, Maximal melanin content	Thinner, Often more oval, Reduced melanin content	1A
2	Epithelial	Hair matrix	Larger volume, thicker diameter	Thinner, more stretched	1B, I
3	Epithelial	Proximal hair matrix	More closed	More open	1B, II
4	Mesenchymal	Dermal papilla stalk	Loose	Densely packed	1C, I
5	Mesenchymal	Dermal papilla shape	More onion-shaped	Often more oval	1C, II
6	Pigmentary	Melanin content and distribution	Maximal, higher melanin content in central hair matrix	Reduced, lower melanin content in central hair matrix	1D, I
7	Pigmentary	gp100+ cells	More evenly distributed, reaching below Auber's line	Maximal number of cells located in precortical matrix	1D, II
Quantitative morphometric criteria					
1	Epithelial	DAPI+ cells below Auber's line	Significantly more DAPI+ cells	Significantly less DAPI+ cells	2A
2	Epithelial	% of Ki-67+ cells below Auber's line	Significantly higher % of Ki-67+ cells	Significantly lower % of Ki-67+ cells	2B
3	Epithelial	% of TUNEL+ cells below Auber's line	Significantly lower % of TUNEL+ cells	Significantly higher % of TUNEL+ cells	2C
4	Mesenchymal	Dermal papilla stalk fibroblasts	Significantly less fibroblasts	Significantly more fibroblasts	2D
5	Mesenchymal	TUNEL+ cells in dermal papilla stalk fibroblasts	Less TUNEL+ cells in dermal papilla stalk fibroblasts	More TUNEL+ cells in dermal papilla stalk fibroblasts	2E
6	Mesenchymal	TUNEL+ cells in dermal papilla	Significantly less TUNEL+ cells	Significantly more TUNEL+ cells	2F
7	Pigmentary	gp100+ cells around the dermal papilla	Significantly more gp100+ cells	Significantly less gp100+ cells	3A
8	Pigmentary	gp100 immunoreactivity around the dermal papilla	Significantly more gp100 immunoreactivity	Significantly less gp100 immunoreactivity	3B
9	Pigmentary	Tyrosinase activity-associated immunoreactivity	More tyrosinase activity-associated immunoreactivity	Less tyrosinase activity-associated immunoreactivity	3C
10	Pigmentary	Melanin content	Significantly higher	Significantly lower	3D

Both qualitative and quantitative parameters are used to distinguish between anagen VI and early catagen in organ-cultured human hair follicles. Four qualitative criteria are based on assessing the morphology of the hair matrix, the dermal papilla and the distribution of pigmentary markers. These criteria are complemented by ten quantitative criteria assessing morphometric parameters of cell number, proliferation, apoptosis and hair follicle pigmentary markers.

human anagen VI from early catagen IV HFs. Availability of such a recognition and classification system is hoped to improve assay sensitivity, accuracy and reproducibility.

Materials and methods

Tissue collection and HF culture

Temporal and occipital non-inflamed human scalp skin was obtained from females undergoing face-lift surgery with informed consent. Anagen VI HFs were isolated according to the Philpott method (5,24,25) and Helsinki guidelines. Isolated HFs were maintained in a 24-well plate with 500 μl serum free Williams E medium (Biochrom, Cambridge, UK) supplemented with 2 mmol/l L-glutamine (Invitrogen, Paisley, UK), 10 ng/ml hydrocortisone (Sigma-Aldrich, Munich, Germany), 10 μg/ml insulin (Sigma-Aldrich) and 1% antibiotic/antimycotic mixture (Gibco, Karlsruhe, Germany). HFs were checked daily. Anagen HFs and HFs that had already entered the regressing stage were immediately embedded in Shandon Cryomatrix (Pittsburgh, PA, USA) and snap frozen in liquid nitrogen. Five to seven longitudinal sections of HFs were processed for immunohistological stainings.

In order to test the substance eflornithine (Sigma-Aldrich) HFs were incubated overnight and on day 1 medium was changed and vehicle or test substance was added. Test groups received eflornithine daily (400 mg/l, 1000 mg/l) and the control HFs were treated daily with the same amount of water instead. The culture medium was replaced every other day and the hair shaft length was measured using a Nikon Diaphot inverted binocular microscope (5). After 6 days the HF culture was stopped, HFs were embedded and cut for further procedures.

Histochemistry

For Masson Fontana staining; cryosections were air dried and fixed in ethanol-acetic acid. The sections were washed in tris-buffered saline (TBS) and distilled water several times. Cryosections were treated with ammoniacal silver solution (Fluka, Seelze, Germany) for 40 min at 56°C in the dark. After washing in distilled water, the sections were treated with 5% aqueous sodium thiosulphate (Merck, Darmstadt, Germany) for 1 min. Next, the sections were washed in running tap water for 3 min and were counterstained in 0.5% aqueous neutral red (Sigma). After washing in distilled water, sections were dehydrated and mounted in Eukitt (O. Kindler, Freiburg, Germany).

Immunohistochemistry

To compare proliferation and apoptosis of HFs in the different hair cycle stages double immunolabelling of Ki-67 mouse anti-Ki-67 antiserum (DAKO, Hamburg, Denmark) and TUNEL (ApopTag Fluorescein In Situ Apoptosis detection kit; Millipore, Berlin, Germany) was performed as described previously (26–29).

HF cryosections were first fixed in 1% paraformaldehyde and then in a mixture of ethanol and acetic acid for NKI/beteb (30). Afterwards the sections were presaturated with normal goat serum (DAKO) and incubated with the primary NKI/beteb antibody (mouse anti-NKI/beteb 1:50 in TBS plus 2% normal goat serum; Monosan, Uden, Netherlands) overnight at 4°C. The cryosections were incubated with a secondary rhodamine-labelled goat anti-mouse antibody (1:200 in TBS, Jackson ImmunoResearch, Newmarket, UK) for 45 min at room temperature after a washing step. Counterstaining was performed with DAPI.

HF melanogenesis was also assessed, using the tyramide-based tyrosinase assay, for tyrosinase activity *in situ* as previously described (31). In this procedure, tyrosinase reacts with biotinyl tyramide, causing the substrate to deposit near the enzyme. These biotinylated deposits are then visualized with streptavidin conjugated to a fluorescent dye. This assay is highly specific and serves as a sensitive indicator of pigment cell distribution.

Results

Qualitative morphological criteria

During examination of cultured human HFs under the dissection microscope, if one is lucky, a low-power visualization of HFs provides first pointers whether the HF is still in anagen VI, or has already entered into early catagen (Fig. 1a). More often, however, it is quite challenging to make such a distinction with any certainty. Therefore we have explored and defined qualitative classification criteria to distinguish anagen VI from early catagen [that is catagen stage I–IV in the murine system, according to Müller-Röver et al. (21)]. These criteria are based on; assessing the morphology of the hair matrix (HM) and the dermal papilla (DP), the distribution of melanin, and the expression of the premelanosomal marker gp100 (Nki/beteb) (Table 1).

Rigorous testing in multiple HF organ culture assays consistently revealed organ-cultured anagen VI HFs to display a HM with a larger volume, a more onion-shaped DP and maximal melanin content when compared to early catagen HFs. Early catagen HFs showed a considerably thinner HM, and the shape of the DP underwent discrete changes. However, it was difficult to objectively, accurately, and reproducibly assess these anagen-catagen transformation-associated changes.

In human anagen VI HFs, the HM shows a larger volume with a thicker diameter, compared to early catagen HFs (Fig. 1b, I). At its proximal end, the HM is more closed, as opposed to a wider opened HM in early in regressing HFs (Fig. 1b, II). The overall shape of the HM also changes during the beginning of catagen development:

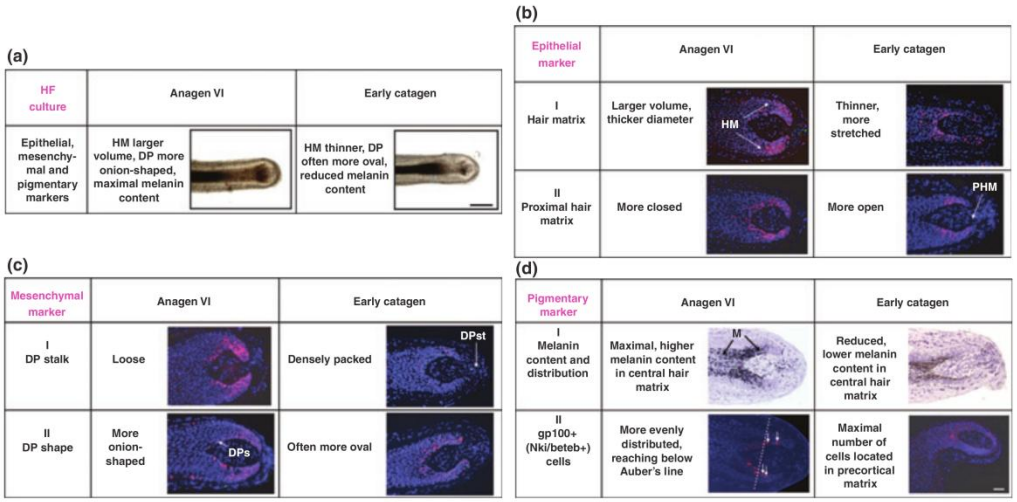

Figure 1. Qualitative morphological criteria to distinguish between anagen VI and early catagen (I–IV). (a) In hair follicle organ culture anagen VI hair follicles show a HM with a larger volume, a dermal papilla which is more onion-shaped and a melanin content which is maximal whereas early catagen hair follicles have a thinner HM, a dermal papilla which is often more oval and reduced melanin content. (b) The hair matrix and its proximal part are epithelial markers which can be used to distinguish between the different hair cycle stages. In anagen VI hair follicles the volume of the hair matrix is larger, the diameter thicker and the proximal part of the hair matrix is more closed when compared to catagen HFs. (c) The dermal papilla stalk and the shape of the dermal papilla are mesenchymal markers for hair cycle staging. In early catagen hair follicles the dermal papilla is more densely packed and its shape is often more oval when compared to anagen VI hair follicles. (d) The melanin content of anagen hair follicles is higher than in catagen follicles and the gp100+ cells are located below Auber's line whereas in early catagen hair follicles gp100+ cells are more often located in the precortical matrix. DP, dermal papilla; DPs, Dermal papilla shape; DPst, dermal papilla stalk; HM, hair matrix; M, melanin; PHM, proximal hair matrix; white arrows indicate gp100+ cells (in red), dotted line assigns the Auber's line, a: Scale bar: 50 μm, b–d: Scale bar: 50 μm.

it gets thinner and more stretched. In addition, the DP stalk and the shape of the DP aid in distinguishing anagen VI from catagen. In early catagen HFs, the fibroblasts which migrate out from the DP towards the connective tissue sheath are more densely packed than during anagen VI, and the shape of the DP is often more oval (Fig. 1c).

The melanin content of anagen HFs, assessed by Masson Fontana, is much higher (Fig. 1d, I). By immunofluorescence microscopy, the premelanosomal marker Nki/beteb shows more immunoreactive cells located below Auber's line in anagen VI HFs, whereas in early catagen HFs gp100+ cells are located predominantly in the precortical matrix (Fig. 1d, II). The reduction of melanin in early catagen is seen even under low-power magnification (Fig. 1a). In addition, detecting the above qualitative catagen-associated changes in DP and HM would enhance the correct staging (Table 1).

Quantitative morphometric criteria

While the qualitative classification criteria are primarily helpful for fast, histological, overview analyses; objective, reproducible and standardized, quantitative criteria are essential for distinguishing anagen VI from early catagen HFs. For this, the number of defined cell populations in specific reference areas was counted, and the measurement of immunoreactivity, using NIH Image software, proved most useful (Table 1, Figs 2 and 3).

As shown in Fig. 2a, anagen VI HFs show significantly more DAPI+ cells, in line with the morphological anagen VI marker, that the HM is larger and thicker at this hair cycle stage. The percentage of Ki-67+ cells (counted below Auber's line) in anagen VI HFs is also significantly higher, compared to early catagen HFs (Fig. 2b). Instead, the number of TUNEL+ cells (below Auber's line), demarcating apoptotic HF cells, is significantly higher in early catagen HFs (Fig. 2c).

Interestingly, we noticed that there were often DP stalk fibroblasts migrating into the connective tissue sheath (CTS) in HFs cultured for a longer period of time. This is perfectly in line with our previous discovery in mice that there is hair cycle-dependent trafficking of fibroblasts between CTS and DP during the murine hair cycle (32). Therefore, counting the number of (supposed migrating) HF fibroblasts in a well-defined reference area proximal of the tip of the matrix keratinocytes might be a useful novel quantitative anagen–catagen distinction parameter. Indeed, significantly more fibroblasts can be found in the DP stalk of early catagen when compared with anagen VI HFs (Fig. 2d).

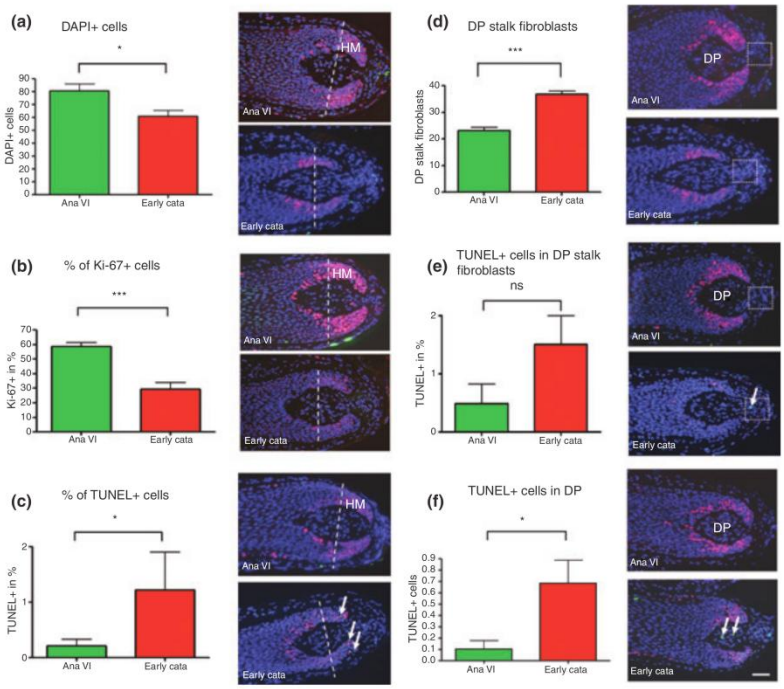

Figure 2. Quantitative morphometric criteria for hair matrix keratinocytes and dermal papilla to distinguish between anagen VI and early catagen (I–IV). (a) There are significantly more DAPI+ cells in anagen VI hair follicles (*$p < 0.05$). (b) The percentage of Ki-67 + in the growth phase of the hair follicles is significantly augmented (***$p < 0.0001$). (c) In early catagen hair follicles there is a significantly higher percentage of TUNEL+ cells (*$p < 0.05$). (d) Significantly more migrating fibroblasts in the dermal papilla stalk can be found in the reference area of catagen hair follicles (***$p < 0.0001$). (e) In the reference area of the dermal papilla, stalk there is a higher percentage of TUNEL+ cells in early catagen hair follicles compared to anagen VI hair follicles (this was not significant). (f) Regarding the central part of dermal papilla, the amount of TUNEL+ cells is significantly augmented in the catagen hair follicle stage (*$p < 0.05$). Data was analysed using the Mann–Whitney test for unpaired samples (GraphPad Prism; GraphPad Software, Inc., San Diego, CA, USA) and are expressed as mean and SEM, $n = 19$ for each group, dotted white square is the reference area which is chosen 200 × 200 with NIH image software; dotted line assigns the Auber's line; white arrows indicate TUNEL+ cells (in green), Ana VI: Anagen VI, Early Cata: Early catagen (catagen I–IV), DP: Dermal papilla, HM: Hair matrix, scale bar: 50 μm.

Furthermore, in this reference field, more TUNEL+ cells can be detected in early catagen HFs compared to anagen VI (Fig. 2e). Also in the central part of the DP, the number of TUNEL+ cells is significantly higher in early catagen versus anagen VI HF stage (Fig. 2f). All these six quantitative morphometric classification criteria (Table 1) become possible by running a single Ki-67/TUNEL stain, which makes this immunohistological assessment a highly instructive and convenient anagen–catagen distinction tool.

Finally, quantitative pigmentary markers proved to offer excellent anagen–catagen distinction parameters (Fig. 3, Table 1). Quantification of the total number of nucleated gp100+ cells that directly surround the DP allows the direct assessment of the melanocytes of the HF pigmentary unit (20). As expected, the expression of this premelanosomal marker (30) is significantly higher in anagen VI HFs compared to early catagen HFs (Fig. 3a). Also, measuring the gp100-associated total immunoreactivity around the DPs reveals significantly more gp100 immunoreactivity in this reference areas of cultured anagen, compared to early catagen HFs (Fig. 3b).

Since tyrosinase is the rate-limiting enzyme for melanogenesis (20), we also assessed whether it can be exploited as a criterion for making the anagen–catagen distinction. As shown in Fig. 3c, this is indeed the case: Tyrosinase activity-associated immunoreactivity is stronger in anagen VI HFs, but did not reach the level of significance in our hands. Therefore, although we do not recommend its employment as a robust quantitative classification parameter, it may best reserved for addressing specific pigmentation research questions related to the anagen VI–catagen switch (Fig. 3c).

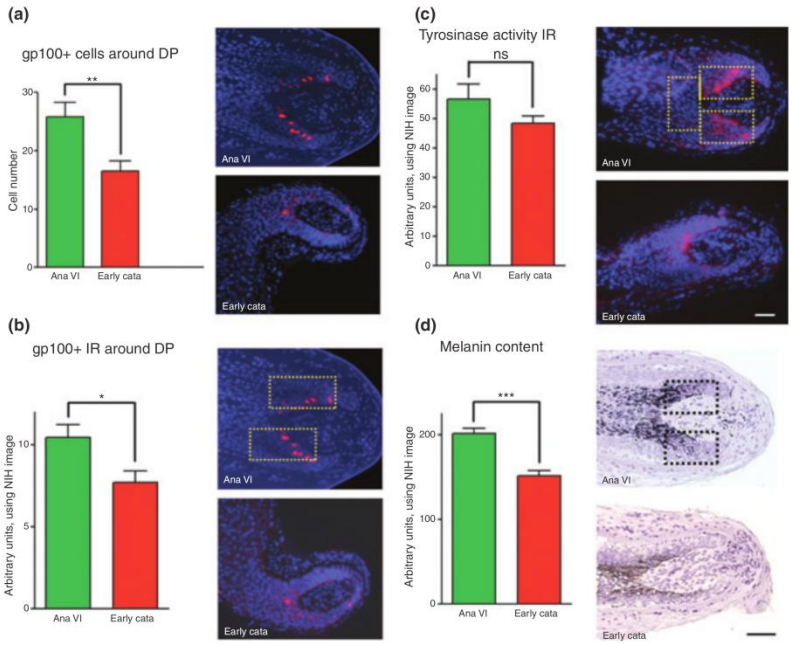

Figure 3. Pigmentary markers (gp100, melanin and tyrosinase) employed for quantitative morphometric criteria to distinguish between anagen VI and early catagen (I–IV). (a) The total number of nucleated gp100+ cells is significantly higher in anagen VI hair follicles compared to early catagen hair follicles (**$p < 0.01$). (b) Measuring the gp100-associated immunoreactivity around the dermal papillae, with NIH Image software, there is significantly more immunoreactivity in the reference areas of cultured anagen hair follicles (*$p < 0.05$). (c) The tyrosinase activity-associated immunoreactivity is higher in anagen VI hair follicles but not significantly augmented. (d) The melanin content is significantly reduced in regressing hair follicles (***$p < 0.0001$). All data were analysed using the Mann–Whitney test for unpaired samples (GraphPad Prism; GraphPad Software, Inc., San Diego, CA, USA) and are expressed as mean and SEM, n = 5–12 hair follicles per group, Ana VI: Anagen VI, Early Cata: Early catagen (catagen I–IV), IR: Immunoreactivity, dotted squares (yellow and black) assign the reference areas for NIH Image, a–c: Scale bar: 50 μm, d: Scale bar: 50 μm.

Instead, simple histomorphometric measurement of the melanin-related 'blackness' in the lateral HM on both sides of the DP proved to be a robust and reliable parameter for distinguishing anagen VI from early catagen HFs (Fig. 3d).

Eflornithine inhibits human hair shaft elongation and induces catagen-like HF regression

When we used the above classification criteria for assessing whether a clinically employed human hair growth inhibitor, eflornithine, can be shown to promote catagen, these parameters turned out to provide dependable and reproducible markers. As expected from previously published clinical work with this agent (33,34), eflornithine significantly impaired human hair shaft elongation *in vitro* (Fig. 4a). More importantly in the current context, treatment with the highest tested dose of eflornithine also promoted catagen development (Fig. 4b), based on the qualitative morphological criteria described above.

Finally, we checked four of our ten quantitative morphometric criteria for reliability. All tested criteria correlated well with the qualitative results. Significantly more DAPI+ cells were found in the matrix below Auber's line in vehicle control HFs compared to eflornithine-treated ones (Fig. 4c). In the same reference area, control HFs also showed significantly more Ki67 + cells (Fig. 4d), while significantly more DP fibroblasts had emigrated into the DP stalk in eflornithine-treated HFs (Fig. 4e). Furthermore, there was a significant decline in the total melanin content in the HM in eflornithine-treated HFs (Fig. 4f). Taken together, this shows that our novel qualitative and quantitative classification system is perfectly suited to objectively assess the hair growth-inhibitory activity in HF organ culture.

Discussion

Previously, when assessing whether organ-cultured human scalp HFs were still in anagen VI or had already entered into catagen, investigators had to rely on fairly ill-defined morphological indicators (22). Their usefulness for classification purposes had not been methodically explored (22),

© 2009 John Wiley & Sons A/S, *Experimental Dermatology*, **19**, 305–312

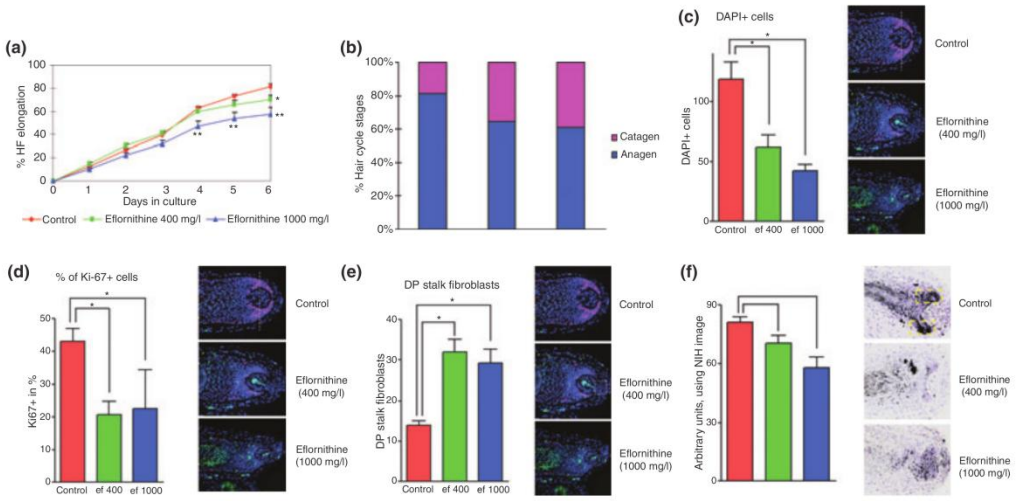

Figure 4. Influence of eflornithine on organ-cultured human scalp hair follicles. (a) Eflornithine significantly promotes catagen induction in cultured human scalp hair follicles (400 mg/l, *p < 0.05 and 1,000 mg/l, **p < 0.005). (b) Eflornithine treatment enhances catagen formation in organ-cultured hair follicles. (c) Significantly more DAPI+ cells are found in the matrix keratinocytes below the Auber's line of control hair follicles (*p < 0.05). (d) Control hair follicles treated with the same amount of water instead of eflornithine show significantly more Ki67+ cells in the hair matrix keratinocytes below the Auber's line (*p < 0.05). (e) Significantly more dermal papilla stalk fibroblasts emigrated out of the dermal papilla in the eflornithine treated hair follicles (*p < 0.05). (f) There is a significant decline of the total melanin content in the hair matrix on both sides of the dermal papilla in the eflornithine treated hair follicles (*p < 0.05, **p < 0.005). All data were analysed using the Mann–Whitney test for unpaired samples (GraphPad Prism; GraphPad Software, Inc., San Diego, CA, USA) and are expressed as mean and SEM, *n* = 18 hair follicles per group.

extensive experience by the investigator was necessary, and assessment relied on drawing analogies to comparable morphological changes in the anagen–catagen transformation of murine HFs *in vivo* (21). In addition, the anagen–catagen transformation in organ-cultured, amputated human scalp HFs shows a number of peculiarities that differ from this transformation *in vivo*, e.g. due to the absence of the bulge, isthmus region, sebaceous gland, and the lack of tissue interactions with the dermis and subcutis. Therefore, it had long been uncertain to which extent morphological criteria that are based on *in vivo* observations, can be extrapolated to HF organ culture conditions. The current methods paper attempts to rectify these shortcomings.

The novel classification system reported here now allows investigators in the field to employ, for the first time, highly standardized, objective, sensitive, quantifiable and reproducible criteria for the determination of whether a test compound prolongs anagen or promotes premature catagen development in human HF organ culture. Depending on the level of accuracy and quantitative assessment required in the individual experimental set-up at hand, investigators can choose from a limited, but comprehensive portfolio of qualitative criteria, which can then be complemented by quantitative test parameters (Table 1). By being able to employ at least two out of the morphological criterions we have provided, researchers are able to classify HFs as anagen VI or early catagen HFs. After having defined the different hair cycle stage groups in this way one can prove this by comparing the quantitative parameter to each other.

By testing different hair growth-inhibitory substances, since the conception of this classification system, we have repeatedly found the following criteria to be particularly instructive, sensitive and reliable and therefore recommend to always include these in a minimal set of parameters for the objective distinction between anagen VI and early catagen in human HF organ culture:

(i) Number of DAPI+ cells below Auber's line; (ii) Percentage of Ki-67+ cells below Auber's line; (iii) Number of DP stalk fibroblasts; (iv) Melanin content of the HM on both sides of the DP.

As any new classification system of this kind, must be put to rigorous testing by regular usage in multiple different laboratories world-wide before becoming universally acceptable. We strongly encourage other investigators in the field to share their personal experience with the proposed system with us and the hair research community at large so as to further optimize the proposed classification system.

We have studied the clinically employed, topically active hair growth-inhibitor eflornithine as a reference compound for testing whether our defined qualitative and quantitative classification criteria generate reproducible and reliable

results this is the case. Although initially developed as an anti-tumor agent, this ornithine decarboxylase inhibitor which inhibits polyamine biosynthesis (35), is highly effective in African trypanosomiasis (sleeping sickness) (36). Upon continued topical application, eflornithine can retard hair shaft formation and/or re-growth, especially in postmenopausal women (37). The same was seen here in human HF organ culture (Fig. 4a). In addition, we provide the first published evidence that eflornithine also promotes the anagen–catagen transformation in cultured human scalp HFs. This further attests to the hair growth-inhibitory properties of eflornithine in the human system and shows that eflornithine can be employed as a good positive control during the preclinical testing of new candidate inhibitors of human hair growth HF organ culture.

The future use of this new classification system by investigators in the field will facilitate the standardized, objective and reproducible determination of whether a test compound really prolongs anagen or promotes premature catagen development in human HF organ culture. Moreover, this new system may stimulate other investigators in the field to now tackle other remaining, important methodological challenges for preclinical hair research in the human system. Examples for such unmet challenges are to develop objective *molecular* criteria defining the exact stage of anagen VI human HFs at the onset and end of HF organ culture, and to allow the objective distinction of human early catagen from later catagen stages *in vitro* and *in vivo*. The current novel classification system should greatly help to close these methodological gaps in basic and applied human hair research.

Acknowledgements

This study was supported in part by a grant from Shiseido, Japan. Namely, the support of Drs. Jiro Kishimoto, Tsutomu Soma and Yumiko Tsuji, Shiseido/Yokohama, is gratefully acknowledged. Additional support was provided by the Manchester NIHR Biomedical Res Center to R.P.

References

1 Paus R, Foitzik K. In search of the ''hair cycle clock'': a guided tour. Differentiation 2004: **72**: 489–511.
2 Stenn K S, Paus R. Controls of hair follicle cycling. Physiol Rev 2001: **81**: 449–494.
3 Schneider M R, Schmidt-Ullrich R, Paus R. Hairy issues: biology of the hair follicle. Curr Biol 2008: In press.
4 Paus R, Cotsarelis G. The biology of hair follicles. N Engl J Med 1999: **341**: 491–497.
5 Philpott M P, Green M R, Kealey T. Human hair growth in vitro. J Cell Sci 1990: **97**: 463–471.
6 Soma T, Tsuji Y, Hibino T. Involvement of transforming growth factor-beta2 in catagen induction during the human hair cycle. J Invest Dermatol 2002: **118**: 993–997.
7 Tsuji Y, Denda S, Soma T, Raftery L, Momoi T, Hibino T. A potential suppressor of TGF-beta delays catagen progression in hair follicles. J Investig Dermatol Symp Proc 2003: **8**: 65–68.
8 Lee Y R, Yamazaki M, Mitsui S, Tsuboi R, Ogawa H. Hepatocyte growth factor (HGF) activator expressed in hair follicles is involved in in vitro HGF-dependent hair follicle elongation. J Dermatol Sci 2001: **25**: 156–163.
9 Jindo T, Tsuboi R, Imai R, Takamori K, Rubin J S, Ogawa H. The effect of hepatocyte growth factor/scatter factor on human hair follicle growth. J Dermatol Sci 1995: **10**: 229–232.
10 Ito T, Ito N, Saathoff M, Bettermann A, Takigawa M, Paus R. Interferon-gamma is a potent inducer of catagen-like changes in cultured human anagen hair follicles. Br J Dermatol 2005: **152**: 623–631.
11 Peters E M, Hansen M G, Overall R W *et al.* Control of human hair growth by neurotrophins: brain-derived neurotrophic factor inhibits hair shaft elongation, induces catagen, and stimulates follicular transforming growth factor beta2 expression. J Invest Dermatol 2005: **124**: 675–685.
12 Peters E M, Liotiri S, Bodo E *et al.* Probing the effects of stress mediators on the human hair follicle: substance P holds central position. Am J Pathol 2007: **171**: 1872–1886.
13 Foitzik K, Krause K, Nixon A J *et al.* Prolactin and its receptor are expressed in murine hair follicle epithelium, show hair cycle-dependent expression, and induce catagen. Am J Pathol 2003: **162**: 1611–1621.
14 Foitzik K, Spexard T, Nakamura M, Halsner U, Paus R. Towards dissecting the pathogenesis of retinoid-induced hair loss: all-trans retinoic acid induces premature hair follicle regression (catagen) by upregulation of transforming growth factor-beta2 in the dermal papilla. J Invest Dermatol 2005: **124**: 1119–1126.
15 Kondo S, Hozumi Y, Aso K. Organ culture of human scalp hair follicles: effect of testosterone and oestrogen on hair growth. Arch Dermatol Res 1990: **282**: 442–445.
16 Philpott M P, Kealey T. Effects of EGF on the morphology and patterns of DNA synthesis in isolated human hair follicles. J Invest Dermatol 1994: **102**: 186–191.
17 Philpott M P, Sanders D A, Kealey T. Effects of insulin and insulin-like growth factors on cultured human hair follicles: IGF-I at physiologic concentrations is an important regulator of hair follicle growth in vitro. J Invest Dermatol 1994: **102**: 857–861.
18 Tobin D J, Slominski A, Botchkarev V, Paus R. The fate of hair follicle melanocytes during the hair growth cycle. J Investig Dermatol Symp Proc 1999: **4**: 323–332.
19 Tobin D J. Human hair pigmentation – biological aspects. Int J Cosmet Sci 2008: **30**: 233–257.
20 Slominski A, Wortsman J, Plonka P M, Schallreuter K U, Paus R, Tobin D J. Hair follicle pigmentation. J Invest Dermatol 2005: **124**: 13–21.
21 Müller-Röver S, Handjiski B, van der Veen C *et al.* A comprehensive guide for the accurate classification of murine hair follicles in distinct hair cycle stages. J Invest Dermatol 2001: **117**: 3–15.
22 Kligman A M. The human hair cycle. J Invest Dermatol 1959: **33**: 307–316.
23 Whiting D A. The Structure of the Human Hair Follicle. Fairfield, NJ: Canfield Publishing, 2004.
24 Sanders D A, Philpott M P, Nicolle F V, Kealey T. The isolation and maintenance of the human pilosebaceous unit. Br J Dermatol 1994: **131**: 166–176.
25 Bodo E, Biro T, Telek A *et al.* A hot new twist to hair biology: involvement of vanilloid receptor-1 (VR1/TRPV1) signaling in human hair growth control. Am J Pathol 2005: **166**: 985–998.
26 Foitzik K, Lindner G, Mueller-Roever S *et al.* Control of murine hair follicle regression (catagen) by TGF-beta1 in vivo. FASEB J 2000: **14**: 752–760.
27 Bodo E, Kovacs I, Telek A *et al.* Vanilloid receptor-1 (VR1) is widely expressed on various epithelial and mesenchymal cell types of human skin. J Invest Dermatol 2004: **123**: 410–413.
28 Peters E M, Stieglitz M G, Liezman C *et al.* p75 Neurotrophin receptor-mediated signaling promotes human hair follicle regression (catagen). Am J Pathol 2006: **168**: 221–234.
29 Kloepper J E, Hendrix S, Bodo E *et al.* Functional role of beta 1 integrin-mediated signalling in the human hair follicle. Exp Cell Res 2008: **314**: 498–508.
30 Singh S K, Nizard C, Kurfurst R, Bonte F, Schnebert S, Tobin D J. The silver locus product (Silv/gp100/Pmel17) as a new tool for the analysis of melanosome transfer in human melanocyte-keratinocyte co-culture. Exp Dermatol 2008: **17**: 418–426.
31 Han R, Baden H P, Brissette J L, Weiner L. Redefining the skin's pigmentary system with a novel tyrosinase assay. Pigment Cell Res 2002: **15**: 290–297.
32 Tobin D J, Gunin A, Magerl M, Handijski B, Paus R. Plasticity and cytokinetic dynamics of the hair follicle mesenchyme: implications for hair growth control. J Invest Dermatol 2003: **120**: 895–904.
33 Soler A P, Gilliard G, Megosh L C, O'Brien T G. Modulation of murine hair follicle function by alterations in ornithine decarboxylase activity. J Invest Dermatol 1996: **106**: 1108–1113.
34 Hynd P I, Nancarrow M J. Inhibition of polyamine synthesis alters hair follicle function and fiber composition. J Invest Dermatol 1996: **106**: 249–253.
35 Poulin R, Lu L, Ackermann B, Bey P, Pegg A E. Mechanism of the irreversible inactivation of mouse ornithine decarboxylase by alpha-difluoromethylornithine. Characterization of sequences at the inhibitor and coenzyme binding sites. J Biol Chem 1992: **267**: 150–158.
36 Pepin J, Milord F, Guern C, Schechter P J. Difluoromethylornithine for arseno-resistant *Trypanosoma brucei* gambiense sleeping sickness. Lancet 1987: **2**: 1431–1433.
37 Hickman J G, Huber F, Palmisano M. Human dermal safety studies with eflornithine HCl 13.9% cream (Vaniqa), a novel treatment for excessive facial hair. Curr Med Res Opin 2001: **16**: 235–244.

APPENDIX C EFFICIENCY RESULTS FOR QPCR VALIDATION EXPERIMENT

Appendix C provides all the efficiency plots (and the corresponding data) for all TaqMan® target genes against the housekeeping gene PPIA used in the thesis. This section corresponds to Chapter 6.18.3 in the thesis where the methodology can be found. Efficiency validations were performed prior to carrying out the qPCR experiments to ensure that the delta delta Ct method could be used to obtain relative expression level results for qPCR experiments performed. In this section each target gene is presented on its own individual page with the efficiency plots and the table containing the data plotted below. The results of the efficiency experiments were used to determine the range of concentrations of cDNA to use for qPCR experiments (A summary table is provided in Section 6.18.3 or alternatively provided in the far right column of all the tables presented here).

Relative efficiency plot and table of results for *Period1* and *PPIA*

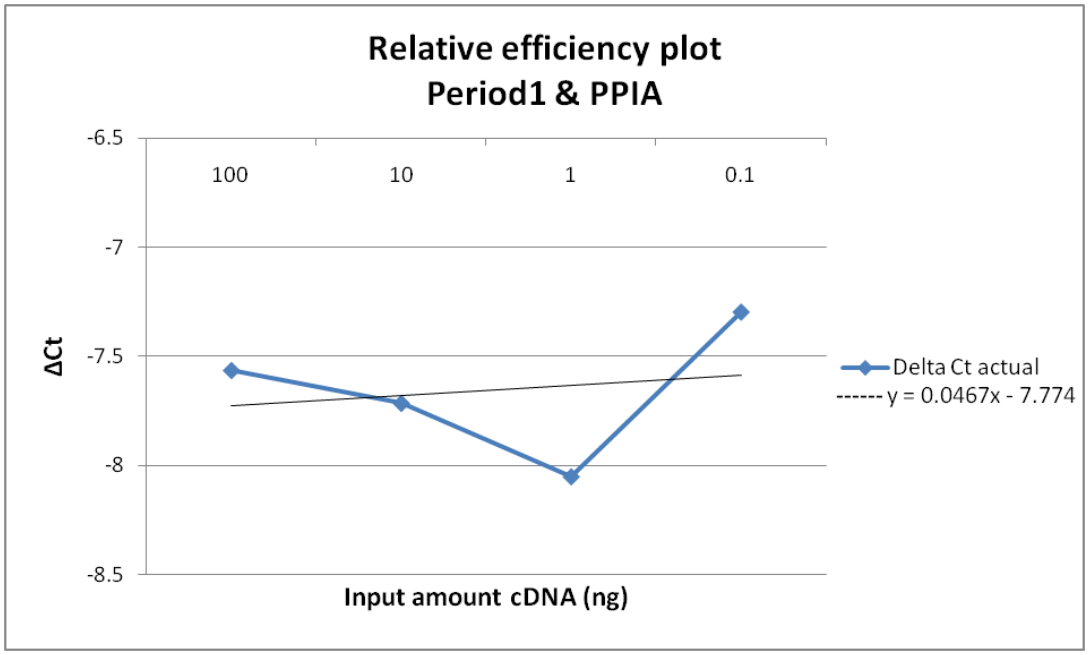

Input concentration cDNA (ng)	PPIA Normaliser gene Average Ct	Period1 Target gene Average Ct	ΔCt PPIA - Period1	Acceptable dynamic range (ng)
100	14.4	22.0	-7.6	0.1 to 100
10	17.8	25.5	-7.7	
1	21.7	29.7	-8.1	
0.1	25.4	32.7	-7.3	
0.01	29.5	36.0	-6.5	
0.001	33.9	40.0	-6.1	

Relative efficiency plot and table of results for *Bmal1* and *PPIA*

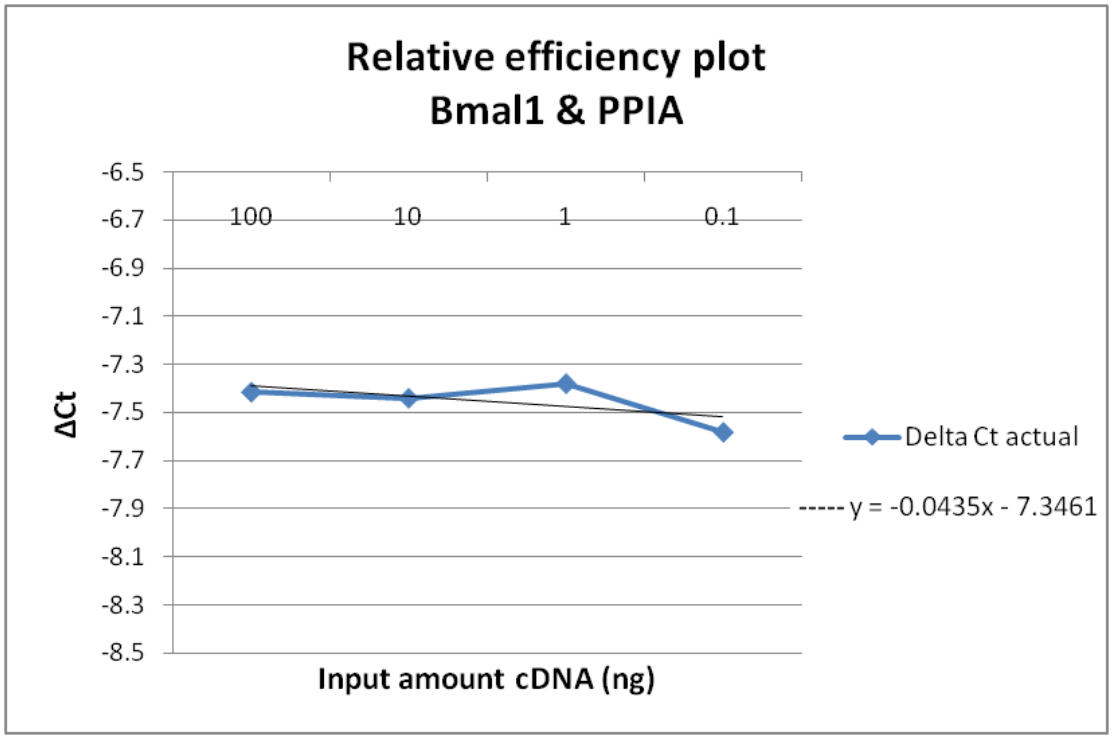

Input concentration cDNA (ng)	PPIA Normaliser gene Average Ct	Bmal1 Target gene Average Ct	ΔCt PPIA - Bmal1	Acceptable dynamic range (ng)
100	14.9	22.3	-7.4	0.1 to 100
10	17.9	25.4	-7.4	
1	21.3	28.7	-7.4	
0.1	24.8	32.4	-7.6	
0.01	28.5	36.4	-7.9	
0.001	31.7	40.0	-8.3	

Relative efficiency plot and table of results for *Clock* and *PPIA*

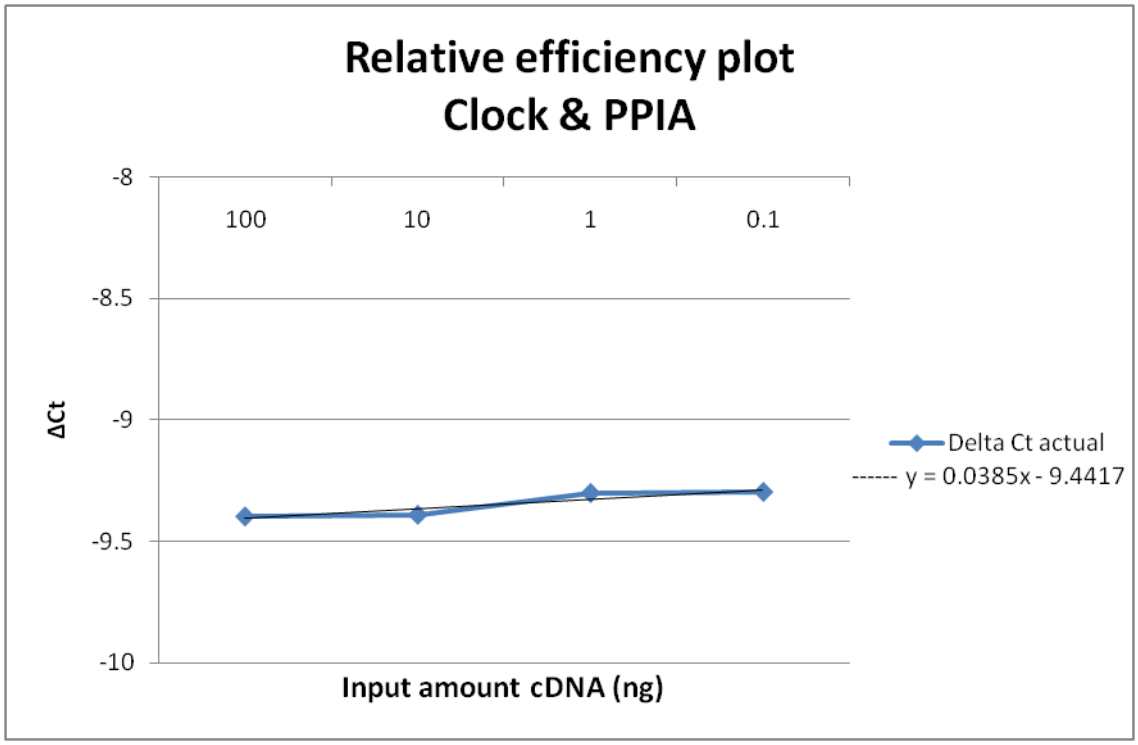

Input concentration cDNA (ng)	PPIA Normaliser gene Average Ct	Clock Target gene Average Ct	ΔCt PPIA - Clock	Acceptable dynamic range (ng)
100	14.9	24.3	-9.4	0.1 to 100
10	17.9	27.3	-9.4	
1	21.3	30.6	-9.3	
0.1	24.8	34.1	-9.3	
0.01	28.5	40.0	-11.5	
0.001	31.7	40.0	-8.3	

Relative efficiency plot and table of results for *Cry1* and *PPIA*

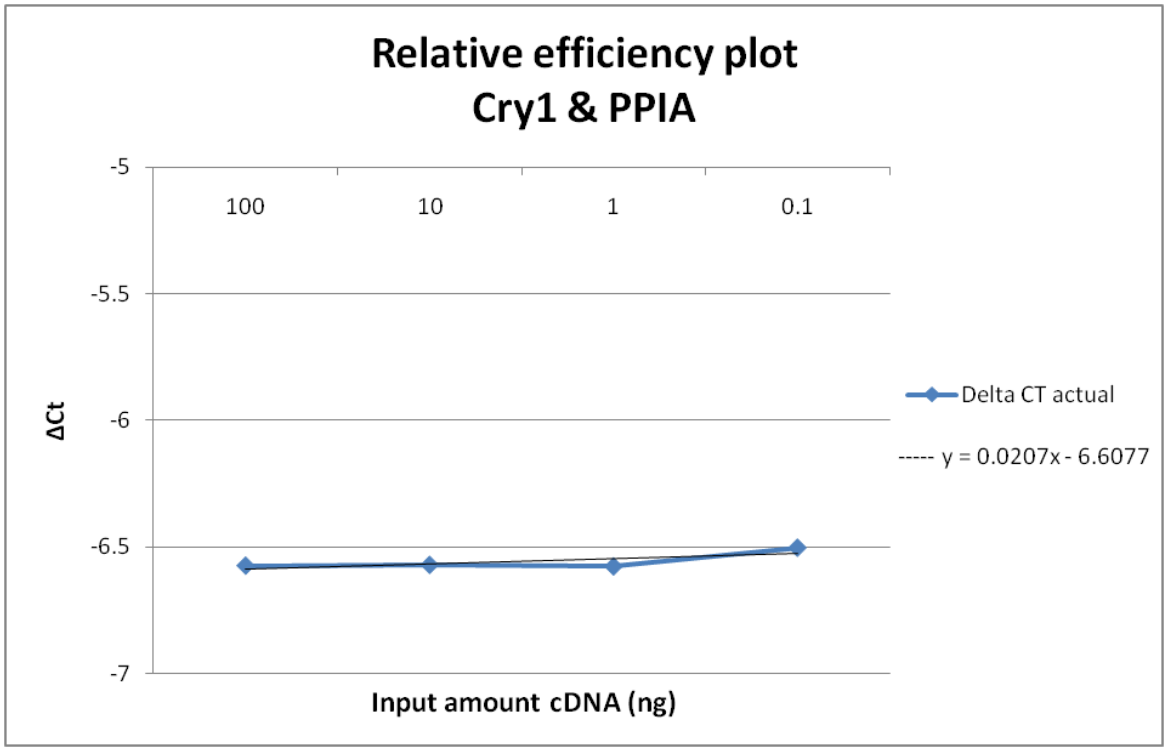

Input concentration cDNA (ng)	PPIA Normaliser gene Average Ct	Cry1 Target gene Average Ct	ΔCt PPIA – Cry1	Acceptable dynamic range (ng)
100	14.9	21.5	-6.6	0.1 to 100
10	17.9	24.5	-6.6	
1	21.3	27.9	-6.6	
0.1	24.8	31.3	-6.5	
0.01	28.5	34.6	-6.1	
0.001	31.7	36.9	-5.2	

Relative efficiency plot and table of results for *Cry2* and *PPIA*

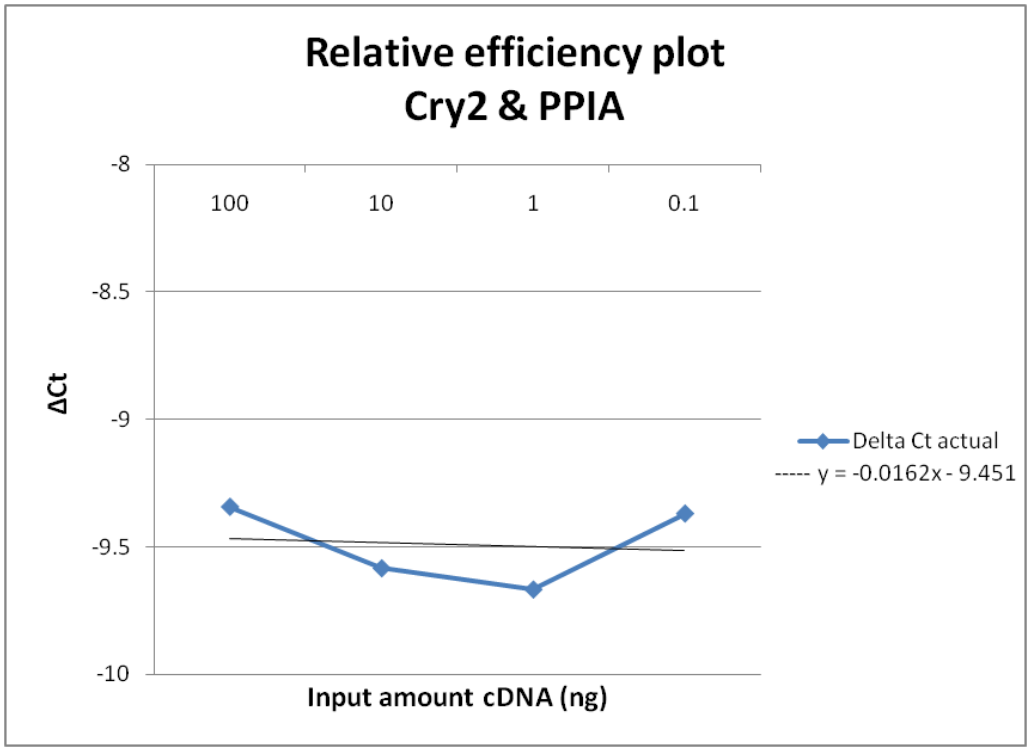

Input concentration cDNA (ng)	PPIA Normaliser gene Average Ct	Cry2 Target gene Average Ct	ΔCt PPIA – Cry2	Acceptable dynamic range (ng)
100	14.9	24.2	-9.3	0.1 to 100
10	17.9	27.5	-9.6	
1	21.3	31.0	-9.7	
0.1	24.8	34.2	-9.4	
0.01	28.5	37.0	-8.5	
0.001	31.7	40.0	-8.3	

Relative efficiency plot and table of results for *Nr1d1* and *PPIA*

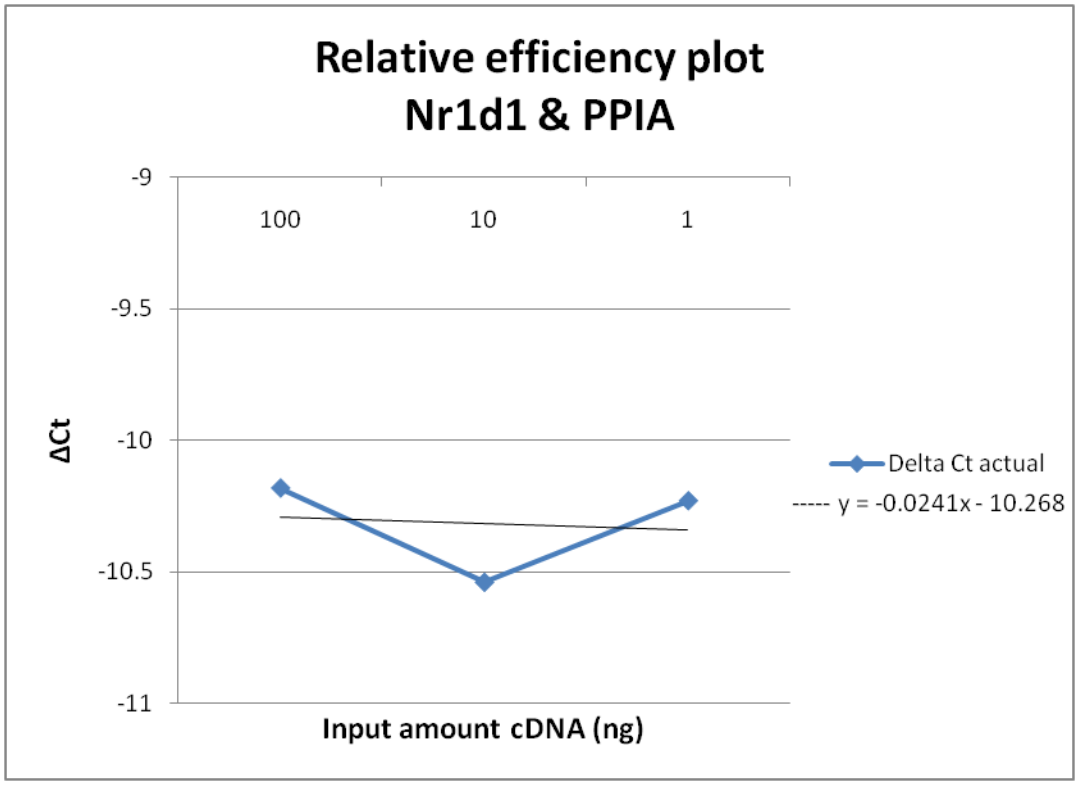

Input concentration cDNA (ng)	PPIA Normaliser gene Average Ct	Nr1d1 Target gene Average Ct	ΔCt PPIA – Nr1d1	Acceptable dynamic range (ng)
100	14.9	25.1	-10.2	1 to 100
10	17.9	28.5	-10.5	
1	21.3	31.5	-10.2	
0.1	24.8	35.8	-10.9	
0.01	28.5	36.7	-8.2	
0.001	31.7	36.7	-5.0	

Relative efficiency plot and table of results for *Cdkn1a* and *PPIA*

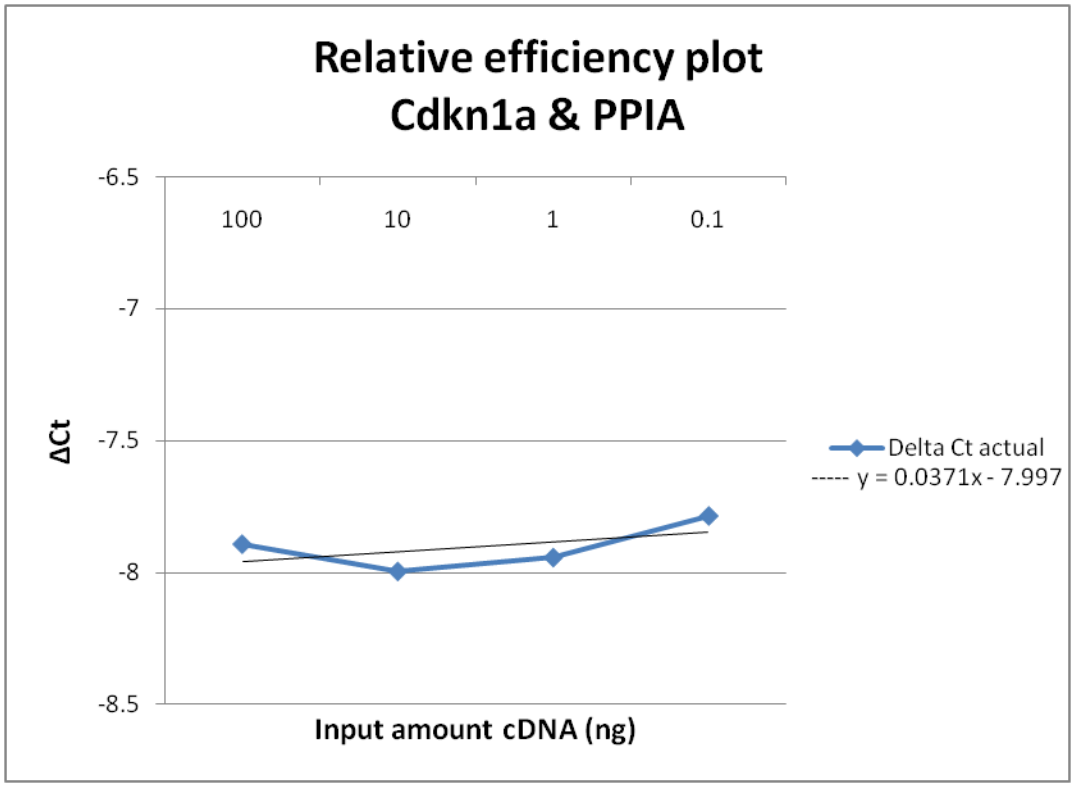

Input concentration cDNA (ng)	PPIA Normaliser gene Average Ct	Cdkn1a Target gene Average Ct	ΔCt PPIA – Cdkn1a	Acceptable dynamic range (ng)
100	14.9	22.8	-7.9	0.1 to 100
10	17.9	25.9	-8.0	
1	21.3	29.2	-7.9	
0.1	24.8	32.6	-7.8	
0.01	28.5	35.9	-7.4	
0.001	31.7	40.0	-8.3	

Relative efficiency plot and table of results for *c-Myc* and *PPIA*

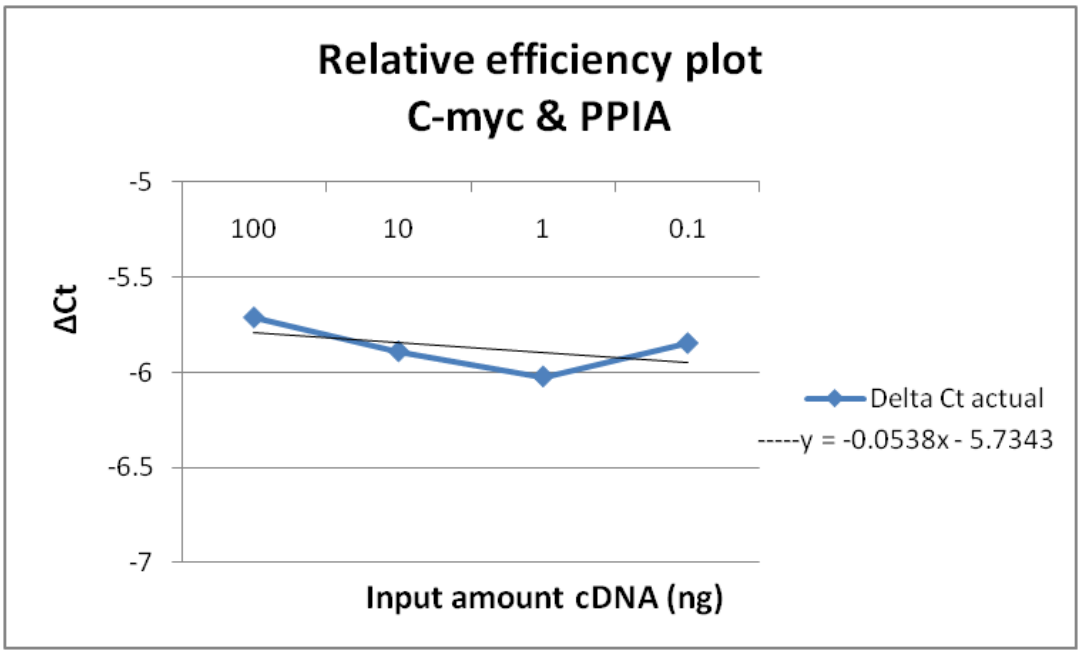

Input concentration cDNA (ng)	PPIA Normaliser gene Average Ct	c-Myc Target gene Average Ct	ΔCt PPIA – c-Myc	Acceptable dynamic range (ng)
100	14.8	20.6	-5.7	0.1 to 100
10	18.0	23.0	-5.9	
1	21.3	27.3	-6.0	
0.1	24.8	30.6	-5.8	
0.01	28.1	34.3	-6.1	
0.001	31.6	34.4	-2.9	

APPENDIX D ADDITIONAL MICROARRAY RESULT: GENE FUNCTIONAL CATEGORIES DOWN-REGULATED GENES IN CATAGEN

Appendix D provides additional data arising from the work detailed in Chapter 8. Human anagen and catagen hair follicle gene expression profiles were obtained via microarray experiments (see Chapters 6 and Chapter 8 for more methodologies and details). An anagen "signature" was defined as the probe set down-regulated in catagen by a fold change of >1.5 in all three patients. Here the functional categories of the genes in the anagen "signature" produced by performing DAVID bioinformatics analysis of this list is provided in the table.

BP = Biological process, MF = molecular function, CC=cell compartment

	Term	*Genes*
CC	intracellular non-membrane-bounded organelle	*KIF5C, KRT31, KRT33A, KRT86, KRTAP3-2, KRT85, MYCN, KRTAP4-7, KRTAP4-6, KRTAP4-5, KRTAP3-3, KRT81, KRTAP2-4, CAMK2N1, KIF5C,KRTAP4-4, SHROOM3, KRTAP2-1, DYNC1I1, KIF26A, KRTAP2-2, KRTAP1-3, KRT37, H2AFJ, KRTAP4-9, KRTAP4-3, KRTAP3-1, KRT73, KRT34, KRTAP4-2, KRT73, KRTAP1-1, KRTAP9-4/9-9, NAV2*
CC	Cytoskeleton	*KIF5C, KRT32, KRT33A, KRT85, KRTAP3-2, KRT86, KRTAP4-7, KRTAP4-6, KRTAP4-5, KRTAP3-3, KRT81, KRTAP2-4, CAMK2N1, KRTAP4-4, SHROOM3, KIF5C, KRTAP2-1, DYNC1I1, KIF26A, KRTAP2-2, KRTAP1-3, KRT37, KRTAP4-9, KRTAP4-3, KRTAP3-1, KRT73, KRT34, KRTAP4-2, KRT73, KRTAP1-1, KRTAP9-4/9-9*
CC	intermediate filament	*KRT33A, KRT31, KRT86, KRTAP3-2, KRT85, KRTAP4-7, KRTAP4-6, KRTAP4-5, KRTAP3-3, KRT81, KRTAP2-4, KRTAP4-4, KRTAP2-1, KRTAP2-2, KRTAP1-3, KRT37, KRTAP4-9, KRTAP4-3, KRTAP3-1, KRT73, KRT34, KRTAP4-2, KRT73, KRTAP1-1, KRTAP9-4/9-9*
CC	keratin filament	*KRTAP2-2, KRTAP1-3, KRT85, KRTAP3-2, KRT86, KRTAP4-7, KRTAP4-9, KRTAP4-3, KRTAP3-1, KRTAP2-4, KRTAP4-6, KRT73, KRTAP4-5, KRTAP4-2, KRTAP3-, KRT73, KRT81, KRTAP1-1, KRTAP9-4/9-9, KRTAP4-4, KRTAP2-1*
MF	structural molecule activity	*KRT33A, KRT31, KRTAP1-3, WNT3, KRTAP3-2, KRT86, KRT85, KRT37, KRTAP3-1, KRT73, KRT34, KRTAP3-3, KRT73, KRT81, KRTAP1-1*
MF	transcription factor activity	*MSX2, SMAD6, DLX1, MYCN, POU4F1, MSX1, DLX2, DLX3*
BP	pattern specification process	*AXIN2, SMAD6, DLX1, WNT3, HHIP, SHROOM3, DLX2, CYP26B1*
BP	neuron differentiation	*KIF5C, EFHD1, DLX1, ID3, POU4F1, KIF5C, DLX2*
BP	Regionalization	*AXIN2, SMAD6, DLX1,WNT3, HHIP, DLX2, CYP26B1*
BP	skeletal system development	*MSX2, AXIN2, DLX1, MSX1, NPR3, DLX2*
BP	cell fate commitment	*DLX1, WNT3, IFRD1,DLX2, CYP26B1*
BP	embryonic morphogenesis	*MSX2, WNT3, SHROOM3, MSX1, DLX2, CYP26B1*
BP	chordate embryonic development	*AXIN2, DLX1, SHROOM3, MSX1,DLX2*
BP	negative regulation of apoptosis	*MSX2, SGK3, SMAD6, DLX1, MSX1*
BP	protein serine/threonine kinase signaling pathway	*MSX2, SMAD6, BAMBI, MSX1*
BP	response to protein stimulus	*MSX2, ID3, MSX1,LY6G6D*
BP	epidermis development	*KRT31,KRT34, KRT85*
BP	negative regulation of signal transduction	*AXIN2, SMAD6, HHIP,CYP26B1*
BP	proximal/distal pattern formation	*Dlx1, Dlx2, Cyp26b2*
BP	BMP signaling pathway	*Msx2,Msx1, SMAD6*
BP	cartilage development	*Msx1, Dlx2*
MF	microtubule motor activity	*KIF5C, DYNC1I1, KIF26A, KIF5C*
BP	appendage morphogenesis	*Msx2,Msx1, Cyp26b2*
BP	forebrain neuron fate commitment	*Dlx1, Dlx2*
BP	regulation of oligodendrocyte differentiation	*Dlx1, Dlx2*
MF	structural constituent of epidermis	*Krtap1-3, Krtap1-1*

APPENDIX E ADDITIONAL MICROARRAY RESULT - FUNCTIONAL CATEGORIES UP-REGULATED GENES IN CATAGEN

Appendix E provides additional data arising from the work detailed in Chapter 8. Human anagen and catagen hair follicle gene expression profiles were obtained via microarray experiments (see Chapters 6 and Chapter 8 for more methodologies and details). The catagen "signature" was defined as the probe set up-regulated in the catagen samples when compared to the anagen samples. (fold change of >1.5 in all three patients). The catagen "signature" produced much less genes and functional categories as seen in the table below (compare to Appendix D – Anagen functional catgegories)

BP = Biological process, MF = molecular function, CC=cell compartment

	Term	Genes
BP	Cell adhesion	*SPP1, COL27A1 COL14A1, TNFAIP6, PARVA, DAB1*
MF	zinc ion binding	*KCND3, FHL1, MMP16*
CC	Cell projection	*SPP1, KCND3, NEFL, PARVA*
CC	extracellular region part	*SPP1, COL27A1, COL14A1, MMP16*
BP	regulation of cellular component size	*SPP1, FHL1, NEFL*
BP	Cell division	*PARD6G*
CC	extracellular matrix	*COL27A1, COL14A1, MMP16*
MF	steroid dehydrogenase activity	*AKR1C2, AKR1C1*
CC	Collagen	*COL27A1, COL14A1*
MF	monocarboxylic acid binding	*AKR1C2, AKR1C1*
BP	regulation of axonogenesis	*SPP1, NEFL*
MF	steroid binding	*AKR1C2, AKR1C1*
BP	response to toxin	*AKR1C1, NEFL*
BP	regulation of neuron projection development	*SPP1, NEFL*
CC	tight junction	*PARD6G*
BP	regulation of cell morphogenesis involved in differentiation	*SPP1, NEFL*